Assessing Past and Future Hazardous Freezing Rain and Wet Snow Events in Manitoba Using a Pseudo-Global Warming Approach

By

Brock Tropea

A Thesis submitted to the Faculty of Graduate Studies of

The University of Manitoba

in partial fulfillment of the requirements of the degree of

MASTER OF SCIENCE

Department of Environment and Geography

University of Manitoba

Winnipeg

Abstract

Freezing precipitation is a major hazard across Canada. Usually occurring in the form of freezing rain and/or wet snow and can damage transportation networks, infrastructure, and vegetation. Under future warming climatic conditions, the characteristics of this precipitation may change but there is great uncertainty. This thesis characterizes damaging freezing precipitation events within Manitoba and examines their future occurrence within a warmer climate.

A total of 10 events were identified, 8 of which were within the WRF period; 5 of these had both freezing rain and wet snow, and the other 3 had freezing rain exclusively. These were characterized using data from the Japanese 55-year Reanalysis (JRA-55), several Environment and Climate Change Canada (ECCC) datasets, and two 4 km Weather Research and Forecasting (WRF) simulations from the National Center for Atmospheric Research (NCAR) from October 2000 to September 2013 (Liu et al. 2017). These were a retrospective control (CTRL) and a pseudo-global warming (PGW) simulation covering CONUS and much of Canada.

Large scale and local factors were associated with these events. Most (9 of 10) showed consistent large scale forcing: a midlatitude cyclone with 500 hPa trough and jet exit enhancing lift, low surface pressure centre nearby, and an atmospheric river. Local factors, such as the elevated terrain of Riding Mountain, influenced 2 events in CTRL and 3 in PGW by altering surface temperature and/or winds to be favourable for freezing precipitation. This terrain is also somewhat co-located with areas of severe ice loading, as shown by the Canadian Standards Association (2015).

In the PGW simulations, these events changed significantly. The 3 events with freezing rain exclusively were in December and January. Of these, 2 (1) had increased (decreased) in extent, precipitation accumulation, and duration. There was no wet snow in these events in CTRL, but it was present in PGW. The other 5 events that had both wet snow and freezing rain, and none had wet snow exclusively. Of these, 1 increased in extent, duration, and accumulation, and another increased in extent, but had similar duration and lesser accumulation. The other 3 events were reduced.

Acknowledgements

Firstly, I thank my advisor Dr. Ronald Stewart for his guidance, knowledge, and patience. Through him I have become a better scientist, student, and person overall. I probably would not have attempted this degree without him.

Thanks to NCAR for providing the WRF CONUS dataset, and particularly Mary Haley, Kyoko Ikeda, and Chi-Fan Shih for assistance with NCL, and advising on the dataset.

Thanks to Grigory Shamov and Ali Kerrache of Westgrid for their assistance with my first usage of cloud HPC computing and Linux.

Thanks to Michael Vieira and Monty Peckover for their insight, data and support.

Both Ruping Mo and Bohdan Kochtubajda of ECCC provided JRA-55 and GEM images, respectively, which were used extensively in this endeavour.

I appreciate the guidance of my colleagues Juris Almonte, Hilary Smith, and Daniel Betancourt. Juris was especially helpful in my first attempts at Python programming, as well helping me make sense of our mutual dataset.

Technical assistance from Scott Kehler and George Liu was greatly appreciated. They helped with plotting shapefiles, getting initial results, and Linux

A thank you goes to Julie Theriault and Vanessa McFadden for providing information about the Chaîné and Castonguay ice loading model.

I thank all of my colleagues in the office. Your friendship is immensely appreciated and allowed me to retain at least a modicum of sanity as I worked on this.

Finally, I thank my parents, who have provided me with more support over the course of my university career than I probably deserve. Without them, I would've never made it this far.

Contents

List of Tables

List of Figures

1. Introduction

1.1. Background and Motivation

Freezing precipitation events are a significant hazard in the cold climate regions of the world. These events, often associated with midlatitude cyclones, impact both the natural world and human society. During these storms, subfreezing liquid or sticky wet snow accretes onto objects and freezes (Figure 1.1). The impact of this excess weight can be accentuated in the presence of wind.

Figure 1.1: Accretion of approximately 3 cm of wet snow onto the branches of a bush during an ongoing wet snowstorm in Winnipeg on October 11, 2019.

There are many types of impacts. For example, power poles/towers topple over or become twisted (Figure 1.2); vegetation is damaged with trees toppling over, snapping, or losing branches (Figure 1.3). Sometimes damaged trees and branches fall onto power lines, snapping them. There can be mortality due to transportation accidents and exposure to cold through power loss. Millions and sometimes billions of dollars of losses are incurred in these events as a result (Hauer et al. 1993; Lecomte et al. 1998; Hauer et al. 2006; Zhou et al. 2011; Armenakis and Nirupama 2014).

Figure 1.2: Collapsed Hydro tower as a result of a wet snowstorm on October 11, 2019. Photo by Manitoba Hydro, used with permission. Retrieved from: https://www.cbc.ca/news/canada/manitoba/manitoba-hydro-snowstorm-powerless-customers-residual-effects-1.5335157

Figure 1.3: Fallen trees and branches on a residential street in Winnipeg as a result of a wet snowstorm on October 11, 2019.

As discussed above, freezing rain, freezing drizzle and wet snow lead to accretion. Sometimes, these forms of precipitation can occur together in a single storm, along with other types of hydrometeors of varying phases occurring before, after, or simultaneously as a mixture (Stewart et al. 2015); this adds to the complexity of accretion. Freezing precipitation and these mixtures are often associated with a precipitation type transition region (Figure 1.4). This is a region in a storm or weather system where, in general, all rain occurs on the warm side and all snow occurs on the cold side while freezing precipitation, various mixtures, and mixed-phase precipitation occurs in between them (Stewart et al. 2015; Almonte and Stewart 2019). These regions can vary between a few to many kilometers across (Stewart et al. 2015), and are closely associated with the location of the 0°C isotherm. Even small changes to temperature and

moisture can alter the type and morphology of precipitation occurring (Stewart et al. 2015; Kochtubajda et al. 2017; Stewart et al. 2019).

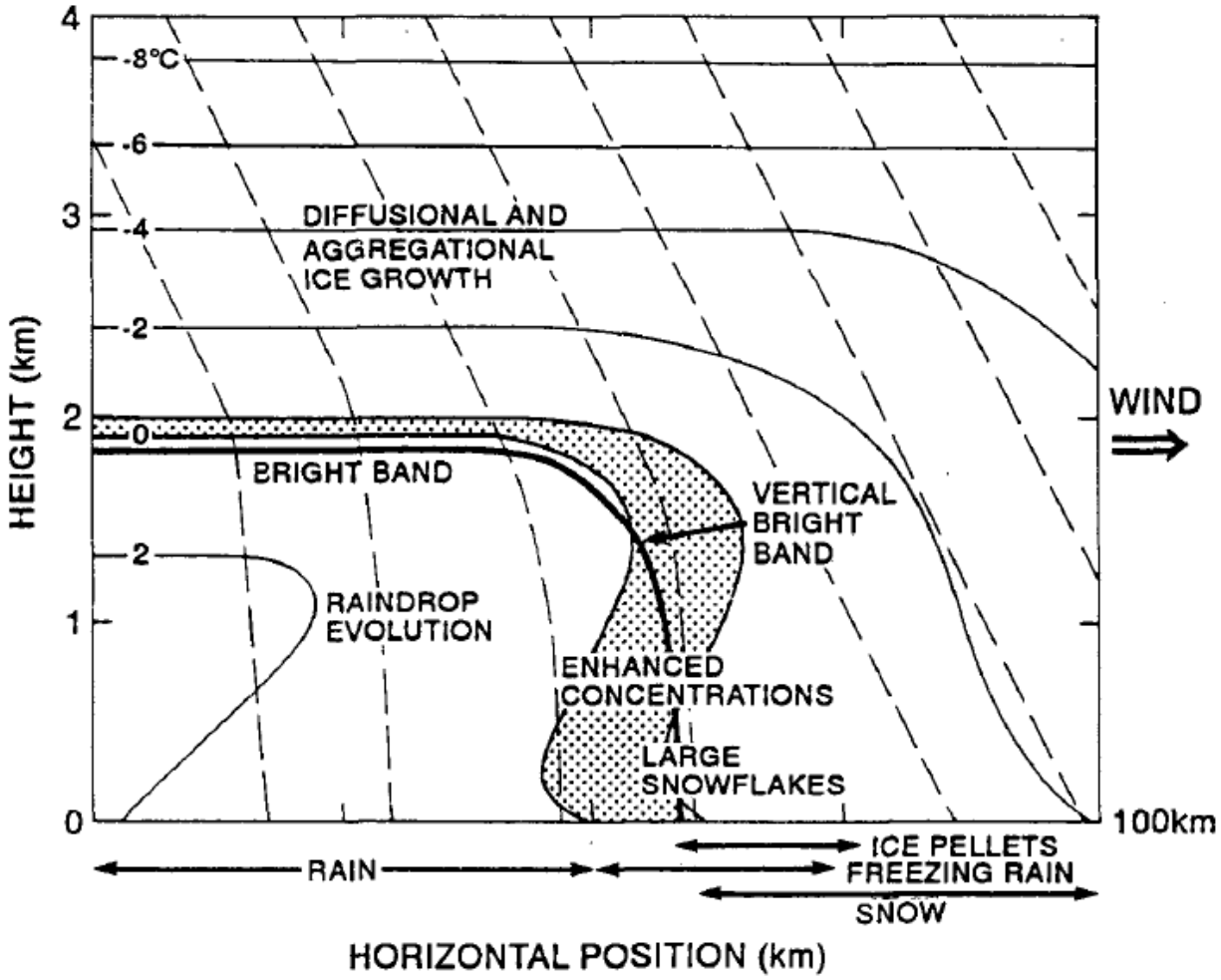

Figure 1.4: Modified schematic vertical cross section from Stewart (1992) showing a precipitation transition region. Some of the microphysical processes in and near this region as well as some of the precipitation types are indicated with text. Solid black contours represent the temperature, the dotted area indicates the region with temperatures very close to 0°C, and dashed lines are illustrative particle trajectories. Wet snow (not shown) occurs most commonly between the region of snow and rain, on the warm side of the near 0°C area. Used with permission.

Particular temperature profiles are generally associated with these types of precipitation shown in Figure 1.5. Freezing rain is typically formed by a snowflake aloft falling into a layer of air that is above 0°C, where it completely melts into a liquid raindrop. It continues to fall below the cloud base into a shallow layer of air below 0°C near the surface, where it becomes

supercooled. Once this occurs, it will immediately begin to freeze on contact with any object it lands on. Wet snow is similar in that a snowflake falls into a warm layer of air aloft, however this warm air generally extends down to the surface. It is also generally shallower than the melting layer in the freezing rain case, which only allows for partial melting of the snowflake. It reaches the surface having partly melted with water intermixed within its crystal lattice; this causes it to become sticky, both to other hydrometeors and to solid objects it lands on. It is also possible that wet snow can reach the surface if the temperature is below 0°C; particles can, for example, partially melt aloft and not be completely refrozen by the time they reach the surface (Stewart et al. 1990; Stewart 1992).

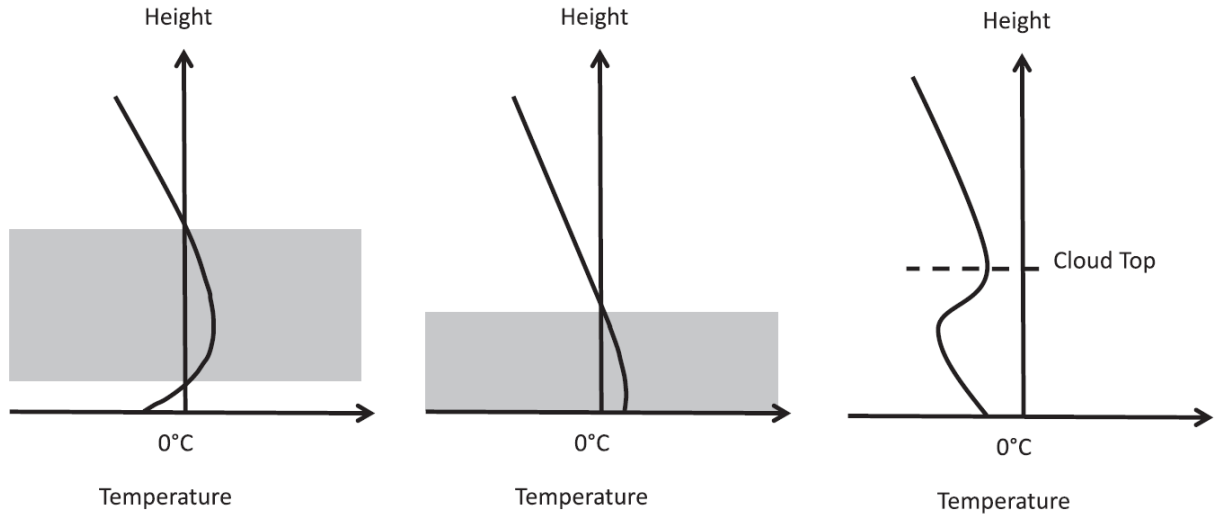

Figure 1.5: Schematic from Stewart et al. (2015) showing the temperature profile associated with freezing rain (left), wet snow (middle), and freezing drizzle (right). The solid black curve is the air temperature, while the gray box represents the melting layer, where temperatures are above 0°C and any frozen particles can melt. Used with permission.

It is critical to note that the melting and freezing that takes place during the evolution of these particles causes extraction and release of latent heat in the surrounding air, which can further alter the precipitation type. This causes freezing rain to be a self-limiting process (Figure 1.6) (Stewart 1984; Lackmann 2011) while wet snow can persist (Figure 1.7), even in the

absence of advection (Lackmann 2011). As well, latent heat can modify the hydrometeor type and/or assist in creating mixtures of types.

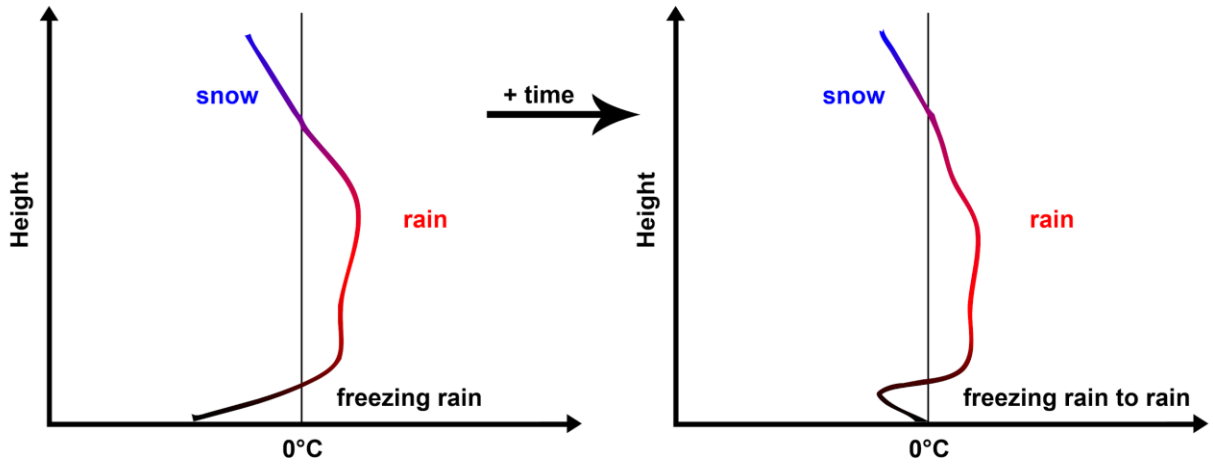

Figure 1.6: Schematic diagram adapted from Lackmann (2011) showing the development of the self-limiting temperature profile associated with freezing rain. The y-axis is the height and the x-axis shows the 0°C reference line. Precipitation type is indicated with text. Time passes between the two plots from left to right.

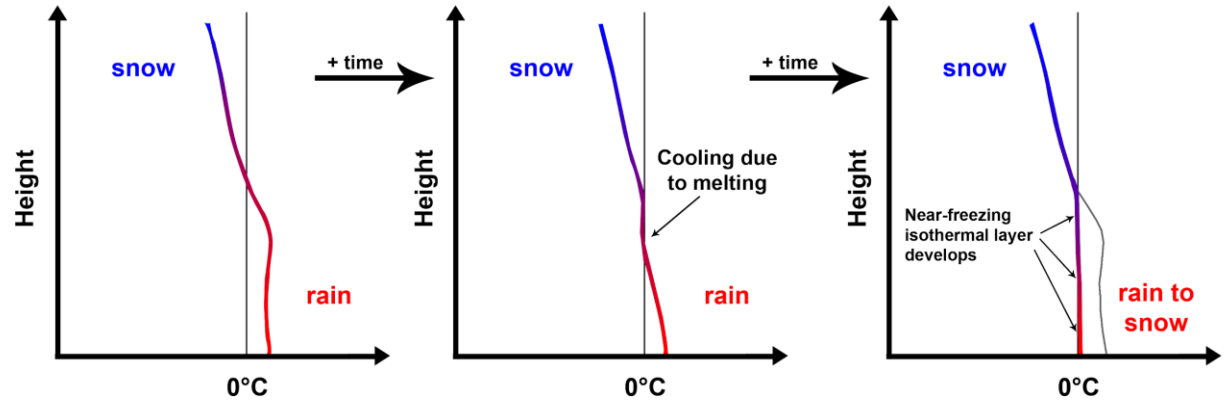

Figure 1.7: Schematic diagram adapted from Lackmann (2011) showing the development of a near 0°C isothermal profile associated with wet snow and rain/snow mixtures. The y-axis is the height and the x-axis shows the 0°C reference line. Precipitation type/mixture is indicated with text. Time passes from left to right, where the initial temperature profile is shown with a gray line.

As mentioned above, the mixed phase and mixed types of precipitation often occur alongside freezing rain and wet snow, though the mechanisms governing exactly which types of

precipitation occur is complex (Figure 1.8). Clouds generating winter precipitation often have a wide distribution of particle types and sizes, which all evolve at differing rates. Hydrometeors falling in the vicinity of the transition region are often subjected to at least partial melting, depending on the depth and temperature of any atmospheric temperature inversions present. The fall velocity and associated trajectory vary with different hydrometeor types, sizes, and mass, which significantly affect the interactions with these various temperature layers. Strong wind shears typically associated with midlatitude cyclones further complicate fall trajectories. As well, liquid water on or within the hydrometeor, or droplets colliding with an ice particle can, under some conditions, freeze and shatter, producing smaller particles of ice. These fragments can begin to grow by deposition and/or accretion, thereby altering the particle size and mass distributions. All precipitation particles will begin to evaporate when they fall below cloud base and this may even lead to complete evaporation. Overall, this is a generalized overview as to how hydrometeor types can occur simultaneously or in sequence near a transition zone.

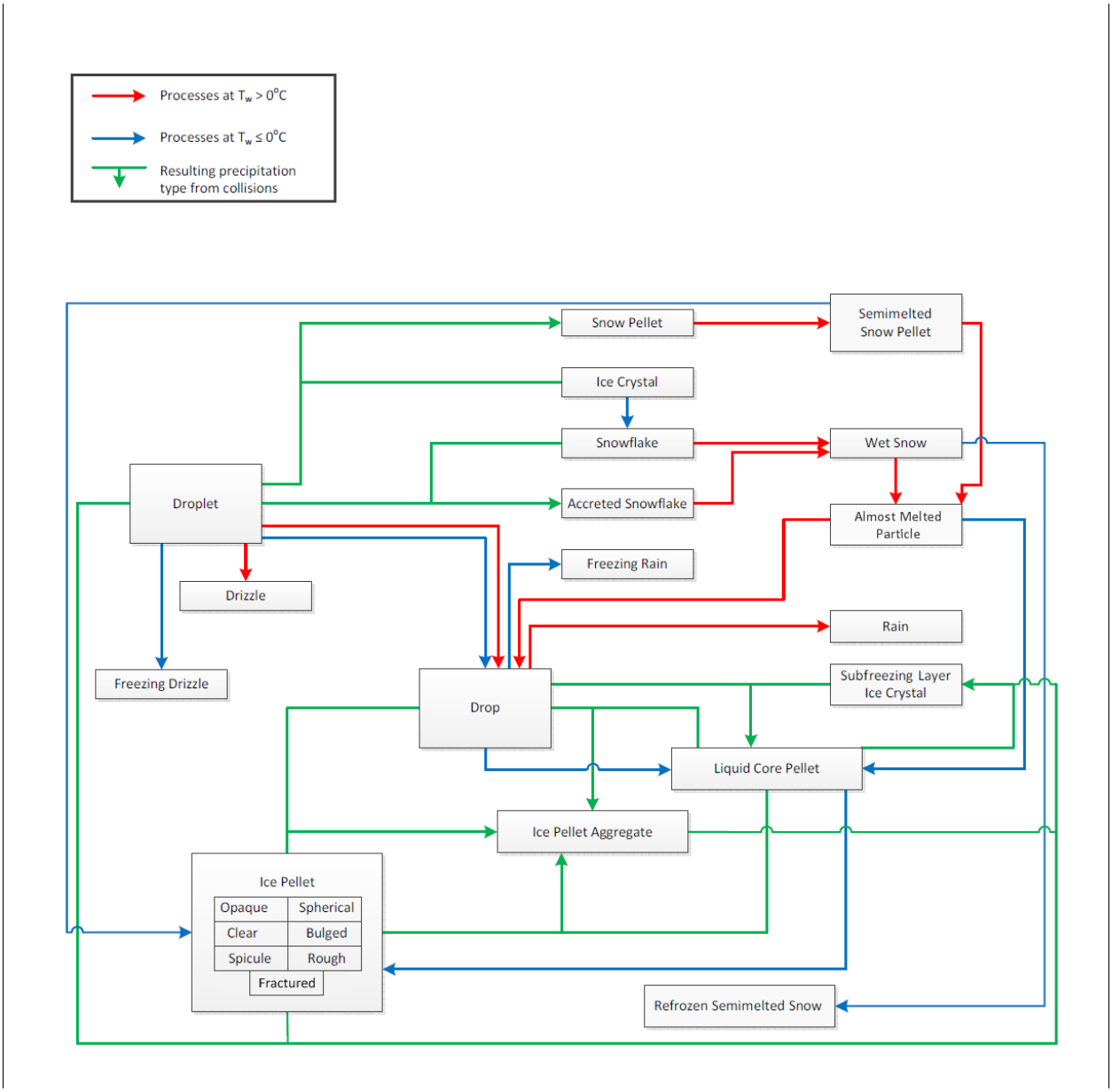

Figure 1.8: Updated flowchart from Stewart et al. (2015) detailing the processes creating the many different types and mixtures of precipitation types occurring near and within a precipitation transition region. Used with permission.

These types of precipitation can occur in many parts of the world, usually in cold climate regions. These types of precipitation are somewhat associated with proximity to large water bodies (usually an ocean) and/or elevated terrain (Cortinas et al. 2004). Large water bodies provide moisture which can be ingested by a storm to enhance it, as well as to moisten the sub-

cloud layer to lessen evaporation and sublimation of the falling precipitation. Elevated terrain alters the low level wind and temperature fields through such mechanisms as upslope flow/cooling, such that they are more favorable for freezing precipitation (Cortinas et al. 2004; Almonte and Stewart 2019). Mechanisms such as cold air damming (Figure 1.9) can also assist in the generation of freezing precipitation, where a layer of sub-freezing air is trapped between a mountain or hillside and a layer of warm air aloft, sometimes with advection refreshing the supplies of warm and cold air (Lackmann 2011).

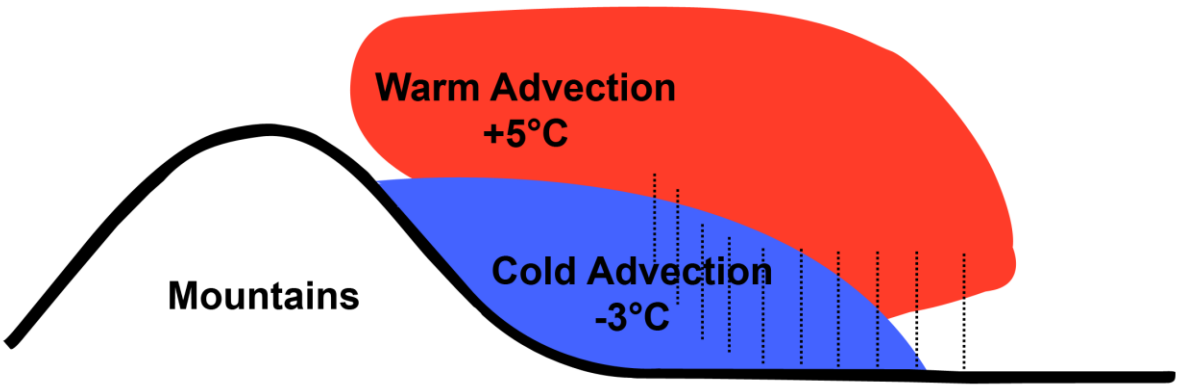

Figure 1.9: Schematic diagram adapted from Lackmann (2011) of a cold air damming situation creating freezing rain. The warm and cold air masses are indicated by colour, while the location of falling rain is indicated by the dotted black lines.

Groisman et al. (2016) examined freezing precipitation in North America and northern Eurasia, and found large areas over both regions with more than 8 freezing rain or drizzle events annually on average. These areas were over the east coast of the United States and Canada, the vicinity of the Great Lakes, and the western part of Russia between the Baltic and Black Seas.

Cortinas et al. (2004) also examined these precipitation types across Canada and the United States. Their results are similar, with freezing rain, drizzle, and ice pellets being closely co-located with the east coast of the United States and Canada, as well as the Great Lakes. They found the median annual hours of freezing rain to be between 10-50 hours in this region,

particularly on the east side of the Great Lakes near the Atlantic Ocean. The median annual freezing rain and drizzle days was similar to Groisman et al. (2016), with a maximum of around 10 days, focused in the same area.

There have been a number of studies that examined freezing precipitation events over Canada and these have generally focused on eastern Canada. However, other parts of Canada also receive these types of precipitation to a lesser extent. For instance, Kochtubajda et al. (2017) examined the occurrence of freezing rain, drizzle, and ice pellets across the Canadian Prairie Provinces, Territories, and the Arctic. Across the Prairies, which includes Manitoba and the adjacent Saskatchewan and Alberta, the average annual number of freezing rain days was generally 1-5, while the number of freezing drizzle and ice pellet days were much higher at 2-12 and 2-14, respectively. The average annual number of hours of freezing rain was found to be generally 1-7, though the maximum annual number of hours was much higher at nearly 30 hours. This suggests that, while freezing rain is not as common in the West, severe events can still occur.

Kochtubajda et al. (2017) noted that freezing precipitation is less common over western Canada partly due to larger amounts of sublimation and evaporation aloft, which reduces the size/amount of freezing precipitation, whereas the lower atmosphere during East Coast events is often near saturation. Chinooks are discussed as an additional mechanism which can assist in the creation of freezing precipitation, by creating a warm layer of air aloft, which may or may not extend to the surface.

Climatological features of freezing precipitation specific to Manitoba were documented by Kochtubajda et al. (2017). It was found that they were associated with the 0°C isotherm, and

this means they usually occur in the shoulder seasons of spring and fall, although they can also occur in the winter months (Cortinas et al. 2004; Kochtubajda et al. 2017).

However, no provincial or storm-scale study has ever been performed on these types of events in Manitoba. One of the primary concerns is from an infrastructure perspective, specifically Manitoba Hydro's operations, which consists of many hydroelectric transmission and distribution lines. Damage to these lines can cut power to many thousands of people locally, as well as neutralizing the ability to transmit power to customers in the United States. The potential costs of these events are of great interest to the province of Manitoba and Manitoba Hydro, as they are a continual problem, occurring every few years (Kochtubajda et al. 2017).

A recent example, as of this writing, is a wet snow event that occurred on October 10-12, 2019. This storm was one of the worst in the history of the province, causing over 266,000 outage reports to Manitoba Hydro (Manitoba Hydro 2019), which took approximately 2 weeks to restore (Dacey 2019). Manitoba Hydro crews had to repair more than 4,000 damaged wooden power poles and approximately 950 km of power lines (The Canadian Press 2019), with estimated repair costs of more than $100,000,000 (Thompson 2019). Estimated costs of the clean-up for the City of Winnipeg are in the tens of millions of dollars, primarily involving the removal of fallen trees and branches (Bergen 2019).

1.2. Changing Hazards in a Warming Climate

As the climate continues to warm in the 21st century due to anthropogenic climate change, the spatiotemporal characteristics of freezing precipitation may change (IPCC 2013; Stewart et al. 2019). Warmer temperatures and the attendant increased water vapour is expected

to have many impacts on global and regional precipitation patterns. The timing, intensity, frequency, and location of precipitation are all expected to change, though the specifics of this remains somewhat unclear. The general consensus is that precipitation will become more variable, with decreases in some regions, increase in others, and extreme events becoming more common (Trenberth 2011; IPCC 2013).

Given the thermodynamic sensitivity of freezing precipitation, it is likely that its spatiotemporal patterns will also be altered. However, there is a great deal of uncertainty regarding all of these changes (IPCC 2013; Stewart et al. 2019). If these precipitation types occur more frequently, with greater severity, at differing times of year, or in areas that otherwise do not typically receive them, they could present a greater hazard to ecosystems and human society.

There is evidence of change in the recent past. Groisman et al. (2016) compared freezing precipitation from 1975-2004 to that of 2005-2014 in North America and Russia in a climatological sense without examining specific events. In North America, they found in general that the annual number of freezing rain days either increased or decreased by 2 on average with no pattern or statistical significance. In the southeastern United States and Canada, a more negative trend of around 1 less day of freezing rain was seen. In British Columbia, Canada, an increase in freezing rain can be seen on the order of 3-5 more days. Across Russia, the changes were more pronounced. There is a decrease in freezing rain along the western border on the order of 1 or 2 fewer days per year, though the pattern is somewhat variable. There is a much clearer pattern of decreased freezing drizzle of 2 fewer days per year across the same area.

Stewart et al. (2019) examined some aspects of future freezing rain over the interior of western Canada, including the climatological northward migration of the 0°C isotherm and the associated precipitation that follows using an ensemble of climate models. They found that in the

central regions of Canada this isotherm moves poleward between 50 and 100 km per decade, though the exact annual locations of this isotherm vary considerably between models, and that changes in freezing rain over the region were relatively low, usually less than 9 additional hours of freezing rain. They note the difficulty of considering projections of specific precipitation types and/or mixtures, due to their complexity of formation. As discussed earlier, these precipitation types are very sensitive to relatively small temperature and moisture changes, especially near the surface. The particle density can also play a role. For example, a denser particle like a snow pellet will fall much farther before melting than a particle of lesser density such as a snowflake; this difference can lead to a different type of precipitation being experienced at the surface. These complications make determining exactly how transition regions will behave in the future very challenging.

Given the potential for significant change in freezing precipitation in the future, and the impacts that these types of precipitation can have on human society and natural ecosystems, it is critical to improve projections of these conditions.

1.3. Objective

Given the lack of research on freezing precipitation events specific to Manitoba despite its importance, the overall objective of this thesis is to better understand the factors leading to freezing precipitation over Manitoba and to begin to examine its future occurrence.

This will be accomplished through addressing two sub-objectives:

1. Characterize 10 freezing rain and wet snow events affecting Manitoba Hydro in particular and determine their primary meteorological and local driving factors.

2. Examine how these freezing rain and wet snow events may change in a future warmer climate assuming thermodynamically-driven change.

2. Data and Methods

The location and key geographical aspects of the study region will be outlined in this section first. Several datasets were utilized and will be described next. Several analytical approaches were used, and the section concludes with a summary of these.

2.1. Study Region

The province of Manitoba is the focus of this thesis (Figure 2.1). It consists of several ecozones, with the southern portion being prairie, the middle being boreal prairie, and the north being mostly boreal shield. It has several large lakes, such as Lake Winnipeg and Lake Manitoba, as well as numerous other smaller lakes, particularly in the north. The most populated city is Winnipeg, the capital, located to the south of Lake Winnipeg, inside the Red River Valley. The province is mostly flat, with increasing elevation in the western half of the province, up to a maximum of 831.2 m above sea level (ASL) at the peak of Baldy Mountain (Bamburak and Christopher 2004). Other important elevated features of the landscape are Riding Mountain and Pembina Mountain, which reach elevations of approximately 762 m ASL (Lang 1974) and 426 m ASL (Upham 1896). These features rise approximately 457 m (Lang 1974) and 90 m (Bamburak and Christopher 2004) above the surrounding land, respectively.

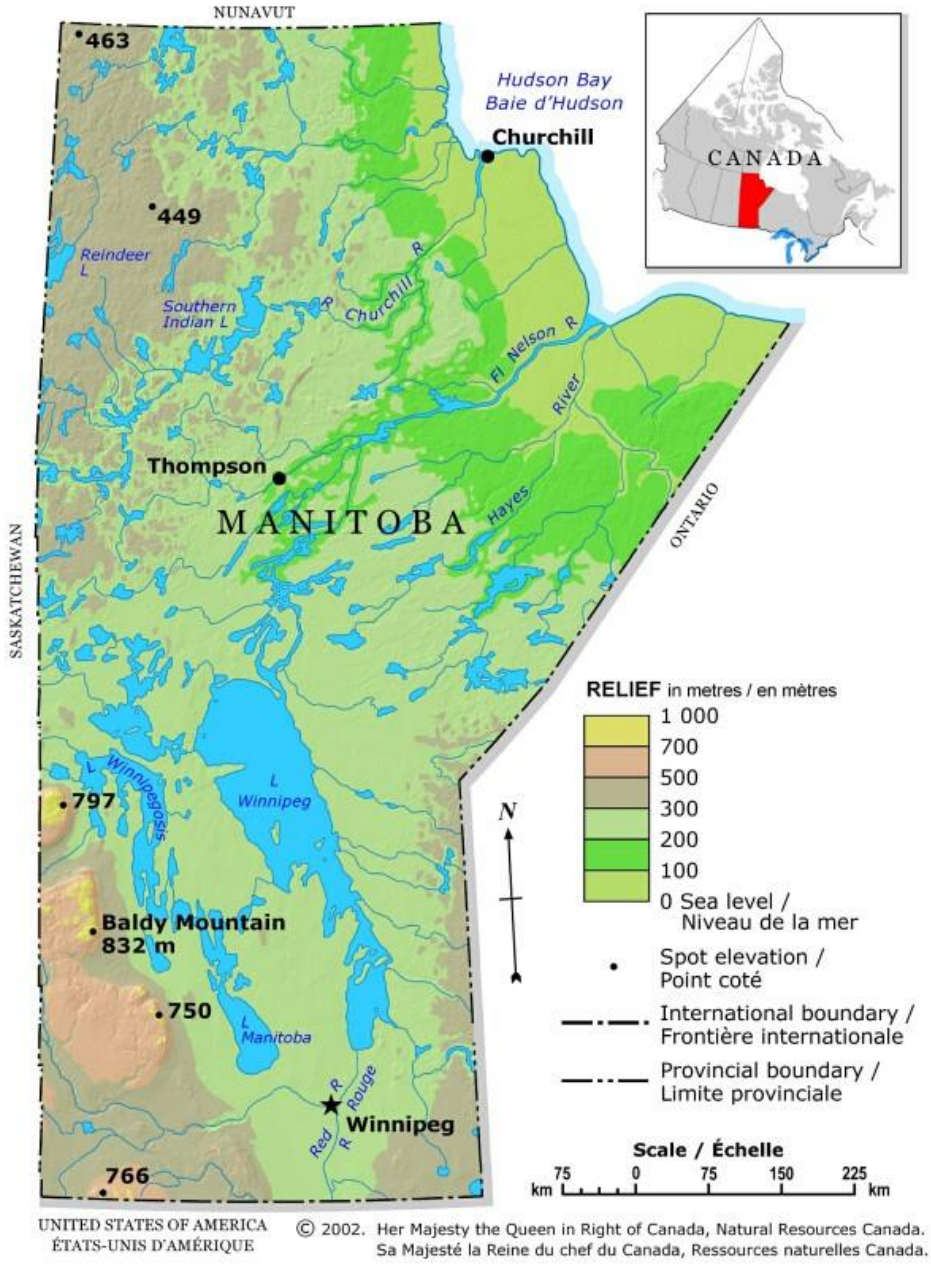

Figure 2.1: Relief map of Manitoba. Contours indicate terrain height, and the large and small black dots represent larger towns and spot elevations, respectively. The black star indicates the location of Winnipeg. The inset image in the top right shows the location of Manitoba within Canada. Retrieved from: https://www.nrcan.gc.ca/maps-tools-publications/maps/atlas-canada/explore-our-maps/reference-maps/16846

There is an extensive network of transmission and distribution lines that are operated by Manitoba Hydro, the majority of which are concentrated in the southern portion of the province. Examples of two of the larger transmission lines are Bipole III, which extends from Winnipeg

northward toward Hudson Bay, and the Manitoba-Minnesota Transmission Project (MMTP; Currently under construction) which extends south from Winnipeg to the US border.

There are 3 areas of climatological severe ice loading in Manitoba (Figure 2.2). These areas were determined by the Canadian Standards Association (CSA) by calculating deterministic ice loads of 19 mm or more (Canadian Standards Association 2015). These areas are co-located with some of the elevated terrain in the western portion of the province, specifically Riding Mountain and Pembina Mountain, as well as the southern Interlake region.

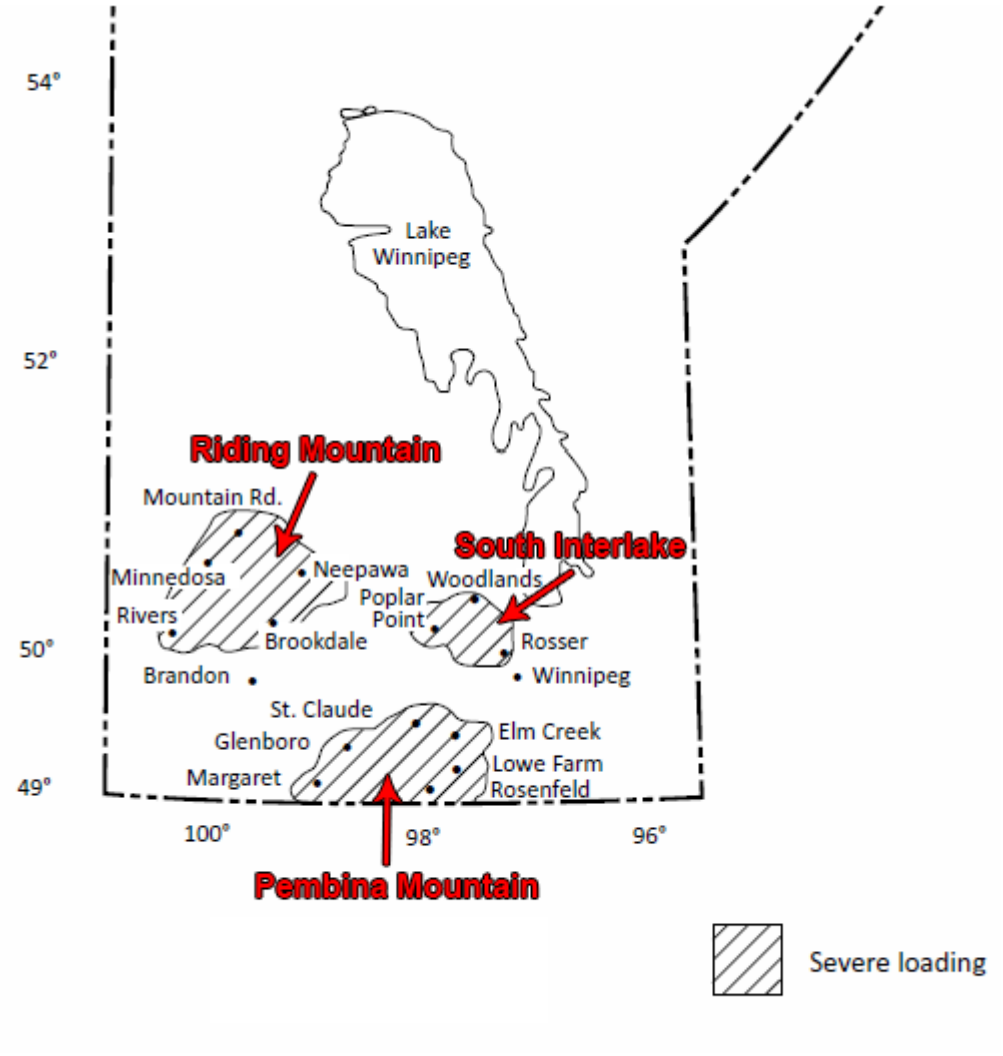

Figure 2.2: Adapted map from the CSA Standards of climatological severe ice loading. Major towns and cities are shown as black dots, while areas of severe ice loading (≥19 mm) are indicated by the hatched areas. Geographic locations that these areas are co-located with are indicated in red.

2.2. Weather Research and Forecasting Model Simulations

To assess the freezing precipitation events in Manitoba and their spatiotemporal characteristics in the future, this study primarily utilizes model output from a pair of simulations generated by the National Center for Atmospheric Research (NCAR). The Weather Research and

Forecasting (WRF) model was used to simulate control (CTRL) and pseudo-global warming (PGW) conditions for the contiguous United States (CONUS). The dataset is described by Rasmussen and Liu (2017) and the model output is discussed by Liu et al. (2017). These simulations are collectively referred to as the WRF CONUS CTRL and PGW simulations.

2.2.1. Description

The model is convection permitting (non-hydrostatic) with no convective parameterization, and was run at 4 km resolution, which allows for good representation of complex terrain interactions (Liu et al. 2017). It uses spectral nudging to maintain the historical overall large scale synoptic flows (2000 km), which keeps storm tracks in the same general location.

The domain of these simulations is 5440 km in the east-west (zonal) direction and 4064 km in the north-south (meridional) direction (Figure 2.3). This domain does not extend far north enough to cover the entirety of Manitoba, only going up to 57.336°N. Thus, the study area within the model that will be considered is from the international border (49°N) up to 55°N to avoid spurious results due to lateral boundary errors associated with limited area models (Almonte and Stewart 2019). The model uses an Arakawa-C grid, with 51 (50) staggered (non-staggered) levels in the vertical, topped at 50 hPa, which use a variable terrain-following coordinate system. The model output is hourly for the surface-based 2D variables, and every 3 hours for the 3D variables aloft. The period of the CTRL and PGW simulations is 13 years, from October 2000 to September 2013.

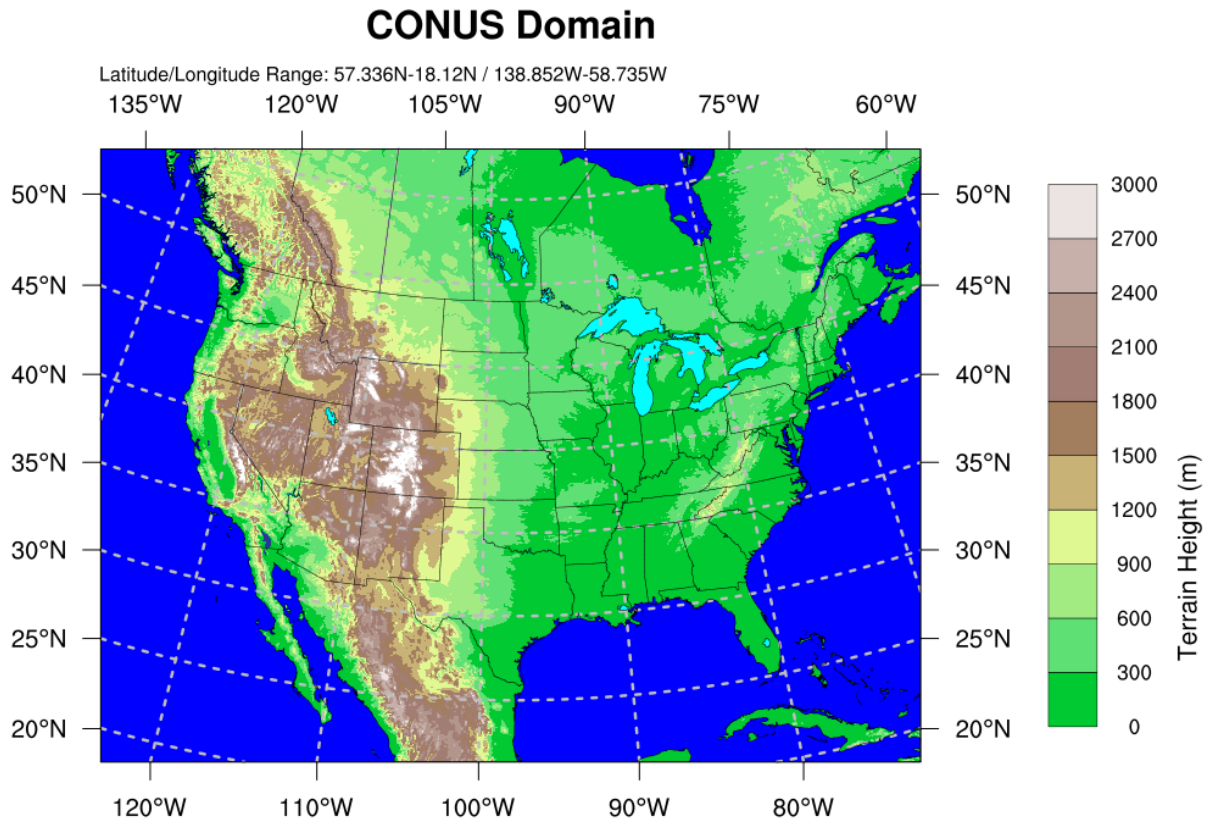

Figure 2.3: The domain of the WRF pseudo-global warming simulations. Contour colours indicate terrain height (m) within the model.

The WRF model's terrain field in Manitoba was used to relate the elevated terrain features, two example transmission projects, and areas of severe ice loading as defined by the Canadian Standards Association (2015). A combination plot of these is shown in Figure 2.4, which illustrates the co-location of the terrain and the severe icing areas.

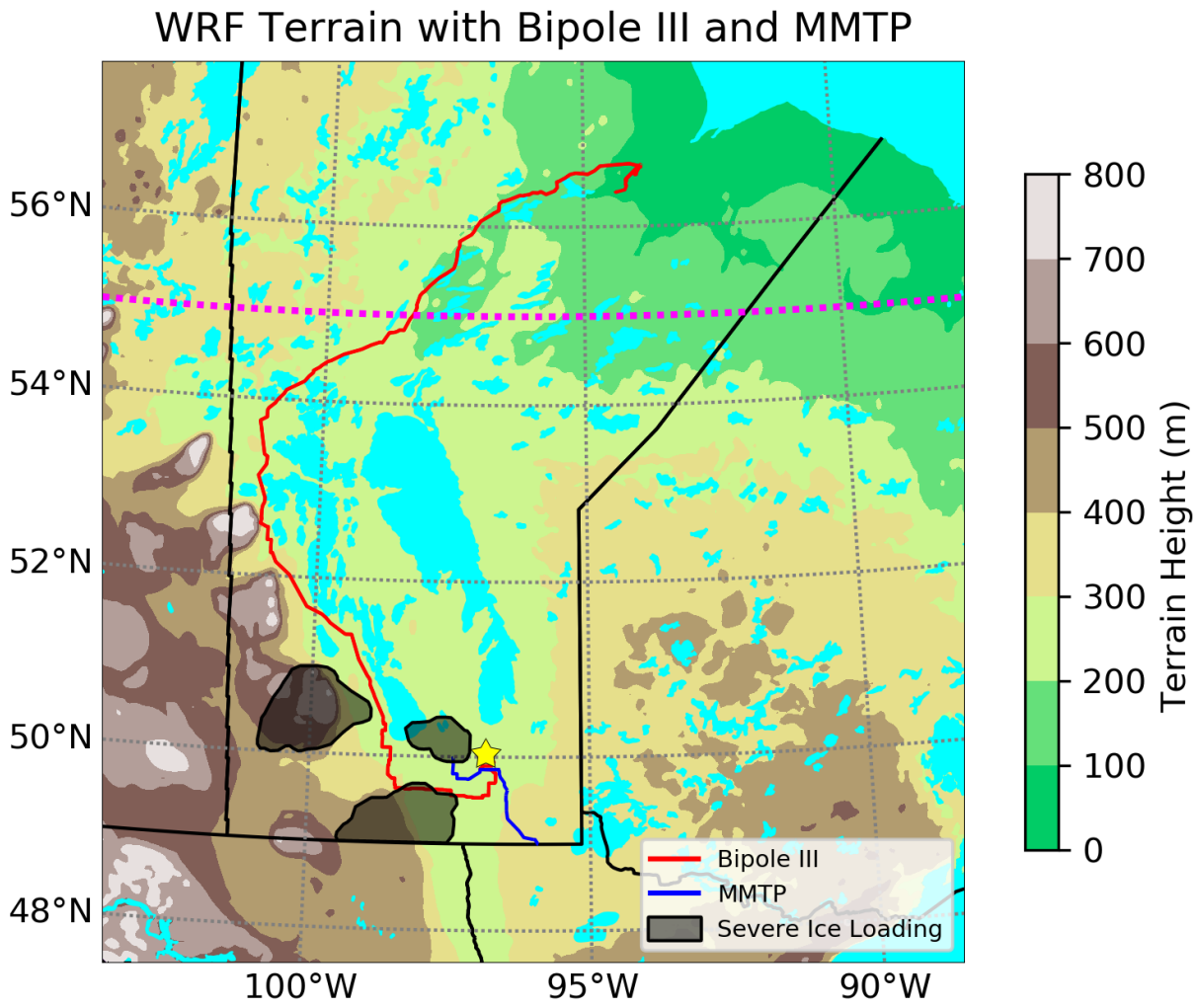

Figure 2.4: Map of the WRF terrain field, and approximate location of two example Manitoba Hydro transmission lines, and areas of severe ice loading. The coloured contours indicate the terrain height (m ASL), the red and blue lines indicate the locations of the Bipole III and MMTP lines respectively, and the shaded black areas indicate climatological severe ice loading as shown by the Canadian Standards Association (2015). The star indicates the location of Winnipeg. The dotted magenta line is 55°N latitude, the northern edge of the domain used in this thesis.

2.2.2. Microphysics: Thompson and Eidhammer (2014)

The microphysics scheme that is used by WRF in these simulations was developed by Thompson and Eidhammer (2014). This is an improved version of a bulk microphysics scheme developed by Thompson et al. (2008) which has been updated to include aerosols. These aerosols are modelled explicitly as cloud condensation nuclei (CCN) and ice condensation nuclei (ICN),

along with five types of water species: cloud water, cloud ice, rain, snow, and a hybrid graupel-hail category. The latter category is calculated by using a variable intercept parameter which is dependent on the mixing ratio of graupel and the amount of supercooled liquid water (Thompson et al. 2008). The addition of these aerosols allows for a more realistic treatment of cloud and ice particle nucleation, especially in mixed-phase clouds where the interactions between aerosols, droplets, ice, and hydrometeors is far more complex than in liquid only clouds. The aerosols are divided into two broad categories: hygroscopic (water friendly) and non-hygroscopic ice nuclei.

Tests of the scheme revealed that, in general, the scheme tends to represent aerosol theory well. In sensitivity experiments the simulations with more aerosols present created more numerous smaller drops, whereas the simulations with less aerosols had larger but fewer drops. Overall, the effect of aerosol inclusion on surface precipitation totals is modest, with statistically insignificant differences compared to observations. However, they did note that the aerosols tended to lead to the creation of more snow and less rain due to inhibited warm rain processes. The scheme underwent further testing in Liu et al. (2017), where they found the scheme performed favourably compared to observations, especially in the winter months.

An important consequence of this scheme is that it explicitly allows calculation of critical winter precipitation types. This output will be utilized later in section 2.5 in precise definitions. One caveat is that the scheme does not consider particles made up of two phases (liquid and solid). It therefore cannot directly consider precipitation types such as liquid core pellets and wet snow (Stewart et al. 2015). In the case of wet snow, for instance, it will convert the portion of snow that melts into liquid water as raindrops, a separate species of hydrometeor.

2.2.3. Pseudo-Global Warming Assumption

The pseudo-global warming simulation is a climate sensitivity and physics experiment, and is described by Rasmussen et al. (2011), Rasmussen et al. (2014), and Liu et al. (2017). The CTRL simulation is a retrospective re-analysis of the current state of the climate, using initial and boundary conditions from the ERA-interim reanalysis, forced every 6 hours:

$$CTRL = ERA\ Interim \tag{2.1}$$

PGW simulates a warmer climate by forcing CTRL with a climate perturbation. The perturbed fields include horizontal wind, geopotential, temperature, specific humidity, sea surface temperature, soil temperature, sea level pressure, and sea ice. This perturbation is the mean change signal from the Representative Concentration Pathway 8.5 (RCP 8.5) emission scenario, using a 19 member CMIP5 ensemble. This is the "business as usual" scenario, and its name refers to the additional 8.5 W m^{-2} net radiative forcing on the Earth's surface expected by the end of the 21st century:

$$PGW = ERA\ Interim + \Delta CMIP5_{RCP8.5} \tag{2.2}$$

where $\Delta CMIP5_{RCP8.5}$ is the 95-year CMIP5 multi-model ensemble-mean change signal using the RCP 8.5 emission scenario:

$$\Delta CMIP5_{RCP8.5} = CMIP5_{2071-2100} - CMIP5_{1976-2005} \tag{2.3}$$

This approach allows for the examination of existing events, and what these same events would look like in a warmer climate if they were to occur in the same area.

There are many advantages to this approach. While the spectral nudging used in CTRL generally keeps storm tracks generally the same, it does allow sub-synoptic flows to evolve naturally and dynamically with the perturbed thermodynamic and dynamic fields in the PGW simulation (Rasmussen et al. 2011; Rasmussen et al. 2014; Liu et al. 2017). This allows for the PGW simulation to depict changes in storm frequency and intensity, due to local scale feedbacks and mesoscale phenomena (Liu et al. 2017). This perturbation represents the difference between two CMIP5 model ensemble mean climates, which frees it from systematic GCM biases, and avoids the internal variability of GCM simulations (Liu et al. 2017).

However, there are disadvantages to this approach. As mentioned, the simulation constrains storm tracks via spectral nudging. As such, PGW represents a warmer future climate with the current weather pattern frequencies, and assumes that storm tracks will overall stay similar (Rasmussen et al. 2011; Rasmussen et al. 2014; Liu et al. 2017). Changes in the future frequency or paths of large scale disturbances/low pressure systems are thus not accounted for. Therefore, these simulations are not a robust prediction of exactly what the future climate will be, but rather present one scenario out of many (Rasmussen et al. 2011; Liu et al. 2017).

2.3. Japanese 55-year Reanalysis (JRA-55)

2.3.1. Description

For synoptic information, data from the Japanese 55-year Reanalysis (JRA-55) was utilized. This is a 6-hour global reanalysis covering the years 1958 to the present (Kobayashi et al. 2015). The reanalysis has a resolution of approximately 55 km, with 60 vertical levels topped at 0.1 hPa, and uses a semi-Lagrangian advection scheme. It was created using the TL319

version of the assimilation data system used by the Japanese Meteorological Agency (JMA), utilizing high quality data primarily from the ERA-40 observational dataset. It is an improvement of the prior Japanese 25-year Reanalysis, which utilizes advancements in the JMA numerical weather prediction capabilities (ie: introduction of 4D-Var analysis), which have greatly reduced the biases and improved the dynamical consistency.

However, some biases remain, such as a warm bias in the upper troposphere, a cold bias in the lower troposphere, excessive precipitation in the tropics, and a dry bias in regions of deep convection (Kobayashi et al. 2015; Kobayshi et al. 2019).

2.3.2. JRA-55 Products

Table 2.2: Summary of JRA-55 products. The product's full name, acronym/designation, and units are on the left. The usage for each of these products in this thesis is in the right column.

Japanese 55-year Reanalysis (JRA-55) Products	
Product	Usage
500 hPa height (dam) and strong wind (W500 ≥ knots)	Find upper disturbances, jet streaks, and attendant forcing for ascension
850 hPa wind (W850, m s^{-1})	Find moist low level jets, refining placement of atmospheric rivers
Integrated water vapor (IWV, kg m^{-2})	Determine overall moisture available to storms
Integrated vapor transport (IVT, kg m^{-1} s^{-1})	Locate atmospheric rivers
Equivalent condensation rate (ECR, mm day^{-1})	Find moisture convergence, areas of maximum precipitation potential from atmospheric rivers
Mean sea level pressure (MSLP, hPa)	Find centre of midlatitude cyclones driving these events, track their progress

The first JRA-55 product used is a 500 hPa height analysis (W500) in dam, which additionally has strong winds of ≥ 50 knots included. This is used to find upper level disturbances and jet streaks. Troughs in the pressure field provide the approximate location where storms are taking place and an indication of the strength and developmental stage of the storm, while the jet streaks mark areas of broad forcing for ascent.

The mean sea level pressure (MSLP) in hPa is a closely related product that gives further insight into the developmental stage of a cyclone, and a more precise idea of what areas at the surface are being affected. It provides the ability to track the path of any storm with more precision.

The winds at the 850 hPa level (W850) in m s^{-1} are used primarily to locate any low level jets.

The equivalent condensation rate (ECR) in mm day^{-1} is the convergence of integrated water vapour flux, and is defined by the maximum possible contribution of the moisture flux convergence to precipitation (Smith 2019). It is useful to infer where the maximum potential precipitation induced from an atmospheric river is, and the total amount.

Integrated vapour transport (IVT) in kg m^{-2} represents the transport of water vapour through the depth of the atmospheric column, and is used to locate atmospheric rivers. An atmospheric river is defined by the American Meteorological Society Glossary of Meteorology (2019) as:

> "A long, narrow, and transient corridor of strong horizontal water vapor transport that is typically associated with a low-level jet stream ahead of the cold front of an extratropical cyclone. The water vapor in atmospheric rivers is supplied by tropical and/or extratropical moisture sources. Atmospheric rivers frequently lead to heavy precipitation

where they are forced upward—for example, by mountains or by ascent in the warm conveyor belt. Horizontal water vapor transport in the midlatitudes occurs primarily in atmospheric rivers and is focused in the lower troposphere. Atmospheric rivers are the largest "rivers" of fresh water on Earth, transporting on average more than double the flow of the Amazon River."

It is integrated from the surface to 300 hPa, using a relation shown in Smith (2019):

$$IVT = g^{-1} \int_{Ps}^{Pt} qV_h dp \tag{2.4}$$

where g is gravitational acceleration (9.8 m s^{-2}), P_s is the surface pressure in hPa, P_t is the top of the atmosphere at 300 hPa, q is the specific humidity of water vapour, V_h is the horizontal transport vector using zonal (u component) and meridional (v component) winds.

Lastly, integrated water vapour (IWV) in kg m^{-2} is the mass of all the water vapour through the depth of the atmospheric column. This is used to provide an estimate of how much water vapour is available to a storm at any one location and time.

2.4. Observational Meteorological Data

This study also makes use of non-model data to provide a baseline of the events and evaluate the model results. Surface weather observations were provided by both Manitoba Hydro and Environment and Climate Change Canada (ECCC), whereas the operational surface and upper air analysis maps and gridded precipitation data were provided solely by ECCC.

2.4.1. Surface Observations

Surface weather observations from Manitoba Hydro were a baseline first guess to help identify the approximate date and type of precipitation and hazards experienced during any freezing precipitation event, which are provided by their own personnel in the field. Note that these observations may differ from the official ECCC ones.

Surface weather observations from ECCC are used to evaluate as many of the events and data from the model as possible. The hourly observations used for evaluation are temperature, relative humidity, wind speed, and wind direction.

2.4.2. Global Environmental Multiscale Analysis Maps

Operational weather analysis maps from ECCC's Global Environmental Multiscale (GEM) model (ECCC 2010) were used to evaluate the dynamical flows within WRF CONUS. The analyses include 500 hPa height, mean sea level pressure, 700 hPa height, and 850 hPa height. Primarily, these analyses were checked against the WRF mean sea level pressure field and 10 meter (surface) winds for congruency, ensuring a reasonably accurate simulation.

2.4.3. Canadian Precipitation Analysis

Data from the Canadian Precipitation Analysis (CaPA) were used to further evaluate the WRF CONUS simulations. CaPA is a gridded composite dataset in GRIB2 format produced by ECCC (ECCC 2019b) and originally described by Mahfouf et al. (2007). It represents a best estimate of 6 and 24-hour precipitation by integrating observational precipitation gauge

measurements, radar quantitative precipitation estimates, and numerical model data (ECCC 2019b). These data are combined in near real time, and uses a statistical interpolation that allows for continuous coverage (ECCC 2016) of 2 differently sized domains and resolutions.

The first configuration is the Regional Deterministic Precipitation Analysis (RDPA), which has the same domain as the Regional Deterministic Prediction System (RDPS) model and has a 10 km resolution. The second configuration is the High Resolution Deterministic Precipitation Analysis (HRDPA), which shares the domain of the High Resolution Deterministic Prediction System (HRDPS) model and has a 2.5 km resolution (ECCC 2019b). One of the key advantages of this dataset is that it provides coverage across the entire country, despite the sparsity of northern observing stations.

Overall, the performance of CaPA is good across the domain, differing seasons, and times of day. However, uncertainties still exist regarding winter and mountainous precipitation, and performance is lesser during summer due to difficulties in producing convective precipitation (Smith 2019). There is a negative bias in winter due to issues associated with measuring solid precipitation, and some authors have found a positive (negative) bias for events with < 2 mm (> 5 mm) (Smith 2019).

2.5. Definitions of Freezing Precipitation

The occurrence of freezing rain, wet snow, and mixed precipitation must be defined. These definitions follow those used by Almonte and Stewart (2019) and they are summarized in Table 2.3. They apply to ECCC surface data, as well as at 2 height levels in WRF: the 2 m surface temperatures (T2) and the ~23-24 m lowest model level temperatures (TK).

Table 2.3: Summary of criteria for freezing precipitation types and mixtures. Check marks indicate when the 0.2 mm criterion was satisfied. A wet-bulb temperature criterion ≤ 0°C was used to exclude rain and wet snow (blue), whereas a criterion > 0°C was used to exclude freezing rain (orange).

Freezing Precipitation Types and Mixtures				
Type or Mixture	**Constituent Precipitation**			
	Snow	Rain	Graupel	Freezing Rain
Freezing Rain	✘	✘	✘	✔
Freezing Rain, Snow	✔	✘	✘	✔
Freezing Rain, Snow, Graupel	✔	✘	✔	✔
Freezing Rain, Graupel	✘	✘	✔	✔
Wet Snow	✔	✘	✘	✘
Wet Snow, Rain	✔	✔	✘	✘
Wet Snow, Rain, Graupel	✔	✔	✔	✘
Rain, Graupel	✘	✔	✔	✘

Freezing precipitation can occur as one type or as a mixture of types. In particular, freezing rain is defined as occurring if the wet bulb temperature is ≤ 0°C, and there is ≥ 0.2 mm of liquid precipitation. Wet snow is defined as occurring if the wet bulb temperature is > 0°C, and there is ≥ 0.2 mm of snow. Mixtures can occur if all of the constituent types are individually ≥ 0.2 mm.

An important issue to note is that wet snow can actually still occur when the wet-bulb temperature is < 0°C and these occurrences are therefore not considered here, which falls outside of these definitions. There are 4 different ways to produce wet snow, as described by Stewart et

al. (1990) and Stewart (1992), with only one having that has to occur at > 0°C. For this thesis, only wet snow at > 0°C can be considered in the WRF simulations, since the microphysical parameterizations do not account for mixed phase snow particles.

The minimum threshold for precipitation is defined as ≥ 0.2 mm h^{-1} because the WRF precipitation data is hourly and ≥ 0.2 mm is the minimum detectable amount of precipitation according to ECCC standards (Environment and Climate Change Canada, 2019a). Anything less is considered "trace" precipitation (Environment and Climate Change Canada, 2019a). It should be noted that using this 0.2 mm threshold may result in the underestimation of the number of occurrences of precipitation (Almonte and Stewart 2019).

The 2 m surface temperature is used because it represents how the precipitation will be experienced by society in general. As well, 2 m is the standard height at which surface observing stations measure temperature, which allows for comparisons and evaluation between WRF and observations from ECCC.

The lowest model level (~23-24 m) temperature is used because this thesis has a focus on the impacts of these events on Manitoba Hydro's infrastructure. The network of distribution lines, 66 kV and below, are of particular interest within Manitoba. Conductors for these lines typically range from 8m to 15m above the ground surface depending on the line configuration and structure (M. Vieira and M. Peckover 2019, personal communication). Therefore, the lowest model level height of ~23-24 m was deemed appropriate, because any freezing precipitation occurring at this level may interact with the power lines, but if it occurs only at 2 m it may not affect these lines.

The reason that the lowest model level height is not an exact number, and is only approximately (~) 23-24 m is because the model uses a hydrostatic terrain-following coordinate system, which creates variation in the height of this layer.

The mean height of this layer was determined by computing the mean height of the mass point (θ), which is the point at the centre of each Arakawa-C grid cell where thermodynamic and mass variables are stored. To derive it, the 3-hourly 3D WRF geopotential height variable (H, in this equation) was used to find the geometric height above sea level (z) of the first 2 staggered layers, which form the bottom and top of the 1st grid cell, using the following relation from Stull (2011a):

$$z = R_0 \cdot H/(R_0 - H) \tag{2.5}$$

where R_0 is the mean radius of the Earth (6,356,766 m) and H is the geopotential height in metres. This value was then divided by 2, which is the midpoint of the grid cell, and the geometric height above sea level (ASL) of the mass point. Subtracting the WRF terrain height value (HGT) from this number yields the geometric height above ground of the mass variable.

The height of this layer was averaged across all event years of the CTRL simulation in the dataset: 2000, 2004, 2005, 2006, and 2012 and the results are shown in Figure 2.5. The mean lowest model level height exhibits approximately 1 meter of rise across the province, with 23 m at the extreme northeastern tip, and 24 m across the majority of the south with patches above 24 m near the U.S. border. The height of the layer is slightly lower at 23.6-23.8 m in the west above the elevated terrain of the province.

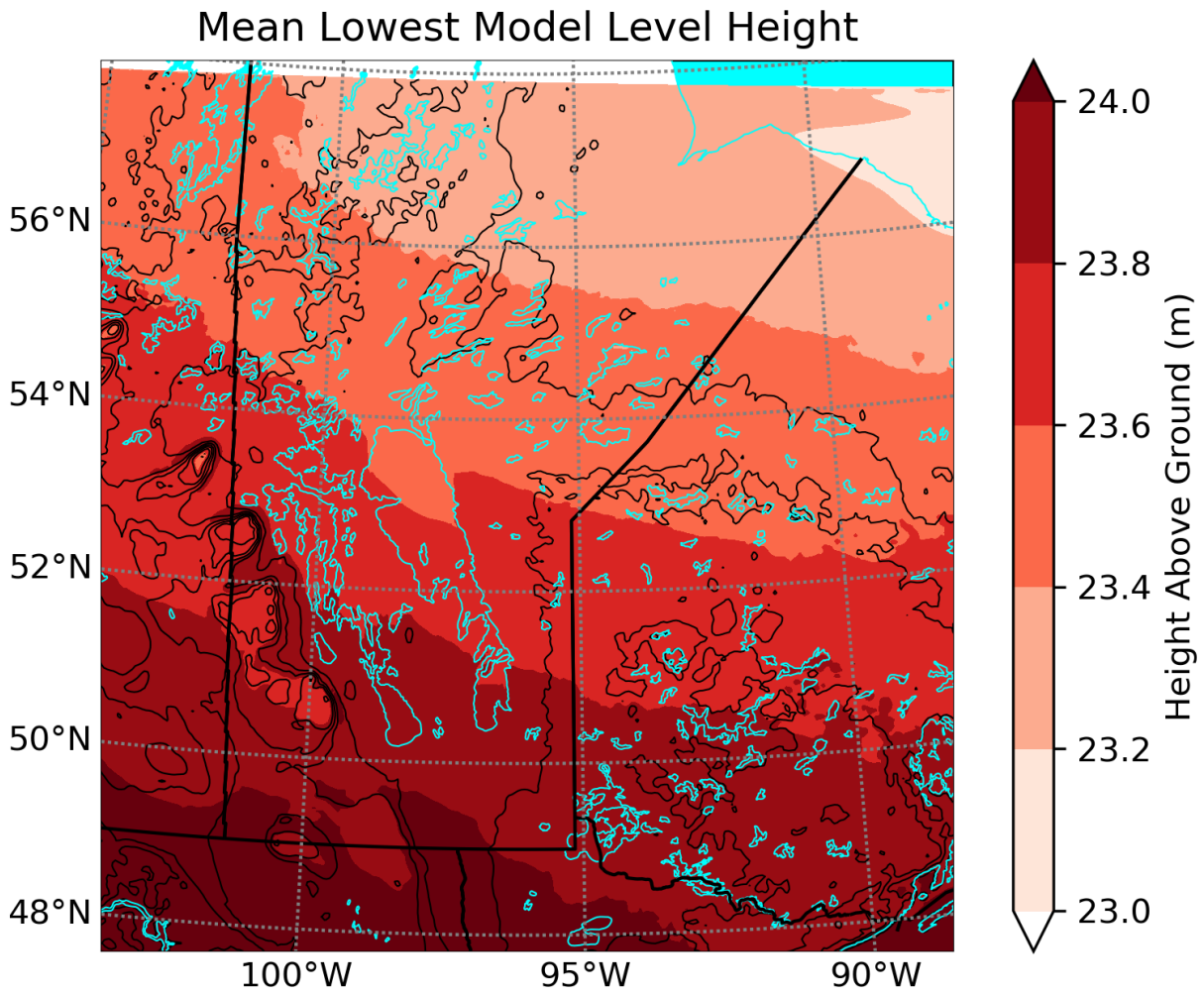

Figure 2.5: The mean height of the lowest model level for years 2000, 2004-2006, and 2012 in the CONUS simulations in Manitoba. Contour colours indicate the geometric height above the ground (m).

The wet bulb temperature is used in the criteria because it provides a threshold for phase change. Hydrometeors fall below the cloud into a layer of sub-saturated air and, through evaporation, they tend to cool to the wet bulb temperature.

However, the wet bulb temperature is not a built-in product of the WRF CONUS dataset, and must be derived. To calculate it, both the lowest model level temperature (TK) and the 2 m temperature (T2), total pressure (P), and mixing ratio of water vapour (QVAPOR) were used with a relatively recent empirical formulation in Stull (2011b), shown below:

$$T_w = T \times atan(0.151977(RH + 18.313659)^{1/2}) +$$
$$atan(T + RH) - atan(RH - 1.676331) + \quad (2.6)$$
$$0.00391838(RH^{3/2} \times atan(0.023101 \times RH) - 4.686035$$

where T is temperature in °C and RH is the relative humidity in percent. Relative humidity is also not provided as a WRF CONUS product, however it can be derived using the National Center for Atmospheric Research (NCAR) Python module called wrf-python, using the "wrf.rh" computational algorithm.

A final important note regarding temperature and these criteria is that WRF has a much higher level of precision for temperature compared to observations. Observations reported by ECCC are reported to either a whole degree Celsius or one tenth degree, which is in accordance with international standards (World Meteorological Organization 2017). Therefore, to maintain consistency between the model and observations, all WRF wet-bulb temperatures will be rounded to the nearest tenth of a degree.

2.6. Analysis Approach

To meet the first sub-objective and characterize the events and the driving factors behind them, a top-down approach was used. Firstly, the large scale/synoptic factors that generated these freezing precipitation events were analyzed. Using the JRA-55, broad flow patterns were considered to determine which are generally favourable to these events over their duration.

Next, the WRF CTRL simulations were used to characterize the freezing precipitation events. This includes plotting the total accumulated amounts of freezing precipitation, as well as

the number of hours of this precipitation that occurred. The overall maximum extent of the event will be considered, as well as the location of the area of maximum precipitation accumulation and duration.

The WRF CTRL simulations were also used to identify local factors that contributed to these freezing precipitation events. Given the association of freezing precipitation with proximity to terrain and large water bodies, the events were examined to determine if terrain interaction in the western portion of the province was taking place, as well as if any lake effect precipitation was occurring via lakes Winnipeg or Manitoba.

To determine which events were affected by terrain, the accumulation and duration of freezing precipitation were plotted against the terrain field within WRF. This was simply to check for spatial correlation between the distribution of the freezing precipitation and the terrain. To further infer terrain interaction in these events, the lowest available wind (U10, V10) at 10 m and temperature at 2 m were plotted against the terrain field in the WRF model, alongside the vertical wind component (W) at 10 m. This allows the large scale visualization of air flowing toward, against, around, as well as ascending (descending) the elevated terrain in Manitoba, and the subsequent cooling (warming) that occurs due to upslope (downslope) flow. In the cases in which it was apparent that the freezing precipitation and wind were interacting with the terrain, vertical cross sections of the terrain, precipitation, temperature, and winds were plotted to visualize this interaction from another more detailed angle. Another benefit of plotting these vertical cross sections is that it allows for very clear visualization of any atmospheric temperature inversions aloft that may be playing a role in the formation of freezing precipitation.

Finally, another important aspect of these events is the associated winds. They are an important factor in the force and stresses exerted on infrastructure and vegetation. The speed of

the wind during and after an event is important, but so is the angle at which the winds intersect. For example, winds striking power lines at a normal (90º) direction will exert far more force than those intersecting the line at a lesser angle. To describe the winds, they were plotted in a time series alongside various other thermodynamic properties which were used to describe event characteristics. In addition, scatter plots of the U and V components of the wind were made to determine the predominant directionality and strength of the wind during any given event.

To address the second sub-objective, the PGW simulations were utilized in a similar manner to the CTRL simulations. Firstly, the number of hours of freezing precipitation and the total accumulation for each event was found and compared to that of CTRL. Any changes in spatial extent and overall severity of the events can be determined by these metrics. Any events in CTRL found to have terrain interaction involved in the precipitation were examined in the same way in PGW, to determine if this factor remained the same. Finally, the wind speeds during and after the events was examined to determine if the speeds and directions changed.

3. Selected Freezing Precipitation Events

3.1. Event List

To address the objectives of this thesis, Manitoba Hydro identified a sample of 10 events with freezing rain and/or wet snow which impacted their operations (Table 3.1). These were identified in response to a regulator's inquiry to Manitoba Hydro (M. Vieira 2019, personal communication).

Table 3.1: A sample of events which had freezing rain and/or wet snow which impacted Manitoba Hydro. The approximate date(s) of the event is shown in the left column, while the hazards associated with it are in the right column.

Event List with Hazards	
Date	**Hazards**
April 27, 1984	Rain, freezing rain, ice pellets
November 6-12, 2000	Rain, wet snow, ice pellets, strong wind
May 11, 2004	Heavy rain, snow, strong wind
October 5, 2005	Wet snow, strong wind
December 14-19, 2005	Snow
December 28, 2005	Snow, rain
January 12-18, 2006	Mostly snow, some rain
October 13, 2006	Wet snow, freezing rain, strong wind
October 4-5, 2012	Rain, wet snow
March 8, 2017	Wet snow

These events were provided with an approximate date range and general area where they occurred, and the hazards associated with that event. It is important to note that many of the events had several types of precipitation, either at the same time or in sequence. As well, events that featured strong winds either during or shortly after the event were identified. Each of these 10 events will be examined to determine what factors led to its occurrence as well as its future features, which will be done systematically according to the methodology outlined in section 2.6.

3.2. Event Time Periods

Before any analysis of the events, they must first be described discretely by defining a precise starting and ending times. The dates given in the initial event list were approximated by Manitoba Hydro. For each event, the dates are mainly focused on the impacts of the hazardous precipitation to infrastructure, and not the meteorology. There is not necessarily hazardous precipitation occurring across the entire date range for each event, and it is possible that hazardous precipitation preceded or followed these dates by 24 hours or more.

Therefore, the CONUS CTRL simulation was used to determine when the precipitation in the events started and stopped exactly, down to an hourly level. The simulation was checked every hour for freezing precipitation and mixtures occurring in Manitoba within and beyond these dates, using several 2D (surface) WRF variables in the surface-based temperature approach, described in Section 2.4.

The methodology for determining the meteorological length of the event within the model is as follows. The date(s) provided by Manitoba Hydro were used as a starting estimated

date range, using all 24 hours of data (from 00 UTC to 23 UTC) for each day in the CTRL simulation.

The start of the event is defined as the first hour (00 UTC) of the first day in the range of days for each event, unless there is already freezing precipitation/mixtures occurring in Manitoba. If they are already occurring at 00 UTC, then time is regressed in 1 hour increments to the hour where the precipitation begins.

The end of the event is defined as the last hour of the last day in the range of days for each event (23 UTC), unless freezing precipitation/mixtures are still occurring at this hour in Manitoba. If they are occurring at this time, then time is advanced forward in 1 hour increments up to and including the last hour where they occur.

In addition, it is desirable to determine if the PGW version of these events have a differing time frame from the CTRL time frame. Although it is useful to directly compare the same time frame between CTRL and PGW, such a comparison partially misses events that begin earlier or persist longer within the PGW simulation. To sufficiently capture these early or extended events, the same treatment was given to the PGW simulation.

The event lengths that were determined using this methodology are shown in Table 3.2. Duration varies greatly from 26 hours up to 228 hours in the longest cases, though it is important to note that these durations are not continuous hours of freezing precipitation/mixtures. The precipitation often comes in waves on separate days; some days have a large amount of precipitation whereas others only have slightly more than trace amounts. More specific spatiotemporal information on event duration can be found in Section 5.2.

Table 3.2: Summary of the length of the events within WRF. The Manitoba Hydro approximate date of the event is the left column, and the length of the event for CTRL and PGW simulations are in the middle and right columns, respectively. Sub-columns indicate the start and end date and time in UTC, and total hours of the events.

Event Length						
Event	**CTRL**			**PGW**		
	Start	End	Hours	Start	End	Hours
November 6-12, 2000	Nov 6 00 UTC	Nov 12 23 UTC	168	Nov 5 14 UTC	Nov 13 16 UTC	195
May 11, 2004	May 11 00 UTC	May 13 03 UTC	52	May 11 00 UTC	May 11 23 UTC	24
October 5, 2005	Oct 5 00 UTC	Oct 6 10 UTC	34	Oct 5 00 UTC	Oct 6 01 UTC	26
December 14-19, 2005	Dec 13 12 UTC	Dec 19 23 UTC	156	Dec 13 12 UTC	Dec 19 23 UTC	156
December 28, 2005	Dec 27 11 UTC	Dec 28 23 UTC	36	Dec 28 00 UTC	Dec 29 01 UTC	24
January 12-18,2006	Jan 11 22 UTC	Jan 18 23 UTC	170	Jan 11 22 UTC	Jan 18 23 UTC	170
October 13, 2006	Oct 11 22 UTC	Oct 14 02 UTC	53	Oct 13 00 UTC	Oct 14 06 UTC	31
October 4-5, 2012	Oct 3 04 UTC	Oct 6 00 UTC	69	Oct 4 00 UTC	Oct 5 23 UTC	48

4. Evaluation of WRF CTRL

The WRF output was compared against observations for the 10 events for any times that data were available. Comparisons were made between the output, surface weather stations, archived radar data, and an operational climate model when possible. The 2 m temperature and the 10 m wind variables are used for this comparison, due to these heights being compliant with the measurement standards followed by ECCC (ECCC 2019c), as established by the World Meteorological Organization (WMO) (World Meteorological Organization 2017).

Collectively, WRF was able to reasonably simulate key aspects of these events. The output was previously evaluated by Liu et al. (2017) who found that the simulations were able to capture the spatiotemporal patterns of sub-seasonal, seasonal, and annual precipitation and temperature across most of the domain. Overall spatial correlation between WRF and the Parameter-elevation Regressions on Independent Slopes Model (PRISM) network used for evaluation of precipitation ranged between 0.68 and 0.987. Liu et al. (2017) further noted that the model exhibits skill in simulating western orographic precipitation. They also noted some weaknesses in that it under-predicts summertime Midwest convection and annual precipitation in the southeast, but overestimates the summer-fall southwest precipitation.

They also noted a warm temperature bias exists year-round, and is worst in the central US and summer, while there is a significant winter-spring cold bias over snowy peaks and near the Great Lakes. Overall temperature spatial correlation ranged between 0.962 and 0.989 (Liu et al. 2017). These biases extend up to the Manitoba border in all cases. Seasonally, the precipitation bias is positive in the winter and spring (30-60 mm, ~50% difference), and is negative in fall and summer (15-90 mm, ~30% difference). The temperature warm bias is strongest in spring (~2-3°C), and the strongest cold bias is in winter (~3-4°C).

4.1. Evaluation Against GEM

The WRF was evaluated against the operational GEM model to determine if it was able to reasonably represent the low level dynamics of these events. Primarily, this means comparing the WRF surface winds to the GEM mean sea level pressure field, though all of the available GEM products are available in Appendix B. Considering the use of spectral nudging in these simulations, flows are expected to be well behaved overall. The product used for this purpose was the mean sea level pressure, which was used to infer the surface wind flow fields in WRF, while the other products were used as a secondary source of evaluation of the overall flow when appropriate.

An example of a comparison between the WRF and GEM is in Figures 4.1 and 4.2, where it can be seen that the direction and overall pattern of the WRF surface winds are in line with the surface pressure pattern in GEM.

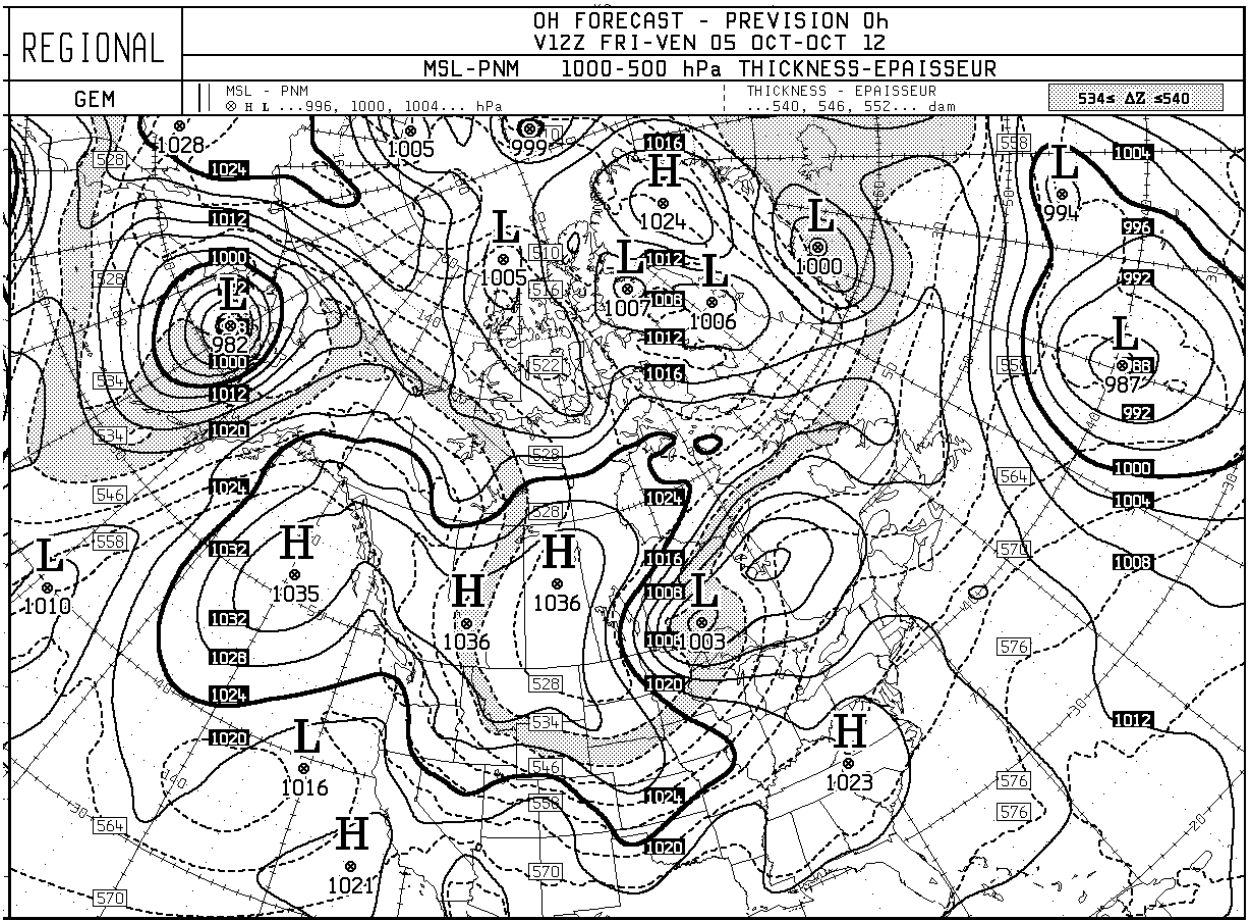

Figure 4.1: GEM analysis of mean sea level pressure and 500 hPa thickness for 5 October, 2012 12 UTC. The solid black contours indicate mean sea level pressure (hPa), while the dashed black contours indicate 1000-500 hPa thickness (dam). The strong low pressure centre in the middle of the image is just east of Manitoba in Ontario at this time.

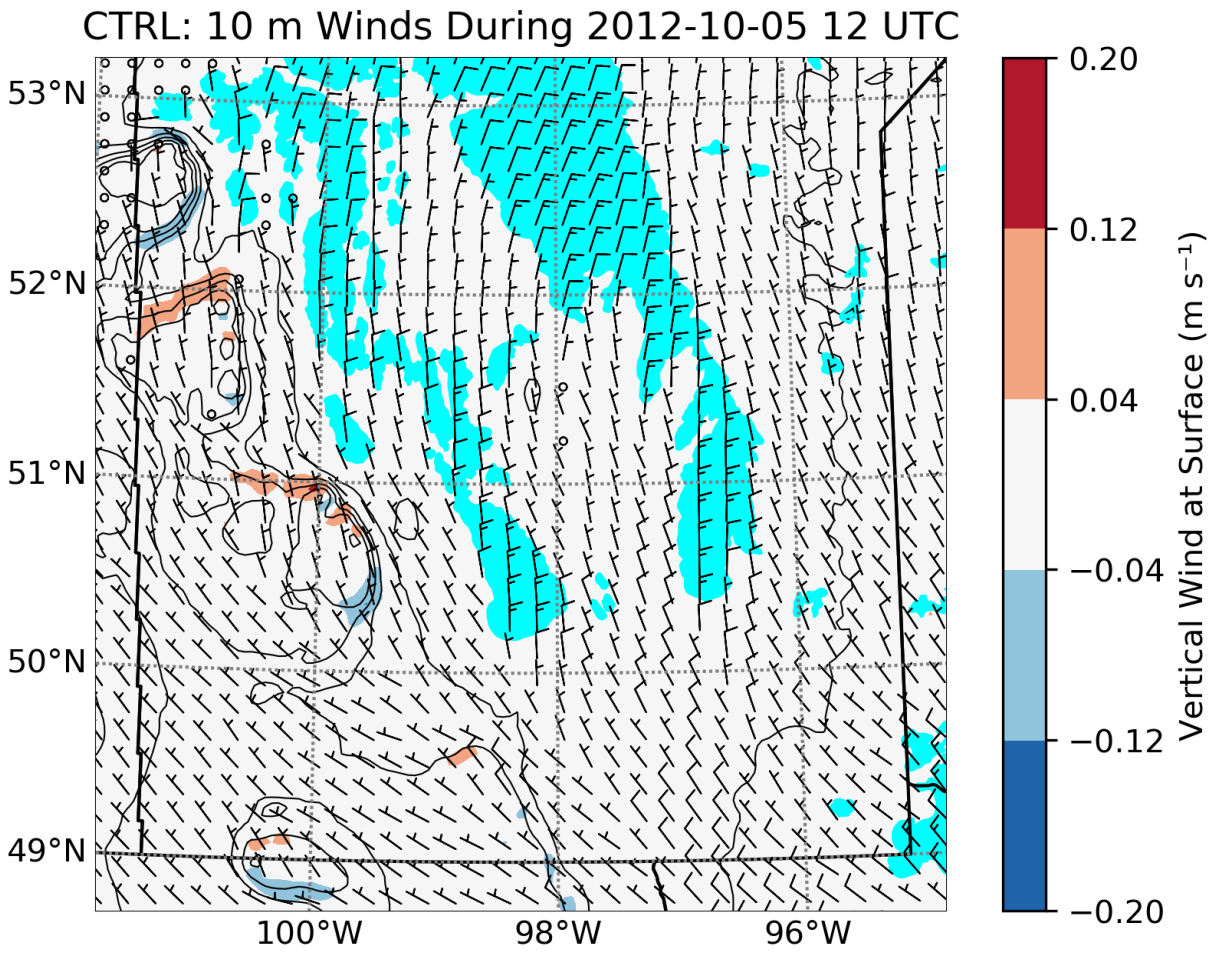

Figure 4.2: WRF 10 m horizontal winds and vertical wind component in the CTRL simulation on 5 October, 2012 12 UTC. The wind barbs represent the 10 m wind speed and direction in m s^{-1}, while the coloured contours indicate the speed of the vertical wind component (W) at the lowest model level in m s^{-1}.

4.2. Evaluation Against CaPA

A total of 6 of the 8 events in the WRF period had CaPA data available for evaluation, which were the events from 2004, 2005, and 2006. The daily accumulated precipitation from CaPA was compared to that of WRF, using a selection of days that covers the entire duration of the event as defined in Table 3.2. These daily accumulations were summed to determine the total event accumulation. The CaPA archive used for this comparison can be found here:

http://collaboration.cmc.ec.gc.ca/science/outgoing/capa.grib/hindcast/capa_hindcast_v2.4/24h/

Overall, WRF performed well for most of the events. The morphology and timing of the precipitation in the storms was captured very well, with major bands/areas of precipitation being closely co-located with CaPA (Figure 4.3). The areas of maximum precipitation also compared well, but were often in slightly different areas and sometimes had slightly higher amounts to that of CaPA (Figure 4.4).

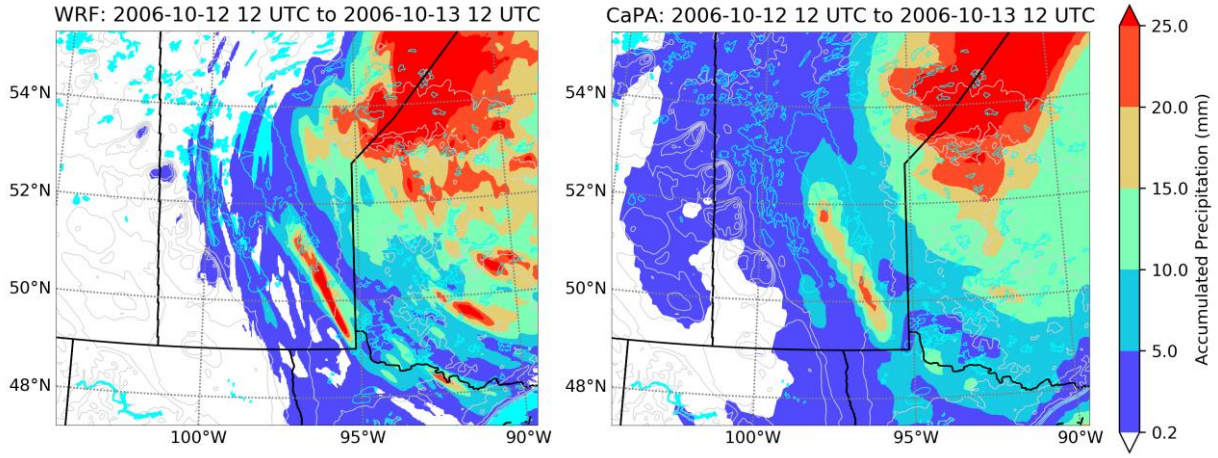

Figure 4.3: Comparison of WRF and CaPA accumulated precipitation for the October 13, 2006 event, between October 12 12 UTC and October 13 12 UTC.

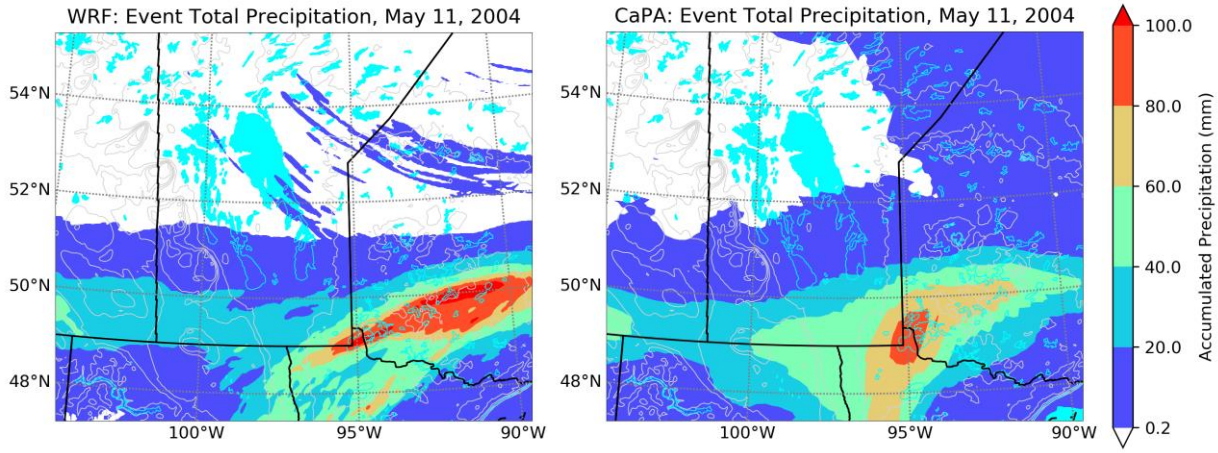

Figure 4.4: Comparison of WRF and CaPA event total accumulated precipitation for the May 11, 2004 event (May 10 12 UTC to May 12 12 UTC). Note that in WRF the area of maximum precipitation is extended to the east into Ontario, and the higher accumulation.

An aspect of the comparison that wasn't as favourable was that, in almost all events, WRF consistently under-predicted the spatial extent of lower precipitation accumulation areas (Figure 4.5). While an extreme example was chosen here, most of the cases did not illustrate this discrepancy. There is some value in this, however, because it means that the WRF simulations are a conservative representation of hazardous precipitation. It can be considered a best case scenario, while the reality may be more hazardous.

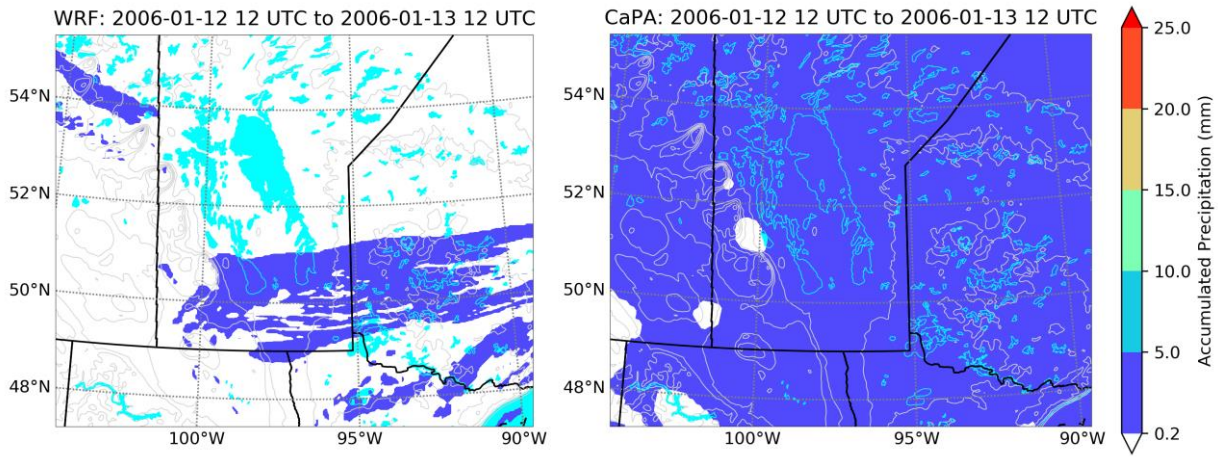

Figure 4.5: Comparison of WRF and CaPA accumulated precipitation from the January 12-18, 2006 event, between January 12 12 UTC and January 13 12 UTC.

The differences between WRF and CaPA are likely due to model resolution, assumptions, and microphysics. WRF is much higher resolution at 4 km, while CaPA uses 10 km model data as one of its data sources. This would explain the more highly detailed convective cells imbedded in the overall storm in WRF. The WRF is non-hydrostatic, meaning it explicitly models convection, while the model used in CaPA is not. Finally, WRF frequently under-predicting lesser amounts of precipitation may be due to the inclusion of aerosols in its microphysics, which have a tendency to reduce this.

4.3. Evaluation Against Surface Observations

WRF CTRL output was compared against observations of temperature, moisture, and wind speed/direction from several surface ECCC stations (Figure 4.6). The stations used for this comparison were chosen due to their approximate homogenous spacing, and/or because they are in a large population centre or near elevated terrain.

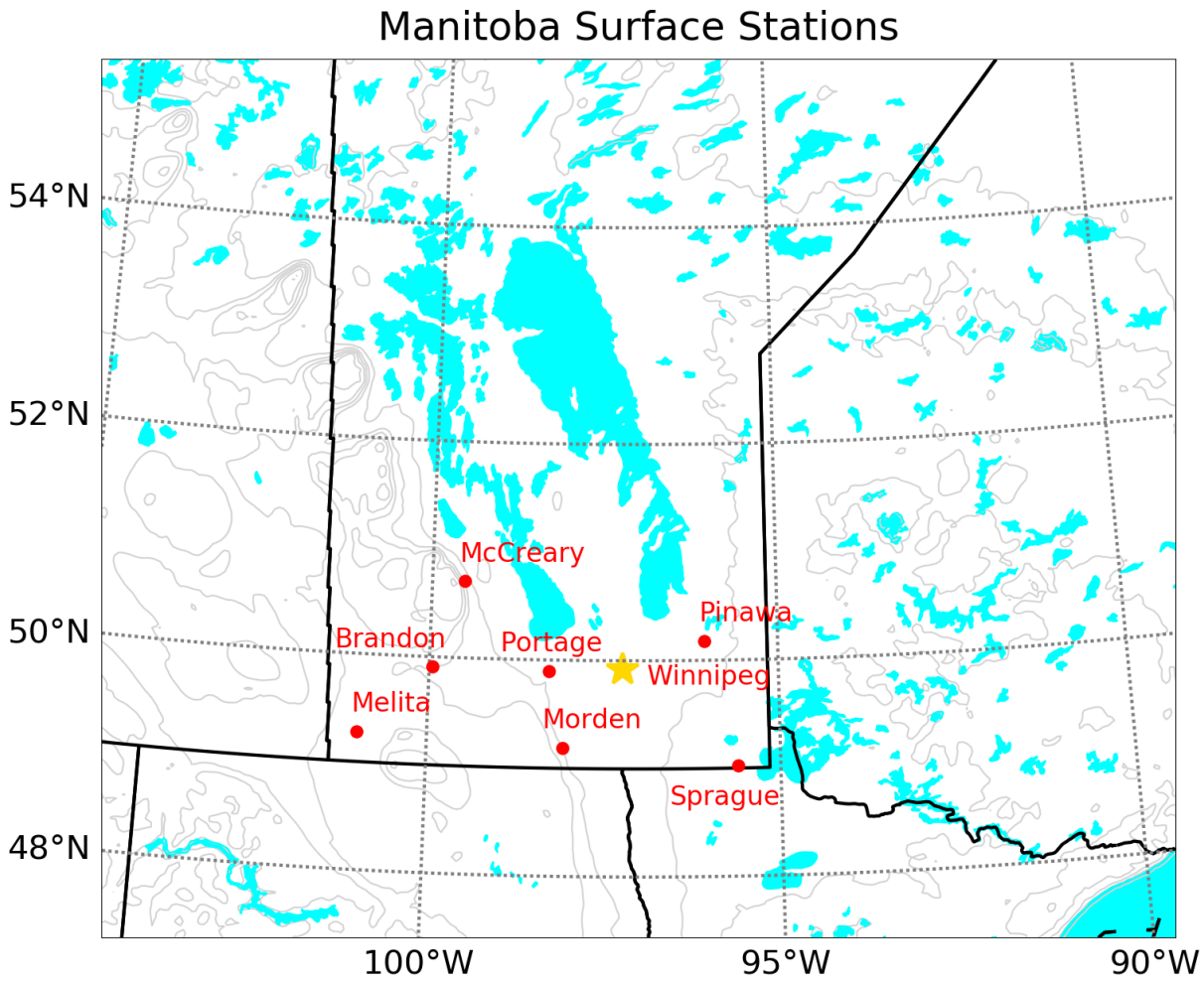

Figure 4.6: Stations in Manitoba used for evaluation of WRF CTRL output.

An evaluation was first made of event mean (Table 4.1) and maximum (Table 4.2) 2 m temperature, relative humidity, and winds at these locations. It is apparent that WRF was able to

generally simulate these parameters, although there were several pervasive relatively small biases, as well as isolated cases of larger biases which occurred during the events that persisted for approximately a week. The biases occurred in both positive and negative directions, but were predominantly negative.

Table 4.1: Mean 2 m temperatures (°C) in the WRF CTRL simulation and from ECCC surface observations, as well the difference between them (WRF-ECCC). The values in each cell are (from top to bottom) the temperatures for WRF, ECCC, and the difference. All values were rounded to 1 decimal place. N/A indicates there was missing data.

Station	**Event**							
	Nov 6-12, 2000	**May 11, 2004**	**Oct 5, 2005**	**Dec 14-19, 2005**	**Dec 28, 2005**	**Jan 12-18, 2006**	**Oct 13, 2006**	**Oct 4-5, 2012**
Melita	14.7 -8.6 -6.1	2.3 0.2 2.0	2.7 0.2 2.5	-17.6 -12.6 -5.0	-0.4 -2.7 2.4	-6.6 -4.8 -1.7	-0.5 -0.1 -0.4	2.7 2.7 0.0
Brandon	-13.1 -6.9 -6.2	1.6 0.7 1.0	2.3 0.8 1.5	-18.4 -13.4 -5.0	-2.5 -3.1 0.6	-10.7 -7.3 -3.5	-0.6 -0.2 -0.4	2.7 3.0 -0.3
McCreary	-11.8 -8.1 -3.6	2.3 1.2 1.0	2.4 1.5 0.9	-15.8 -12.3 -3.5	-4.0 2.3 -1.7	-11.9 -8.3 -3.7	-0.3 0.9 -1.2	2.8 2.7 0.1
Portage Southport	-12.1 4.7 -7.4	1.9 0.7 1.3	2.8 2 0.8	-17.5 -11.7 -5.8	-2.6 -1.9 -0.7	-11.8 -6.7 -5.1	-0.1 1.1 -1.2	4.0 3.6 0.4
Morden	-10.4 -3.9 -6.5	2.2 1.1 1.1	2.1 1.5 0.7	-16.0 -11.0 -5.0	-1.5 -1.4 -0.1	-9.6 -5.5 -4.1	0.3 1.3 -1.1	4.0 3.5 0.5
Winnipeg Airport	-9.2 -2.1 -7.1	2.7 1.2 1.5	3.1 N/A N/A	-16.4 -10.6 -5.8	-2.7 -1.7 -1.0	-12.0 -7.2 -4.7	0.9 1.1 -0.2	5.0 N/A N/A
Pinawa	-5.3 0.4 -5.7	1.2 0.5 0.7	1.8 1.6 0.2	-13.3 -9.6 -3.6	-3.0 -1.8 -1.2	-11.2 -8.9 -2.3	-1.4 -1.2 -0.1	3.3 3.3 0.0
Sprague	-1.1 0.9 -2.1	1.9 1.9 0.0	1.8 2.9 -1.1	-13.2 -9.8 -3.4	-1.8 -2.3 0.5	-10.3 -7.4 -2.9	-1.2 -1.3 0.1	3.6 N/A N/A
Mean Difference	-5.9	1.1	0.8	-4.6	-0.2	-3.5	-0.6	0.1

Table 4.2: Maximum 2 m temperatures (°C) in the WRF CTRL simulation and from ECCC surface observations, as well the difference between them (WRF-ECCC). The values in each cell are (from top to bottom) the temperatures for WRF, ECCC, and the difference. All values were rounded to 1 decimal place. N/A indicates there was missing data.

Station	**Event**							
	Nov 6-12, 2000	**May 11, 2004**	**Oct 5, 2005**	**Dec 14-19, 2005**	**Dec 28, 2005**	**Jan 12-18, 2006**	**Oct 13, 2006**	**Oct 4-5, 2012**
Melita	2.3 3.2 -0.9	10.0 8.6 1.4	6.1 5.1 1.0	0.5 0.4 0.1	0.5 -1.9 2.4	3.4 2.7 0.7	6.0 7.1 -1.1	9.2 7.3 1.9
Brandon	1.2 3.5 -2.3	8.5 8.9 0.4	6.4 4.6 1.8	-4.6 -1.6 -3.0	-1.3 -2.3 1.0	-3.6 -1.9 -1.7	5.6 5.9 -0.3	9.8 7.1 2.7
McCreary	-1.8 1.8 -3.6	7.9 6.8 1.1	6.5 4.2 2.3	-5.9 -2.9 -3.0	-1.3 -1.8 0.5	-4.1 -1.8 -2.3	4.6 5.0 -0.4	9.4 8.3 1.1
Portage Southport	1.2 5.3 -4.1	7.3 8.2 -0.9	6.5 6.0 0.5	-5.2 -0.4 -4.8	-0.7 -1.0 0.3	-2.7 -1.2 -1.5	4.7 5.7 -1.0	13.2 11.2 2.0
Morden	7.6 6.5 1.1	8.0 9.8 0.0	7.8 6.7 1.1	-5.2 -0.5 -4.7	-0.4 -0.2 -0.2	-0.3 -0.8 0.5	5.6 6.6 -1.0	13.4 12.2 1.2
Winnipeg Airport	8.4 9.6 -1.2	8.0 7.5 0.5	7.8 6.8 1.0	-2.8 0.7 -3.5	-0.5 -0.9 0.4	-0.1 0.0 -0.1	4.2 4.8 -0.6	15.4 9.7 5.7
Pinawa	9.4 9.1 0.3	6.2 6.0 0.2	7.5 6.1 1.4	-0.9 -0.2 -0.7	-0.1 -0.8 0.7	0.2 -0.2 0.4	2.1 1.7 0.4	11.6 10.7 0.9
Sprague	9.5 9.5 0.0	8.2 7.8 0.4	6.5 5.7 0.8	-0.8 0.6 -1.4	1.3 -1.3 2.6	-0.2 -0.2 0.0	2.6 1.7 0.9	12.4 11.6 0.8
Mean Difference	-1.3	0.4	1.2	-2.6	1.0	-0.5	-0.4	2.0

The hourly information was then examined using a time series, all of which can be found in Appendix D. The event in which the simulation captured the temperature best is the October 4-5, 2012 event (Figure 4.7). With a few exceptions, such as at Sprague and over the October 5 00 UTC - 18 UTC period at Brandon, the temperature is captured well. Relative humidity was in general simulated well although there were periods of considerable difference. The winds are also generally well captured.

Note that the station at Sprague suffered power loss during this event, and as a result, no data is available after October 4 15 UTC. Power was restored and the station resumed operation on October 9, 2012.

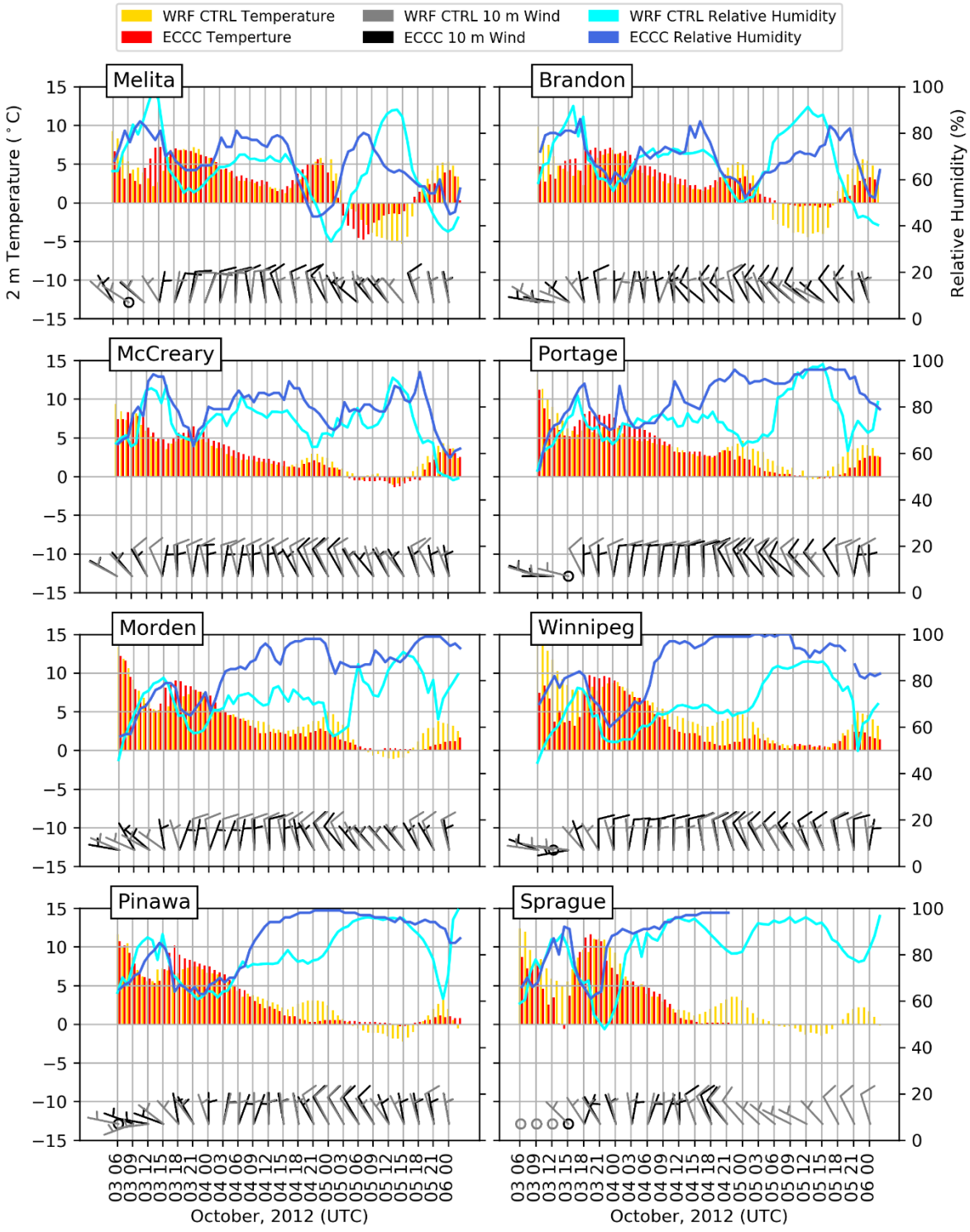

Figure 4.7: Time series of the surface (2 m) temperature (°C), relative humidity (%), and 10 m winds at 8 ECCC surface observation stations, and their attendant locations in WRF during the October 4-5, 2012 event. Temperature is indicated on the left and relative humidity is on the right. Winds are shown as wind barbs in m s^{-1}.

WRF did not simulate the observations as well in other events, such as the May 11, 2004 event (Figure 4.8). There were wide variations between WRF and observations, particularly for temperature and moisture. A warm bias exists for much of the event (for example, Winnipeg); sometimes this occurred when temperatures in the observations were below 0°C (for example, Melita). The winds were also handled relatively poorly at Sprague, with differences between the model and observations of nearly 90° in some cases. This might be linked with Sprague being located in a densely forested area, where the surface roughness of the trees causes more turbulent motion in the boundary layer and near the surface; the model may not have captured this well.

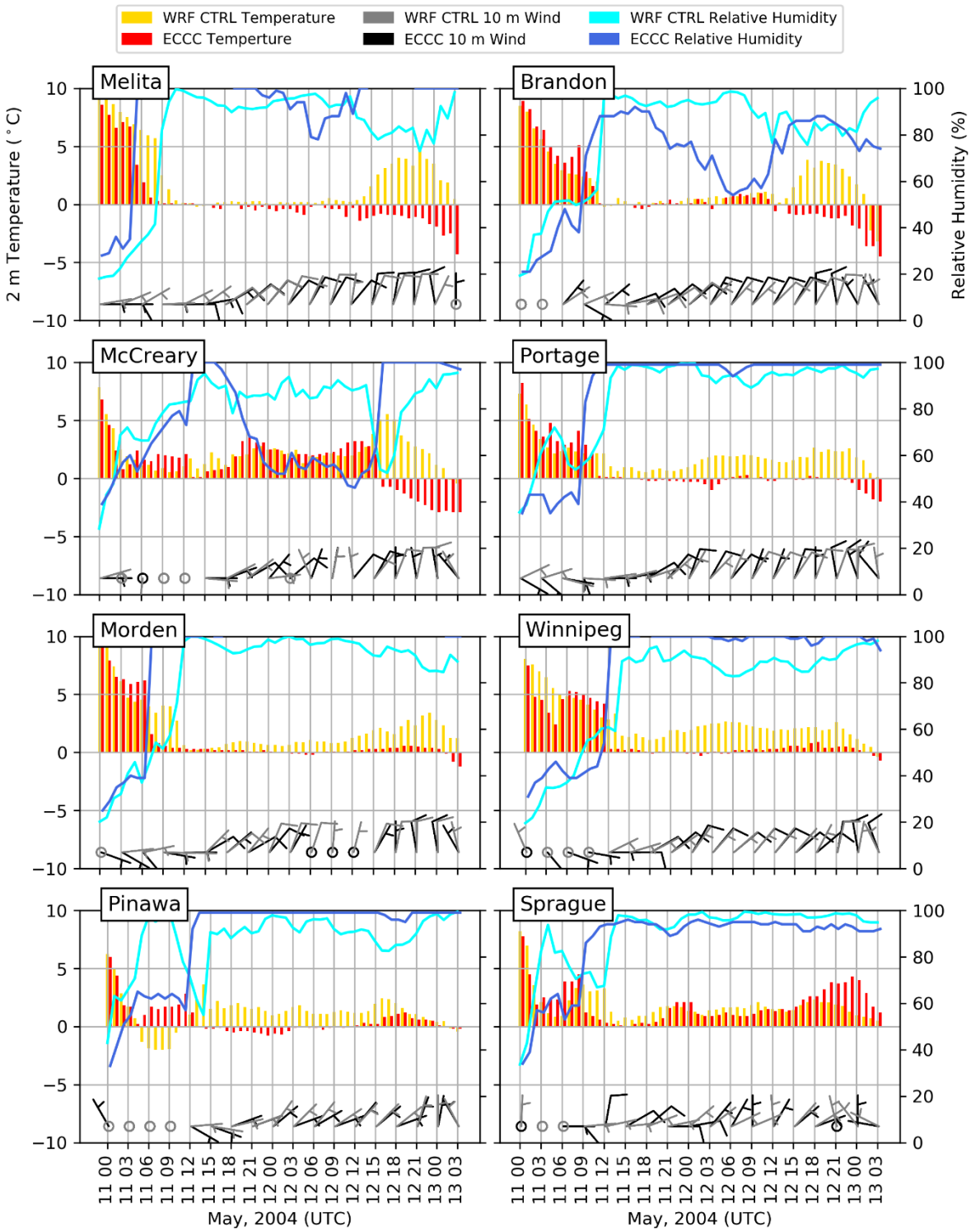

Figure 4.8: Time series comparing the surface (2 m) temperature, relative humidity, and 10 m winds at 8 ECCC surface observation stations, and their attendant locations in WRF during the May 11, 2004 event. Temperature is indicated on the left and relative humidity is on the right. Winds are shown as wind barbs in m s^{-1}.

Overall, WRF CTRL is useful for achieving the objectives of this study but it certainly did not achieve a perfect simulation. For the longer events, there was a mean cold bias of approximately 4-5°C, while the shorter events showed lesser mean warm biases of 0-1°C. Across all the events, WRF had a -1.6°C bias for the mean temperatures compared to observations. The maximum temperatures did not have an appreciable bias, however this number is less meaningful given that biases exist in both the positive and negative directions.

5. Event Characteristics

5.1. Synoptic Scale Factors

Analysis at the synoptic scale revealed three overall patterns; select examples will be shown in the following subsections. All 10 events are detailed in full in Appendix A, and have been summarized in Table 5.1.

Table 5.1: Summary of large scale features associated with each event as they appear on the JRA-55 images. Green cells indicate that a feature was nearby or in Manitoba during the event, and red cells indicate the feature was not observed. Text inside the cell indicates where the feature was located during the event relative to the centre of Manitoba, if applicable.

JRA-55 Analysis Summary				
Event	500 hPa Trough	Atmospheric River	Surface Low	Jet Streak Exit
April 27, 1984	Southwest	South	South	
November 6-12, 2000	Southwest	South	South	
May 11, 2004	Southwest	South	South	
October 5, 2005	Southwest	South-southeast	South-southeast	
December 14-19, 2005	South-southwest	Southeast	South	
December 28, 2005				
January 12-18, 2006	Southwest	West	South	
October 13, 2006	East	Northeast	East	
October 4-5, 2012	Southwest	East	Southeast	
March 8, 2017	Southwest	Northeast	East	

First, 9 of the 10 clearly showed that large scale dynamics/flows were playing a role in these events, and often showed very similar synoptic typing. All but one of the events shows a 500 hPa trough in the vicinity of the province, slightly before or during the dates listed by Manitoba Hydro. These troughs are associated with a midlatitude cyclone, and usually have a jet streak left exit positioned such that it enhanced the lift available to the storm. Typically, these upper disturbances would approach Manitoba's borders from the west, south, or southwest, and move in an easterly, northerly, or northeasterly direction. This results in it passing directly over southern Manitoba, close to the international border or in North Dakota, or just east of Manitoba in Ontario. The tilts of these troughs were often different for each event, varying between a positive tilt, no tilt, and a negative tilt.

The events also had an accompanying low surface pressure centre nearby, which often followed similar tracks to the 500 hPa trough as it moved eastward. Typically, the low pressure centre would reside in Manitoba, or in one of the neighbouring provinces or states.

Additionally, an atmospheric river was present in the events, but often taking different paths into the storm. Most of the time, the atmospheric river would flow northward from the Gulf of Mexico, directly into Manitoba or the storm.

One event that is representative of the 9 similar events (April 27, 1984) will be discussed to illustrate these features (Figures 5.1 - 5.3). The second pattern exists in the October 13, 2006 event, which shows a different flow path for the atmospheric river involved. Third, an event which was dissimilar to the rest will be discussed, December 28, 2005.

5.1.1. Representative Event: April 27, 1984

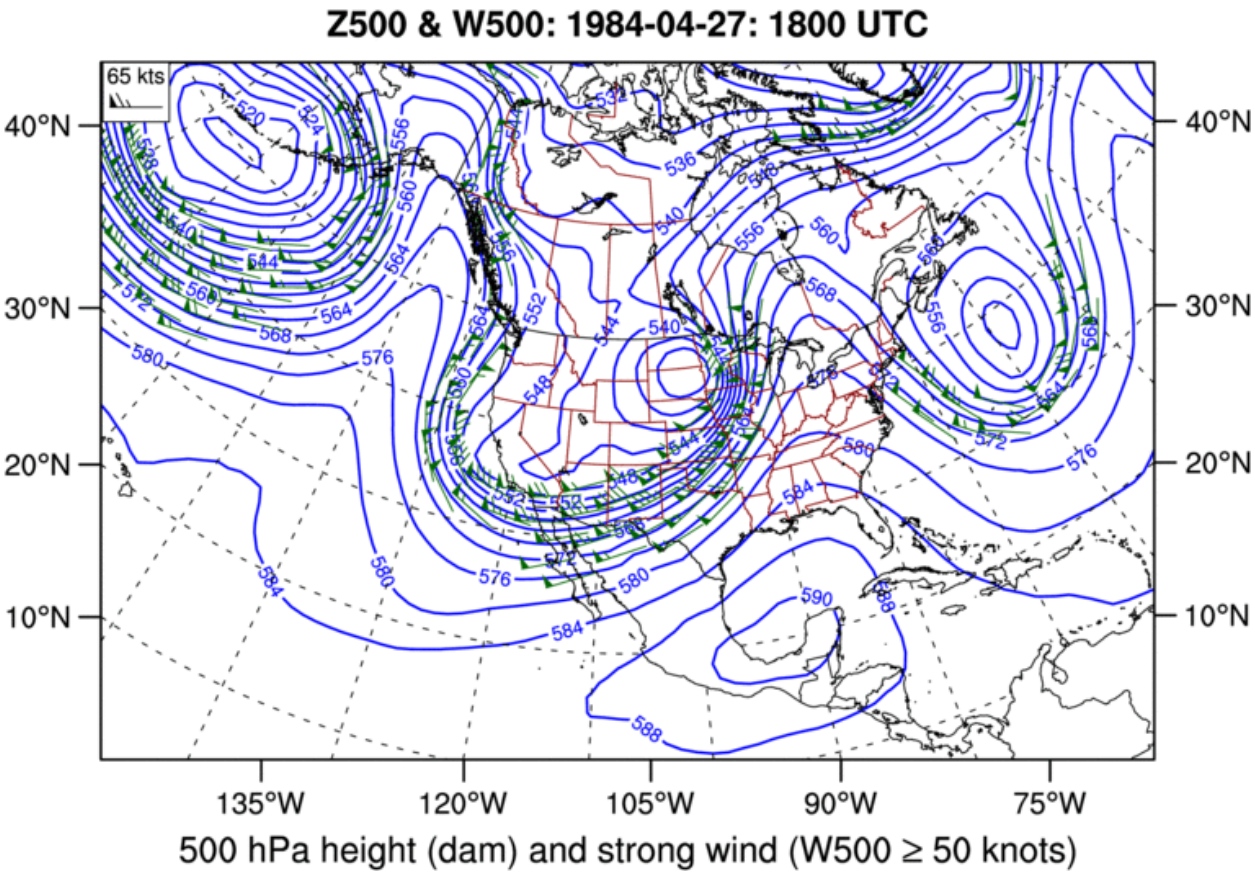

Figure 5.1: JRA-55 500 hPa height analysis for 27 April 1984 18 UTC. Height contours are shown in blue, while strong winds are indicated with a green wind barb. The left jet streak exit is directly over southern Manitoba.

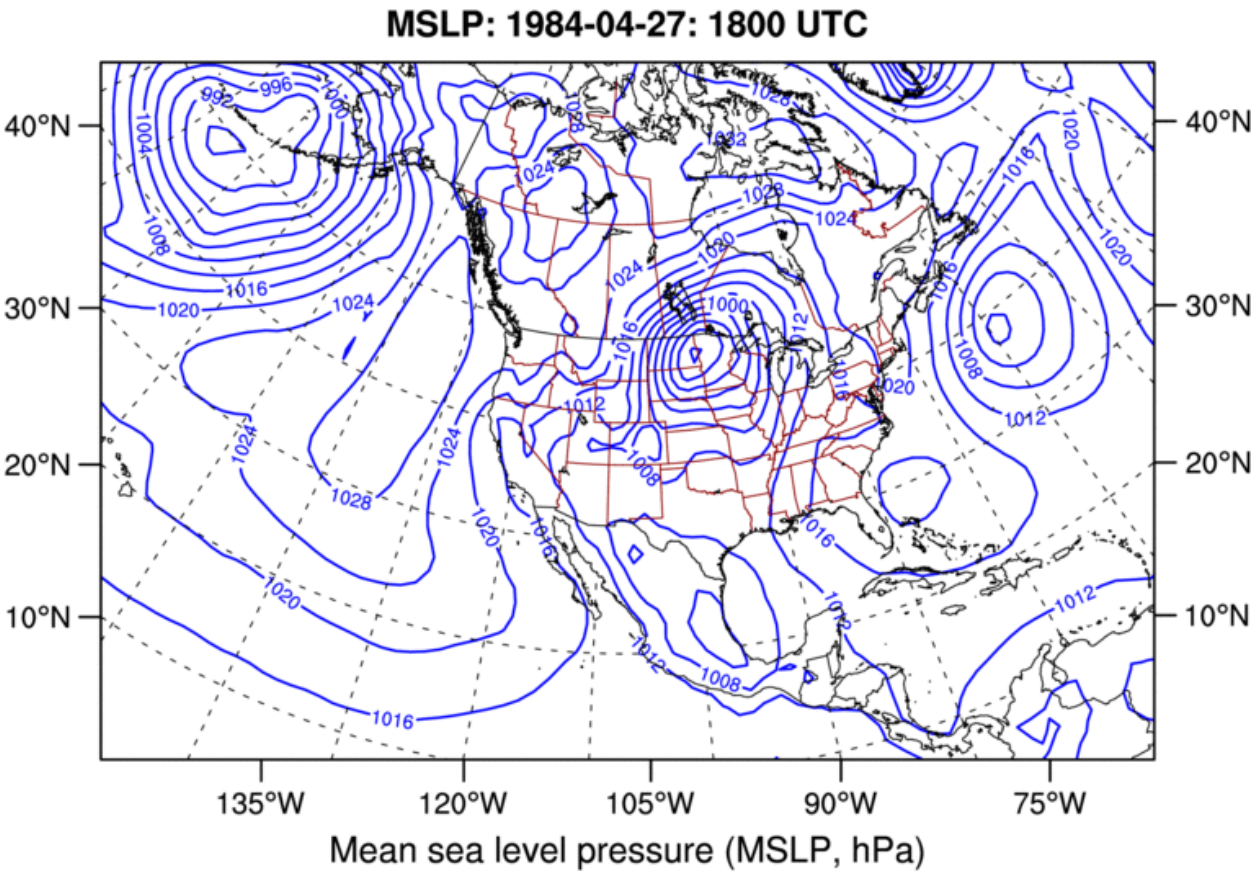

Figure 5.2: JRA-55 mean sea level pressure analysis for 27 April 1984 18 UTC. Mean sea level pressure contours are shown in blue. The low pressure centre is directly south of Winnipeg, Manitoba, straddling the border of North Dakota and Minnesota.

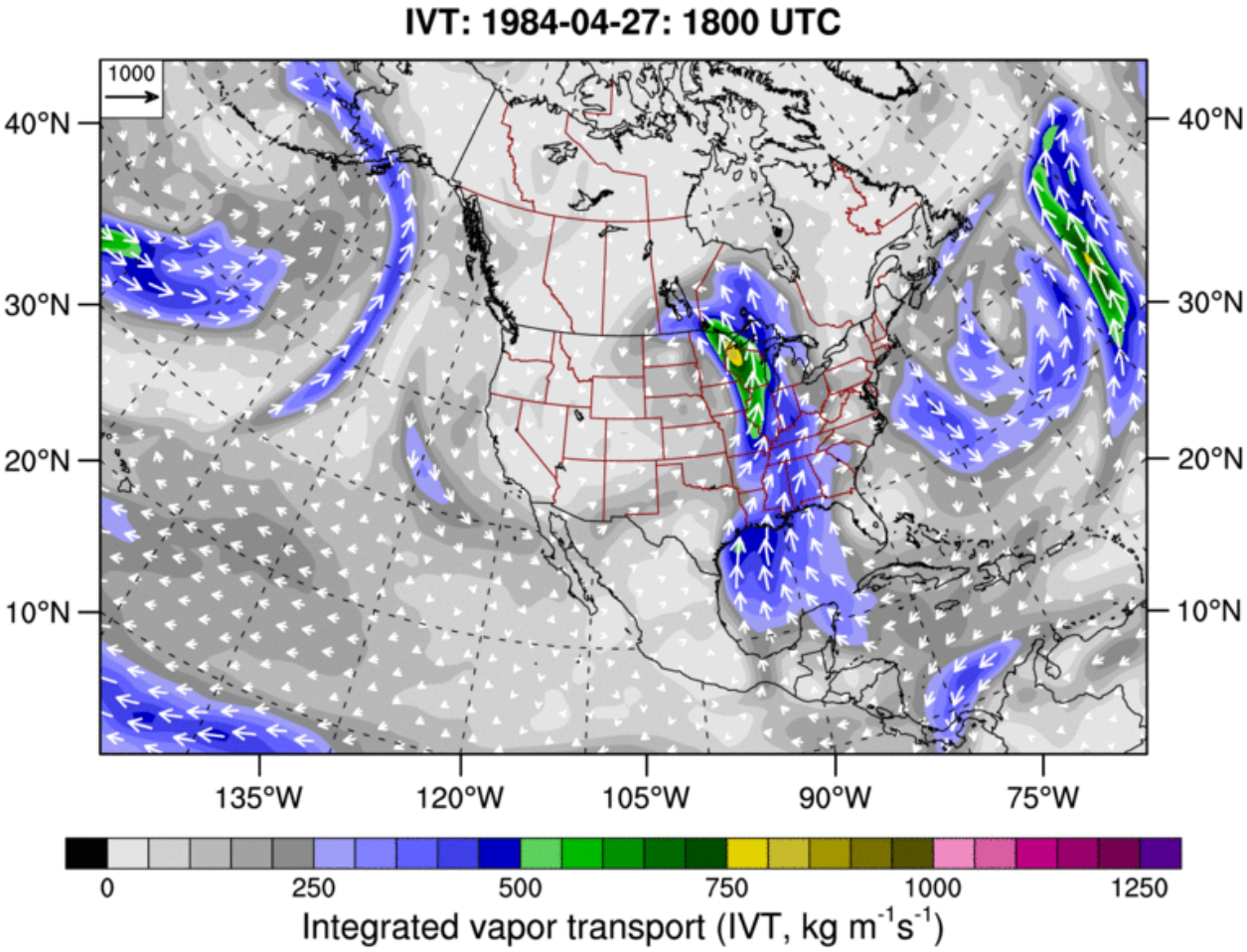

Figure 5.3: JRA-55 integrated vapour transport analysis for 27 April 1984 18 UTC. Coloured contours show the amount of integrated vapour transport. The white arrows indicate mean column flow speed and direction, and the direction any atmospheric rivers that may be present. By definition, the atmospheric river is indicated by 250 IVT (blue) or higher.

5.1.2. Variations in Atmospheric River Flows

In one case, October 13 2006, the atmospheric river flows northeastward, northward, and then follows the curvature of the low pressure centre of the storm, persisting even as it tracks eastward (Figure 5.4). This results in the moisture associated with the atmospheric river entering the storm on the northern side of the low, likely behind the cold front.

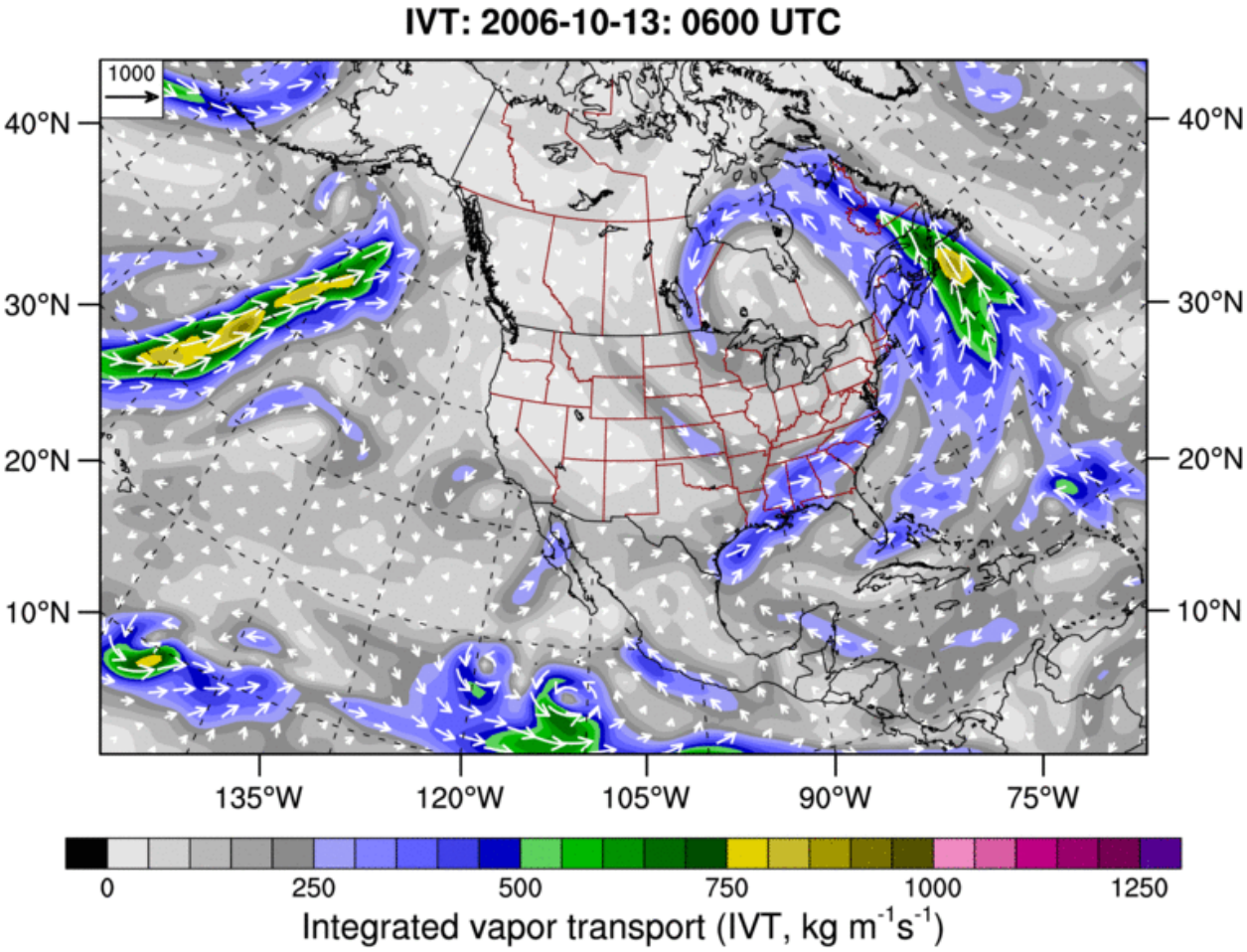

Figure 5.4: JRA-55 integrated vapour transport analysis for 13 October 2006 06 UTC. Coloured contours show the amount of integrated vapour transport. The white arrows indicate mean column flow speed and direction, and the direction any atmospheric rivers that may be present. By definition, the atmospheric river is indicated by IVT values greater than or equal to 250 units (blue).

5.1.3. Dissimilar Event: December 28, 2005

The event that does not show the same large scale forcing as the others occurred on December 28, 2005. The 500 hPa flow is mostly zonal in the days leading up the 28th, with very little deviation from this pattern even after December 28 (Figure 5.5). There is a very weak shortwave perturbation in the 500 hPa flow that precedes the event, but this is unlikely to enhance the storm a significant amount.

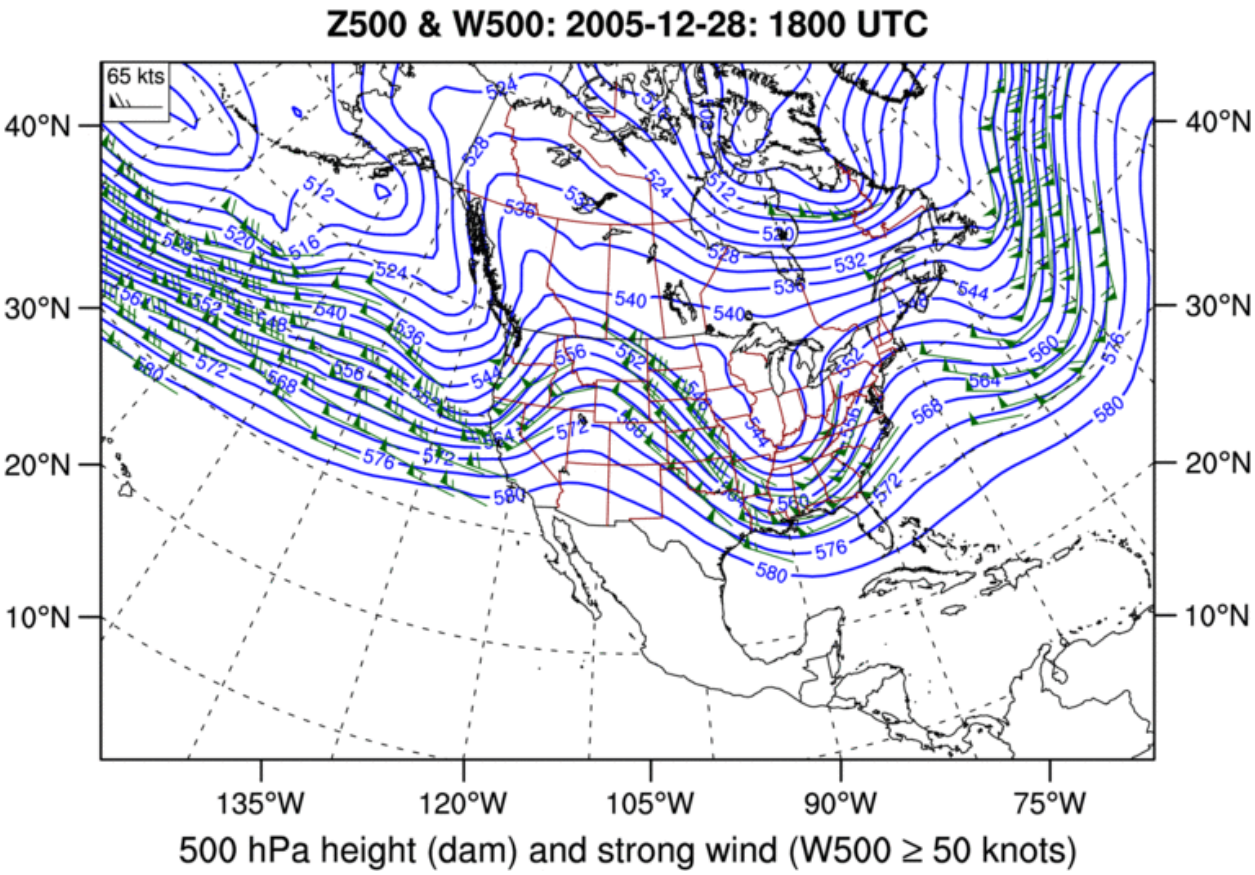

Figure 5.5: JRA-55 500 hPa analysis for 28 December 2005 18 UTC. Height contours are shown in blue, while strong winds are indicated with a green wind barb. The 500 hPa flow is zonal throughout this event.

The mean sea level pressure field does not feature any meaningful low pressure centre that is associated with a trough of any reasonable strength (Figure 5.6). There exists a broad, relatively weak low pressure area of 1002 hPa that is just northeast of Manitoba for the majority of the event, associated with the weak 500 hPa shortwave perturbation. Both the low surface pressure centre and this upper disturbance move away from Manitoba quickly before the event begins.

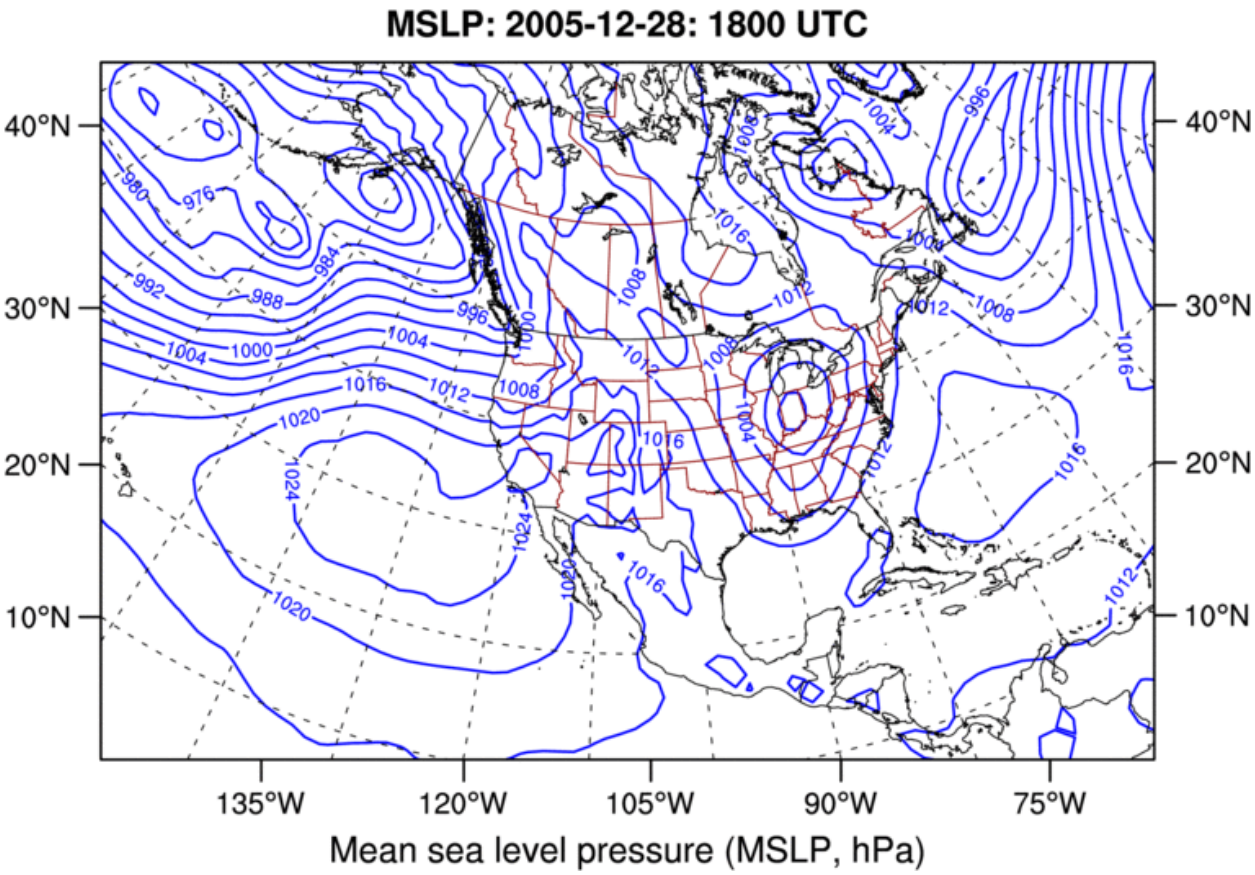

Figure 5.6: JRA-55 mean sea level pressure analysis for 28 December 2005 18 UTC. Mean sea level pressure contours are shown in blue.

An atmospheric river does not enter Manitoba or any of the surrounding area at any point before, during, or after the event (Figure 5.7).

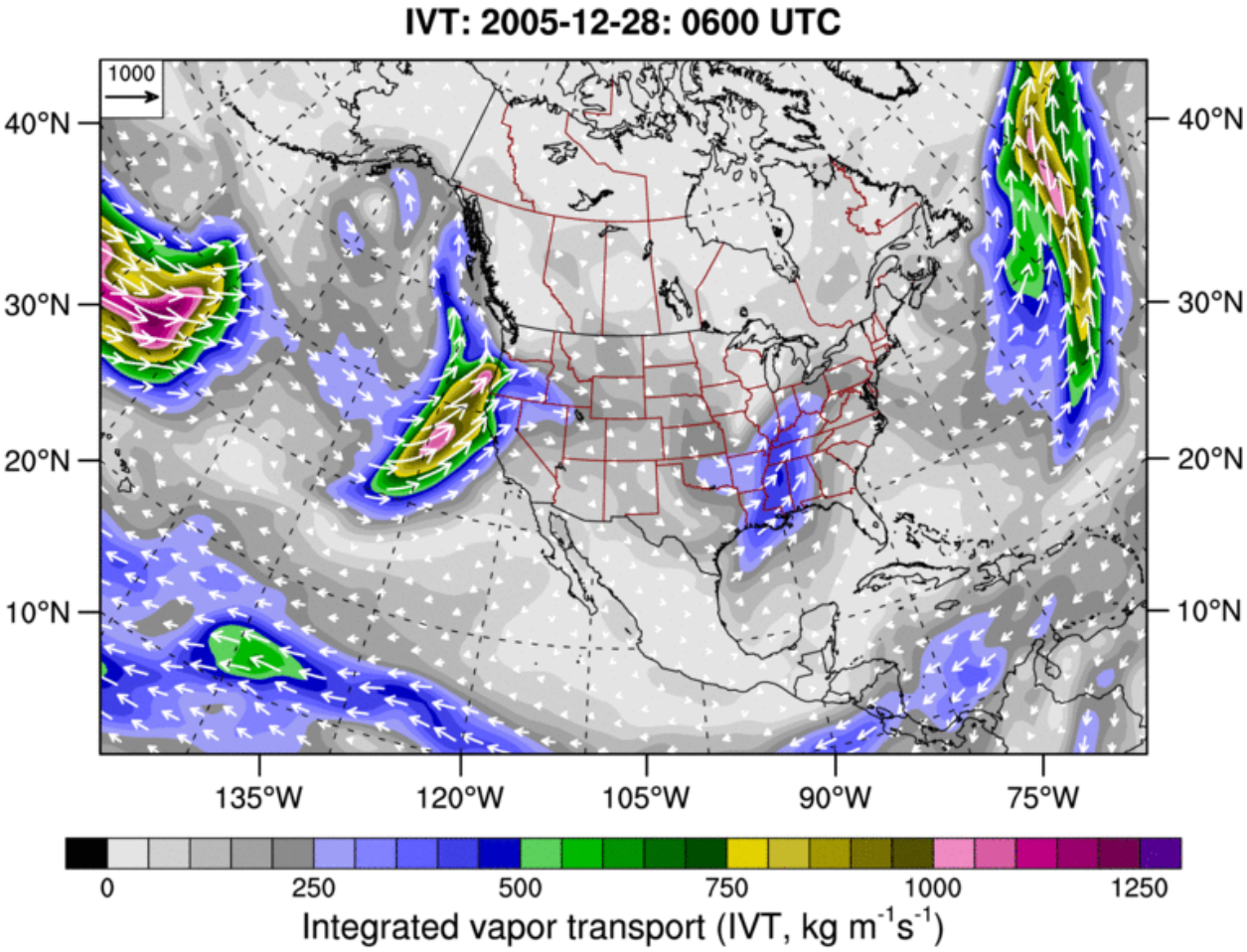

Figure 5.7: JRA-55 integrated vapour transport analysis for 28 December 2005 06 UTC. Coloured contours show the amount of integrated vapour transport. The white arrows indicate mean column flow speed and direction, and the direction any atmospheric rivers that may be present. There was no atmospheric river during this event.

ECR indicates relatively low amounts of condensation between 0-10 mm occurring in Manitoba beginning on 27 December 2005 06 UTC, with a maximum of 20-30 mm on 28 December 2005 06 UTC in the western portion of Manitoba (Figure 5.8). However, both IVT and IWV do not show significant moisture at any point.

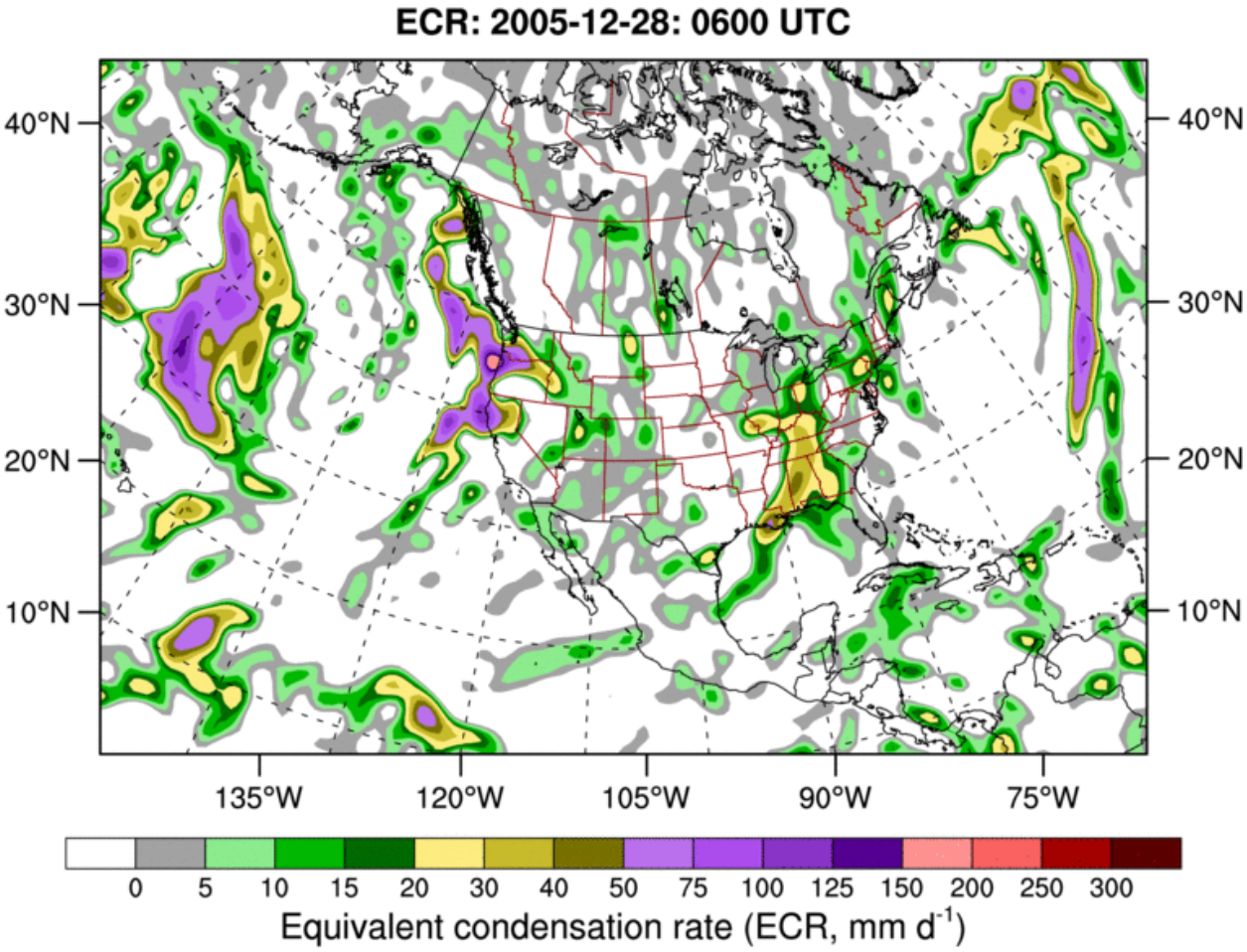

Figure 5.8: JRA-55 equivalent condensation rate analysis for 28 December 2005 06 UTC. The colour contours indicate the maximum amount of precipitation that could occur via moisture flux convergence. Note that there was no atmospheric river flowing into Manitoba at this time.

5.1.4. Summary of Synoptic Factors

The preceding analyses illustrated that different large scale conditions led to the 10 selected events. Most (9) had a similar large scale structure including an atmospheric river but one was associated with a lack of atmospheric river. Collectively, it is important that different large scale conditions can lead to substantial freezing precipitation.

5.2. Characterization of Precipitation

Each of the 10 events is characterized by their precipitation amount, spatial extent, duration, and intensity. First, the types of precipitation occurring within each event were assessed in the CTRL simulation (Table 5.2). Note that throughout the rest of the paper, the abbreviations WTSN, FZRA, SN, RN, and GR are used for wet snow, freezing rain, snow, rain, and graupel, respectively.

Table 5.2: Generalized summary of the types of freezing precipitation and associated mixtures within the CTRL simulation. The blue (orange) rows indicate freezing rain (wet snow) types, and the numbers in each cell represent the approximate maximum cumulative amount of precipitation (liquid equivalent in mm) over the duration of the event within Manitoba. The numbers used are derived from the contours in Figure 5.9 and similar figures, and it is indicated anywhere these numbers were clearly under or over the contour threshold.

Freezing Precipitation Types and Mixtures in CTRL									
Type or Mixture	**Event**								**Type Total (mm)**
	Nov 6-12, 2000	May 11, 2004	Oct 5, 2005	Dec 14-19, 2005	Dec 28, 2005	Jan 12-18, 2006	Oct 13, 2006	Oct 4-5, 2012	
Freezing Rain	**>25**	**15**	**5**	**<5**	**10**	**10**	**5**	**5**	**80**
Freezing Rain, Snow	**5**	**15**	**15**	**0**	**5**	**5**	**5**	**5**	**55**
Freezing Rain, Snow, Graupel	**5**	**10**	**5**	**0**	**5**	**5**	**0**	**5**	**35**
Freezing Rain, Graupel	**15**	**10**	**5**	**<5**	**10**	**5**	**0**	**5**	**55**
Wet Snow	**5**	**>25**	**>25**	**0**	**0**	**0**	**20**	**15**	**90**
Wet Snow, Rain	**5**	**>25**	**>25**	**0**	**0**	**0**	**25**	**20**	**100**
Wet Snow, Rain, Graupel	**5**	**25**	**>25**	**0**	**0**	**0**	**0**	**15**	**70**
Rain, Graupel	**5**	**>25**	**>25**	**0**	**0**	**0**	**0**	**5**	**60**
Event Total (mm)	**70**	**150**	**130**	**10**	**30**	**25**	**55**	**75**	**545**

It is important to note that these numbers (and those of Table 6.1) are approximate. They provide an overall sense of precipitation occurrence, but they do not take into account the overall spatial extent or maximum amount of any event or type. The numbers indicate the maximum amount the precipitation accumulated over the duration of the event at any one grid location

within Manitoba, according to the contour values used in Figure 5.9 and similar figures. However, most of the other grid locations likely did not receive this amount; they may have received less. As well, it is indicated any time the highest contour value was exceeded, which did occur several times. Therefore, many of the amounts were less than the numbers indicated across much of the province, while sometimes the highest values were greater than 25 mm.

To illustrate these issues, Figures 5.9 and 5.10 show examples of the under-representation and over-representation, respectively. The maximum accumulated precipitation in Figure 5.9 reaches 49.3 mm, but the highest contour is 25, so this was classified as ">25". In Figure 5.10, there are small areas where the precipitation reaches up to the 10 mm contour and was classified as such, yet much of the province experienced less than this or no precipitation at all.

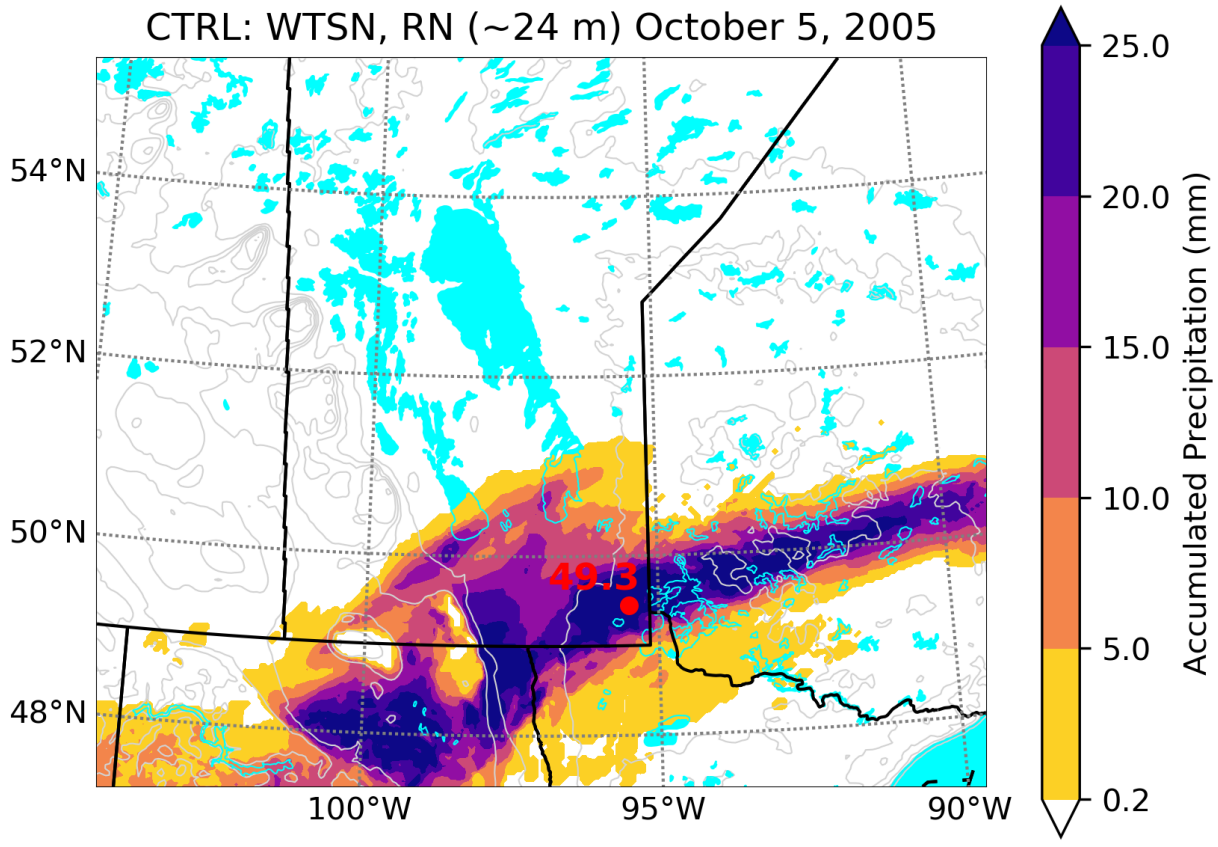

Figure 5.9: WRF CTRL accumulated wet snow (WTSN), rain (RN) mixture at the lowest model level (~24 m) for the October 5, 2005 event. The red dot indicates the maximum accumulation in the image.

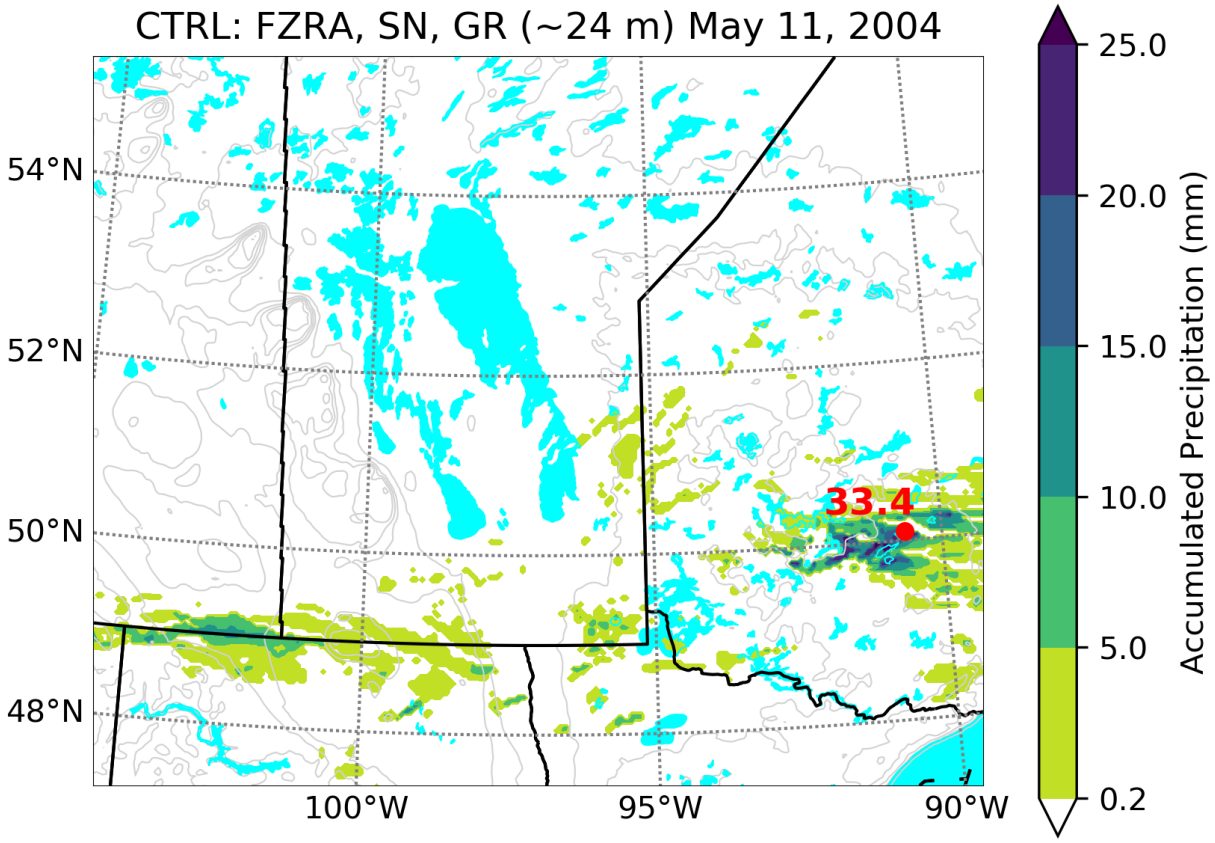

Figure 5.10: WRF CTRL accumulated freezing rain (FZRA), snow (SN), graupel (GR) mixture at the lowest model level (~24 m) for the May 11, 2004 event. The red dot indicates the maximum accumulation in the image.

An additional consideration arises if there is an appreciable difference in the amount or type of precipitation experienced at different model levels in WRF. This is important because while the ~24 m level is primarily being used in this study. If a future comparison is made to 2 m surface observations of precipitation, these values could be different. To examine this, precipitation information was extracted from each grid point in a sub-domain within WRF over the duration of the events. This domain represents southern Manitoba, where most of the freezing precipitation fell, and the majority of the population lives (Figure 5.11).

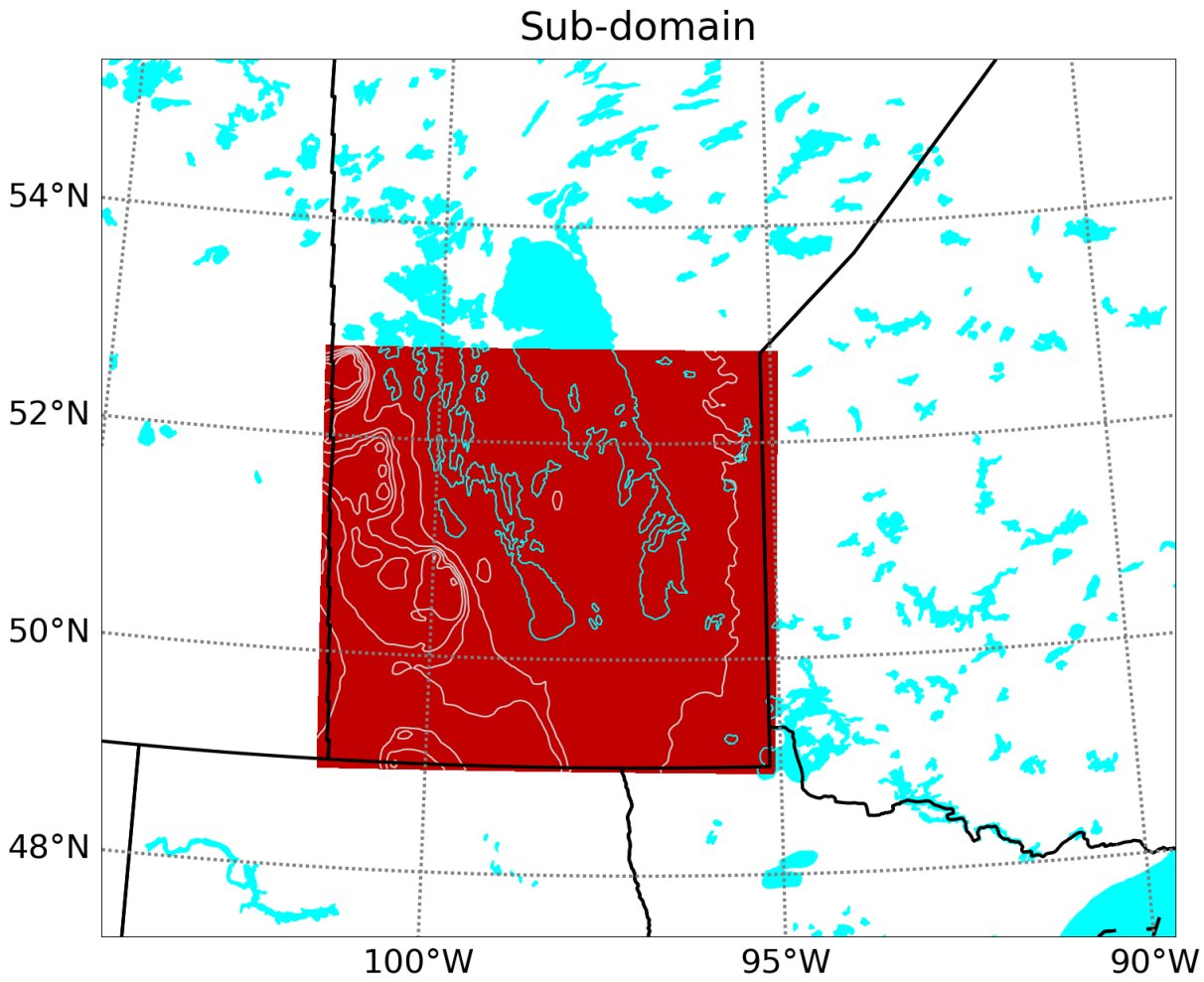

Figure 5.11: Sub-domain of the WRF model that covers the southern half of Manitoba, with an area of 207,680 km².

Comparing the WRF precipitation at these 2 levels shows homogeneity overall in both its duration and accumulated amounts with the major exception being wet snow, with ~15% higher amounts at the 2 m level compared to ~24 m (Figure 5.12). This pattern is similar when examining duration. This could be due to snow having a longer time to melt in a near-surface warm layer that extends through both levels, or perhaps the warm layer is extremely shallow, existing only under the ~24 m level.

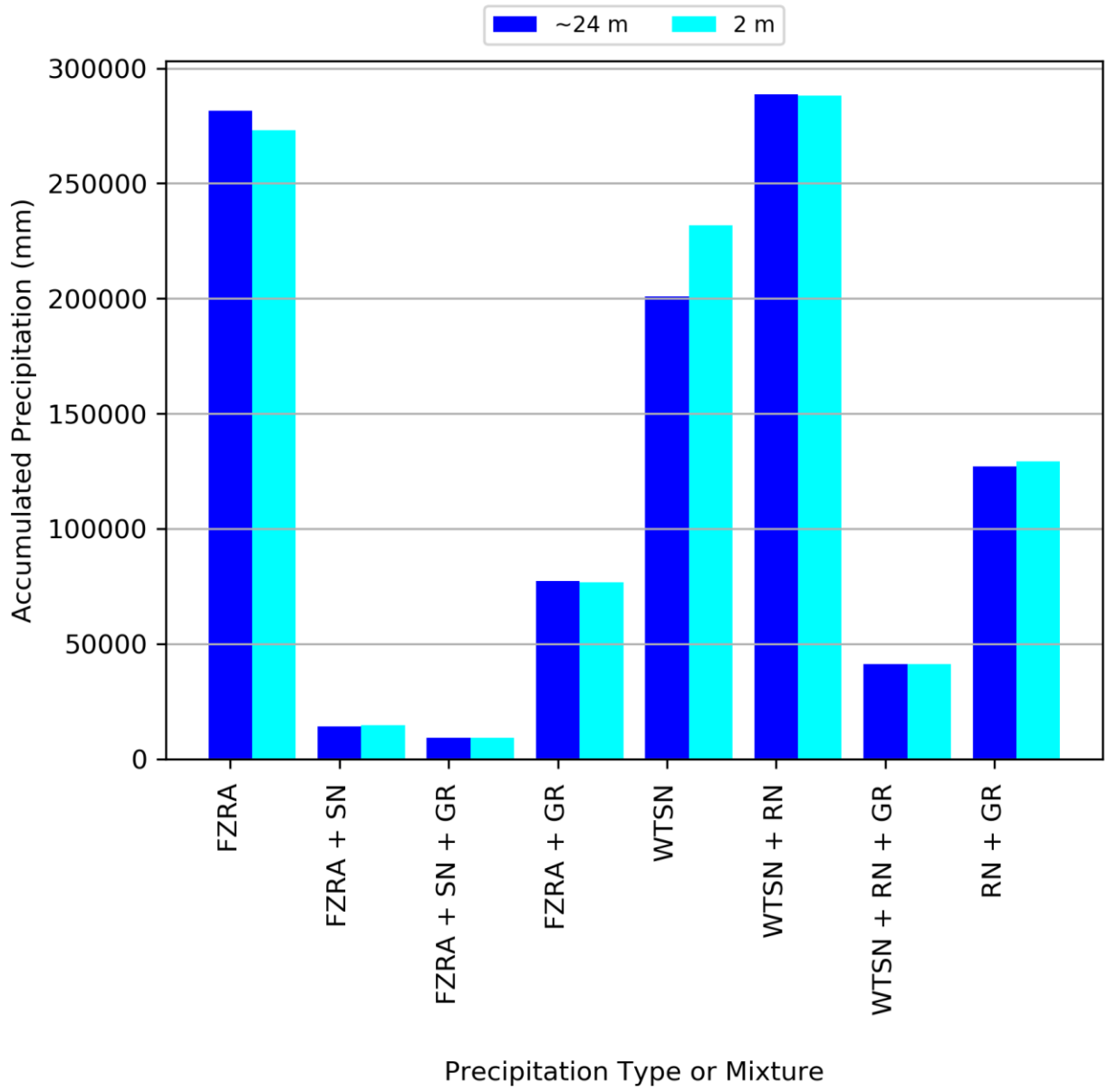

Figure 5.12: A comparison summation of accumulated freezing precipitation types at 2 different model height levels extracted from each WRF grid point over the duration of all events across the southern half of Manitoba.

Additionally, the intensity of freezing precipitation at the 2 levels was examined (Figure 5.13). The overall pattern was skewed toward lighter amounts of precipitation at both levels, and is similar to those of accumulation and duration. The rate criteria used to determine intensity

category are those used operationally by ECCC, namely light = 0.2 - 2.5 mm h^{-1}, moderate = 2.6 - 7.5 mm h^{-1}, and heavy = 7 mm h^{-1} + (ECCC 2019a).

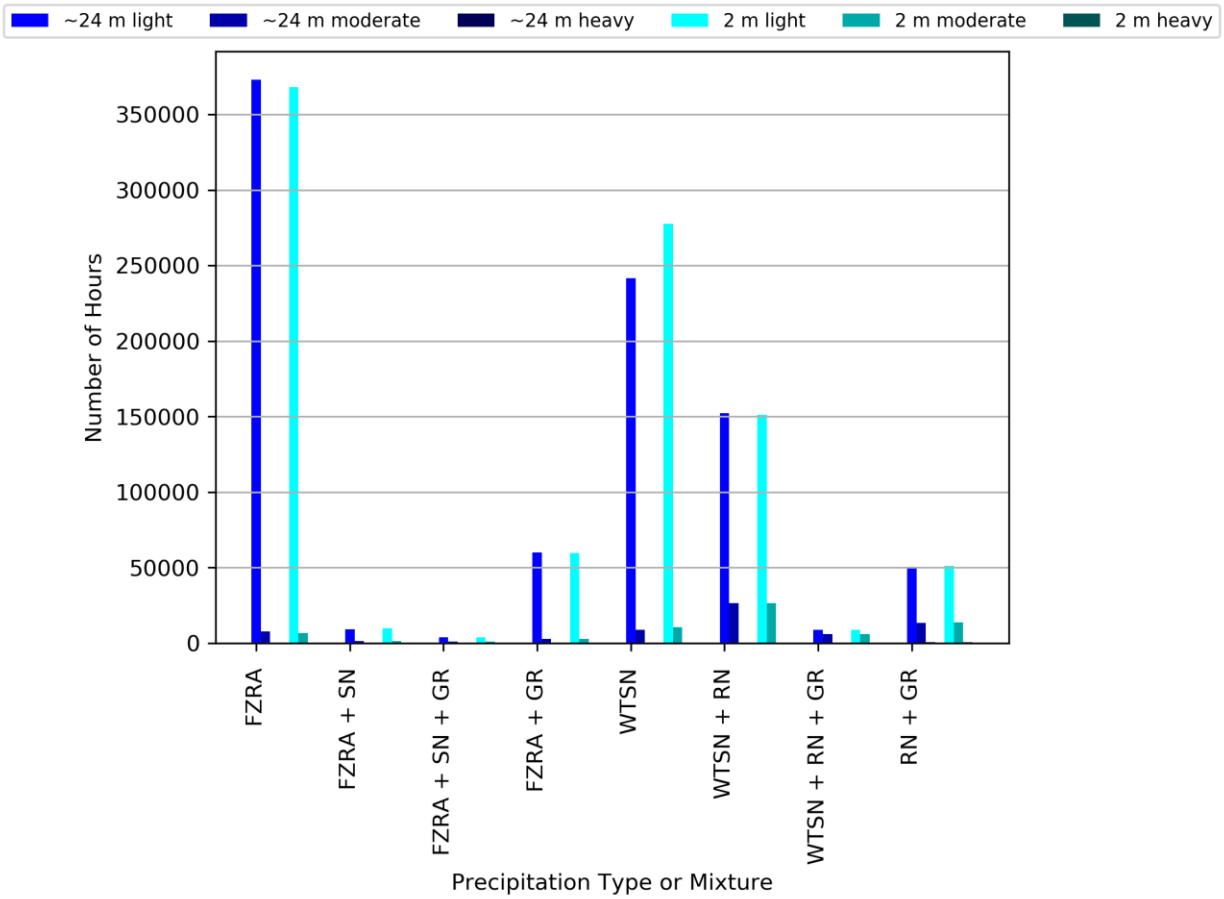

Figure 5.13: Comparison of intensity of freezing precipitation at 2 different model height levels extracted from each WRF grid point over the duration of all events across the southern half of Manitoba. The rates used for the categories of intensity are light = 0.2 - 2.5 mm h^{-1}, moderate = 2.6- 7.5 mm h^{-1}, and heavy = 7 mm h^{-1} +.

5.2.1. Freezing Rain and Mixtures

As shown in Table 5.2, freezing rain and mixtures were more common in their occurrence than wet snow and mixtures, though the amount of precipitation was lower. Freezing rain by itself was more dominant than freezing rain mixtures.

The November 6-12, 2000 event had the largest amount of freezing rain (Figure 5.14) and it affected Manitoba and North Dakota.

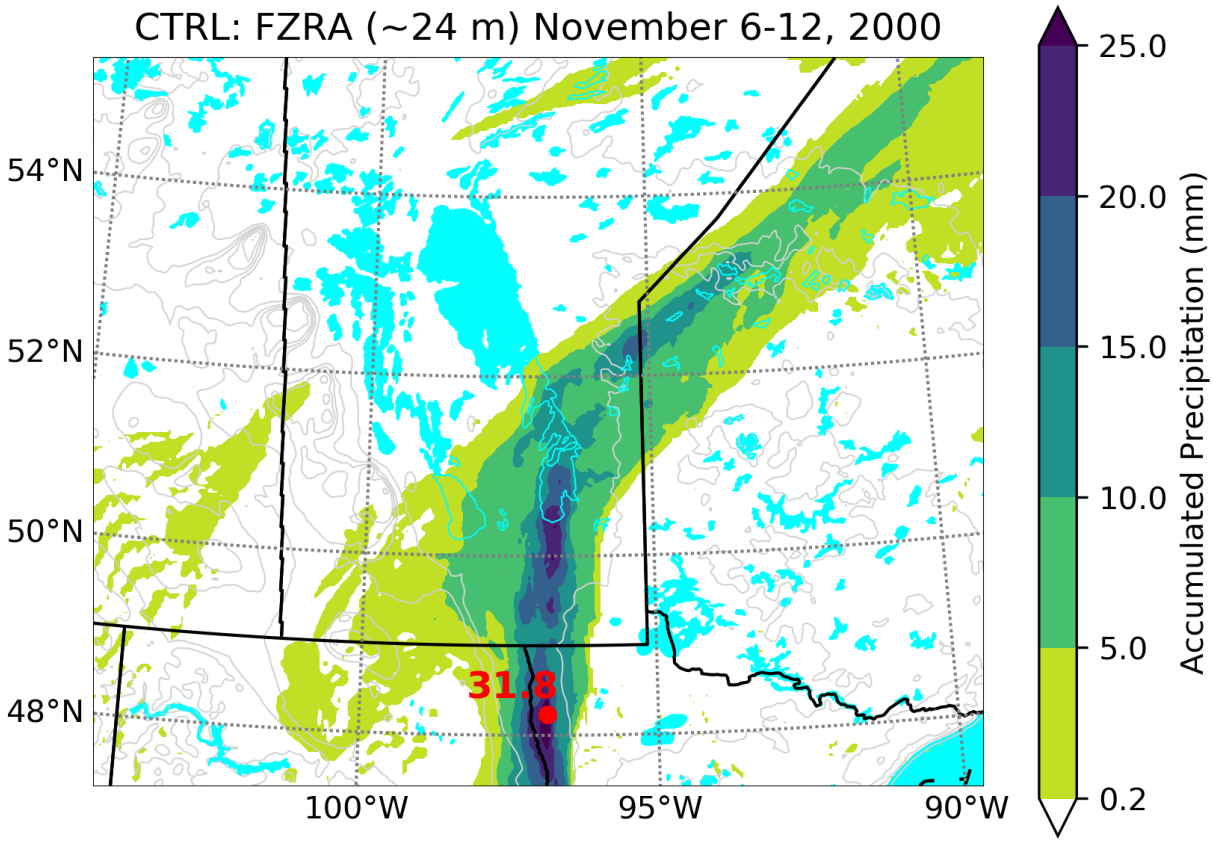

Figure 5.14: WRF CTRL accumulated freezing rain at the lowest model level (~24 m) for the November 6-12, 2000 event. The red dot indicates the maximum accumulation in the image.

The pattern of precipitation suggests that lake effect precipitation was taking place. However, this pattern is more likely the result of the orientation of a strong warm front parallel to the lake during this event (Figure 5.15).

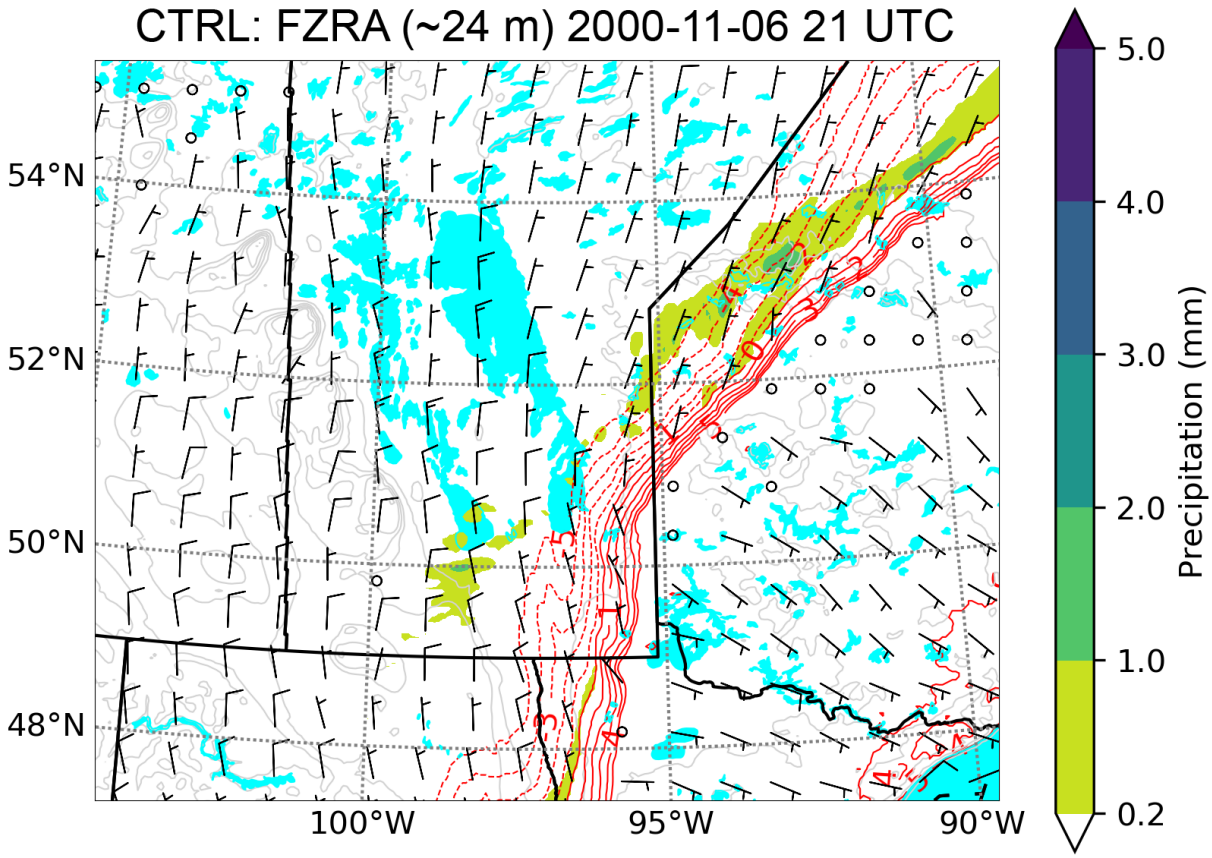

Figure 5.15: Freezing rain during November 6, 2000 21 UTC in CTRL. Red contours indicate lowest model level (~24 m) wet-bulb temperature in °C with dashed and solid contours indicating temperatures < 0°C and ≥ 0°C, respectively. Coloured contours indicate the hourly accumulated precipitation. Wind barbs are in m s^{-1}.

5.2.2. Wet Snow and Mixtures

Wet snow did not occur in the coldest winter months of December and January, but when it did occur in the warmer months, the precipitation amount was much greater than that of freezing rain and mixtures. The overall most dominant type was the mixture of wet snow and rain, with the qualitative cumulative contour analysis exceeding 100 mm across all events.

The October 5, 2005 event had the highest amount of wet snow and mixtures out of all of the events, peaking 49.3 mm over the course of 34 hours (Figure 5.16).

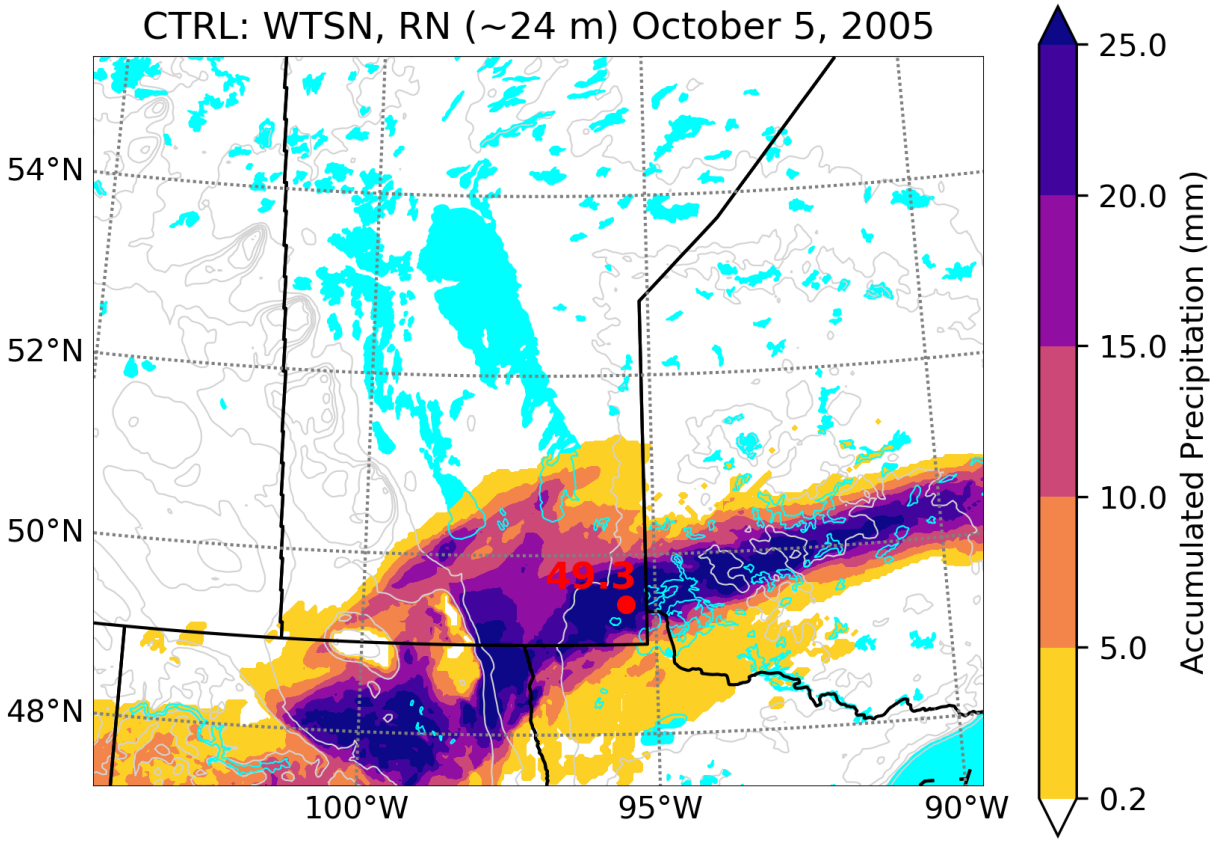

Figure 5.16: WRF CTRL accumulated wet snow, rain mixture at the lowest model level (~24 m) for the October 5, 2005 event. The red dot indicates the maximum accumulation in the image.

The spatial distributions of duration and accumulation were similar for all of the events, for both types, and as such will not be shown in similar maps.

5.3. Local Factors

5.3.1. Terrain

Terrain plays a significant role in 2 of the events in CTRL, which is either Riding Mountain and the nearby elevated terrain in the west, or sometimes Pembina Mountain in the south. In all cases where there is terrain interaction, air flowing up or down these slopes

experience cooling or warming, respectively. This creates a situation in which the top of the slope is near or 0°C, compared to the base where temperatures may be a few degrees above freezing. This can change the precipitation falling on or near these areas.

For example, in the May 11, 2004 event, temperatures at the top of Riding Mountain and Pembina Mountain were lower (near 0°C) than the surrounding air (~2-5°C), due to upslope flow and cooling (Figure 5.17). However, temperatures near the base were still above freezing by a few degrees. When this area was blanketed by snow, all of the snow falling on top of the mountains stayed frozen, whereas any snow that fell into the warmer air began to melt into wet snow (Figure 5.18).

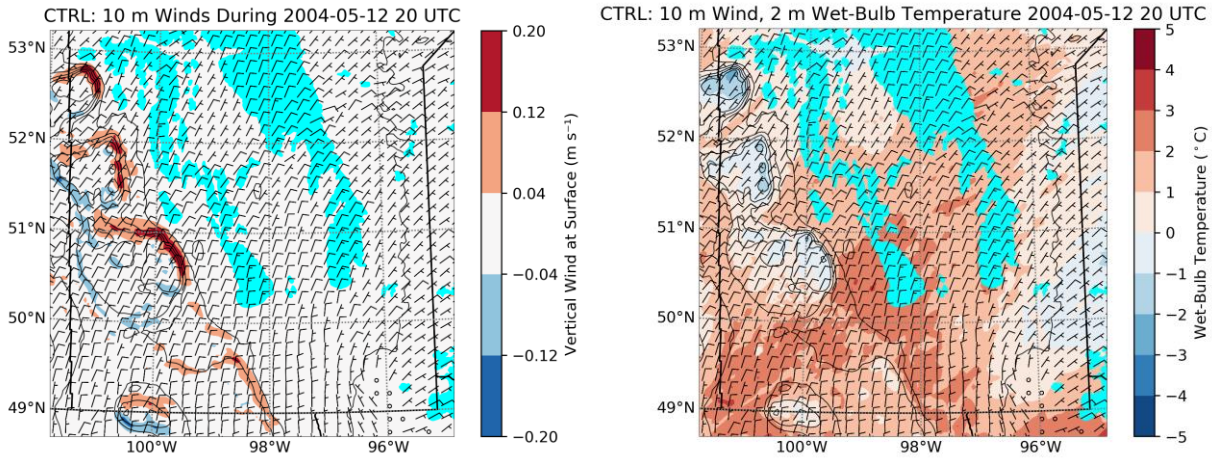

Figure 5.17: WRF CTRL temperature differential across and wind interaction with Riding Mountain during the May 11, 2004 event. The left panel is the 10 m winds, and coloured contours indicating the 2 m wet-bulb temperature. The right panel is the 10 m winds, and the vertical wind component (W) at the lowest model level (~24 m).

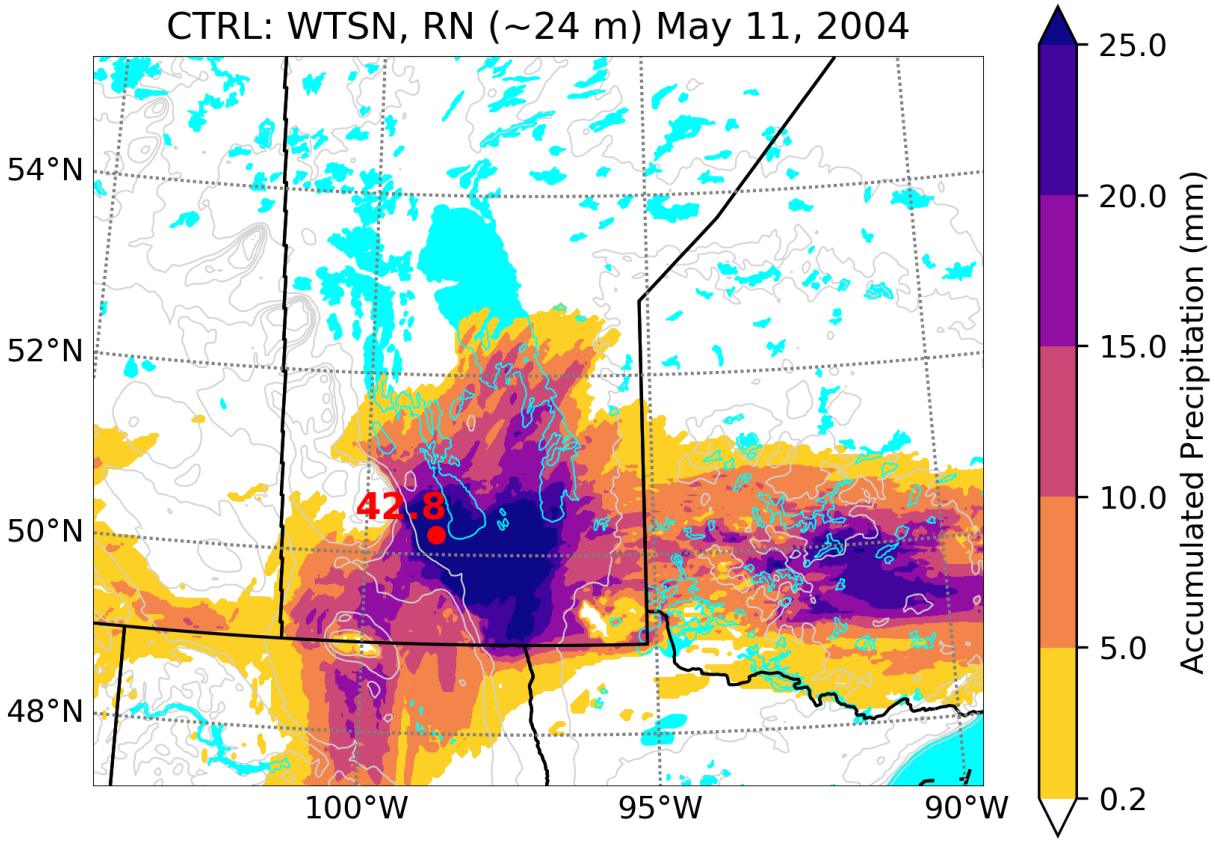

Figure 5.18: WRF CTRL accumulated wet snow, rain mixture at the lowest model level (~24 m) for the May 11, 2004 event. The red dot indicates the maximum accumulation in the image.

A vertical cross section across the slope of Riding Mountain illustrates these conditions from a different perspective (Figures 5.19 and 5.20). The area underneath the red isotherm indicates air that was above 0°C, but had snow falling into it and partially melting into wet snow.

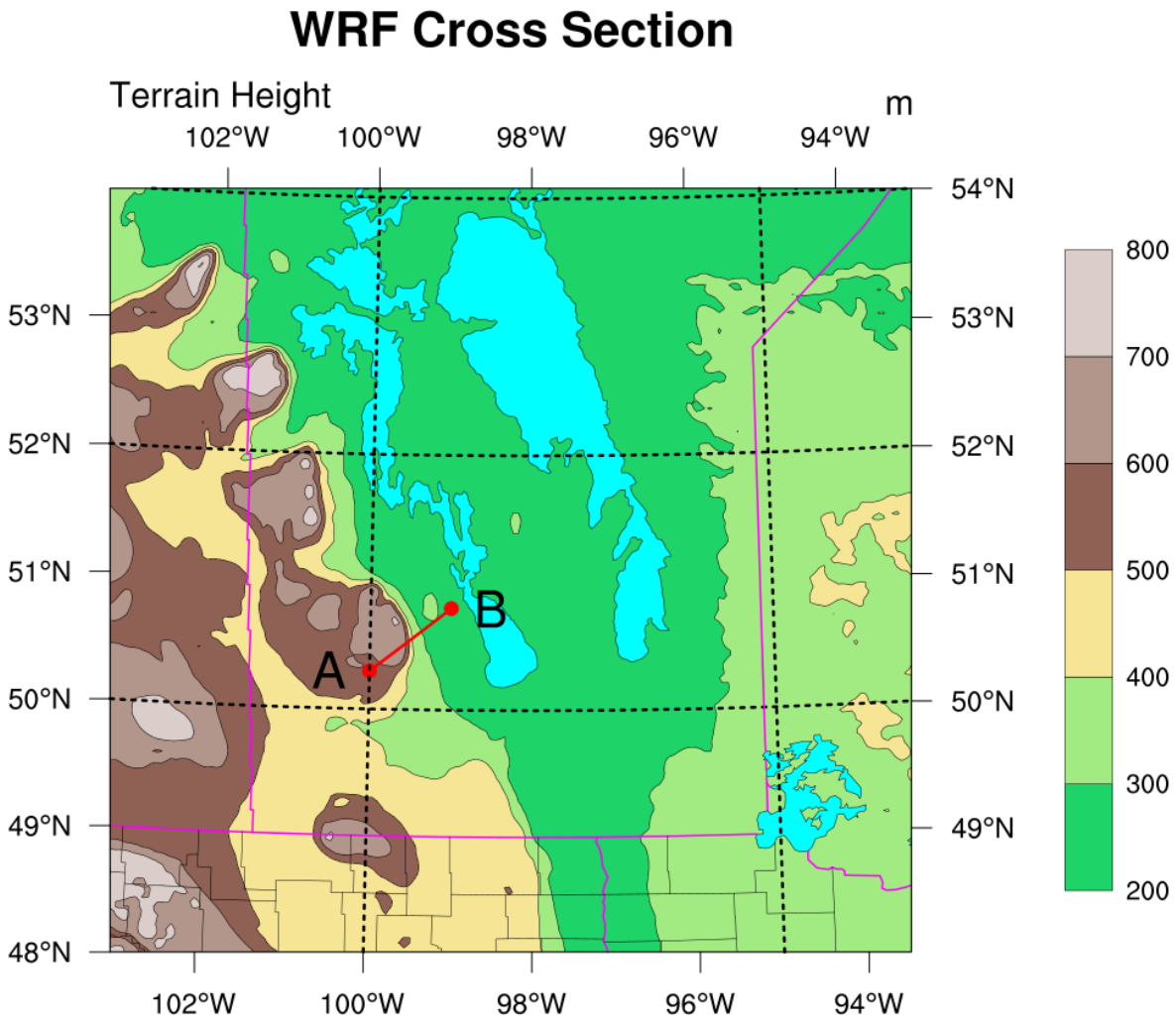

Figure 5.19: Location of vertical cross-section in Figure 5.20. Coloured contours indicate the terrain height (m). The cross section is along the red line from A to B.

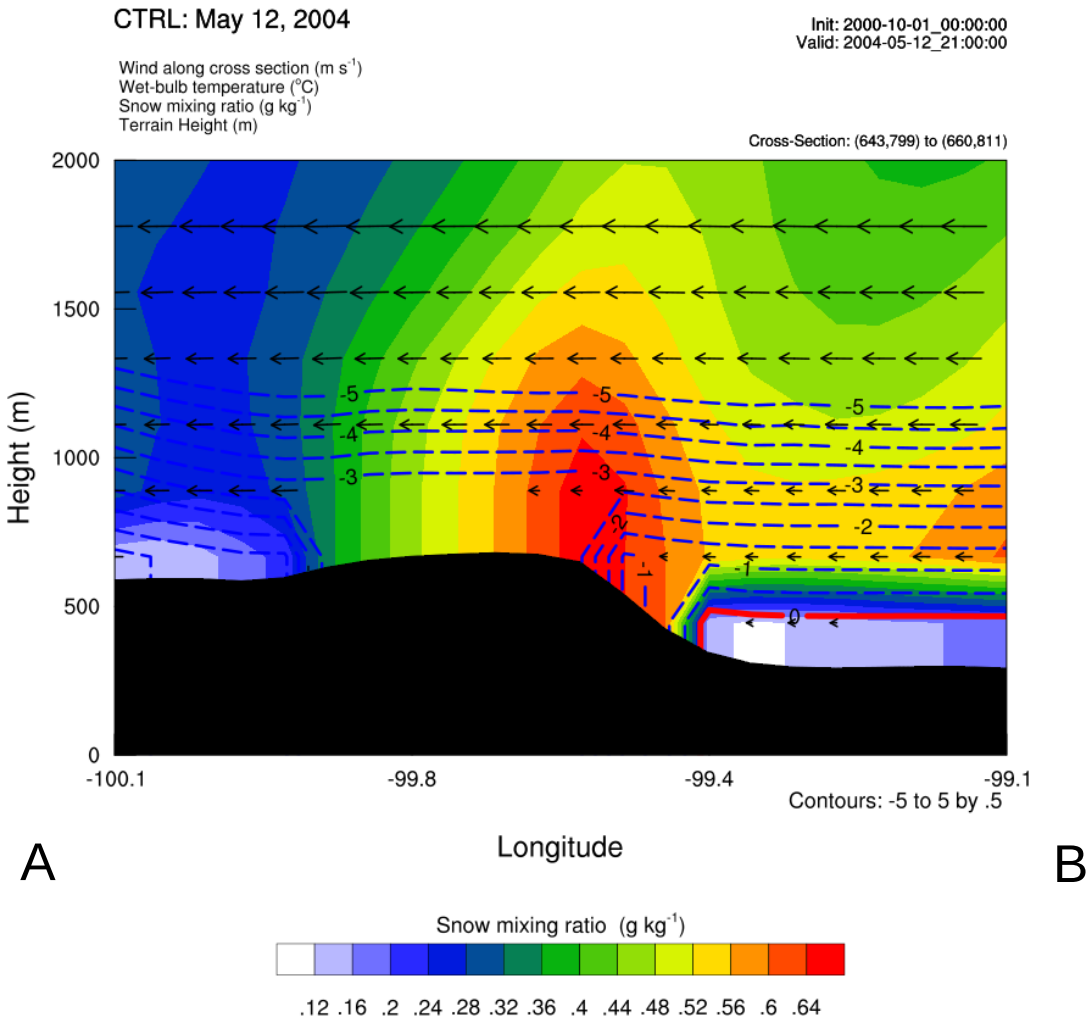

Figure 5.20: Vertical cross-section depicting a wet snow situation over Riding Mountain on May 12, 2004 at 21 UTC in the WRF CTRL simulation. Coloured contours are the snow mixing ratio. The dashed blue, solid thick red, and solid red isolines indicate temperatures below, at, and above 0°C, respectively. Wind speed and direction are indicated with arrows. The black area is the terrain.

The approximate 100-200 m of elevation change between Pembina Mountain and the floodplains of southern Manitoba is adequate to alter the type of precipitation that is occurring via the same temperature differential seen at Riding Mountain. It occurs in several events, such as in the October 5, 2005 event (Figure 5.21), and the previously discussed May 11, 2004 event (Figure 5.22). The precipitation contours are co-located closely with Pembina Mountain, with the

wet snow, rain mixture concentrated on the low side and the freezing rain falling on the high side.

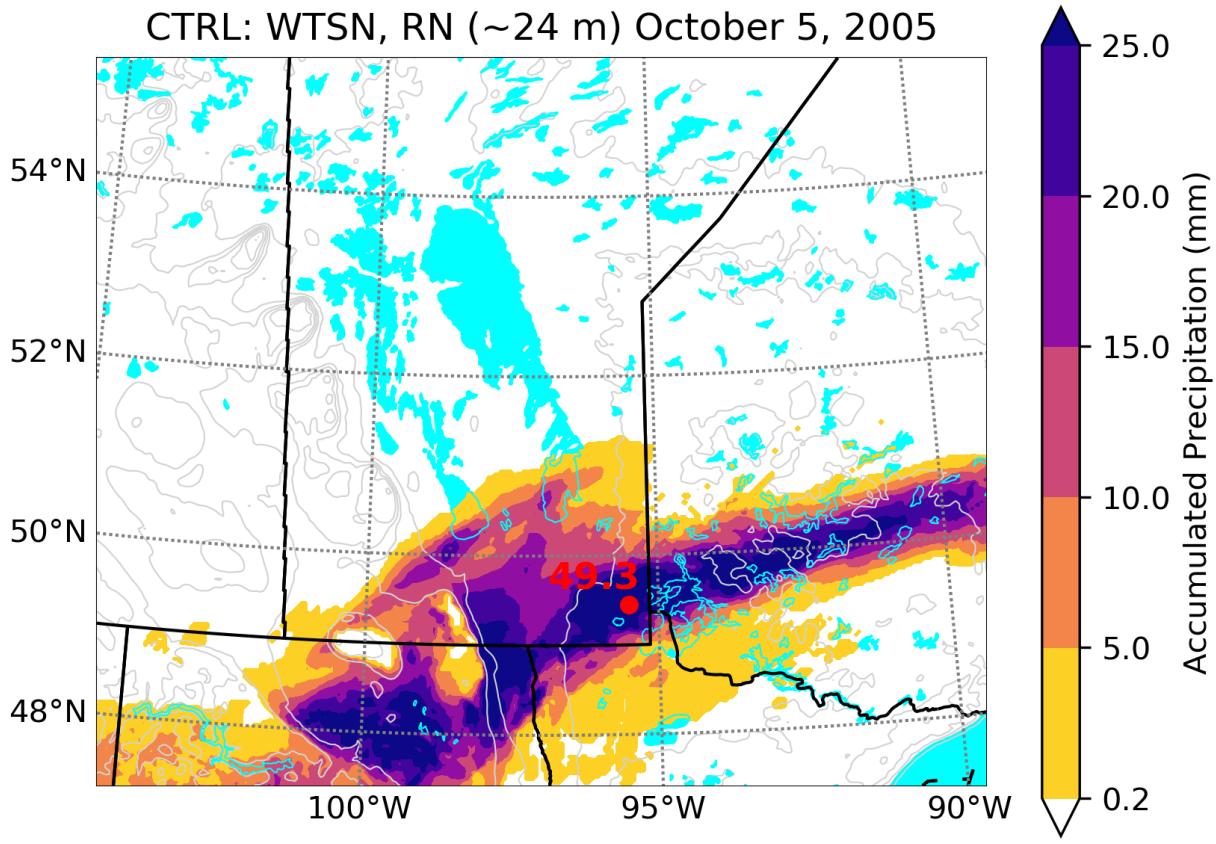

Figure 5.21: WRF CTRL accumulated wet snow, rain mixture at the lowest model level (~24 m) for the October 5, 2005 event. The red dot indicates the maximum accumulation in the image.

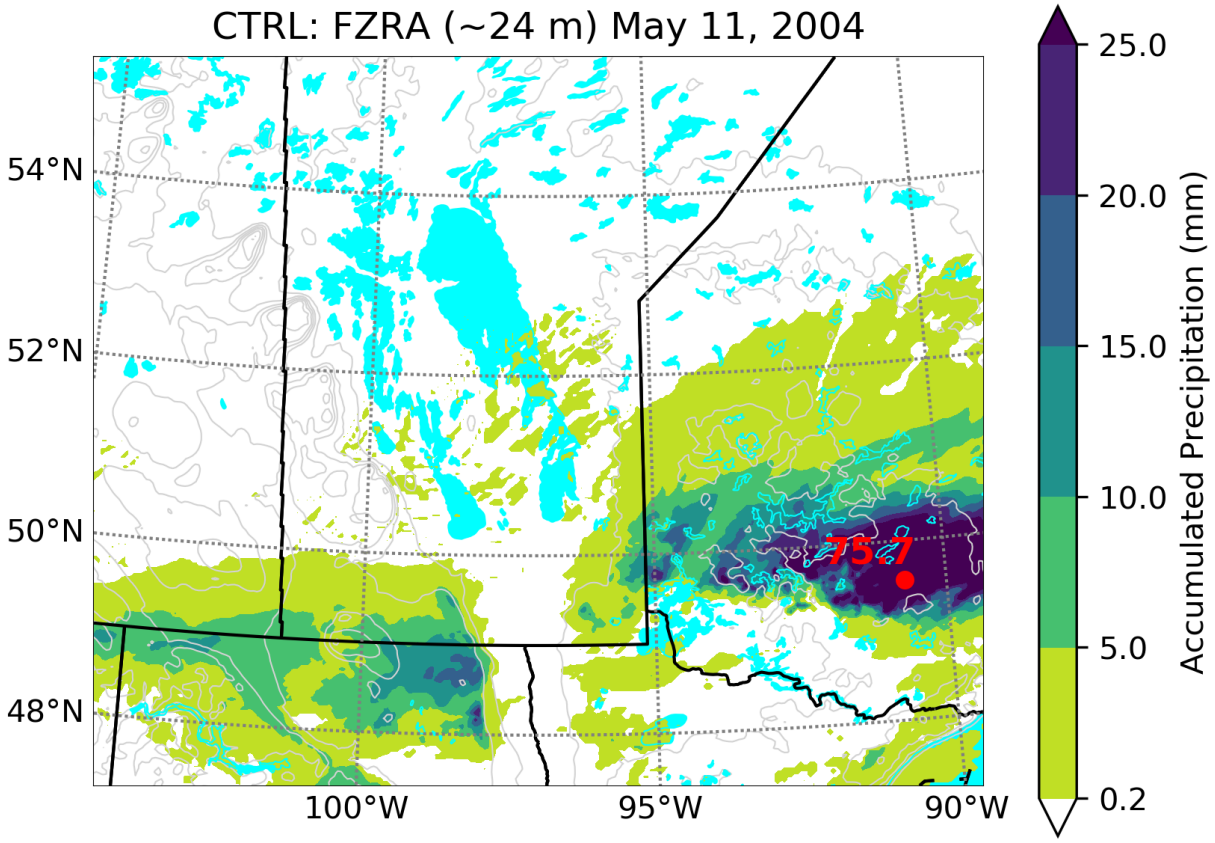

Figure 5.22: WRF CTRL accumulated freezing rain at the lowest model level (~24 m) for the May 11, 2004 event. The red dot indicates the maximum accumulation in the image.

5.3.2. Lake Effects

An additional consideration is that these events may also be influenced by the two large lakes within Manitoba: Lake Winnipeg and Lake Manitoba. Although freezing precipitation is typically associated with proximity to large water bodies, this is generally considered in relation to an ocean, not lakes (Cortinas et al. 2004).

There are two events within which lake effect may have contributed to freezing rain or wet snow. These were the October 13, 2006 event (Figure 5.23) and the October 4-5, 2012 event (Figure 5.24). Northerly subfreezing air flows lengthwise over the long fetch of Lake Winnipeg near sunset, while the temperature just above the surrounding land and lake is below and above

freezing, respectively. This causes temperatures downwind of the lake to be slightly above freezing as well, which allows for the generation of a wet snow, rain mixture.

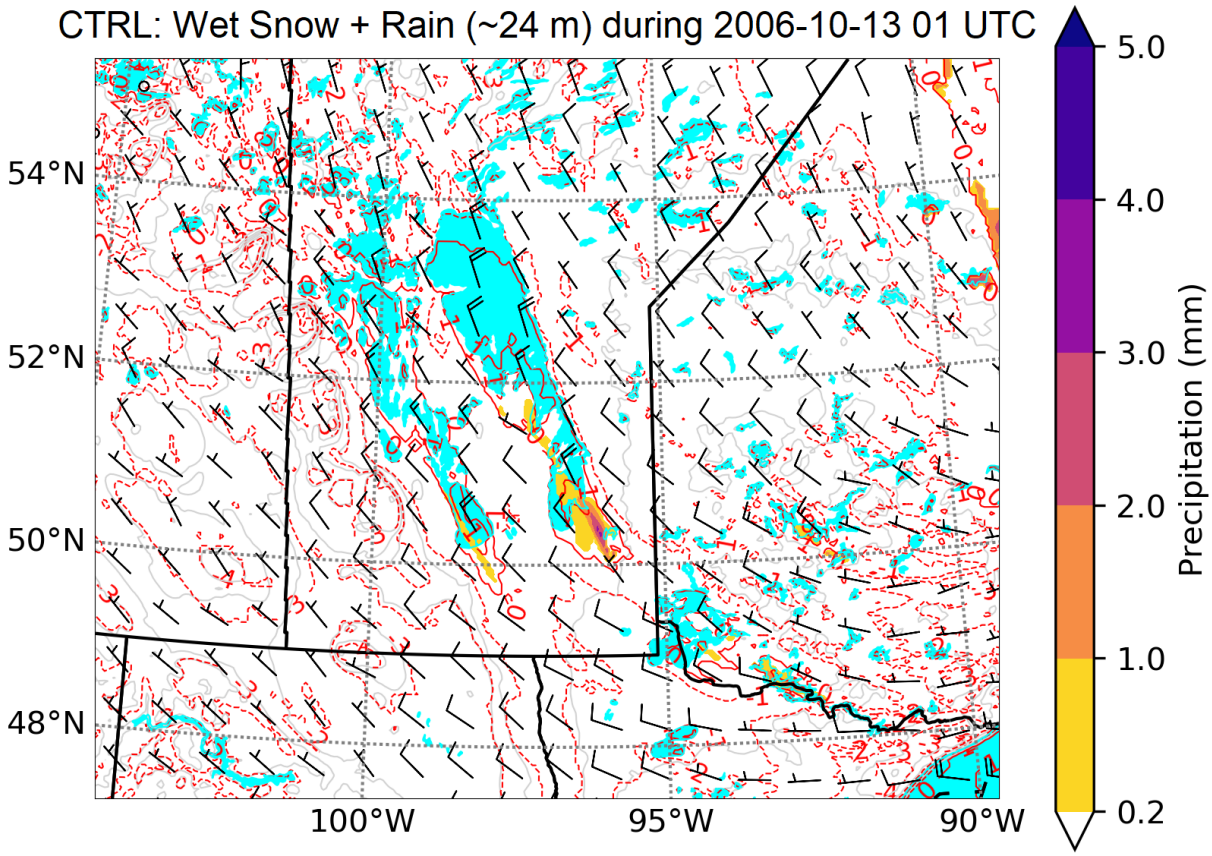

Figure 5.23: Lake effect wet snow, rain mixture during October 13, 2006 01 UTC in CTRL. Red contours indicate lowest model level (~24 m) wet-bulb temperature in °C with dashed and solid contours indicating temperatures < 0°C and ≥ 0°C, respectively. Coloured contours indicate the hourly accumulated precipitation. Wind barbs are in m s^{-1}.

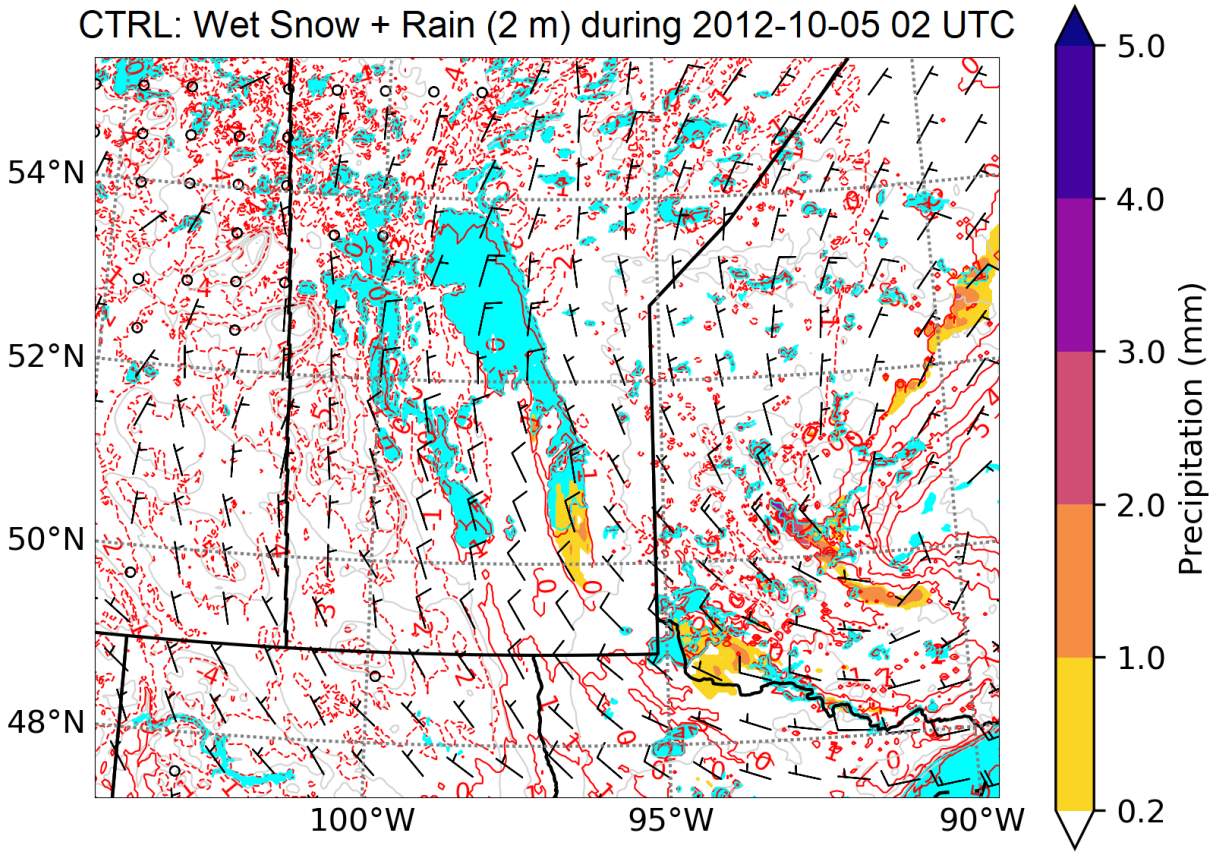

Figure 5.24: Lake effect wet snow, rain mixture during October 5, 2012 02 UTC in CTRL. Red contours indicate lowest model level (~24 m) wet-bulb temperature in °C with dashed and solid contours indicating temperatures < 0°C and ≥ 0°C, respectively. Coloured contours indicate the hourly accumulated precipitation. Wind barbs are in m s^{-1}.

The amount and spatial extent of precipitation generated in this process is relatively small (0.2-4 mm). However, it still contributes to these events and is included in the analysis of total accumulation, event length and other parameters.

5.4. Characterization of Surface Winds

The stress imparted on power lines with ice accreted on them is increased greatly by strong winds. There were 4 events in which winds in both WRF and the observations reached

speeds between 15 and 20 m s^{-1} (54 - 72 km h^{-1}). These were the May 11, 2004, October 5, 2005, December 14-19, 2005, and the October 13, 2006 events. The event with the strongest winds was the October 13, 2006 event (Figure 5.25), particularly in Portage la Prairie and Winnipeg. WRF did tend to underestimate the winds in the most extreme cases, however.

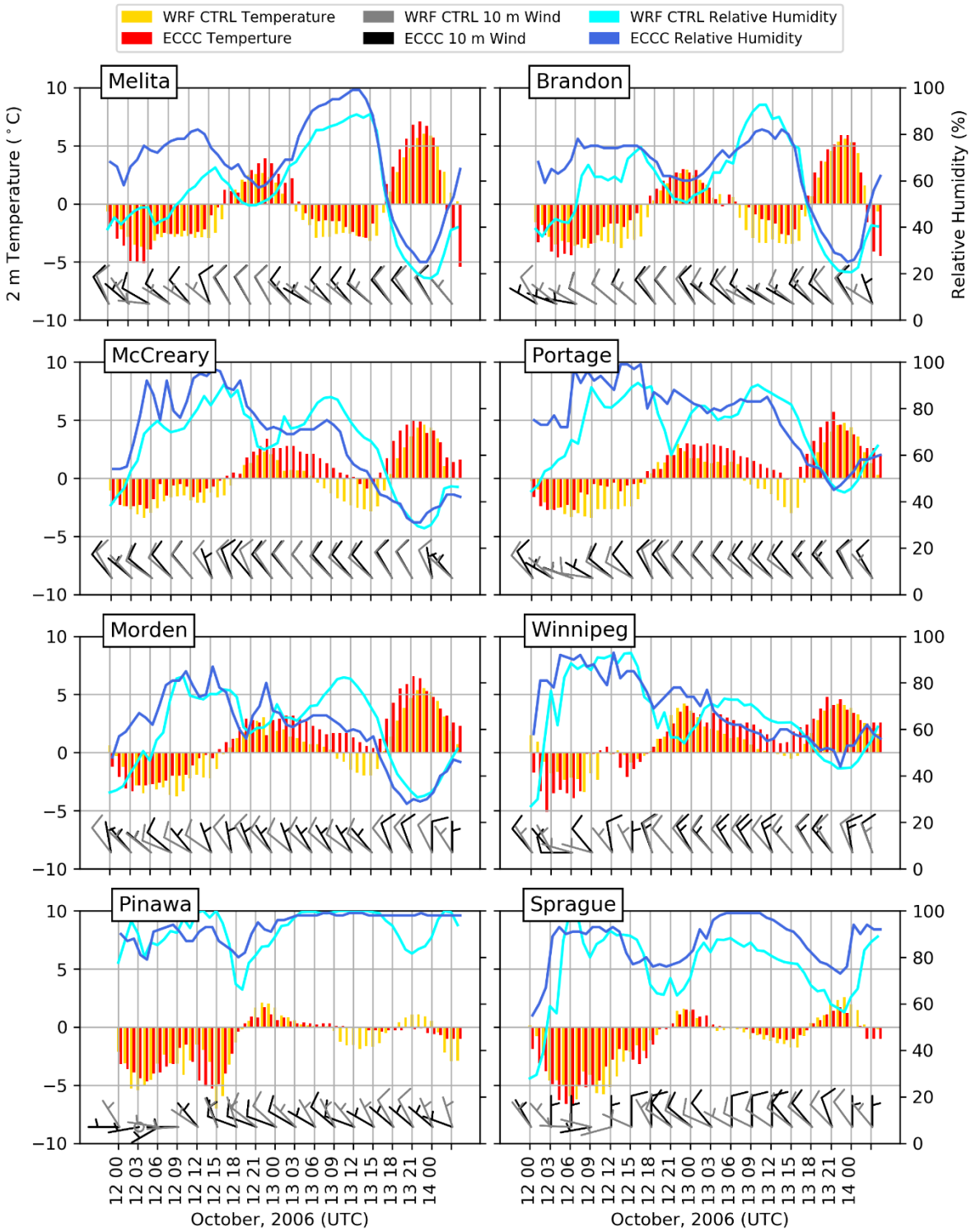

Figure 5.25: Time series comparing the surface (2 m) temperature (°C), relative humidity (%), and 10 m winds at 8 surface stations, and their attendant locations in WRF during the October 13, 2006 event. Temperature is indicated on the left and relative humidity is on the right. Winds are shown as wind barbs in m s^{-1}.

As well as the strength of the wind, its directionality is important when considering stresses exerted on a power line. Winds hitting the line closer to a normal angle will exert more force than at angles that are more acute or obtuse, which can put lines that are oriented in, for example, a north/south or east/west direction at more or less risk. To determine the overall strength of the wind in these events, and the predominant directionality, the U and V components during the event were plotted for the duration of each (Figure 5.26).

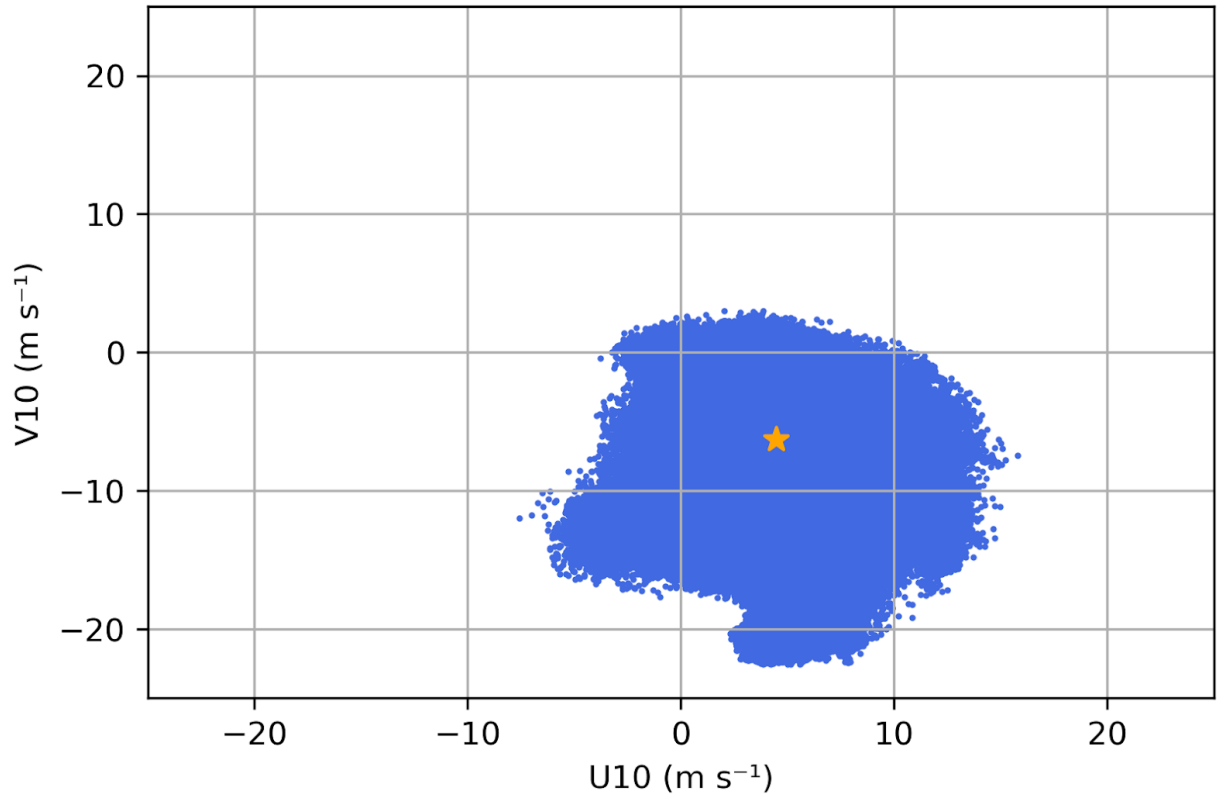

Figure 5.26: Scatterplot of the U and V wind components (m s^{-1}) at 10 m during the October 13, 2006 event in CTRL. The star indicates the overall mean wind for the event.

Six of the 8 events in WRF showed event sustained winds near or exceeding 20 m s^{-1} (70 km h^{-1}), which is significant. In the strongest event, as shown above, the winds peaked at nearly 80 km h^{-1}. The prevailing directionality of these winds was northerly, with 5 of the 6 events

having a strong northerly component. There were strong westerlies in 2 events and easterlies in 2 events (Figure 5.27), such as in the example below.

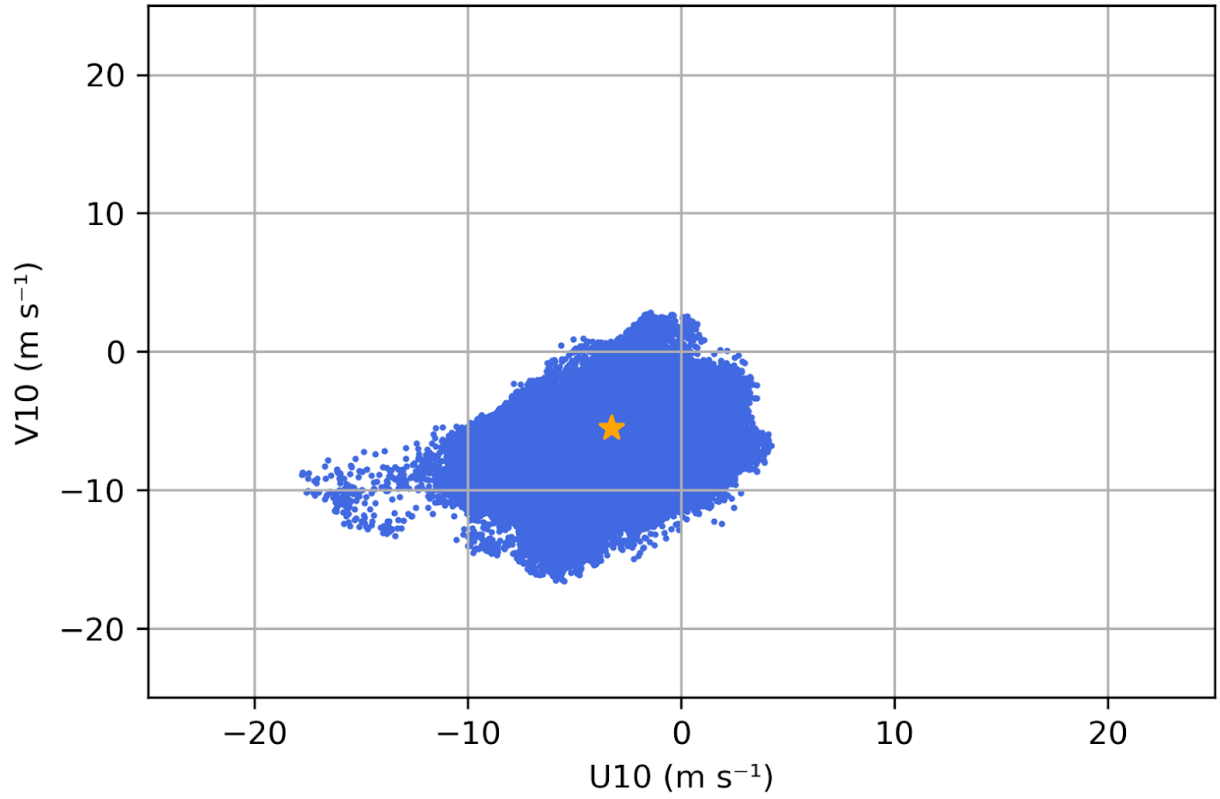

Figure 5.27: Scatterplot of the U and V wind components (m s^{-1}) at 10 m during the October 5, 2005 event in CTRL. The star indicates the overall mean wind for the event.

There was one event that lacked a strong northerly component, the December 14-19, 2005 event, still had a strong westerly component (Figure 5.28). Winds in the other directions were not necessarily weak, with values hovering around 30 km h^{-1}.

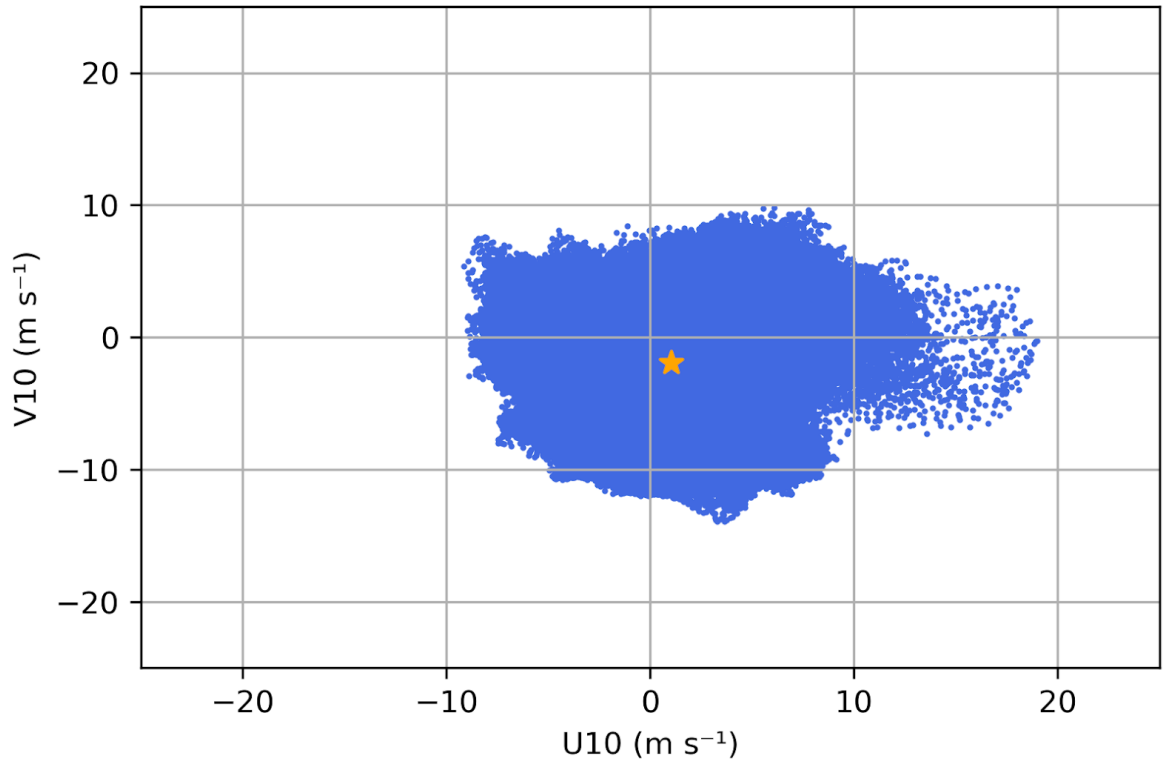

Figure 5.28: Scatterplot of the U and V wind components (m s^{-1}) at 10 m during the December 14-19, 2005 event in CTRL. The star indicates the overall mean wind for the event.

Based on these analyses, power lines oriented in a west/east manner were subjected to the strongest winds overall, with 5 of the 6 events with strong wind having the northerly component being strongest. The hazard to north/south oriented lines was slightly less, however 4 of the 6 events also had a strong zonal component. Two of the 8 events in WRF did not have particularly strong winds, which were the December 28, 2005 and January 12-18, 2006 event.

6. Events in the Pseudo-Global Warming Projection

6.1. Changes in Freezing Precipitation

Significant changes in the spatial extent/pattern, duration, and total accumulation of these events were associated with the pseudo-global warming simulations. Using the same contour plot analysis across the entire region from section 5.2, an approximate 13% increase in total accumulated precipitation was found comparing PGW to CTRL (Table 6.1). The changes were mixed in the case of freezing rain cases, with some types increasing or decreasing ±20%. Wet snow and mixtures were more consistent with an average amount increase of approximately 30%. Consistent between CTRL and PGW were the dominant precipitation types; these continued to be freezing rain alone and a wet snow, rain mixture, although there was a substantial increase (~83%) in the rain, graupel mixture.

A consistent pattern across almost all of the events was that freezing rain and wet snow tended to occur farther north in PGW compared to CTRL. Either their overall spatial extent increased and spread over these higher latitudes, or the focal point of the event (the area of maximum precipitation) occurred at a higher latitude. This pattern arises because the location of the 0°C isotherm shifts northward. This will be shown in subsequent Sub-Sections 6.1.1. and 6.1.2.

Table 6.1: Summary of the types of freezing precipitation and associated mixtures within the PGW simulation. The blue (orange) rows indicate freezing rain (wet snow) types, and the numbers in each cell represent the approximate maximum cumulative amount of precipitation (liquid equivalent in mm) for the event in Manitoba. The numbers used are derived from the contours in Figure 5.9 and similar figures.

Freezing Precipitation Types and Mixtures in PGW										
Type or Mixture	**Event**								**Type Total (mm)**	**Change vs. CTRL (%)**
	Nov 6-12, 2000	May 11, 2004	Oct 5, 2005	Dec 14-19, 2005	Dec 28, 2005	Jan 12-18, 2006	Oct 13, 2006	Oct 4-5, 2012		
Freezing Rain	**>25**	**0**	**0**	**5**	**5**	**25**	**5**	**0**	**65**	**-18.2**
Freezing Rain, Snow	**5**	**0**	**0**	**5**	**<5**	**10**	**5**	**0**	**30**	**-14.3**
Freezing Rain, Snow, Graupel	**<15**	**0**	**0**	**5**	**<10**	**10**	**5**	**0**	**45**	**18.2**
Freezing Rain, Graupel	**>25**	**0**	**0**	**5**	**<10**	**15**	**5**	**0**	**60**	**9.1**
Wet Snow	**<20**	**<25**	**5**	**10**	**<5**	**20**	**20**	**5**	**110**	**22.2**
Wet Snow, Rain	**20**	**>25**	**5**	**10**	**<10**	**25**	**>25**	**10**	**130**	**30**
Wet Snow, Rain, Graupel	**10**	**<20**	**0**	**5**	**<10**	**15**	**5**	**0**	**65**	**-7.1**
Rain, Graupel	**>25**	**>25**	**>25**	**0**	**5**	**5**	**0**	**>25**	**110**	**83.3**
Event Total (mm)	**145**	**95**	**35**	**45**	**60**	**125**	**70**	**40**	**615**	
Change vs. CTRL (%)	**107**	**-37**	**-73**	**350**	**100**	**400**	**27**	**-47**	**13**	

Using the sub-domain shown in Figure 5.11, we can infer more specific information about the overall changes in these precipitation types (Figure 6.1), as it includes data regarding spatial extent as well as maximum accumulations. Extracting precipitation information from each grid point shows different results from those in Table 6.1, where the amounts were estimated by set contours. Freezing rain shows an approximate 200-300% increase in accumulated precipitation over CTRL values, whereas wet snow shows a decrease of approximately 50%, with the exception of the rain, graupel mixture increasing by 100%.

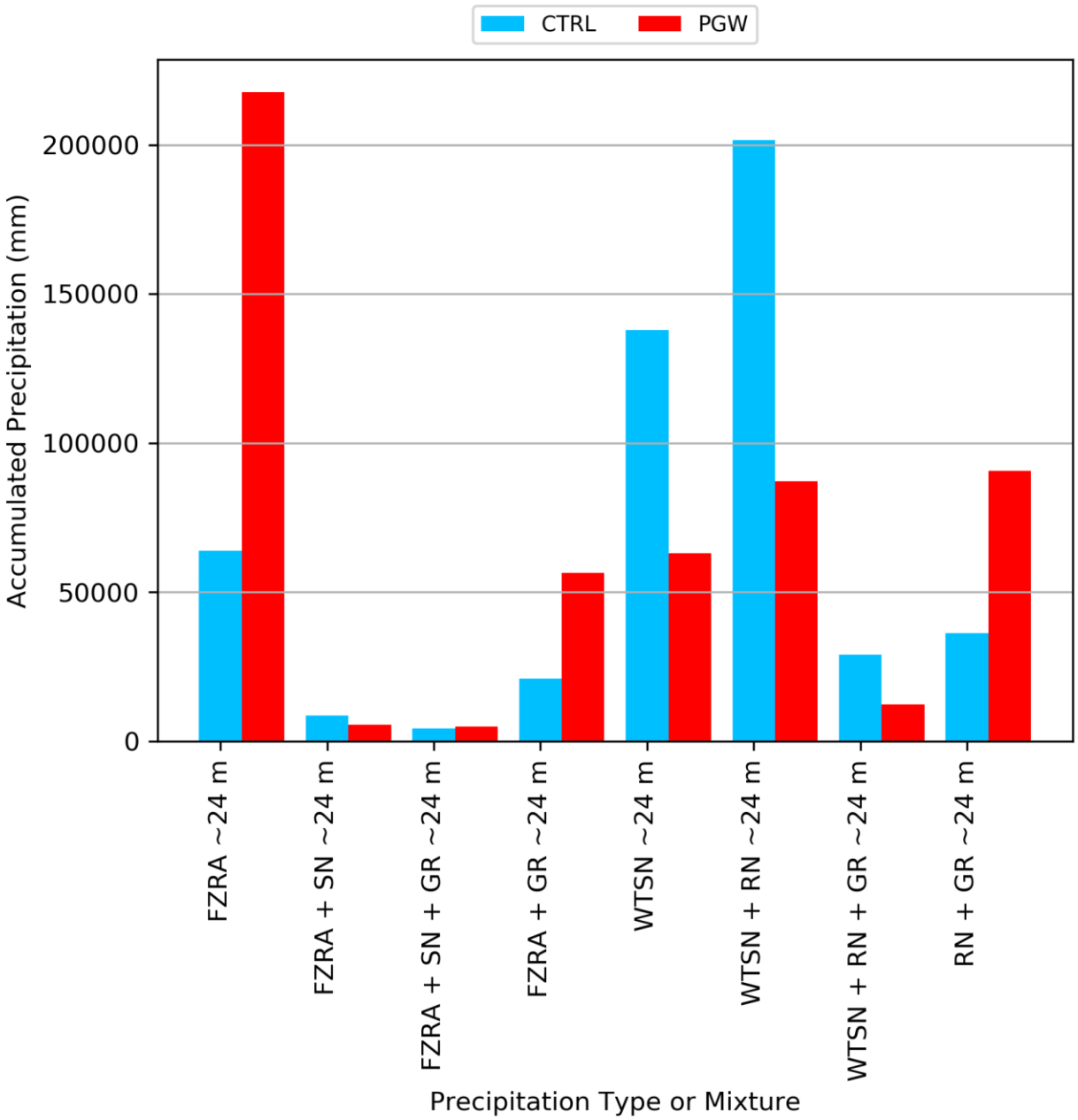

Figure 6.1: A summation of each of the types of accumulated precipitation at each WRF grid point for all of the events across southern Manitoba south of ~53°N. Precipitation type is indicated along the x-axis and the total amount is indicated by the y-axis.

The distribution of the types of precipitation shows a similar pattern to the totaled amounts (Figure 6.2). There is a marked increase in freezing rain, particularly in the upper 25% of accumulations. In CTRL, the maximum accumulation for freezing rain in any event was

approximately 26 mm, whereas in PGW it is more than double, at 58 mm. This suggests that, while freezing rain may not become more common overall, the extreme cases can be significantly enhanced.

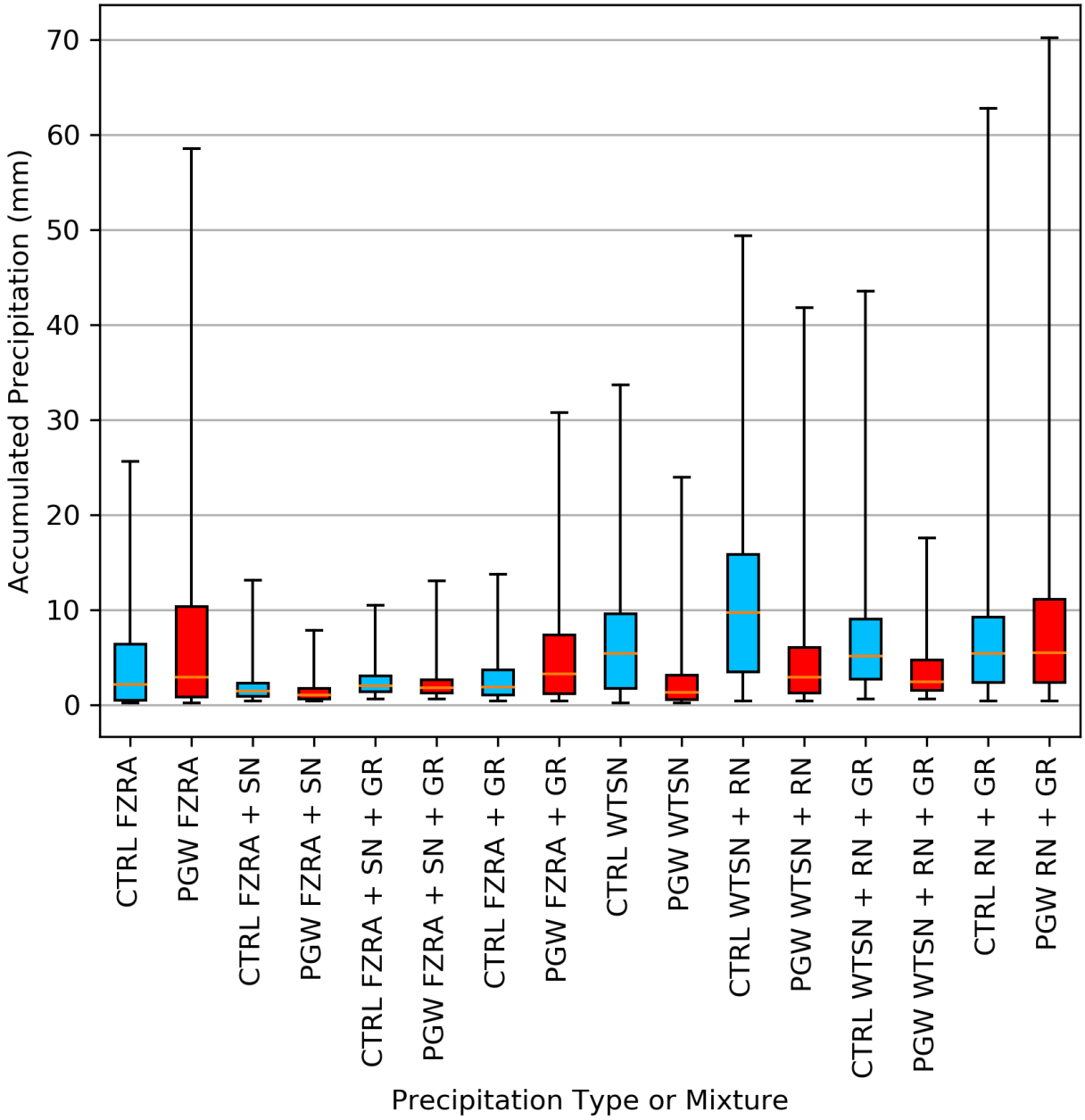

Figure 6.2: Distributions of the accumulated precipitation for each type of precipitation at each WRF grid point for all of the events across southern Manitoba. Precipitation type is indicated on the x-axis and the total amount is on the y-axis. Blue and red boxes are the CTRL and PGW values, respectively. The box and whisker plots illustrate the median, 25th and 75th percentiles, as well as the minimum and maximum values.

Changes in duration are slightly different to that of accumulation, with a subtler pattern of change (Figure 6.3). Generally, the same types of precipitation increase or decrease, though not to the same magnitude as the accumulation.

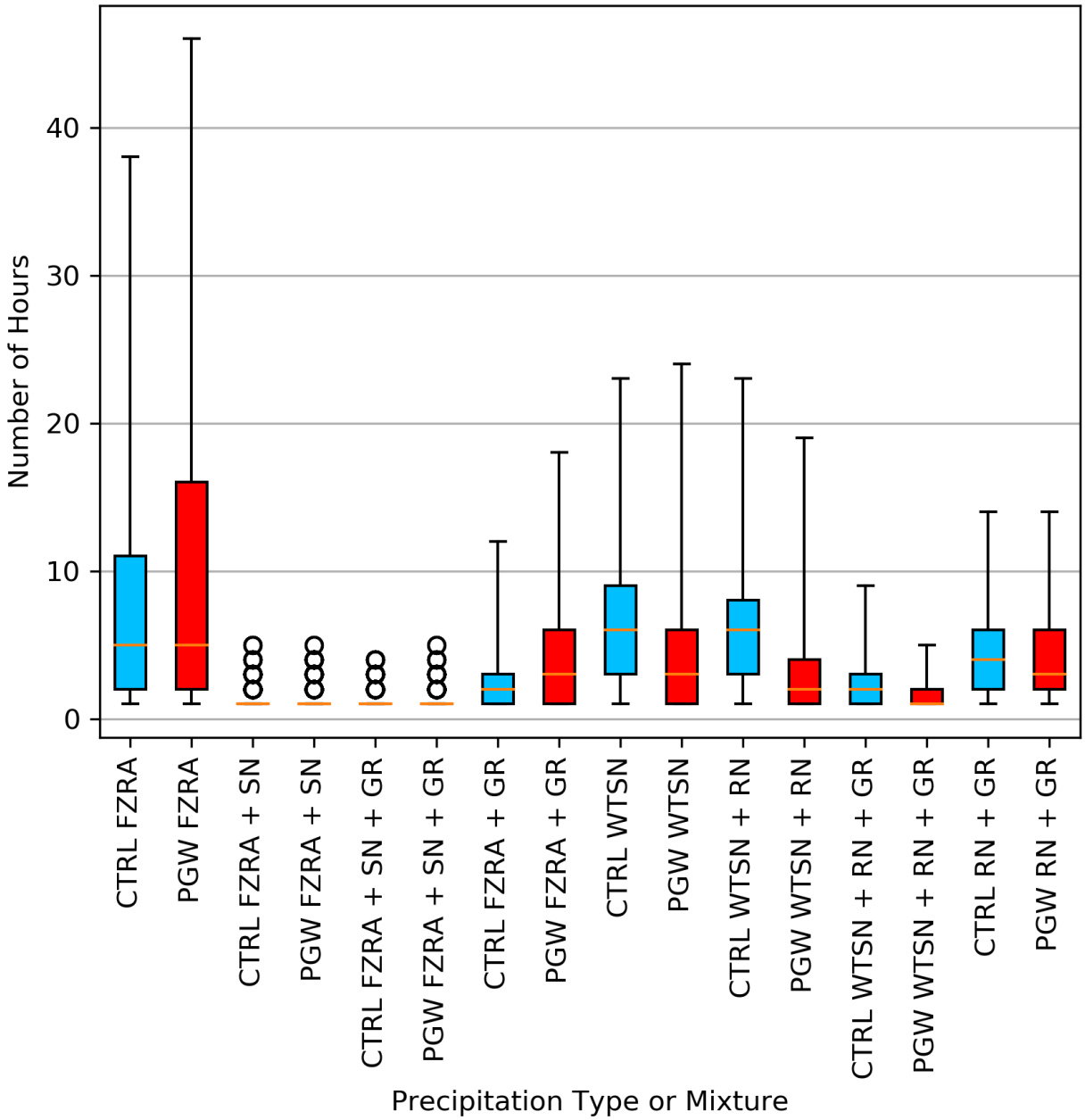

Figure 6.3: Distributions of the number of hours of precipitation for each type of precipitation at each WRF grid point for all of the events across southern Manitoba. Precipitation type is indicated on the x-axis and the total amount is on the y-axis. Blue and red boxes are the CTRL and PGW values, respectively. The box and whisker plots illustrate the median, 25th and 75th percentiles, as well as the minimum and maximum values. Circles indicate insufficient data to plot.

The dominant intensities of precipitation in PGW are similar to that of CTRL, with light intensity freezing precipitation being the most common (Figure 6.4). Heavy freezing precipitation is extremely rare in both simulations.

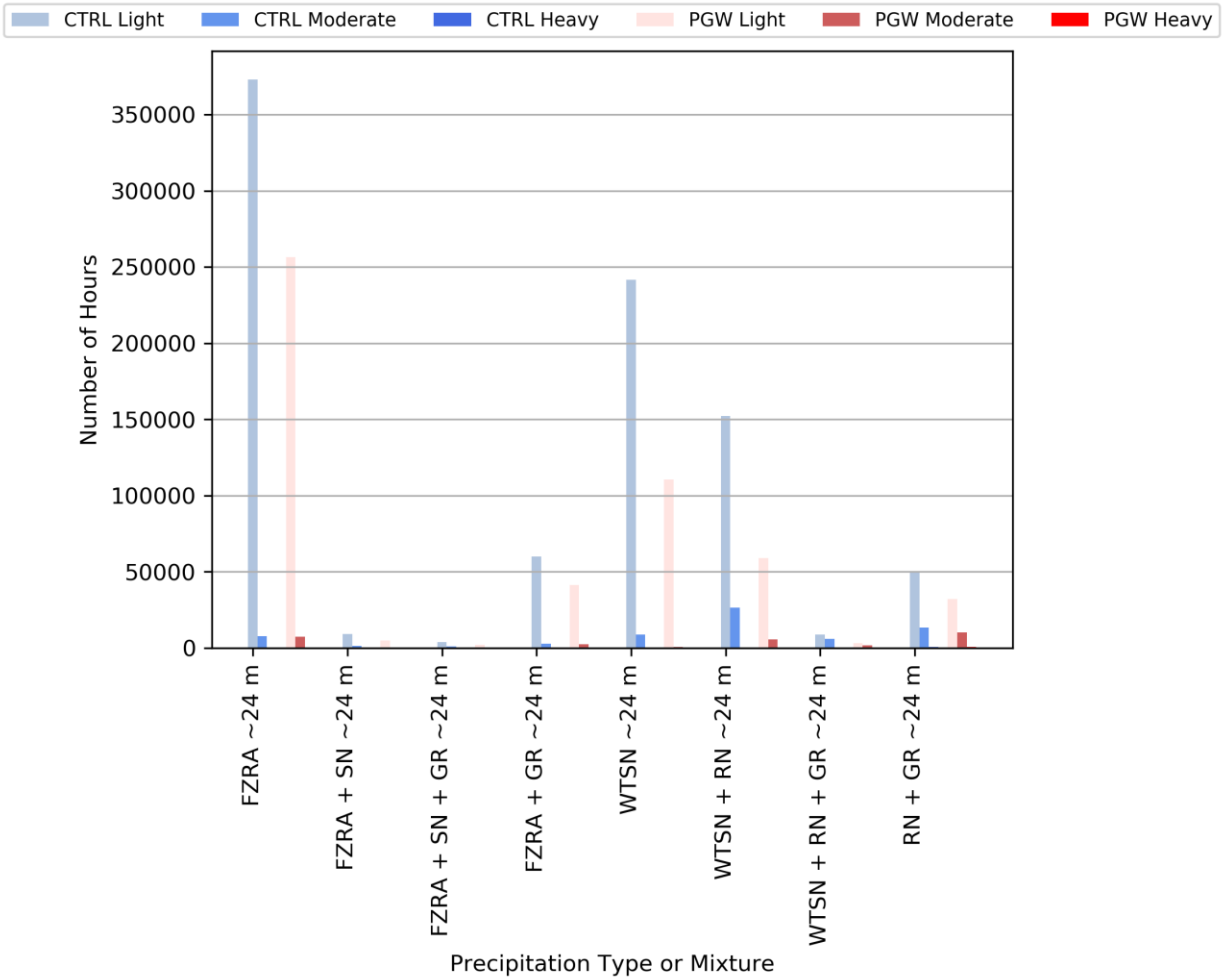

Figure 6.4: Intensity of freezing precipitation types in PGW compared to CTRL. Blue and red coloured bars represent CTRL and PGW, respectively.

A summary of overall statistics and changes in the means and maxes of freezing precipitation using the sub-domain is shown in Table 6.2. In general, the PGW simulation enhanced the freezing rain values, and reduced wet snow values. Freezing rain and mixtures' mean and maximum accumulation and duration increased between 24% and 59% on average. The intensity of this type was mostly unchanged. Wet snow and mixtures were reduced in all

aspects between 14% and 42% on average. The specific aspects of the individual events can still be seen in this summary, such as the significant enhancement of freezing rain in the November 6-12, 2000 event, which shows up as a 122% and 128% increase to mean and maximum accumulation.

Table 6.2: Summary of changes to mean and maximum freezing precipitation types and mixtures using the sub-domain for all of the events. Cell values represent the mean and maximum, separated with a slash. The type or mixture is listed in the leftmost column. The 2nd, 3rd, and 4th columns are the accumulation, duration, and intensity, respectively. Each of these is subdivided into CTRL, PGW, and % difference between CTRL and PGW sub-columns. The table groups freezing rain and mixtures and wet snow and mixtures using blue and orange, respectively. Beneath each group are the average values.

Summary of Changes to Mean and Maximum Freezing Precipitation									
Type or Mixture	**Accumulation (mm)**			**Duration (# Hours)**			**Intensity (mm h^{-1})**		
	CTRL	PGW	% Diff.	CTRL	PGW	% Diff.	CTRL	PGW	% Diff.
Freezing Rain and Mixtures									
Freezing Rain	3.9 / 25.6	8.7 / 58.5	122 / 128	7.2 / 38	10.6 / 46	47 / 21	0.5 / 5.2	0.8 / 7.0	51 / 34
Freezing Rain, Snow	1.9 / 13.1	1.3 / 7.9	-29 / -40	1.1 / 5	1.2 / 5	8 / 0	1.6 / 7.1	1.1 / 5.2	-34 / -26
Freezing Rain, Snow, Graupel	2.4 / 10.5	2.2 / 13.0	-11 / 24	1.2 / 4	1.2 / 5	-2 / 25	2.0 / 8.0	1.8 / 5.8	-9 / -27
Freezing Rain, Graupel	2.6 / 13.8	5.2 / 30.7	100 / 123	2.4 / 12	4.0 / 18	68 / 50	1.1 / 5.1	1.3 / 5.9	19 / 16
Average	**2.7 / 15.8**	**4.4 / 27.5**	**46 / 59**	**3.0 / 14.8**	**4.3 / 18.5**	**30 / 24**	**1.3 / 6.4**	**1.3 / 6.0**	**7 / -1**
Wet Snow and Mixtures									
Wet Snow	6.4 / 33.7	2.3 / 23.9	-64 / -29	6.5 / 23	4.1 / 24	-38 / 4	1.0 / 11.0	0.6 / 4.8	-43 / -57
Wet Snow, Rain	11.0 / 49.3	4.3 / 41.8	-61 / -15	6.2 / 23	3.2 / 19	-49 / -17	1.8 / 12.4	1.3 / 7.9	-24 / -37
Wet Snow, Rain, Graupel	7.2 / 43.5	3.4 / 17.6	-53 / -60	2.6 / 9	1.4 / 5	-46 / -44	2.8 / 17.9	2.5 / 9.8	-11 / -45
Rain, Graupel	7.6 / 62.8	8.3 / 70.2	8 / 12	4.5 / 14	3.9 / 14	-12 / 0	1.7 / 17.2	2.1 / 22.2	23 / 29
Average	**8.1 / 47.3**	**4.6 / 38.4**	**-42 / -23**	**4.9 / 17.3**	**3.1 / 15.5**	**-36 / -14**	**1.8 / 14.6**	**1.6 / 11.2**	**-14 / -27**

6.1.1. Freezing Rain and Mixtures

All of the freezing rain in the events changed, sometimes significantly (Table 6.3). All 8 of the events had at least some freezing rain, with 3 of them having freezing rain exclusively, which were in December and January, while the other 5 had both freezing rain and wet snow. Across all 8 events, freezing rain increased (decreased) in 3 (4) events. One of the 8 events had a similar accumulation and duration, but reduced extent. All events showed the freezing rain occurring farther north in PGW than in CTRL. Note that the extent and maximum latitude was determined qualitatively by visual inspection.

Table 6.3: Summary of the spatial characteristics, duration, and total accumulation of freezing rain for all the events in the CTRL simulations as well as in the PGW simulations. The latter data are shown in brackets. Green and red text indicates an increase and decrease, respectively.

Freezing Rain					
Event	Maximum Hours	Extent	Latitude of Maximum Precipitation	Maximum Latitude	Accumulation (mm)
Nov 6-12, 2000	31-35 (**41-43**)	+	52°N (**53°N**)	Domain edge (**Domain edge**)	20-30 (**≥50**)
May 11, 2004	16-20 (**0**)	-	50°N (**N/A**)	N/A	10-15 (**0**)
Dec 14-19, 2005	1-5 (**6-10**)	+	~50°N (**~53°N**)	~50°N (**~ 54°N**)	≤1 (**8-10**)
Dec 28, 2005	6-10 (**1-5**)	-	50°N (**~53°N**)	~50°N (**~ 52°N**)	5-10 (**≤2**)
Oct 5, 2005	1-2 (**0**)	-	51°N	51°N	≤5 (**0**)
Jan 12-18, 2006	11-15 (**21-23**)	+	~50°N (**51°N**)	~51°N (**53°N**)	5-10 (**20-25**)
Oct 13, 2006	1-2 (**1-2**)	-	55°N (**54°N**)	55°N (**54°N**)	≤5 (**≤5**)
Oct 4-5 2012	1-2 (**0**)	-	53°N (**N/A**)	53°N (**N/A**)	≤10 (**0**)

The two events with freezing rain that were enhanced the most were the November 6-12, 2000 event (Figure 6.5) and the January 12-18, 2006 event (Figure 6.6). In these events, both the spatial extent and amount of precipitation were greatly enhanced.

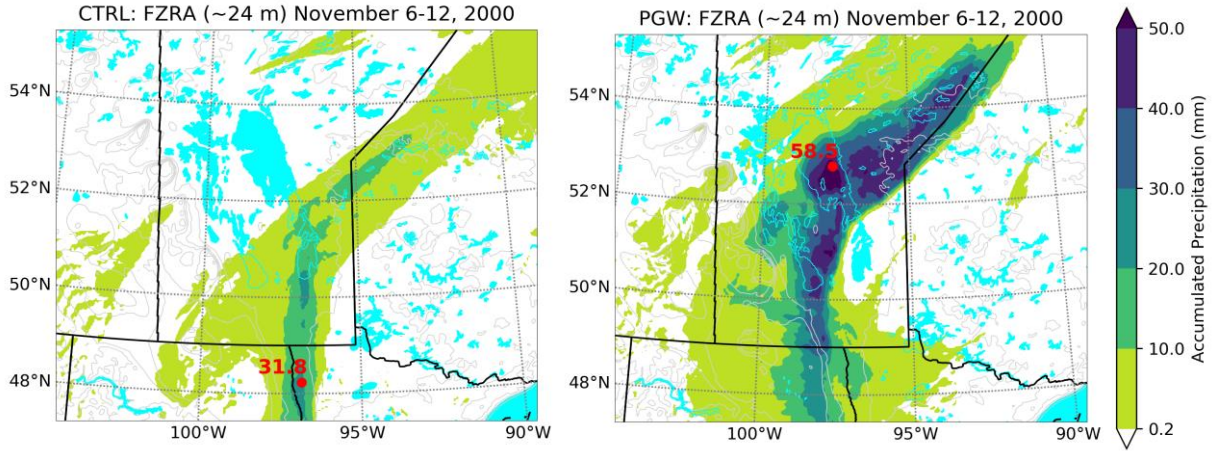

Figure 6.5: WRF PGW accumulated freezing rain at the lowest model level (~24 m) for the November 6-12, 2000 event in CTRL (left) and PGW (right). The red dot indicates the maximum accumulation in the image.

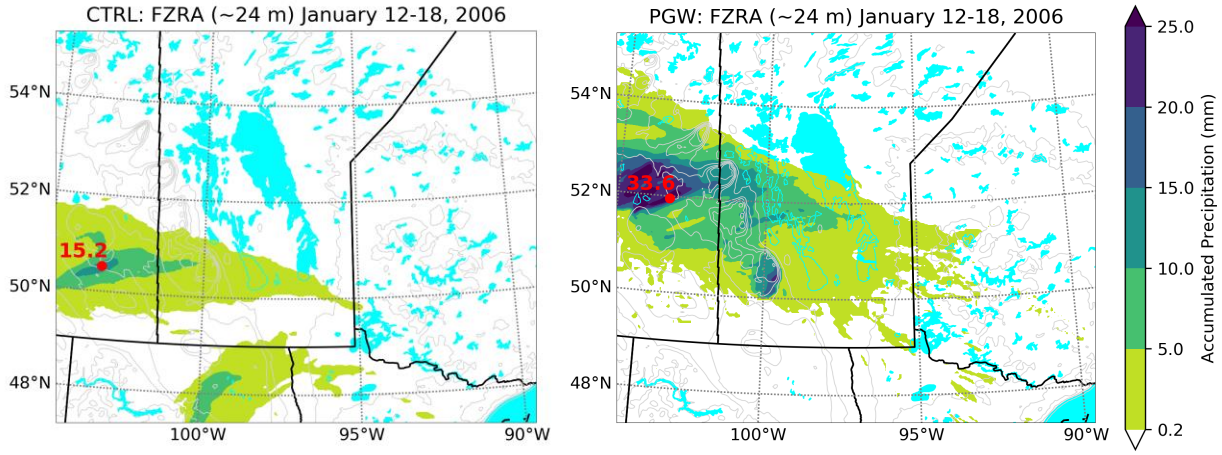

Figure 6.6: WRF PGW accumulated freezing rain at the lowest model level (~24 m) for the January 12-18, 2006 event in CTRL (left) and PGW (right). The red dot indicates the maximum accumulation in the image.

The mixed results for enhancement and reduction of freezing rain are consistent with previous studies, such as Groisman et al. (2016). The increase could be due to multiple factors. The relatively specific thermodynamic/dynamic conditions that produce freezing rain would

generally have continued in these future warmer climate simulations; these conditions are typically associated with an occluded midlatitude cyclone. However, water vapour would also be more readily available in these future climate simulations. This includes sub-cloud regions that would increase loss due to evaporation below cloud base. In contrast, rain would also be increased due to the warmer conditions and this would tend to decrease freezing rain occurrences.

6.1.2. Wet Snow and Mixtures

There were 5 events that had wet snow, all of which occurred alongside freezing rain (Table 6.4). In PGW, 1 increased in extent, duration, and accumulation, and another increased in extent, but had similar duration and lesser accumulation. The other 3 were reduced in extent, duration, and accumulation. All cases showed the precipitation occurring farther north or at the same latitude, compared to CTRL. There were 3 instances in which there was no wet snow in CTRL, but it was present in PGW, and all of these instances were in December and January.

Table 6.4: Summary of the spatial characteristics, duration, and total accumulation of wet snow for all the events in the CTRL simulations as well as in the PGW simulations. The latter data are shown in brackets. Green and red text indicates an increase and decrease, respectively.

Wet Snow					
Event	Maximum Hours	Extent	Latitude of Maximum Precipitation	Maximum Latitude	Accumulation (mm)
Nov 6-12, 2000	1-5 (**21-30**)	+	52°N (**55°N**)	52°N (**Domain edge**)	≤10 (**18-19**)
May 11, 2004	26-27 (**21-30**)	-	50°N (**51°N**)	53°N (**54°N**)	26 (**23-24**)
Dec 14-19, 2005	0 (**11-20**)	+	N/A (**52°N**)	N/A (**54°N**)	0 (**5-10**)
Dec 28, 2005	0 (**1-5**)	+	N/A (**53°N**)	N/A (**53°N**)	0 (**3-4**)
Oct 5, 2005	16-20 (**1-5**)	-	~50°N (**51°N**)	~51°N (**51°N**)	25-30 (**≤5**)
Jan 12-18, 2006	0 (**21-30**)	+	N/A (**53°N**)	N/A (**~54°N**)	0 (**15-20**)
Oct 13, 2006	21-25 (**21-22**)	-	51°N (**~54°N**)	Domain edge (**Domain edge**)	18-19 (**15-20**)
Oct 4-5, 2012	26-29 (**1-5**)	+	~50°N (**52°N**)	Domain edge (**52°N**)	10-20 (**≤10**)

The events with wet snow were reduced in most aspects. The most prominent example is the October 4-5, 2012 event, which was significant in CTRL, but was reduced to being nearly absent from Manitoba in PGW (Figure 6.7). A notable aspect of this event is that, although the reduction in spatial extent made it a non-hazard in Manitoba, the maximum accumulation nearly doubled, exceeding 60 mm.

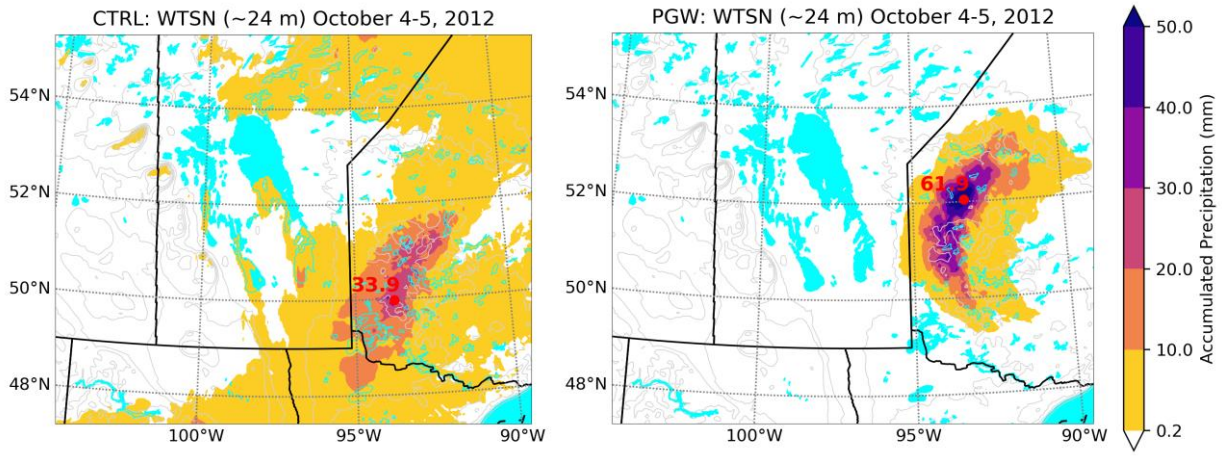

Figure 6.7: WRF PGW accumulated wet snow at the lowest model level (~24 m) for the October 4-5, 2012 event in CTRL (left) and PGW (right). The red dot indicates the maximum accumulation in the image.

Some of the events were reduced, but only in some aspects. The October 13, 2006 event is an example of an event that suffered a reduction in maximum accumulation, but wet snow was more widespread compared to CTRL (Figure 6.8).

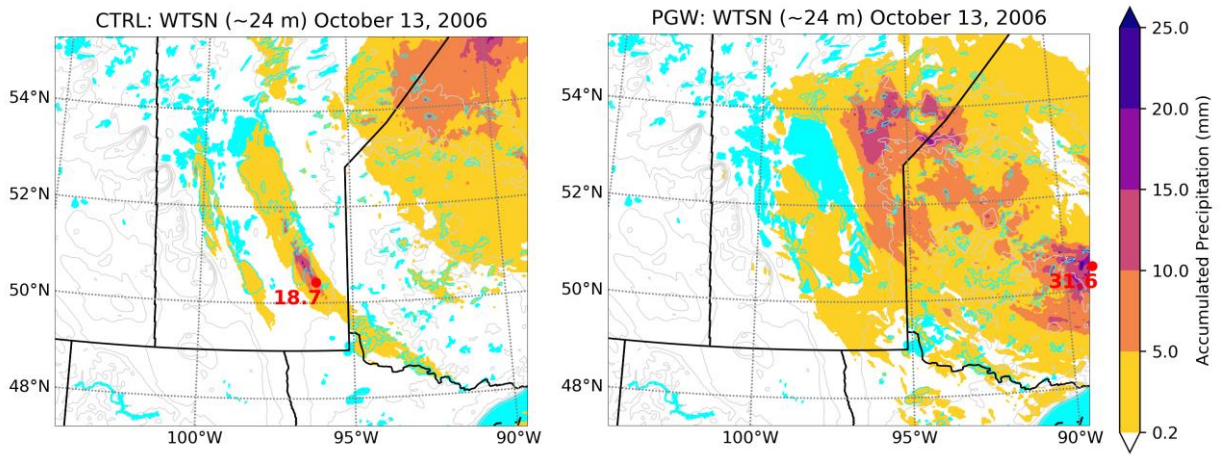

Figure 6.8: WRF PGW accumulated wet snow at the lowest model level (~24 m) for the October 13, 2006 event in CTRL (left) and PGW (right). The red dot indicates the maximum accumulation in the image.

Three events showed wet snow occurring in PGW whereas there was none in CTRL. A notable example of this is the January 12-18, 2006 event (Figure 6.9)

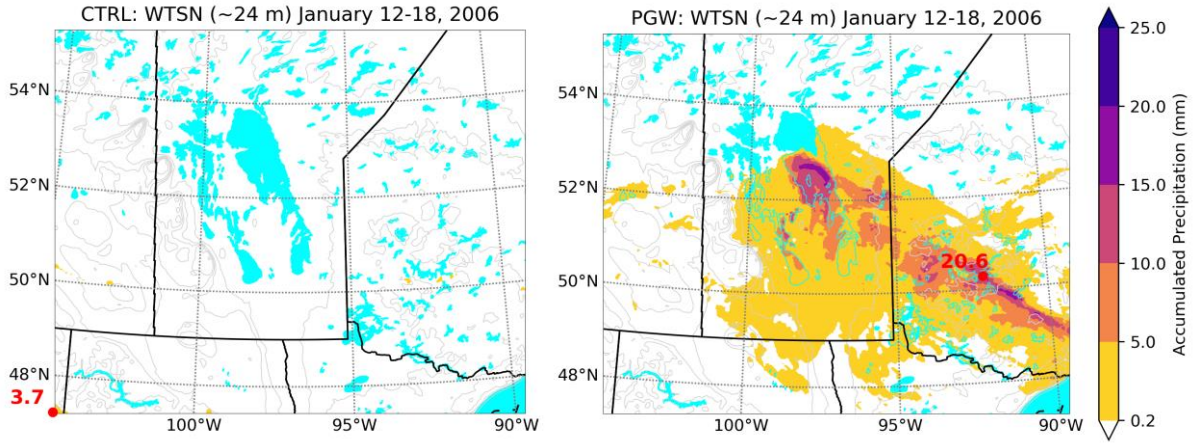

Figure 6.9: WRF PGW accumulated wet snow at the lowest model level (~24 m) for the January 12-18, 2006 event in CTRL (left) and PGW (right). The red dot indicates the maximum accumulation in the image.

Changes in wet snow occurrence/severity were more unidirectional. The decrease in the majority of events arises because, in the warmer climate, more of the precipitation melted completely into rain before reaching the surface.

There were 3 new instances of wet snow in PGW in all the coldest winter months (December and January). This suggests that these precipitation types, normally associated with the shoulder seasons, now occurred in the warmer winter months instead of "dry" snow.

6.2. Changes in Local Factors

There were some changes in local factors in PGW, which are summarized in Table 6.5. CTRL had 2 events, the May 11, 2004 and October 5, 2005 event, which showed terrain interaction taking place. There were 3 events in PGW with terrain interaction: November 6-12, 2000, May 11, 2004, and January 12-18, 2006. Lake effects were slightly reduced in PGW, with it only being evident in the October 13, 2006 event, slightly farther north.

Table 6.5: Summary of the local factors of terrain and lake effects for all events in the CTRL simulations as well as in the PGW simulations. The latter data are shown in brackets.

Precipitation Type	**Freezing Rain**		**Wet Snow**	
Event	Terrain	Lake Effects	Terrain	Lake Effects
Nov 6-12, 2000	No (**Yes**)	No (**No**)	No (**No**)	No (**No**)
May 11, 2004	Yes (**No**)	No (**No**)	Yes (**Yes**)	No (**No**)
Dec 14-19, 2005	No (**No**)	No (**No**)	No (**No**)	No (**No**)
Dec 28, 2005	No (**No**)	No (**No**)	No (**No**)	No (**No**)
Oct 5, 2005	No (**No**)	No (**No**)	Yes (**No**)	No (**No**)
Jan 12-18, 2006	No (**Yes**)	No (**No**)	No (**Yes**)	No (**No**)
Oct 13, 2006	No (**No**)	No (**No**)	No (**No**)	Yes (**Yes**)
Oct 4-5 2012	No (**No**)	No (**No**)	No (**No**)	Yes (**No**)

6.2.1. Terrain

Terrain interaction occurred in 3 events in the PGW simulation, compared with 2 in CTRL. One example is from the PGW version of the May 11, 2004 event (Figure 6.10), which shows a reversal of the precipitation pattern seen in CTRL (Figure 5.18) in which a wet snow, rain mixture is concentrated at the top of Riding Mountain instead of the lower areas to the east. A cross section shows snow falling into an above freezing layer at the peak of Riding Mountain (Figure 6.11). Small gravity wave-like perturbations in the temperature field show that there was localized increased vertical motion from upslope flow; these motions may have been enough to

induce the production of snow. As the night progressed, radiational cooling, possibly enhanced by the sublimation of falling snow, caused temperatures in the immediate area to drop below freezing, halting the wet snow.

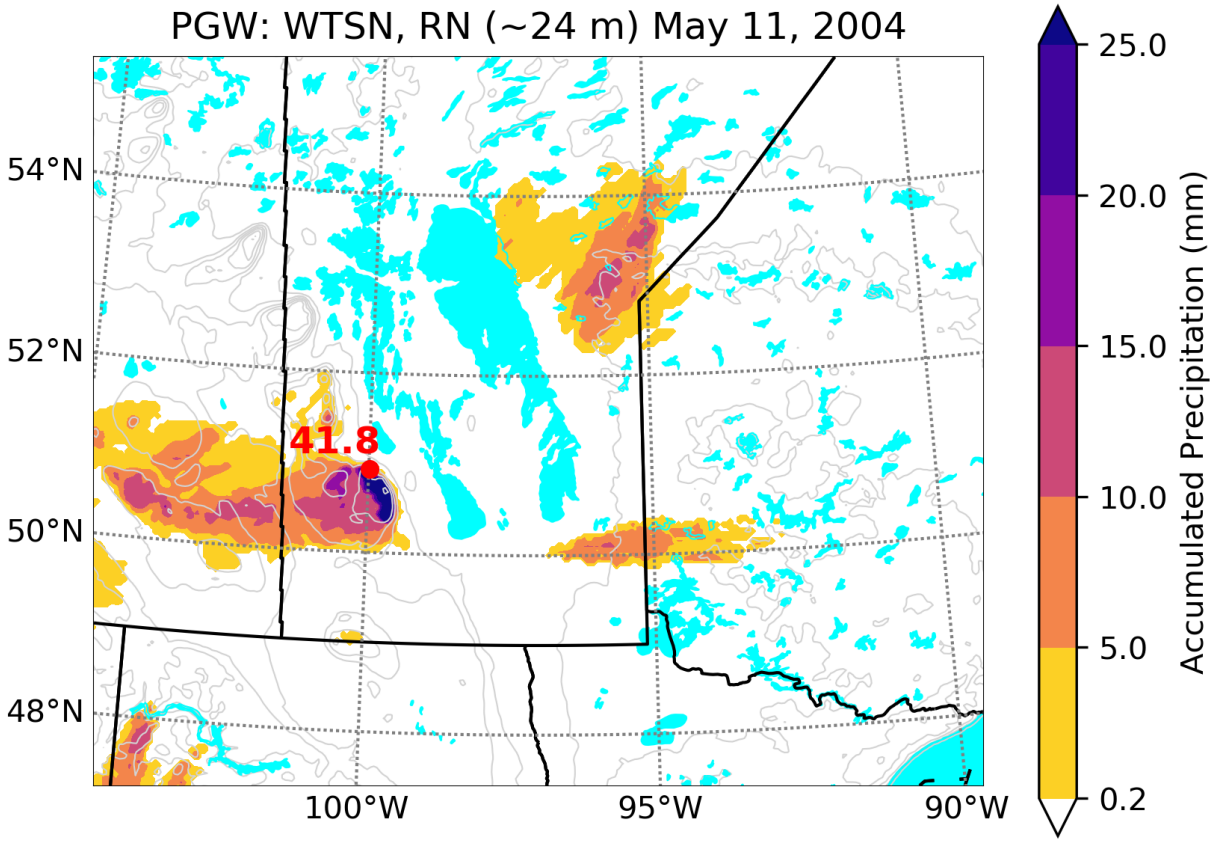

Figure 6.10: WRF PGW accumulated wet snow, rain mixture at the lowest model level (~24 m) for the May 11, 2004 event. The red dot indicates the maximum accumulation in the image.

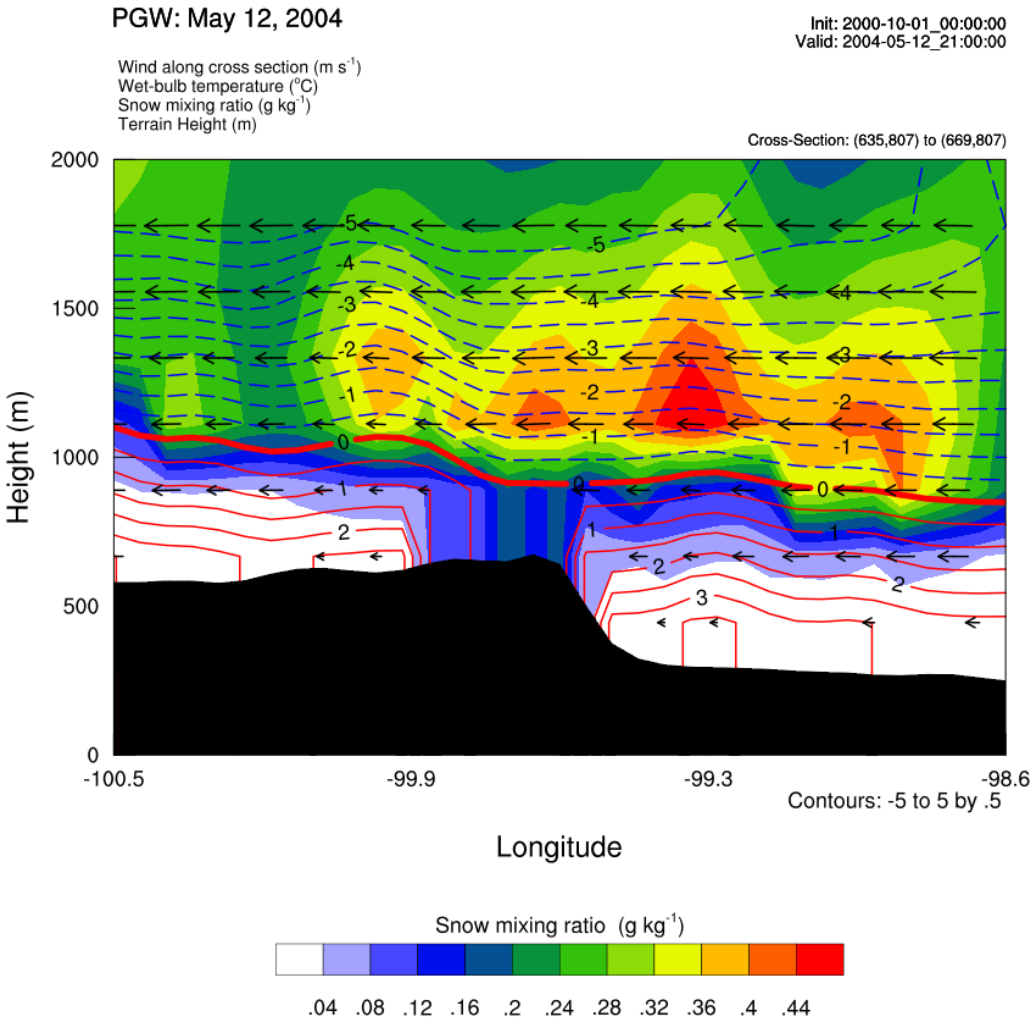

Figure 6.11: Vertical cross-section depicting a wet snow situation over Riding Mountain on May 12, 2004 at 21 UTC in the WRF PGW simulation. Coloured contours are the snow mixing ratio. The dashed blue, solid thick red, and solid red isolines indicate temperatures below, at, and above 0°C, respectively. Wind speed and direction are indicated with arrows. The black area is the terrain.

This flow pattern and temperature differential can assist in the generation of freezing rain and mixtures in a similar way. In the PGW simulation of the January 12-18, 2006 event, air that flowed up the slopes of Riding Mountain was cooled such that temperatures at the top were sub-freezing. Freezing rain and mixtures were enhanced at the top, whereas precipitation falling at the base was mostly rain (Figure 6.12).

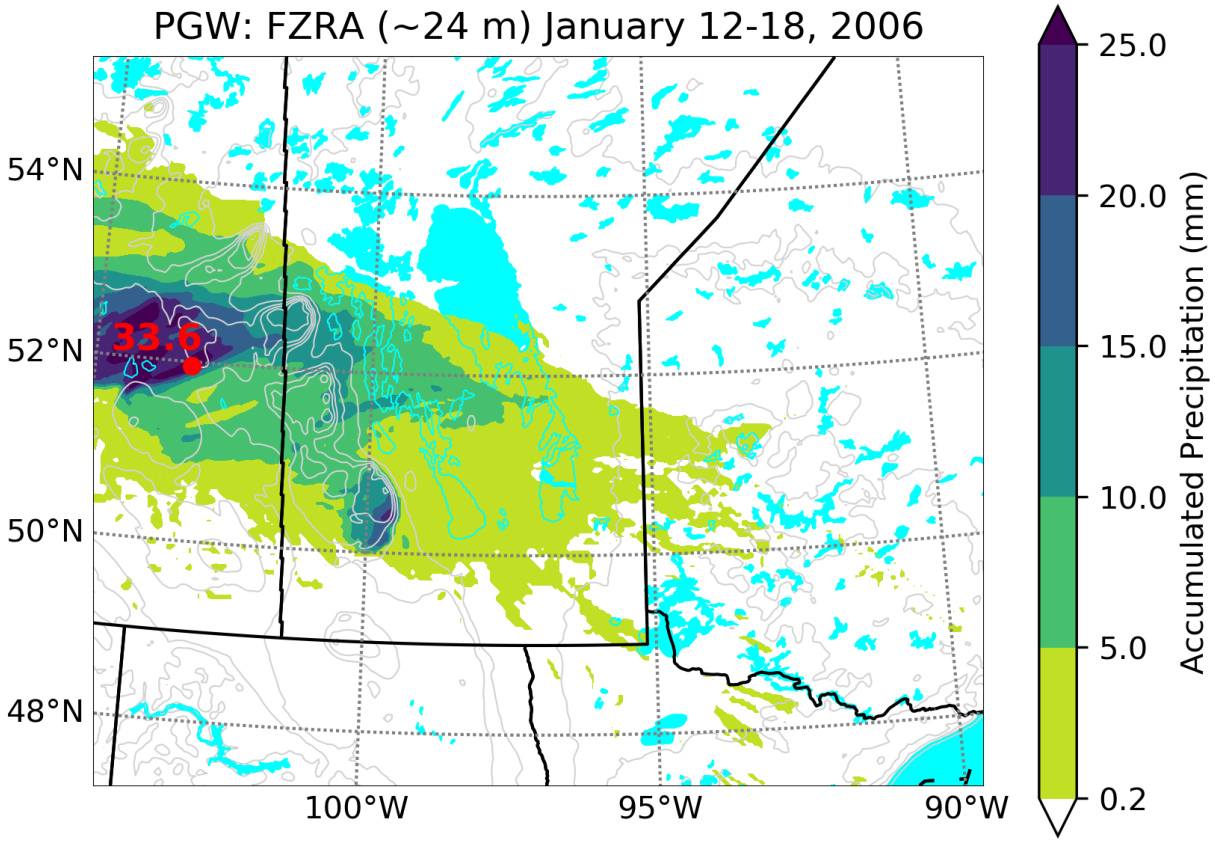

Figure 6.12: WRF PGW accumulated freezing rain at the lowest model level (~24 m) in the January 12-18, 2006 event. The red dot indicates the maximum accumulation in the image.

Cross sections suggest many potential mechanisms acting at once in this event. These include an inversion aloft entering the province from the west, localized heating along the slopes possibly due to latent heat release from the freezing of raindrops, as well the upslope flow that was also observed in the prior event that was discussed (Figures 6.13 - 6.15). A longer time series of this event is shown in Appendix C.

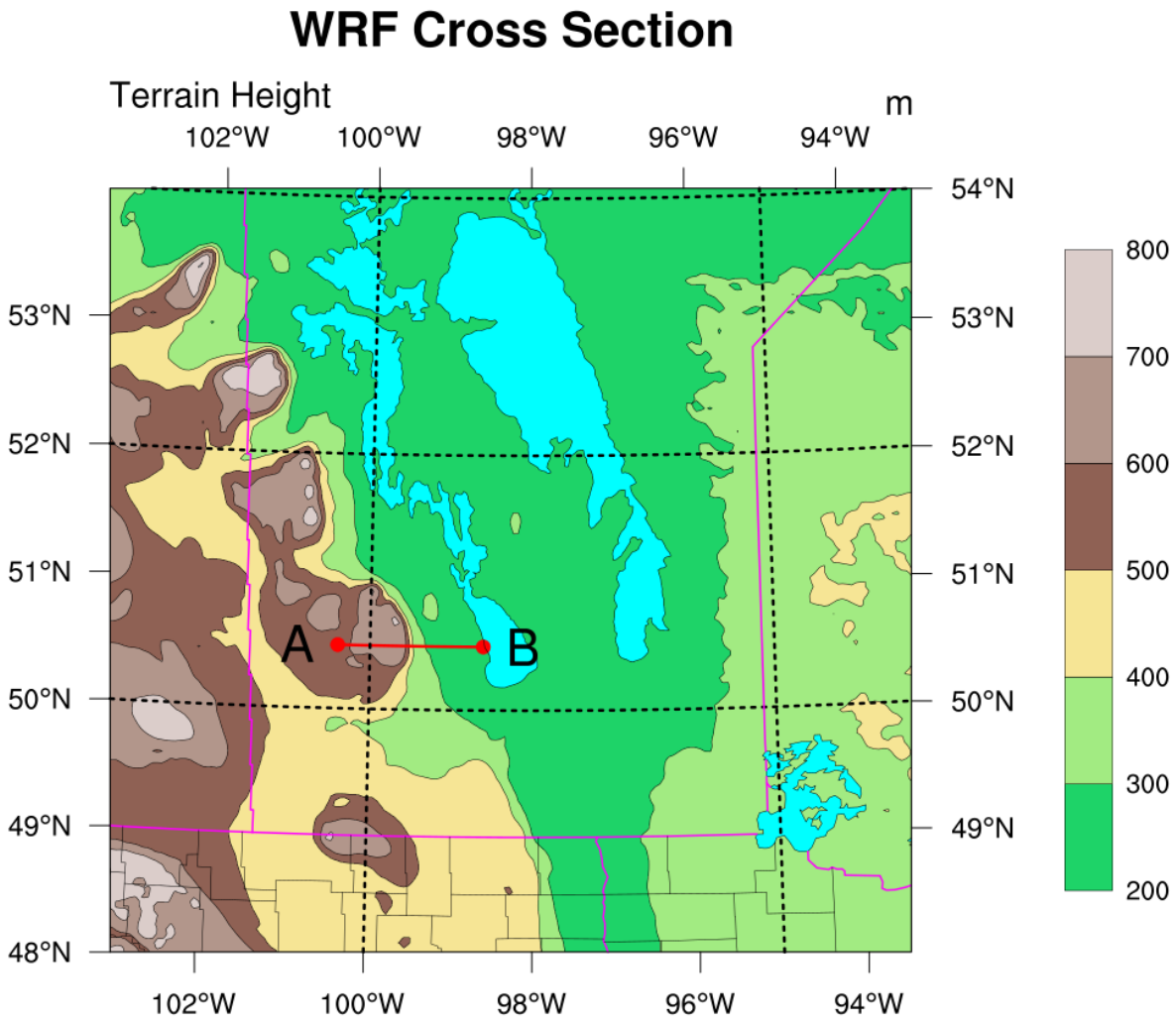

Figure 6.13: Location of vertical cross-section in Figures 6.14 and 6.15. Coloured contours indicate the terrain height (m). The cross section is along the red line from A to B.

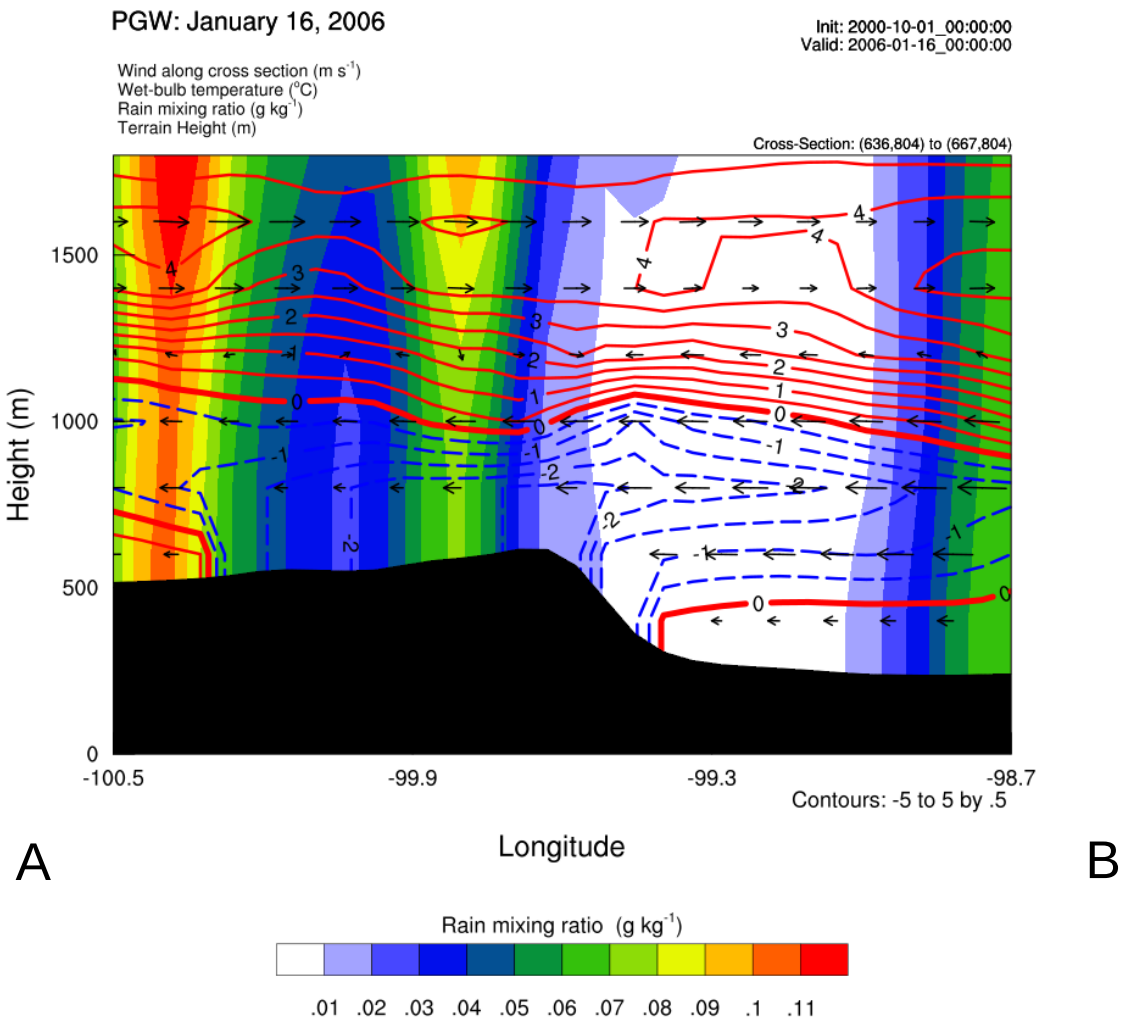

Figure 6.14: Vertical cross-section depicting a wet snow situation over Riding Mountain on January 16, 2006 at 00 UTC in the WRF PGW simulation. Coloured contours are the rain mixing ratio. The dashed blue, solid thick red, and solid red isolines indicate temperatures below, at, and above 0°C, respectively. Wind speed and direction are indicated with arrows. The black area is the terrain.

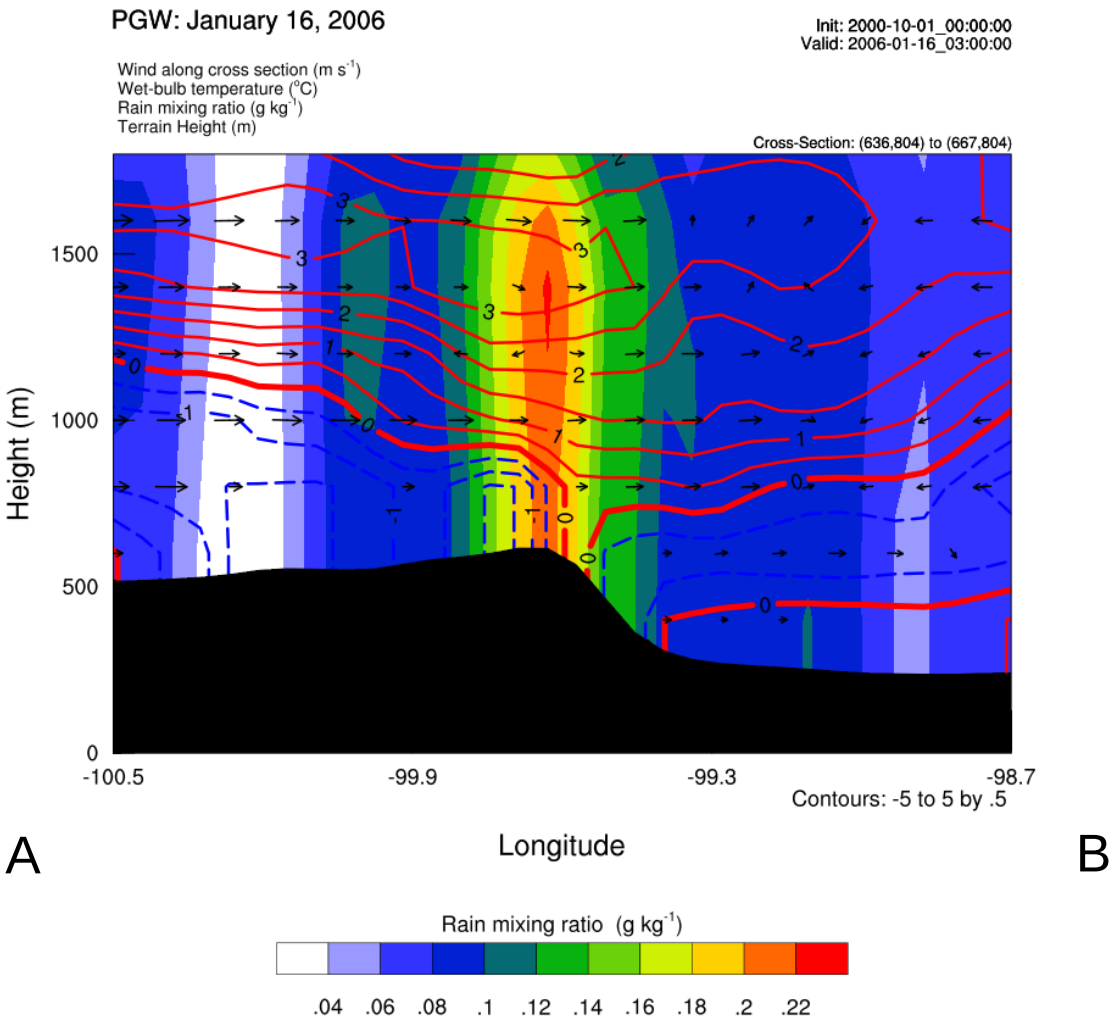

Figure 6.15: Vertical cross-section depicting a wet snow situation over Riding Mountain on January 16, 2006 at 3 UTC in the WRF PGW simulation. Coloured contours are the rain mixing ratio. The dashed blue, solid thick red, and solid red isolines indicate temperatures below, at, and above 0°C, respectively. Wind speed and direction are indicated with arrows. The black area is the terrain.

6.2.2. Lake Effects

The influence of the lakes on freezing precipitation was reduced in PGW compared to CTRL. In the October 13, 2006 event, there was still a modicum of precipitation being generated on the flanks of the lakes, though it was slightly farther north (Figure 6.16). The 2012 event, which was the other event with lake effects, did not have any precipitation generated through

these means. The event in PGW was significantly reduced in spatial extent and was almost absent from Manitoba.

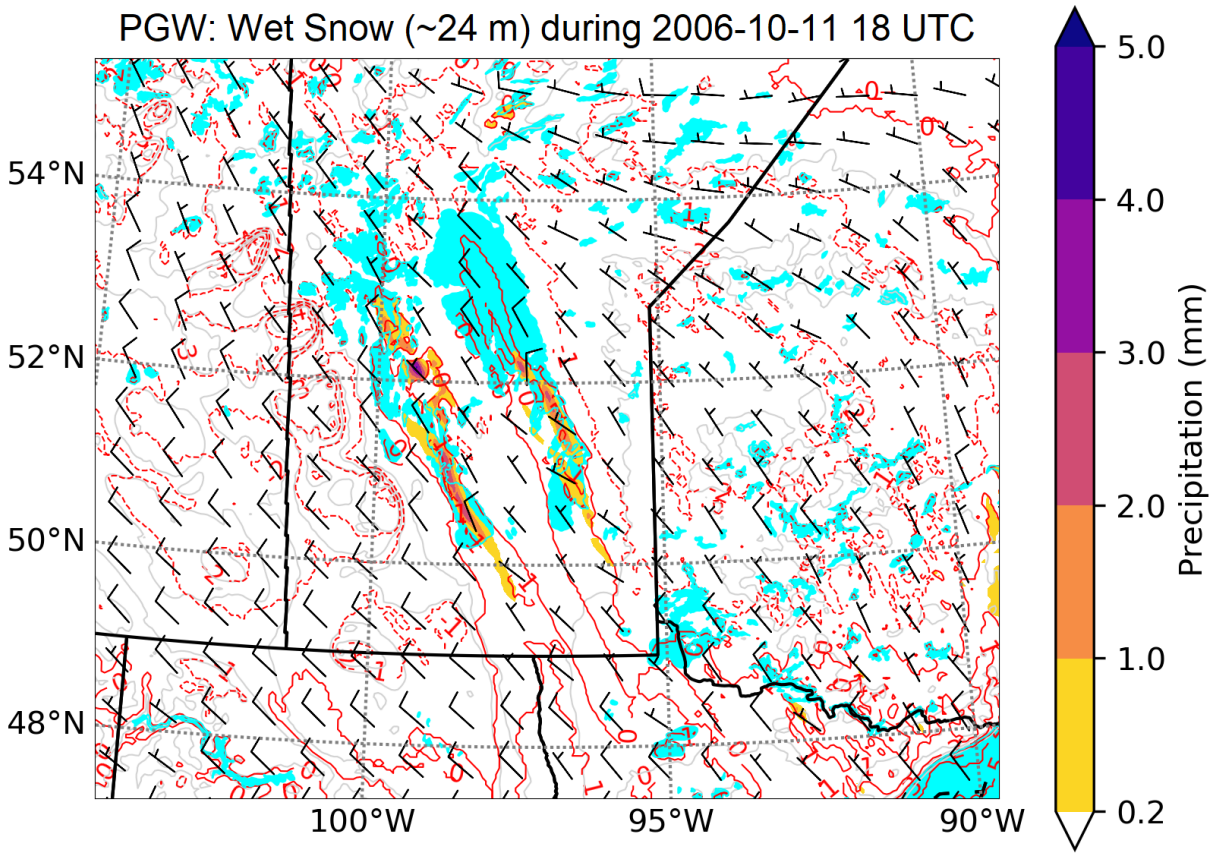

Figure 6.16: Lake effect precipitation being generated during the October 13, 2006 event in the PGW simulation. Red solid and dashed contours indicate wet-bulb temperatures above and below 0°C, respectively. Coloured contours indicate precipitation accumulation. Winds are indicated with wind barbs in m s^{-1}.

None of the other events in PGW generated any significant detectable lake effect precipitation.

6.3. Changes in Surface Winds

The surface winds saw no discernible changes to either their overall direction or strength in PGW. Figure 6.17 shows a scatterplot comparing the U and V wind components of CTRL and PGW for October 13, 2006, which had the strongest winds of all the events. Similar scatterplots for all of the events show little to no change as well.

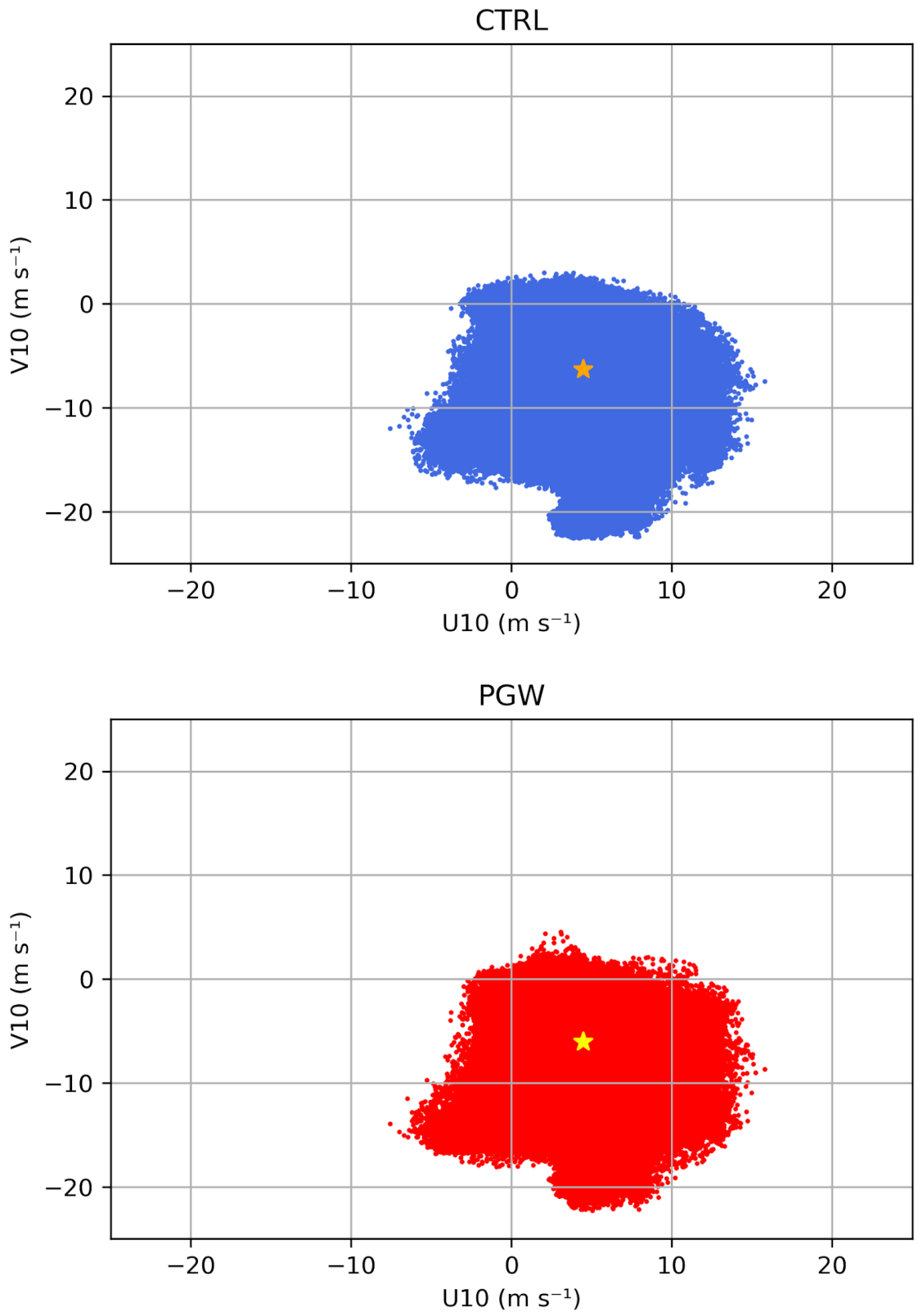

Figure 6.17: Scatterplot showing the U and V 10 m winds within the CTRL and PGW simulations. The stars in each plot indicate the mean winds for each simulation.

The 8 stations used for evaluation in Section 4.3 can also be used for examining wind changes in the PGW simulations. Figure 6.18 shows a comparison between PGW and CTRL for the October 13, 2006 event. The winds show a similar pattern of little to no change, often being identical, shown by the wind barbs overlapping.

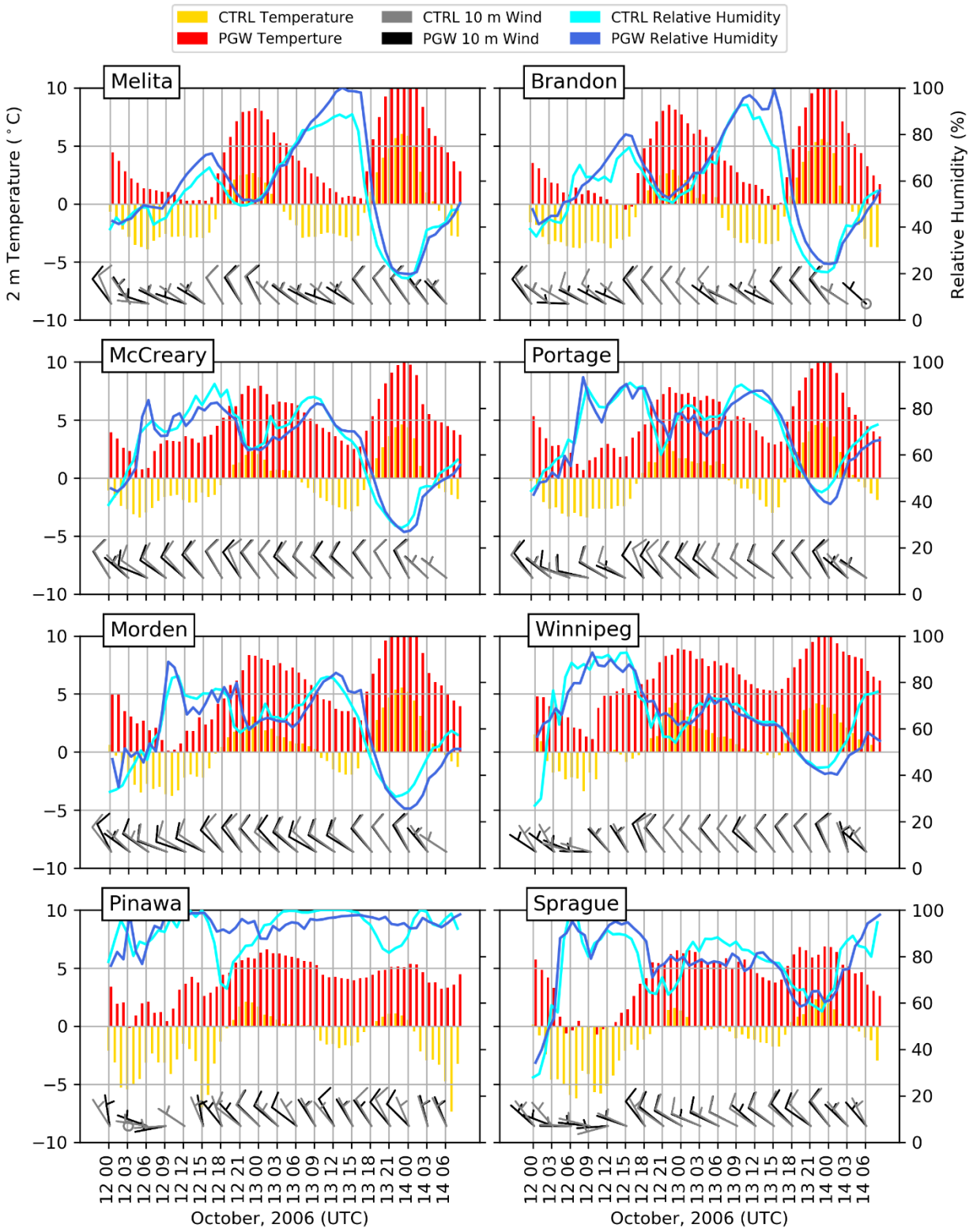

Figure 6.18: Time series comparing 2 m temperature, relative humidity, and 10 m winds between CTRL and PGW for the same 8 stations used in the evaluation of WRF.

7. Concluding Remarks and Future Work

7.1. Concluding Remarks

This thesis has examined several significant impacts from freezing rain and wet snow events that have impacted Manitoba. Multiple conclusions can be drawn from this study.

Manitoba occasionally experiences significant impacts from freezing rain and wet snow events, which occur every few years and sometimes multiple times in the same year. These events can affect infrastructure a great deal, including Manitoba Hydro. For them, the impacts include physical damage to their hydroelectric transmission/distribution network, due to the conductor and/or line being stressed from the additional weight and force exerted on them via accretion and wind.

Manitoba Hydro provided a list of 10 different events spanning approximately the past 3 decades. All featured one or a mixture of freezing rain, wet snow, and strong winds. These 10 events were examined with a variety of observational and model datasets.

The primary model dataset used in the analysis was output from the Weather Research and Forecasting (WRF) model that simulated many of these events as well as their features under a pseudo-global warming (PGW) assumption. This method allows for assessment of climate sensitivities assuming thermodynamically-driven change, although it has limitations in that it is not a robust prediction of a future climate, and it constrains changes in synoptic-scale flows and thus storm tracks. The Thompson and Eidhammer aerosol-aware microphysics scheme is used, which has the main limitation of not representing mixed phase particles. Although WRF did not perfectly simulate the events and their associated precipitation types, its products represent

essential information. Across all the events, WRF had a mean -1.6°C cold bias for surface temperatures compared to observations.

The areas of severe ice loading, as shown by the Canadian Standards Association, were found to be co-located to two areas of elevated terrain in the province (Canadian Standards Association 2015), which agrees with previous findings of freezing precipitation, such as Cortinas et al. (2004). These are Riding Mountain and Pembina Mountain (also known as the Manitoba Escarpment), which rise approximately 457 m (Lang 1974) and 90 m (Bamburak and Christopher 2004) above the surrounding land, respectively. In addition, a third area was co-located in the southern Interlake region.

The 10 events were analyzed on a synoptic scale. It was found that 9 of the 10 events were associated with large scale forcing, often with very similar overall flow patterns. These events were caused by a midlatitude cyclone, with a 500 hPa trough and often with an associated left jet exit, positioned in such a way that the jet streak enhanced the lift available to the storm. Typically, these upper disturbances would approach Manitoba's borders from the west or south, and move in an easterly or northeasterly direction. This results with them passing either directly aloft of southern Manitoba, close to the international border to the south in North Dakota in the United States, or just east of Manitoba in Ontario. The events also had a related low surface pressure centre nearby, which often followed the 500 hPa trough as it moved eastward.

Nearly all the events included an associated atmospheric river. They would flow northward off the Gulf of Mexico, and would usually enter the storms through the south. However, they would occasionally travel cyclonically around the low pressure centre as it tracked toward the east. This results in the atmospheric river entering different parts of the storm, such as in the northeast quadrant. Normally, an atmospheric river enters these storms behind the

warm front, and just ahead of the cold front. It may be the case that the events which feature an atmospheric river wrapping around the storm may enter it behind the cold front or at a different stage of occlusion than is normal. It is unknown if this makes a difference on the type of precipitation experienced in these events.

The December 28, 2005 event had a different synoptic setup. The event occurred just ahead of a relatively weak 500 hPa ridge, which had a small shortwave perturbation embedded in it. As could be expected, there was no significant area of low surface pressure associated with this event, given the lack of upper level forcing. The event also didn't feature an atmospheric river in any way. Precipitation amounts in the event were relatively low in comparison to others as a result of these factors. The freezing rain that did occur during this event is likely associated with warm air aloft which is associated with the aforementioned upper air ridge, where a portion or lobe of this warm air positioned itself over Manitoba. However, given the lack of advection of fresh cold air at the lower levels, the self-limiting nature of freezing rain caused the event to end fairly quickly.

Local factors such as topography influenced 2 of the events in the CTRL simulation by altering the low level temperature and wind fields to be more favourable to the generation of freezing precipitation. Specifically, the elevated terrain in the western part of the province, such as Riding Mountain or Pembina Mountain, are the primary features in this interaction. In the case of freezing rain, sub-freezing air flowing from an easterly direction would flow up against the eastern side of Riding Mountain, while a warm air inversion aloft (approximately 1-2 km above MSL) would enter the province from the west. This created a temperature stratification in the atmosphere with very cold temperatures aloft, temperatures above freezing near the top of the boundary layer, and sub-freezing temperatures at the surface. This allows freezing rain to occur

on the eastern side of Riding Mountain as the cold air is trapped between the inversion and the terrain.

Another interaction with topography occurred when the air near the surface is slightly above 0°C, (1-5°C). As the air flows from an easterly direction and upslope in the western portion of the province (approximately 450 m above surrounding area) it would cool to a sub-freezing temperature, creating a temperature differential across the slope. If this air were to rise over this same distance, it would cool approximately 4.5°C dry adiabatically or 2.7°C wet adiabatically. This allowed freezing rain to occur near or on the higher elevation, but not in the lower lying floodplain that makes up the central and eastern portions of the province, where it falls as rain in the warmer temperatures. Wet snow is generated in a similar manner. Any snow that falls into the lower lying areas of the province in the east, falls into a shallow layer of slightly warmer (1-5°C) air exists near the surface, which causes it to partially melt into wet snow. This was again notable on the eastern side of Riding Mountain, where the air existing at the base of the elevation change was warmer, which created wet snow, while the air at the top of the elevation change was sub-freezing and allowed for "dry" snow.

The presence of large lakes can also play a role. When Lake Winnipeg and/or Lake Manitoba were open (not covered in ice), it allowed for warming and moistening of the above air, generating precipitation. In the two events in which this was evident, the associated precipitation was mostly wet snow (0.2-4 mm), with a small amount of freezing rain (0.2-2 mm) over a limited area.

Analyses of the surface winds showed that the majority (6 of 8) of the events had strong winds. Five of these 6 events typically had a strong northerly wind component, though 2 had a strong easterly component, and another 2 had a strong westerly component. The strongest wind

components in these events would typically peak at 20 m s^{-1} (~70 km h^{-1}) or more in CTRL. This suggests that power lines oriented west/east were subjected most often to hazardous winds, though lines oriented north/south were subjected to these stresses almost as often.

There were significant changes in both freezing rain and wet snow between the CTRL and PGW simulations. In the CTRL simulation, all 8 events had freezing rain. Three of these events had freezing rain exclusively, which occurred in December and January, while the other 5 had both freezing rain and wet snow. In the PGW simulation, 3 of these 8 events increased in spatial extent, total accumulation, and duration, whereas 4 events were reduced in relation to these features. One event had similar accumulation and duration, but reduced extent. In general, freezing rain and mixtures were enhanced between 24 and 59% on average. Freezing rain occurring alone was more prevalent than mixtures involving it, and it had an increase in accumulation of approximately 125%. Specifically, the upper quartile of the accumulation distribution increased the most, going from a maximum of approximately 26 mm to 58 mm. The interquartile range increased as well, though median values remained similar. A large portion of this increase occurred due to the November 6-12, 2000 event being greatly enhanced in PGW. This suggests that while freezing rain may not be more common in the future, the extremes could be enhanced significantly.

For wet snow, 5 events in the CTRL simulation had this type and it occurred alongside freezing rain in all cases. There were no exclusively wet snow events. Only 1 of these events increased in spatial extent, total accumulation, and duration. One event had an increased spatial extent, but similar duration and lesser accumulation. The other 3 events were reduced in spatial extent, accumulation, and duration. In general, wet snow and mixtures were reduced between 14 and 42% on average. Wet snow and rain occurring as a mixture was more prevalent than wet

snow by itself or any mixtures in its category. Although most types of wet snow and mixtures were reduced, the mixture of rain and graupel increased in accumulation and intensity by approximately 10 and 25%, respectively. The median for rain and graupel accumulation was unchanged, but again the upper 25% of the accumulation distribution was increased. It was increased by approximately 8 mm, making it far less than the increase for freezing rain.

Importantly, there were 3 instances in which no wet snow was present in the CTRL simulation, but it was present in the PGW simulation. All of these instances were in the winter months of December and January, which were exclusively freezing rain events in CTRL. These months do not normally experience the required high-enough temperatures to generate wet snow. This could suggest that, although overall wet snow events will not necessarily be more common in a future warmer climate, they will occur more often in winter, as opposed to the shoulder seasons of fall and spring.

Another important point is that all freezing precipitation types in PGW tended to occur farther north than in CTRL, regardless of whether the event had reduced or increased accumulation, duration, or extent. Due to the constrained synoptic flows in PGW, this more northerly occurrence is primarily due to thermodynamic factors that can be altered at the mesoscale by, for example, varying terrain height.

Within PGW, the role of terrain and lakes continued to be important. There were 3 events affected by these factors in PGW; one event illustrated effects on freezing rain, one illustrated effects on wet snow, and one illustrated effects on both types.

Surface winds were overall unchanged in their speed or directionality in PGW in all the events. Slight variations existed at certain grid points, but flow fields were similar between the two simulations. The usage of spectral nudging in these simulations only allowed for evolution

of mesoscale and microscale dynamics. This suggests that their contribution to the overall wind is minimal, and that synoptic scale dynamics are the primary forcing for winds.

The interpretability of these results in relation to a future warmer climate depends on the manner and degree through which global and synoptic scale atmospheric flows change. If they change significantly, it is possible that storms generating freezing precipitation in the future will more commonly occur in different areas than those presented here.

In conclusion, a thesis has been completed on the features of 10 freezing rain and wet snow events affecting Manitoba. Although uncommon, these major events are sometimes affected significantly by local terrain and lakes. Changes are expected in their occurrence and spatiotemporal characteristics in the future climate.

7.2. Future Work

Although this research has addressed critical issues related to freezing precipitation and the possible changes in a future climate, it is also recognized that many atmospheric-related issues need to be further investigated.

An important limitation is that it focused on only 10 events. The complete 13-year WRF CONUS information should be examined to assess overall patterns in a more comprehensive manner.

More comprehensive assessment of the model outputs of precipitation type compared to the temperature is warranted, as well as evaluation of these against observations. This would offer additional insight as to the efficacy of the surface temperature approach, as well model

biases. Although the model does show some temperature bias overall, these biases may be smaller during the actual periods with freezing precipitation.

Although some of the processes responsible for freezing precipitation were investigated, more details at every scale should be examined. A more precise synoptic typing for each event and each freezing precipitation type would be desirable. For example, the relationship between the spatiotemporal characteristics of troughs, fronts, low pressure centres, and atmospheric rivers should be related to specific freezing precipitation types.

The role played by terrain and lakes in the events was examined, although more investigation is desirable. For example, it is unclear at what temperature the WRF land surface model determines when the lakes in the province freeze over, and how this ice cover is represented.

Inferences of future conditions were based on the pseudo-global warming approach and thus did not consider dynamic changes at the synoptic scale. Similar analyses need to be carried out using actual climate scenario information that would consider, for example, storm track changes. This would potentially allow inferences into hazardous precipitation occurring in new areas, as well as any changes in surface winds.

Although not addressed directly in this thesis, a motivation was the impact of wet snow and freezing rain on structures. Several comments can be made regarding this issue. First of all, the type of precipitation varied greatly within each event and between events. Associated icing would similarly be complex since it would arise from different precipitation types, combinations and ordering. Secondly, wind speed and direction also varied within and between events. This would again lead to variations in icing features. Third, under PGW conditions, precipitation and wind fields changed somewhat and this, qualitatively, would lead to altered icing conditions.

Fourth, it would have been desirable to quantify the impacts of varying precipitation types and winds on structures but this was not possible. To do it adequately, icing models must account for the varying precipitation types, temperature and wind. There are icing models that can be applied in general with examples being those described by Chaîné and Castonguay (1974) and another by Chaîné and Skeates (1974). Even these models may be insufficient however; it is not apparent that they can adequately simulate icing under the varying precipitation types, including mixtures/combinations, actually experienced. As Chaîné and Castonguay (1974) pointed out, another issue is that winds need to be accounted for at sub-hourly scales; such data are not even available from the observational information, nor WRF output.

References

Almonte, J. D., and R. E. Stewart, 2019: Precipitation transition regions over the southern Canadian Cordillera during January–April 2010 and under a pseudo-global-warming assumption. *Hydrology and Earth System Sciences*, **23**, 3665-3682, https://doi.org/10.5194/hess-23-3665-2019.

American Meteorological Society, 2019: atmospheric river. Accessed 22 January 2020, http://glossary.ametsoc.org/wiki/Atmospheric_river.

Armenakis C., and N. Nirupama, 2014: Urban impacts of ice storms: Toronto December 2013. *Nat. Hazards*, **74**, 1291-1298.

Bamburak, J. D., and J. E. Christopher, 2004: Mesozoic stratigraphy of the Manitoba escarpment. *WCSB/TGI II Field Trip Guide.* Manitoba Geological Survey and Saskatchewan Geological Survey, 83 pp.

Bergen, R., 2019: Storm damage to hydro system could cost record $100M or more, Manitoba Hydro says. CBC News, accessed 26 October 2019, https://www.cbc.ca/news/canada/manitoba/manitoba-hydro-storm-damage-1.5328221.

Canadian Standards Association, 2015: C22.3 No.1-15 Overhead Systems, 191 pp, https://store.csagroup.org/ccrz__ProductDetails?viewState=DetailView&cartID=&portalUser=&store=&cclcl=en_US&sku=C22.3%20NO.%201-15.

Chaîné, P. M., and G. Castonguay, 1974: New Approach to radial ice thickness concept applied to bundle-like conductors. Canadian Climate Centre Internal Report, Industrial Meteorology-Study IV. Atmospheric Environment Service, Downsview, Ontario.

Chaîné, P. M., and P. Skeates, 1974: Wind and ice loading criteria selection. Canadian Climate Centre Internal Report, Industrial Meteorology - Study III. Atmospheric Environment Service, Downsview, Ontario, Canada.

Cortinas Jr., J. V., B. C. Bernstein, C. C. Robbin, and J. W. Strapp, 2004: An analysis of freezing rain, freezing drizzle, and ice pellets across the United States and Canada: 1976–90. *Wea. Forecasting*, **19**(2), 377-390.

Dacey, E., 2019: Power nearly restored, Red River crests after early fall snowstorm in Manitoba. Global News, accessed 26 October 2019, https://globalnews.ca/news/6080982/power-nearly-restored-red-river-crests-after-early-fall-snowstorm-in-manitoba/.

Environment and Climate Change Canada, 2010: GEM The Global Environmental Multiscale Model. Accessed 26 October 2019, http://collaboration.cmc.ec.gc.ca/science/rpn/gef_html_public/index.html.

Environment and Climate Change Canada, 2016: The Canadian Precipitation Analysis(CaPA) Information Leaflet. Accessed 27 October 2019, http://collaboration.cmc.ec.gc.ca/cmc/cmoi/product_guide/docs/lib/capa_information_leaflet_e.pdf.

Environment and Climate Change Canada, 2019a: Glossary. Accessed 17 October 2019, https://climate.weather.gc.ca/glossary_e.html.

Environment and Climate Change Canada, 2019b: CMC Product Guide: The Canadian Precipitation Analysis System (CaPA). Accessed 27 October 2019, http://collaboration.cmc.ec.gc.ca/cmc/cmoi/product_guide/submenus/capa_e.html.

Environment and Climate Change Canada, 2019c: MANOBS Manual of Surface Weather Observations. Environment and Climate Change Canada, 159 pp.

Groisman, P. Y., O. N. Bulygina, X. Yin, R. S. Vose, S. K. Gulev, I. Hanssen-Bauer, and E. Førland, 2016: Recent changes in the frequency of freezing precipitation in North America and Northern Eurasia. *Environ. Res. Lett.*, **11**(4), 045007.

Hauer, R. J., W. Wang, and J. O. Dawson, 1993: Ice storm damage to urban trees. *Journal of Arboriculture*, **19**(4), 187-194.

Hauer, R. J., J. O. Jeffery, and L. P. Werner, 2006: *Trees and Ice Storms: The Development of Ice Storm–Resistant Urban Tree Populations (Second Edition)*. U.S. Department of Agriculture: Forest Service -- National Agroforestry Center, 20 pp.

IPCC, 2013: *Climate Change 2013: The Physical Science Basis. Contribution of Working Group I to the Fifth Assessment Report of the Intergovernmental Panel on Climate Change*, Stocker, T. F., D. Qin, G. K. Plattner, M. Tignor, S. K. Allen, J. Boschung, A. Nauels, Y. Xia, V. Bex and P. M. Midgley, Eds., Cambridge University Press, Cambridge, United Kingdom and New York, NY, USA, 1535 pp.

Jeong, D. I., L. Sushama, M. J. F. Vieira, and K. A. Koenig, 2018: Projected changes to extreme ice loads for overhead transmission lines across Canada. *Sustainable Cities and Society*, **39**, 639-649, https://doi.org/10.1016/j.scs.2018.03.017.

Kobayashi, S., and Coauthors, 2015: The JRA-55 reanalysis: general specifications and basic characteristics. *J. Meteorol. Soc. Jpn.*, **93**(1), 5-48, https://doi.org/10.2151/jmsj.2015-001.

Kobayashi, S., and National Center for Atmospheric Research Staff (Eds), 2019: The Climate Data Guide: JRA-55. Accessed 14 September 2019, https://climatedataguide.ucar.edu/climate-data/jra-55.

Kochtubajda, B., C. Mooney, and R. Stewart, 2017: Characteristics, atmospheric drivers and occurrence patterns of freezing precipitation and ice pellets over the Prairie Provinces and

Arctic Territories of Canada: 1964–2005. *Atmospheric Research*, **191**, 115-127. http://dx.doi.org/10.1016/j.atmosres.2017.03.005.

Lackmann, G., 2011, *Midlatitude Synoptic Meteorology: Dynamics, Analysis, and Forecasting*, American Meteorological Society, 345 pp.

Lang, A. H., 1974: *Guide to the Geology of Riding Mountain National Park*. Information Canada, 68 pp.

Lecomte, E. L., A. W. Pang, and J. W. Russell, 1998: *Ice Storm '98.* Institute for Catastrophic Loss Reduction, 37 pp.

Liu, C., and Coauthors, 2017: Continental-scale convection-permitting modeling of the current and future climate of North America. *Clim. Dyn.,* **49**(1-2), 71-95, https://doi.org/10.1007/s00382-016-3327-9.

Mahfouf, J. F., B. Brasnett, and S. Gagnon, 2007: A Canadian precipitation analysis (CaPA) project: description and preliminary results, Atmos. Ocean, **45**, 1-17, https://doi.org/10.3137/ao.v450101.

Manitoba Hydro, 2019: Winter storm response. Accessed 26 October 2019, https://www.hydro.mb.ca/outages/storm_response/.

Poots, G., 1996: *Ice and Snow Accretion on Structures.* Research Studies Press, 338 pp.

Rasmussen, R., and Coauthors, 2011: High-resolution coupled climate runoff simulations of seasonal snowfall over Colorado: a process study of current and warmer climate. *J. Climate*, **24**, 3015-3048, https://doi.org/10.1175/2010JCLI3985.1.

Rasmussen, R., and Coauthors, 2014: Climate change impacts on the water balance of the Colorado headwaters: high-resolution regional climate model simulations. *J. Hydrometeor.*, **15**, 1091-1116, https://doi.org/10.1175/JHM-D-13-0118.1.

Rasmussen, R., and C. Liu., 2017: High resolution WRF simulations of the current and future climate of North America. Research Data Archive at the National Center for Atmospheric Research, Computational and Information Systems Laboratory, accessed 17 October 2019, https://doi.org/10.5065/D6V40SXP.

Smith, H., 2019: Major precipitation events and the 2009 Red River flood. M. Sc. thesis, Dept. of Environment, Earth, and Geography, University of Manitoba, 189 pp, https://mspace.lib.umanitoba.ca/xmlui/handle/1993/33828.

Stewart, R. E., 1984: Deep 0 C isothermal layers within precipitation bands over southern Ontario. *Journal of Geophysical Research: Atmospheres*, **89**(D2), 2567-2572.

Stewart, R. E., R. W. Crawford, N. R. Donaldson, T. B. Low, and B. E. Sheppard, 1990: Precipitation and Environmental Conditions during Accretion in Canadian East Coast Winter Storms. *Journal of Applied Meteorology*, **29**, 525-538.

Stewart, R. E., 1992: Precipitation Types in the Transition Region of Winter Storms. *Bull. Amer. Meteor. Soc.*, **73**(3), 287-296.

Stewart, R. E., J. M. Thériault, and W. Henson, 2015: On the characteristics of and processes producing winter precipitation types near 0°C. *Bull. Amer. Meteor. Soc.*, **96**(4), 623-639, https://doi.org/10.1175/BAMS-D-14-00032.1.

Stewart, R. E., and Coauthors, 2019: Summary and synthesis of Changing Cold Regions Network (CCRN) research in the interior of western Canada – Part 1: Projected climate and meteorology. *Hydrol. Earth Syst. Sci.*, **23**, 3437-3455, https://doi.org/10.5194/hess-23-3437-2019.

Stull, R., 2011a: *Meteorology for Scientists & Engineers, 3rd Edition*, University of British Columbia. 938 pp.

Stull, R., 2011b: Wet-bulb temperature from relative humidity and air temperature. *J. Appl. Meteor. Climatol.*, **50**, 2267-2269, https://doi.org/10.1175/JAMC-D-11-0143.1.

The Canadian Press, 2019: Power fully restored two weeks after major snowstorm hit Manitoba. City News, accessed 26 October 2019, https://edmonton.citynews.ca/2019/10/25/power-fully-restored-two-weeks-after-major-snowstorm-hit-manitoba/.

Thompson, G., P. R. Field, R. M. Rasmussen, and W. D. Hall, 2008: Explicit forecasts of winter precipitation using an improved bulk microphysics scheme. Part II: implementation of a new snow parameterization. *Mon. Wea. Rev.*, **136**, 5095-5115.

Thompson, G., and T. Eidhammer, 2014: Study of aerosol impacts on clouds and precipitation development in a large winter cyclone. *J. Atmos. Sci.*, **71**, 3636-3658.

Thompson, S., 2019: Storm repair estimates total more than $100 million: Manitoba Hydro. Global News, accessed 26 October 2019, https://globalnews.ca/news/6059635/storm-repair-estimates-total-more-than-100-million-manitoba-hydro/.

Trenberth, K. E., 2011: Changes in precipitation with climate change. *Clim. Res.*, **47**, 123-138.

Upham, W., 1896, *The Glacial Lake Agassiz (Volume 25)*, U.S. Government Printing Office, 658 pp.

World Meteorological Organization, 2017: *Guide to Meteorological Instruments and Methods of Observation.* World Meteorological Organization, 1165 pp.

Zhou, B., and Coauthors, 2011: The great 2008 Chinese ice storm - its socioeconomic-ecological impact and sustainability lessons learned. *Bull. Amer. Meteor. Soc.*, **92**(1), 47-60.

Appendix A: JRA-55

This section contains a selection of images from the JRA-55 for each of the 10 events. For each event, all images are at the same time, and were selected to illustrate the large scale features described in the text. The images (in order) are:

- 500 hPa height analysis (dam) and strong winds (≥50 knots)
- 850 hPa winds (m s^{-1})
- Mean sea level pressure (hPa)
- Integrated Vapour Transport (kg m^{-1} s^{-1})
- Equivalent condensation rate (ECR, mm day^{-1})
- Integrated water vapor (IWV, kg m^{-2})

A1: April 27, 1984

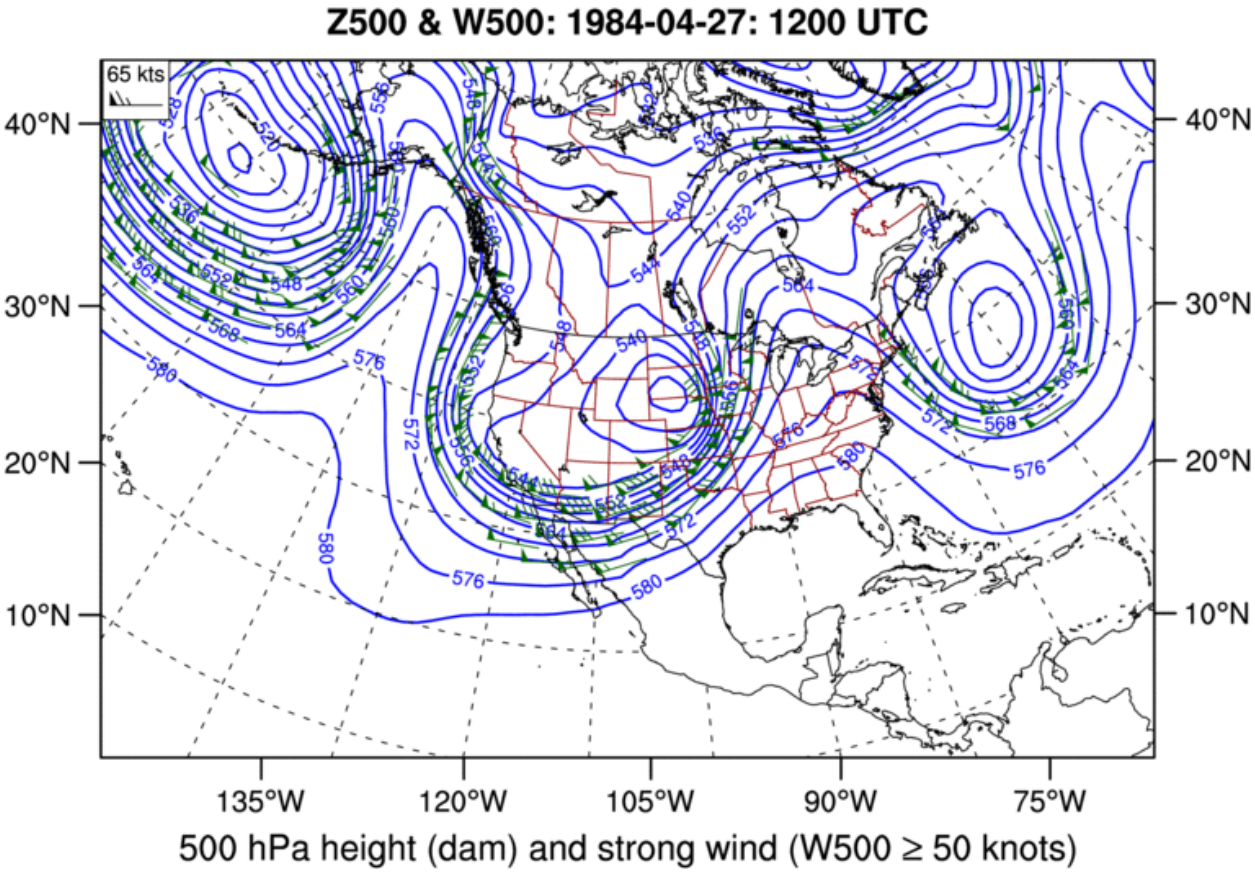

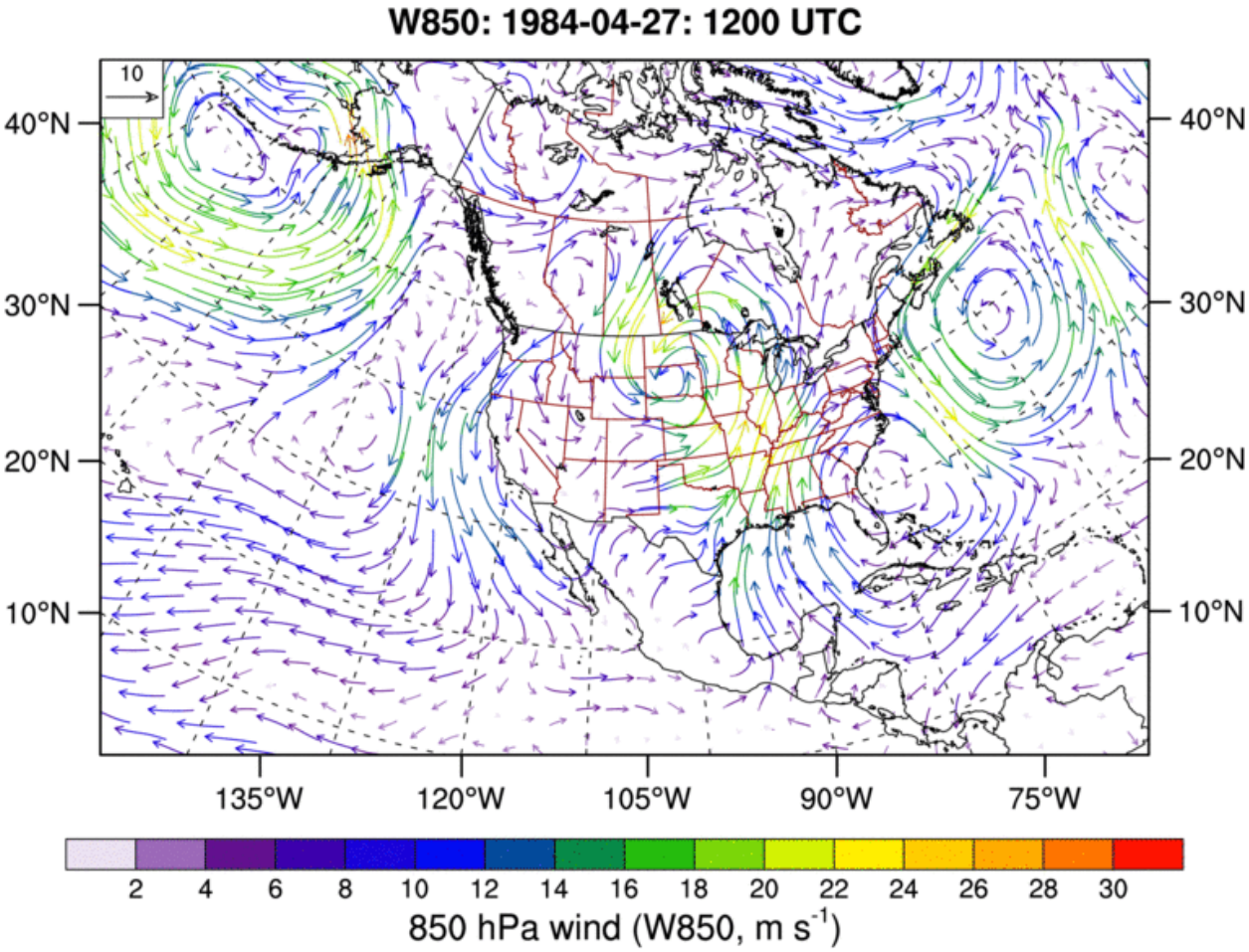
W850: 1984-04-27: 1200 UTC
10
40°N
30°N
20°N
10°N
135°W
120°W
105°W
90°W
75°W
2 4 6 8 10 12 14 16 18 20 22 24 26 28 30
850 hPa wind (W850, m s-1)

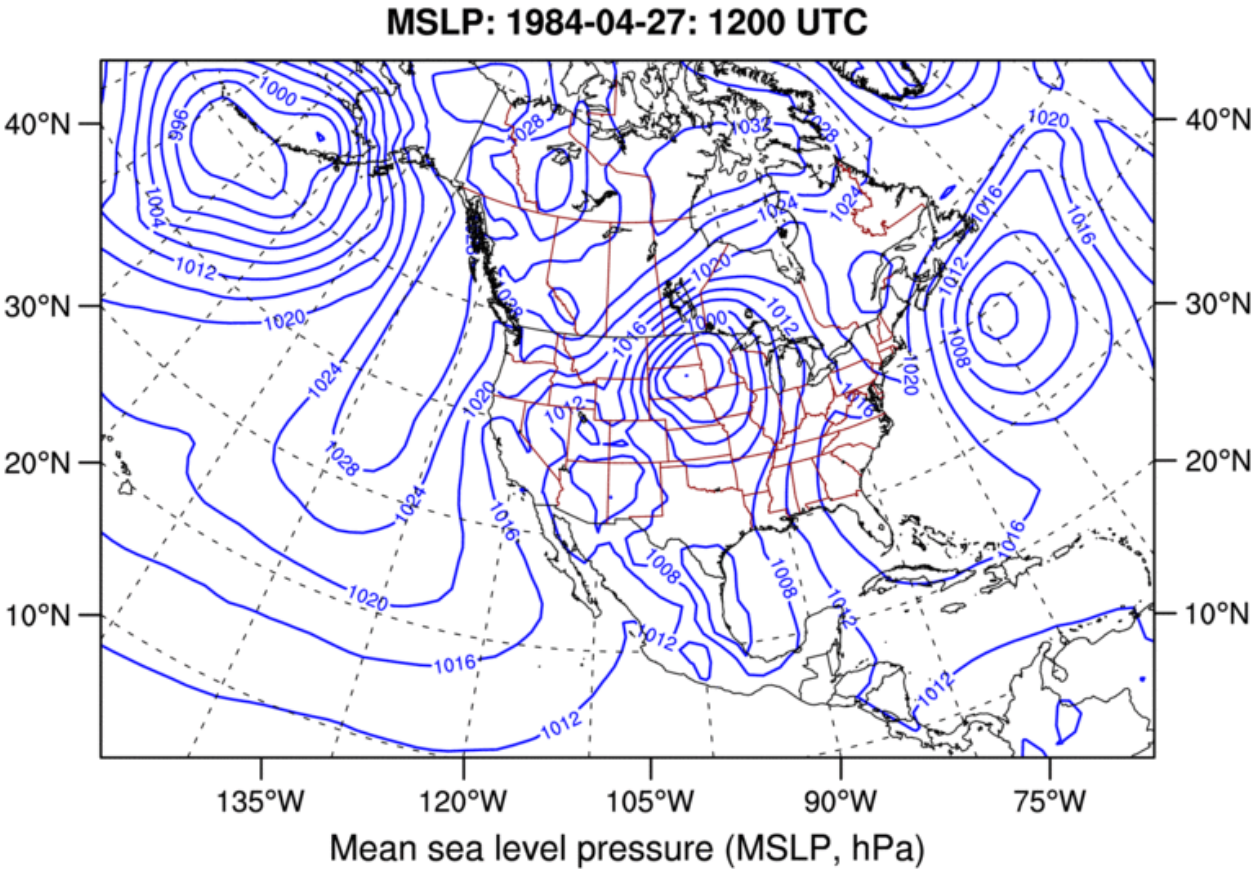
MSLP: 1984-04-27: 1200 UTC
40°N
30°N
20°N
10°N
135°W
120°W
105°W
90°W
75°W
Mean sea level pressure (MSLP, hPa)

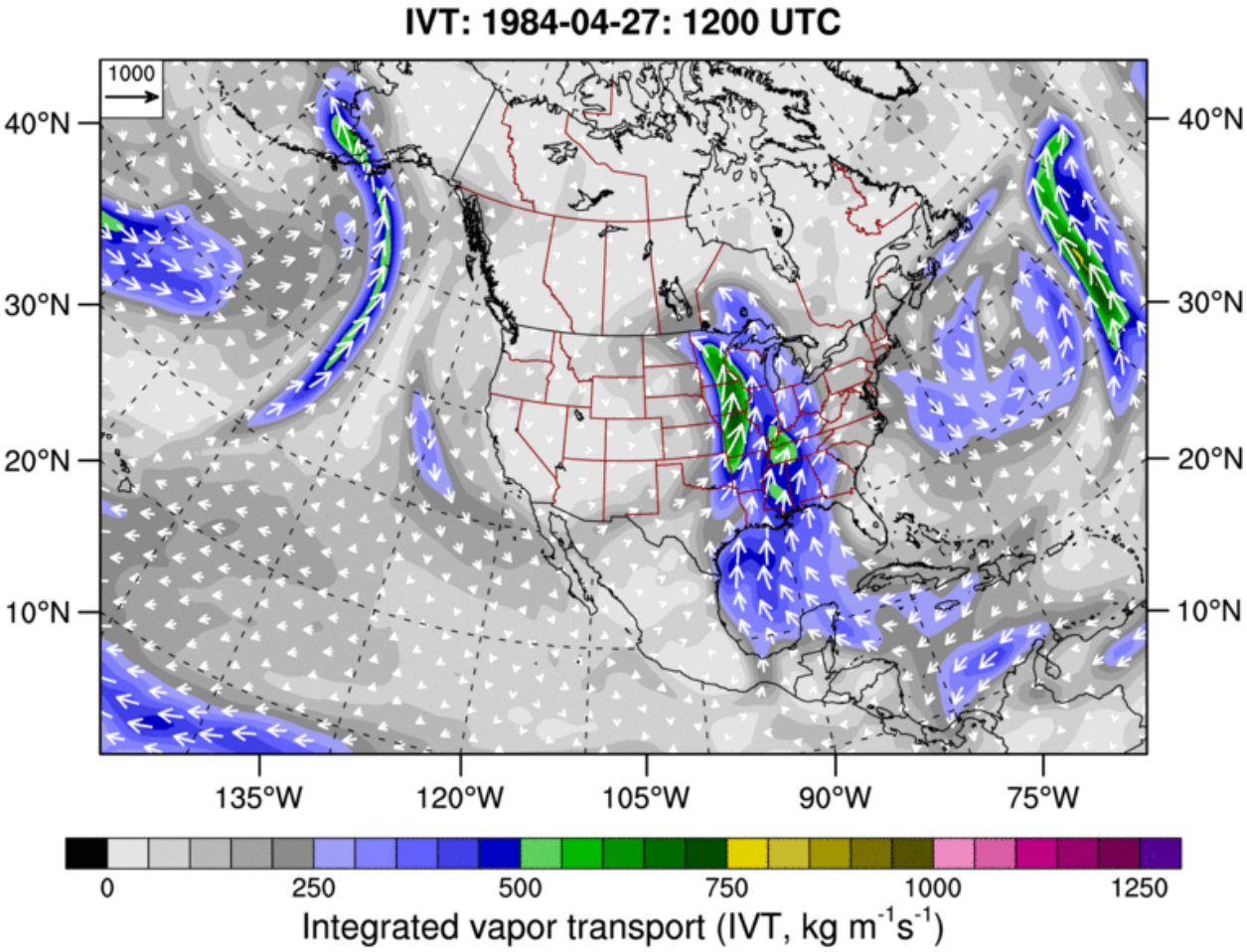
IVT: 1984-04-27: 1200 UTC
1000
40°N
30°N
20°N
10°N
135°W
120°W
105°W
90°W
75°W
0
250
500
750
1000
1250
Integrated vapor transport (IVT, kg m-1s-1)

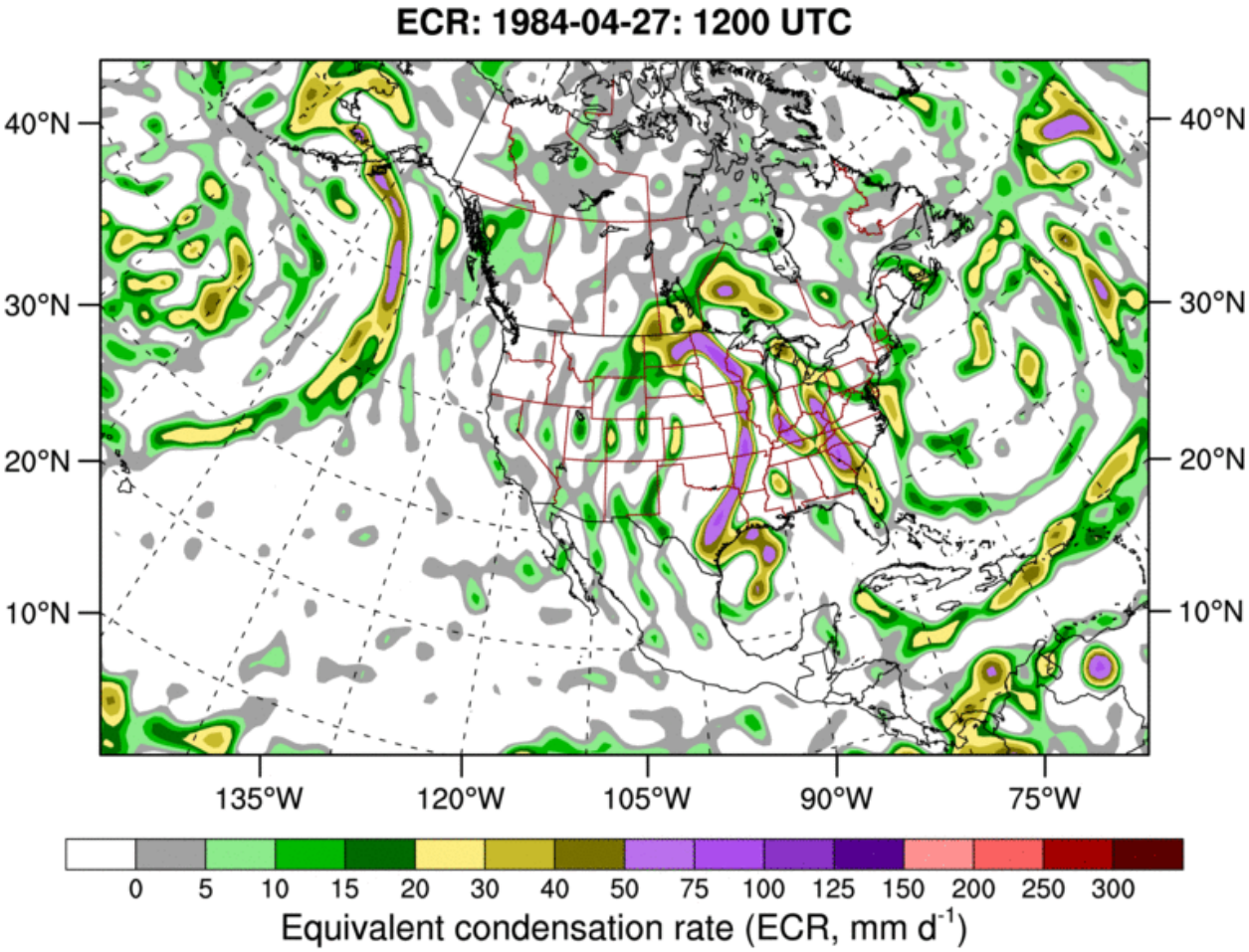
ECR: 1984-04-27: 1200 UTC
40°N
30°N
20°N
10°N
135°W
120°W
105°W
90°W
75°W
0 5 10 15 20 30 40 50 75 100 125 150 200 250 300
Equivalent condensation rate (ECR, mm d-1)

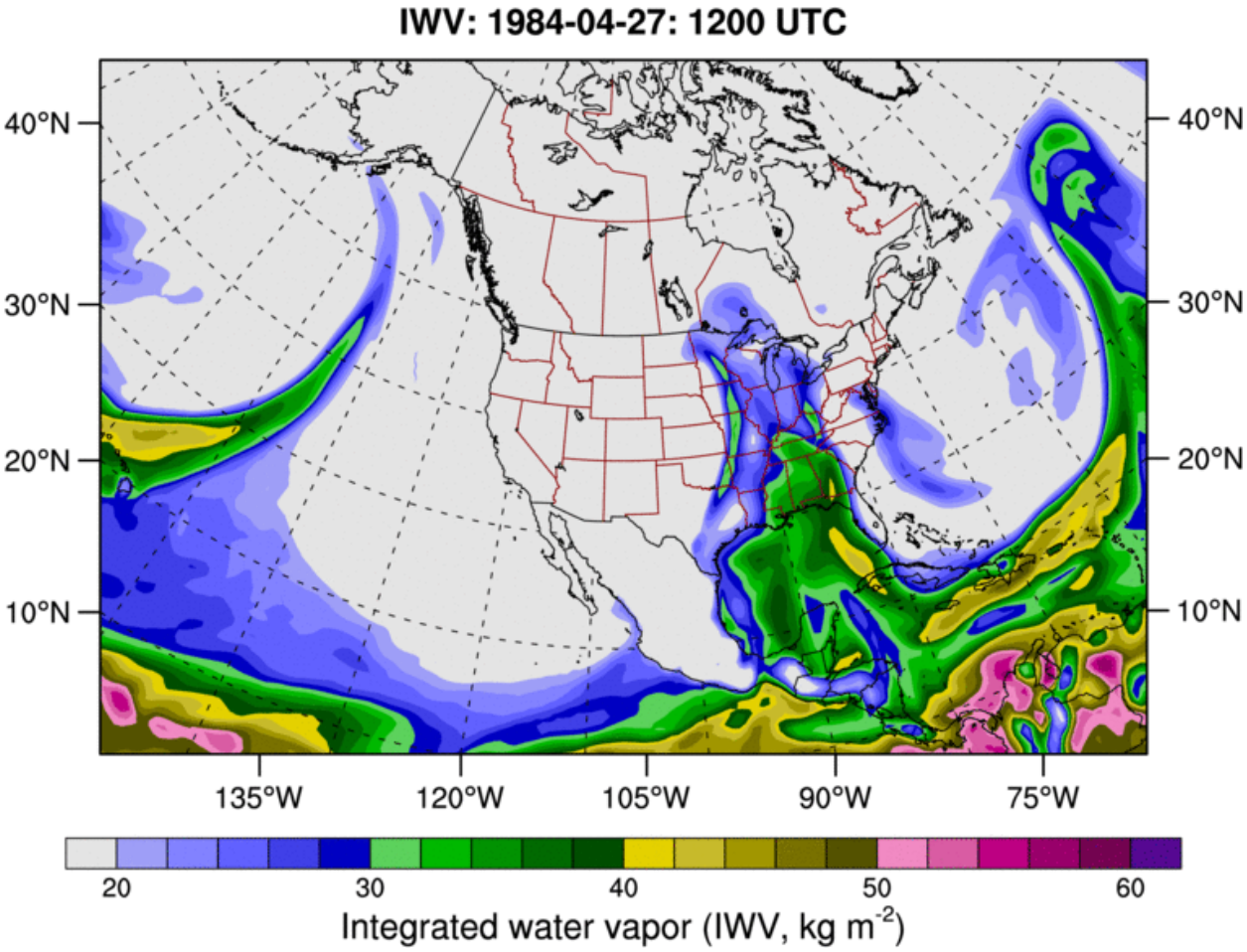
IWV: 1984-04-27: 1200 UTC
40°N
30°N
20°N
10°N
135°W
120°W
105°W
90°W
75°W
20
30
40
50
60
Integrated water vapor (IWV, kg m-2)

A2: November 6-12, 2000

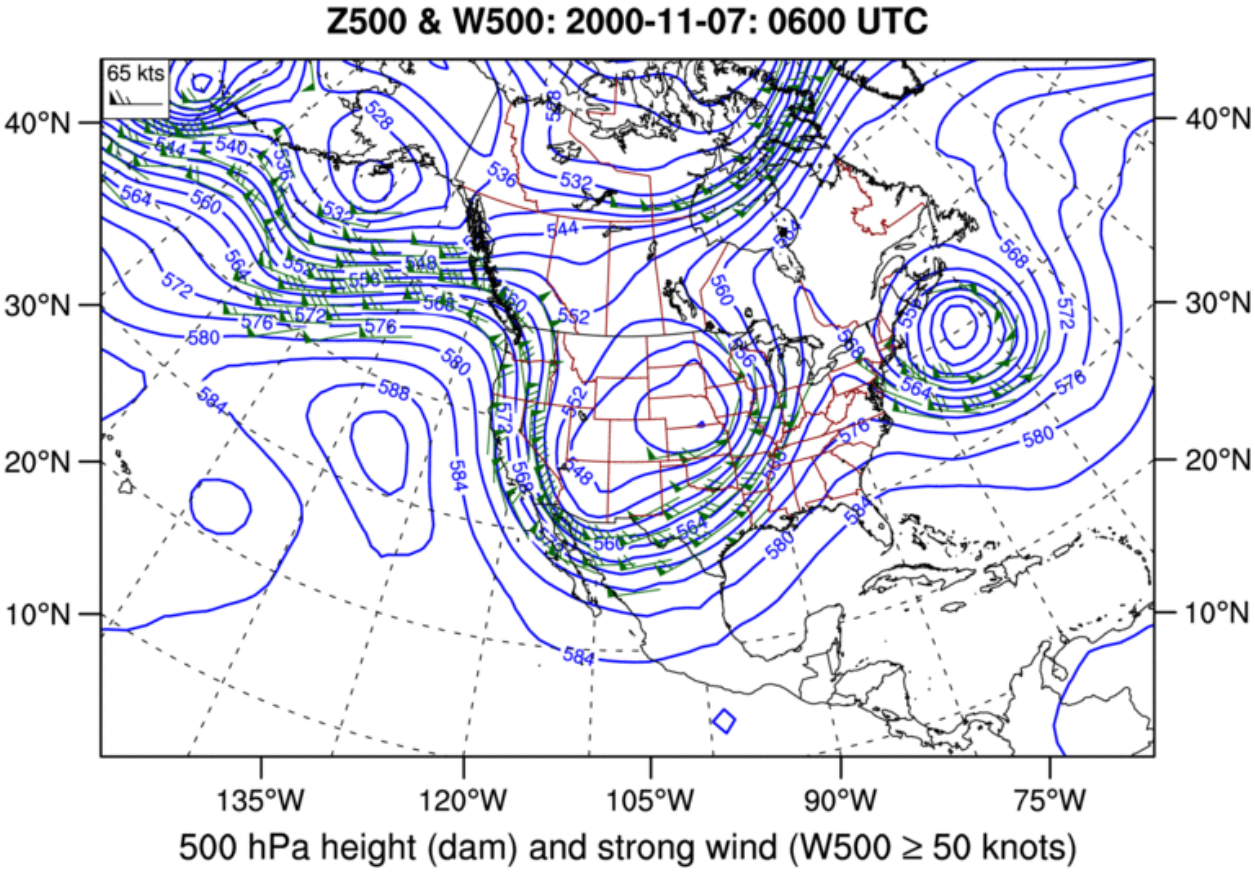

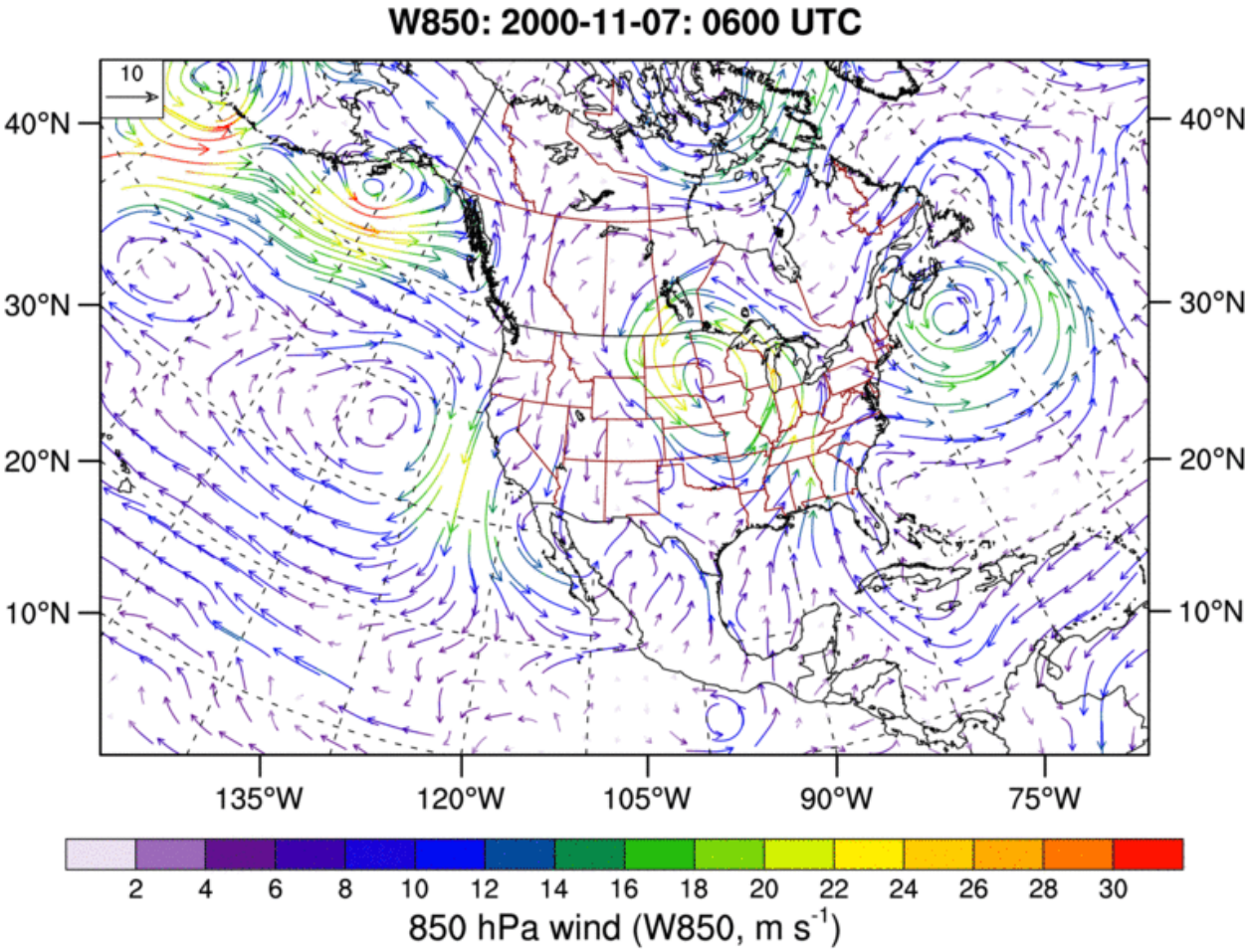
W850: 2000-11-07: 0600 UTC
10
40°N
30°N
20°N
10°N
135°W
120°W
105°W
90°W
75°W
2 4 6 8 10 12 14 16 18 20 22 24 26 28 30
850 hPa wind (W850, m s-1)

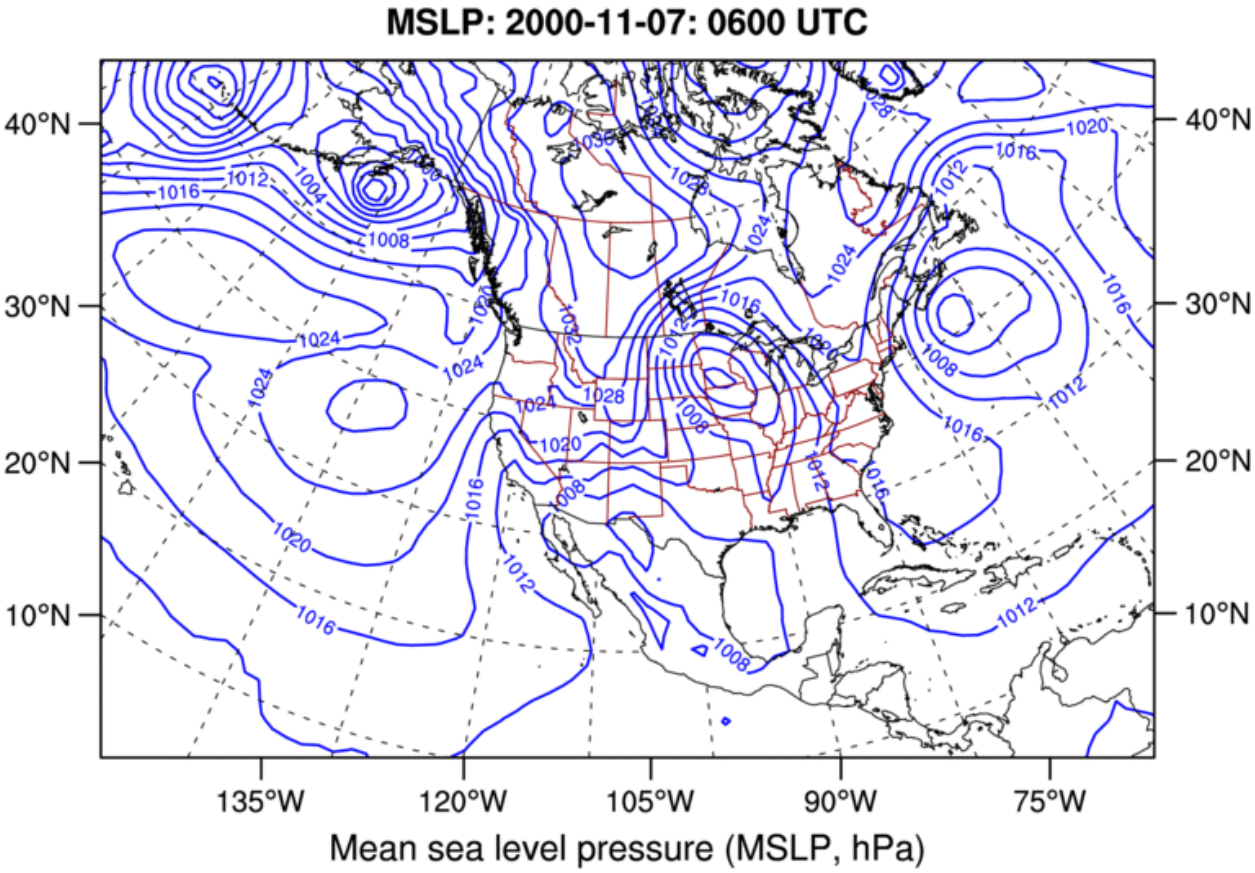
MSLP: 2000-11-07: 0600 UTC
40°N
30°N
20°N
10°N
135°W
120°W
105°W
90°W
75°W
Mean sea level pressure (MSLP, hPa)

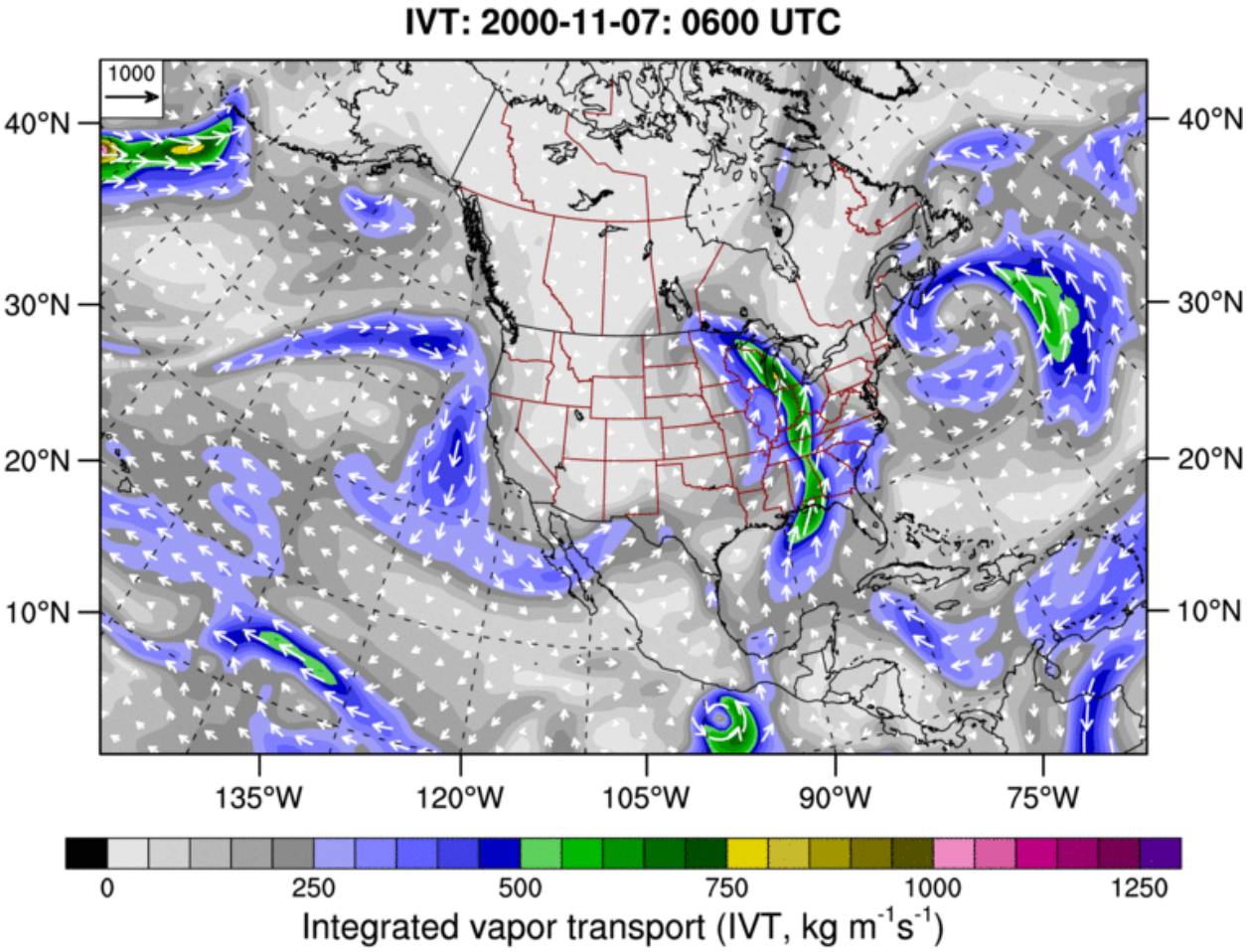
IVT: 2000-11-07: 0600 UTC
1000
40°N
30°N
20°N
10°N
135°W
120°W
105°W
90°W
75°W
0
250
500
750
1000
1250
Integrated vapor transport (IVT, kg m-1s-1)

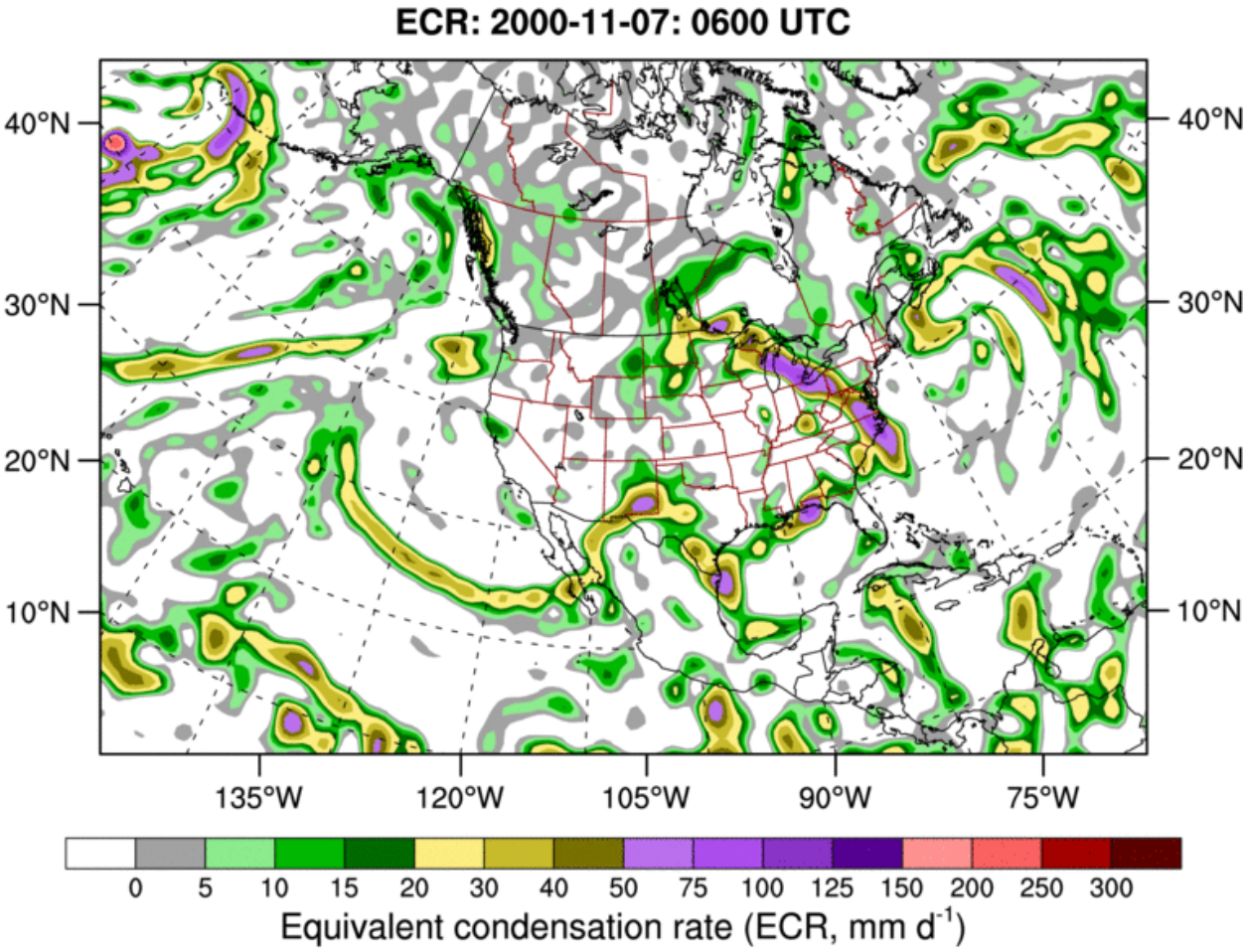
ECR: 2000-11-07: 0600 UTC
40°N
30°N
20°N
10°N
135°W
120°W
105°W
90°W
75°W
0
5
10
15
20
30
40
50
75
100
125
150
200
250
300
Equivalent condensation rate (ECR, mm d-1)

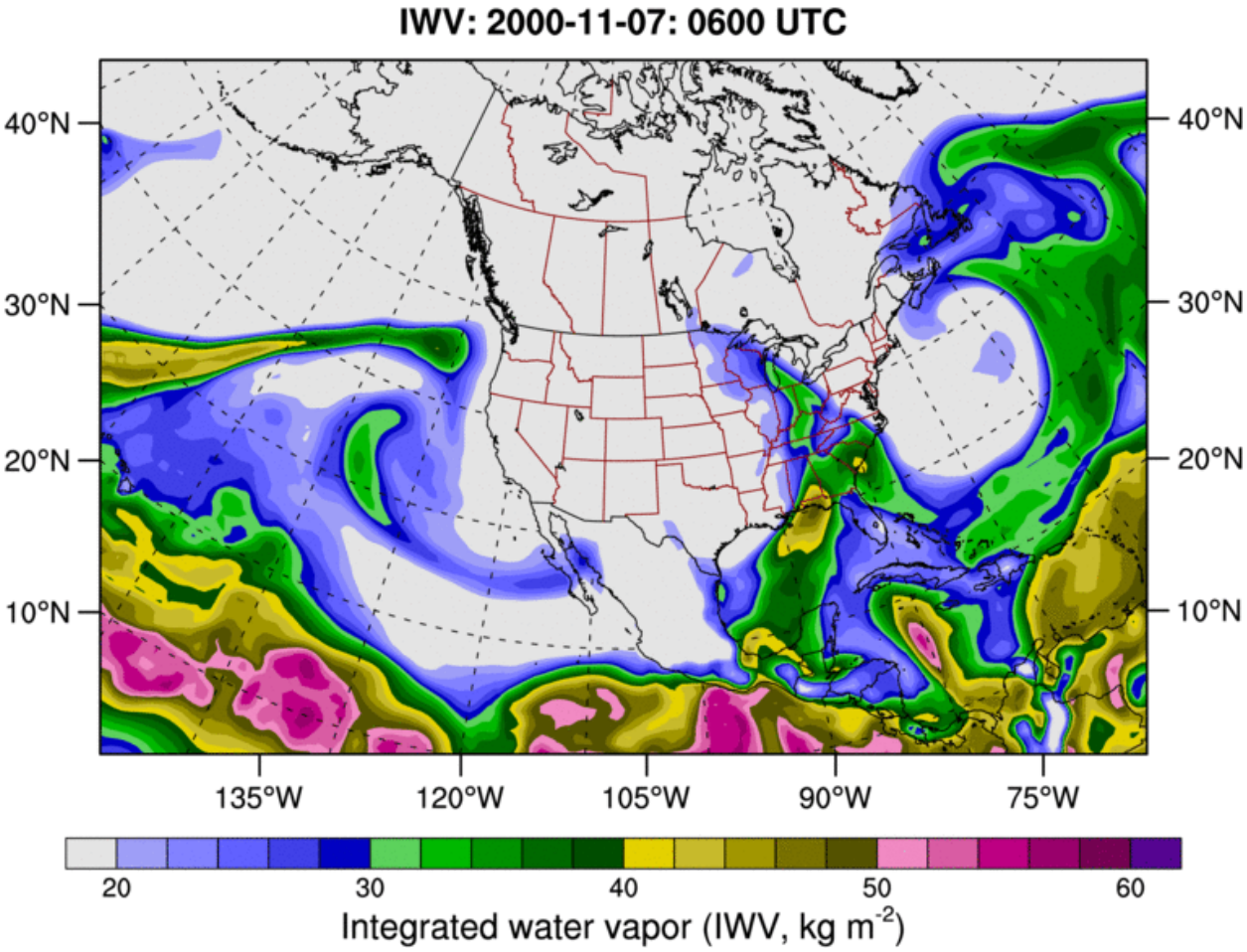
IWV: 2000-11-07: 0600 UTC
40°N
30°N
20°N
10°N
135°W
120°W
105°W
90°W
75°W
20
30
40
50
60
Integrated water vapor (IWV, kg m-2)

A3: May 11, 2004

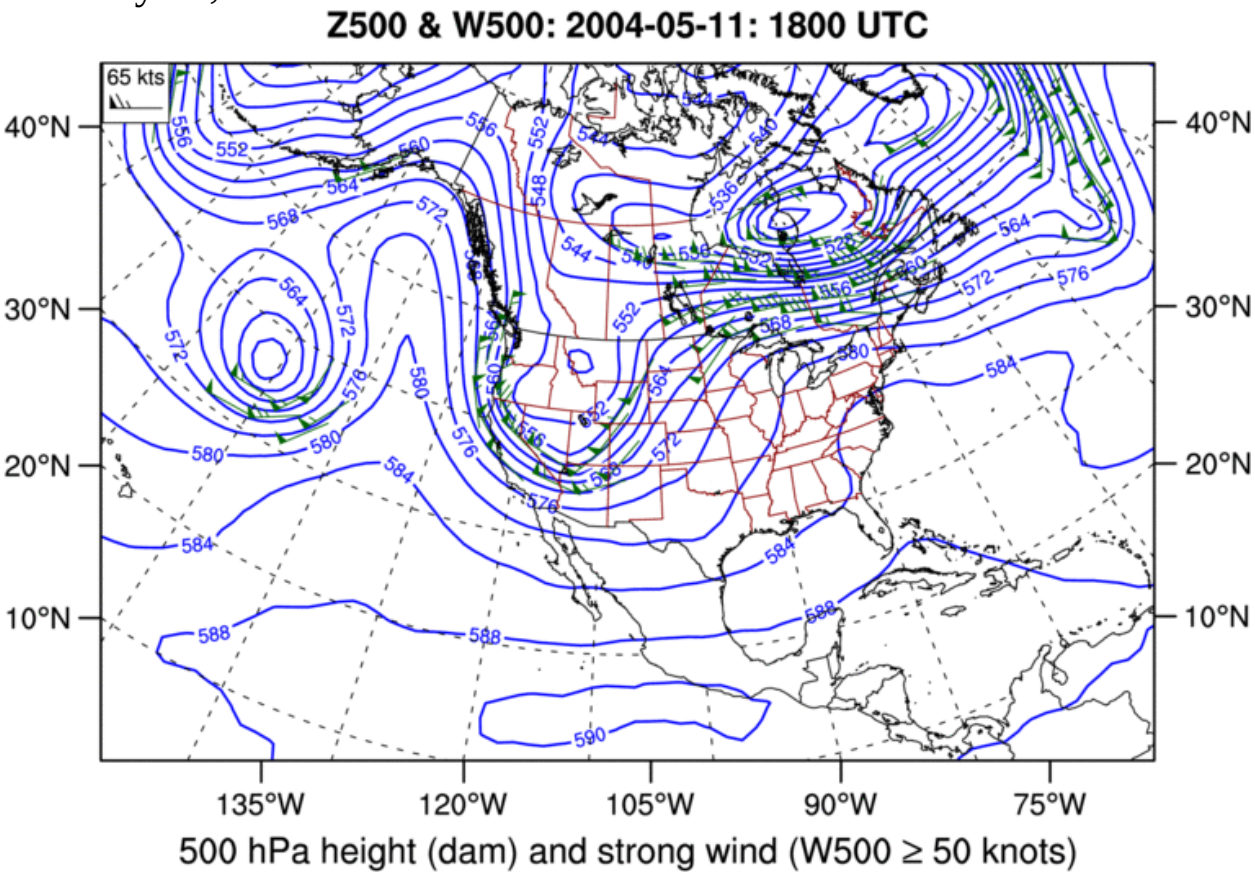

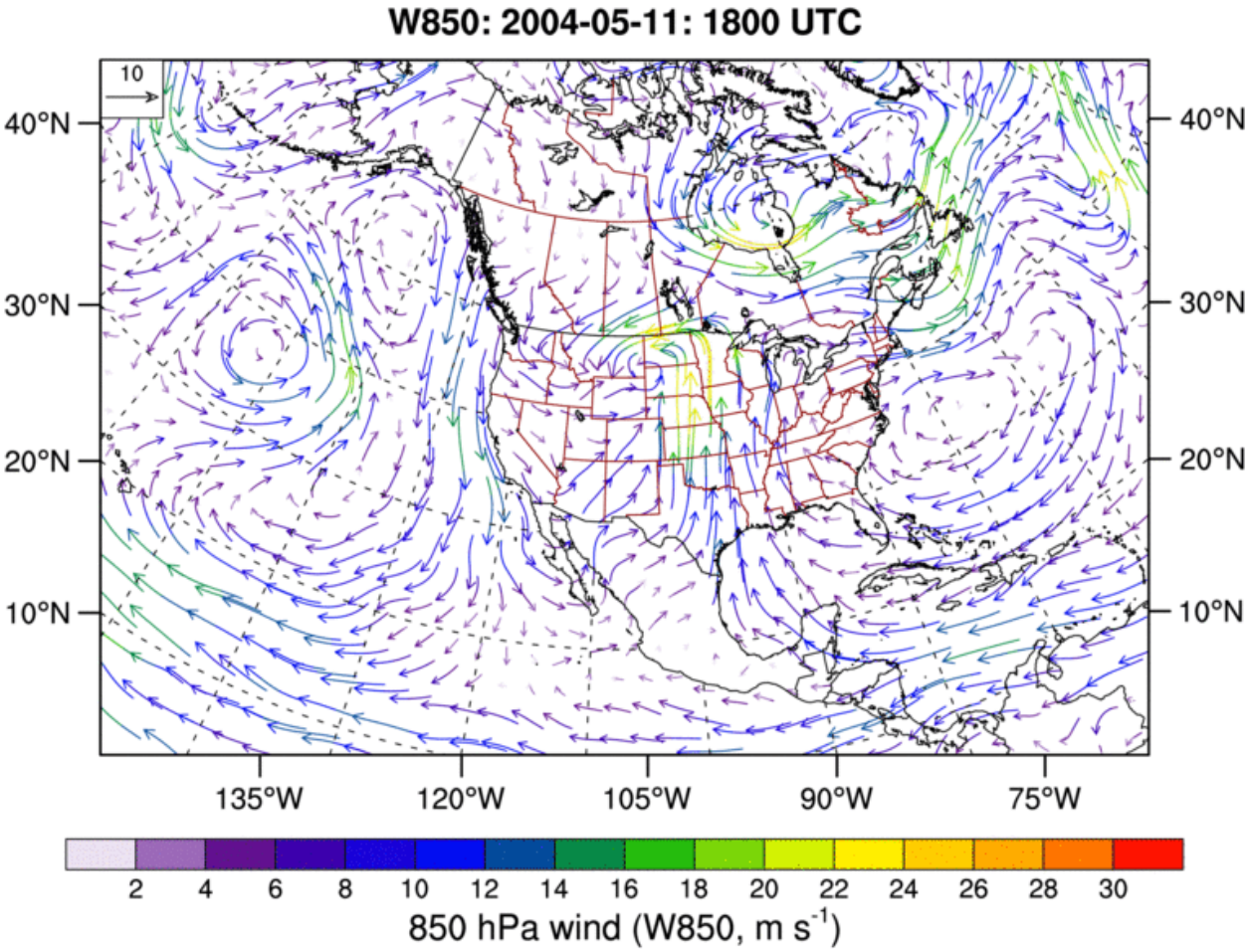
W850: 2004-05-11: 1800 UTC
10
40°N
30°N
20°N
10°N
135°W
120°W
105°W
90°W
75°W
2
4
6
8
10
12
14
16
18
20
22
24
26
28
30
850 hPa wind (W850, m s-1)

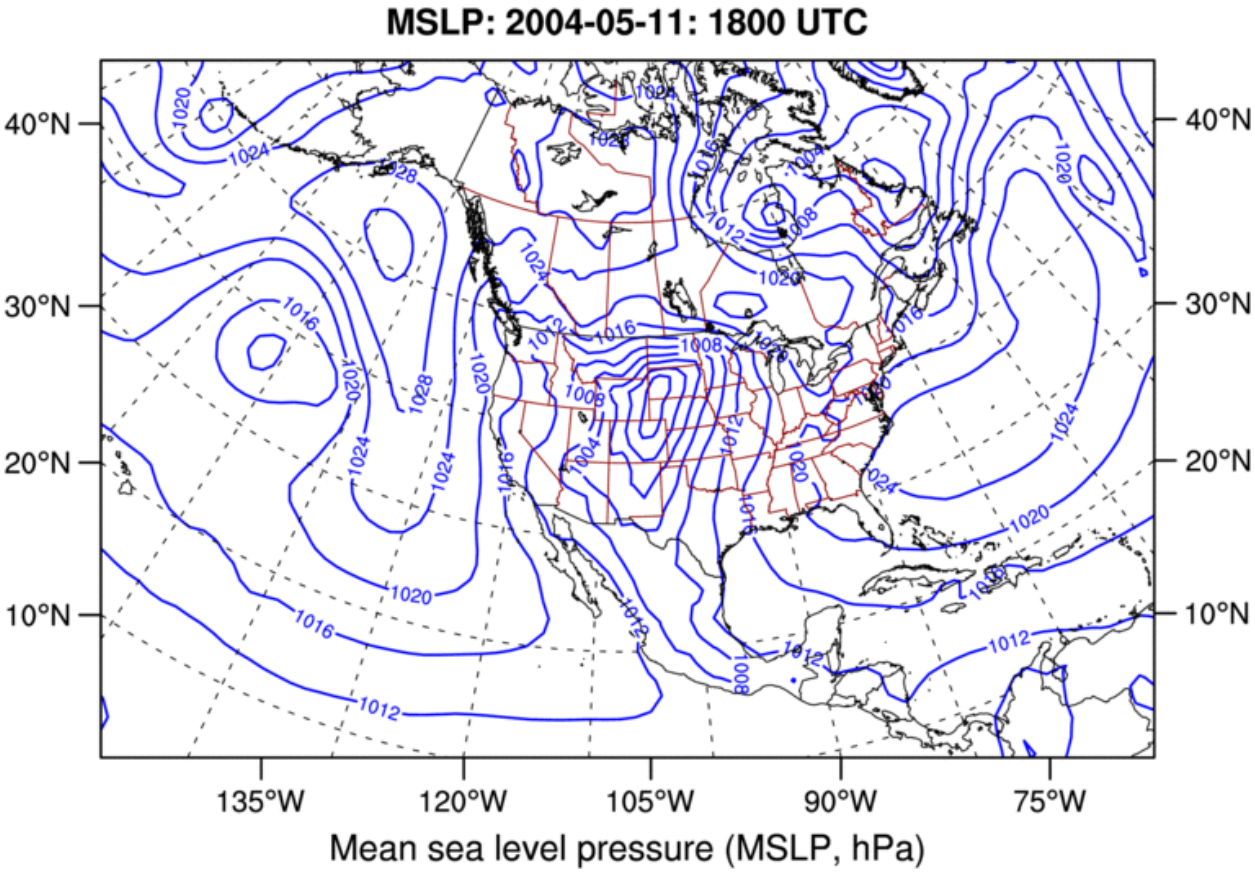
MSLP: 2004-05-11: 1800 UTC
40°N
30°N
20°N
10°N
135°W
120°W
105°W
90°W
75°W
Mean sea level pressure (MSLP, hPa)

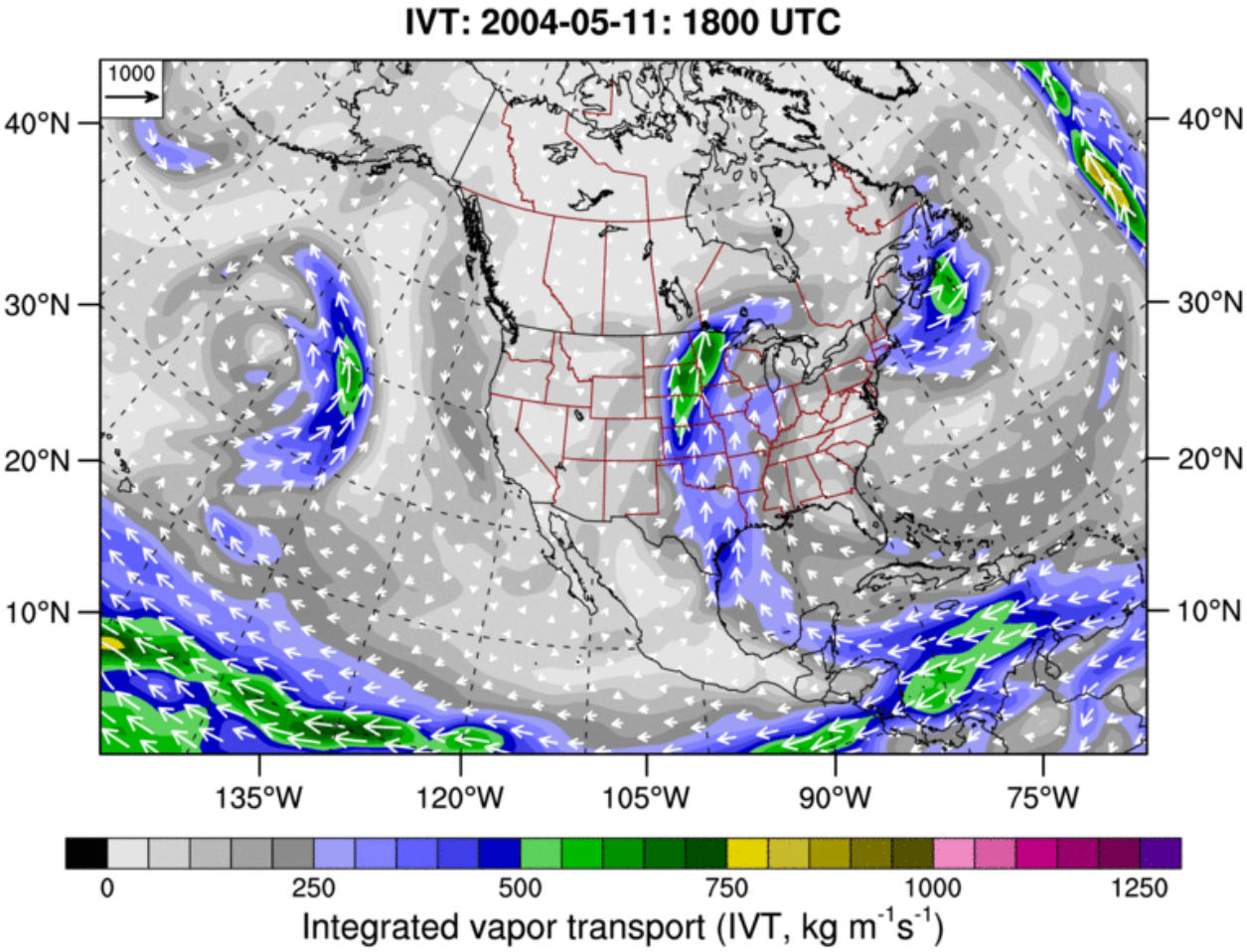
IVT: 2004-05-11: 1800 UTC
1000
40°N
30°N
20°N
10°N
135°W
120°W
105°W
90°W
75°W
0
250
500
750
1000
1250
Integrated vapor transport (IVT, kg m-1s-1)

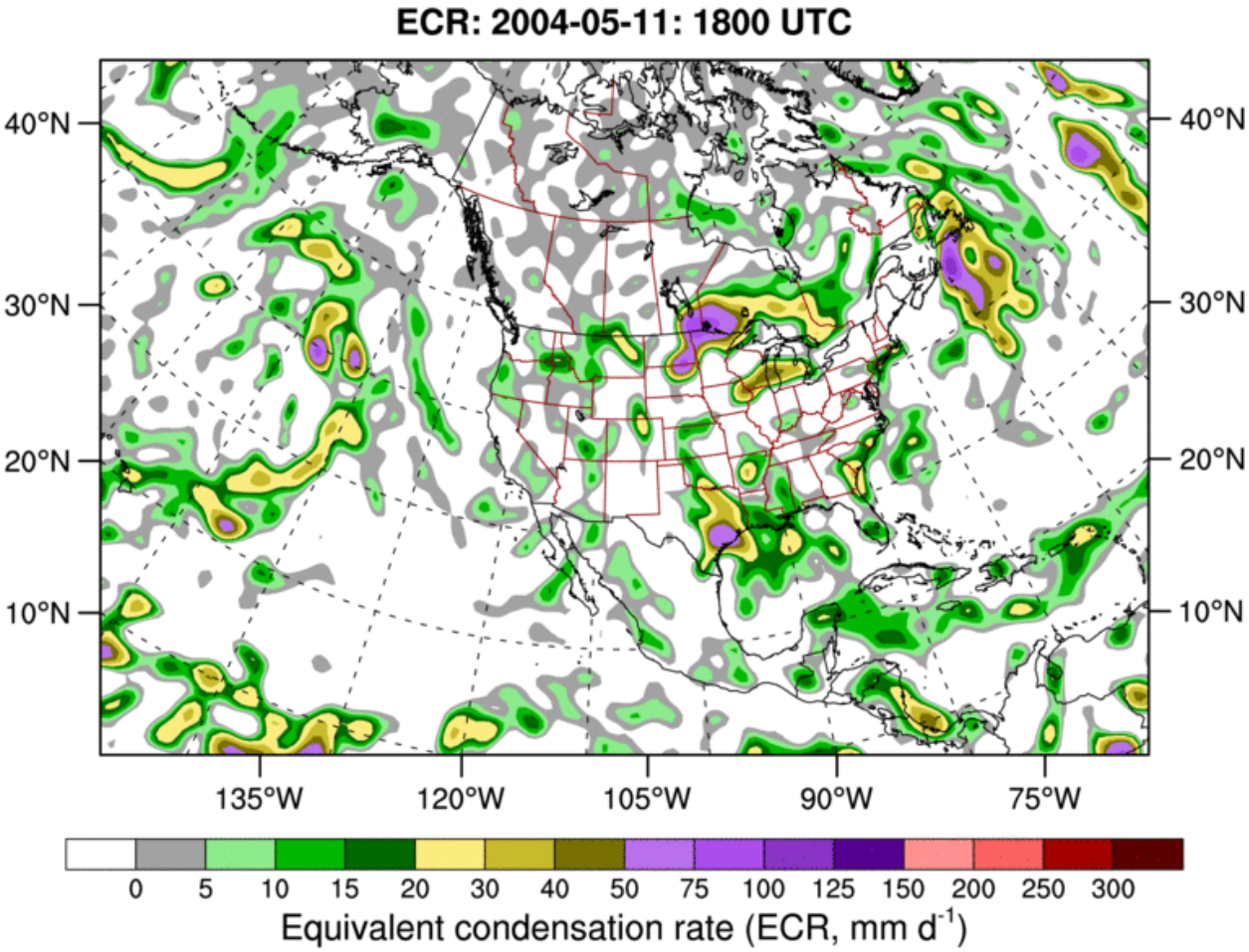
ECR: 2004-05-11: 1800 UTC
40°N
30°N
20°N
10°N
135°W
120°W
105°W
90°W
75°W
0
5
10
15
20
30
40
50
75
100
125
150
200
250
300
Equivalent condensation rate (ECR, mm d-1)

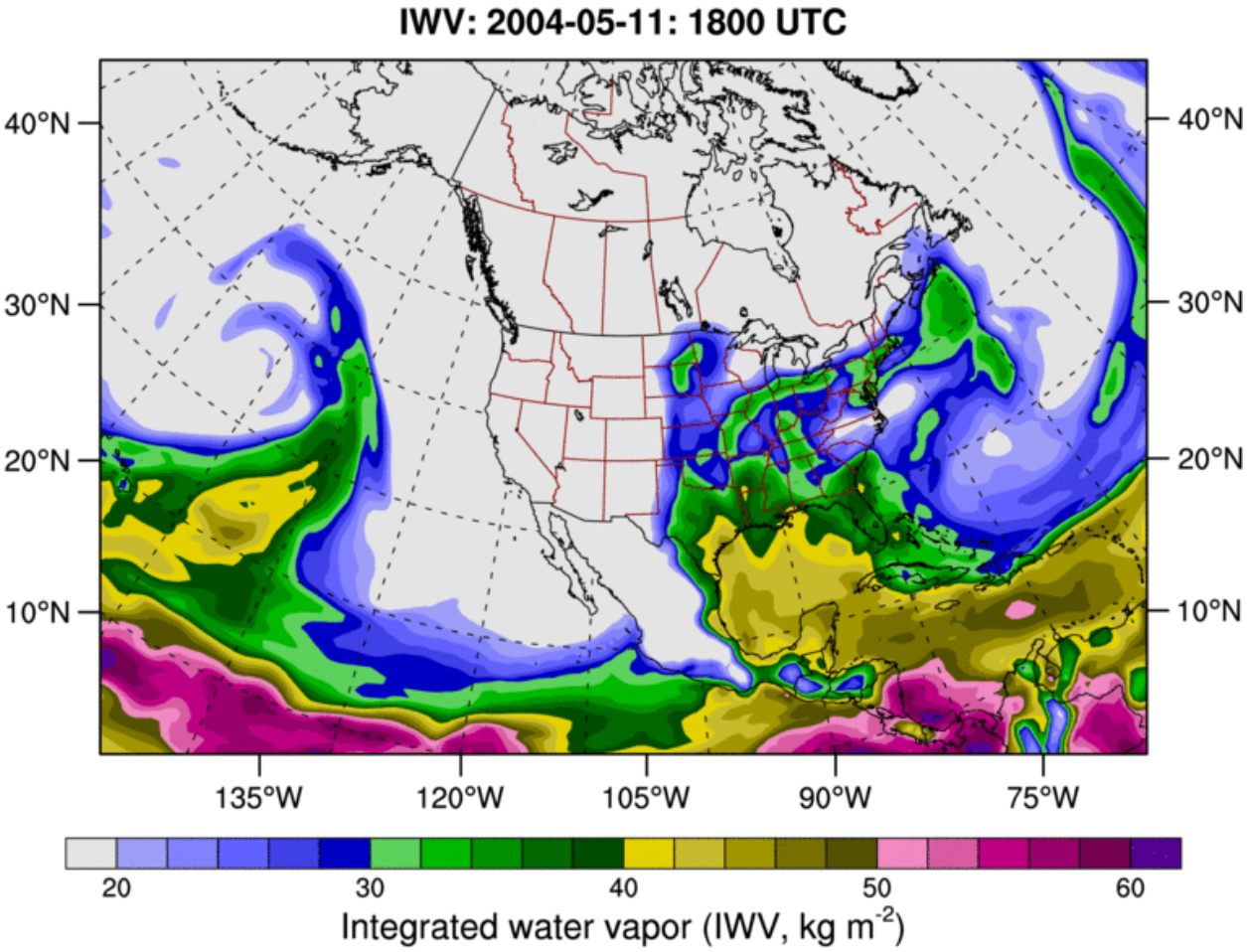
IWV: 2004-05-11: 1800 UTC
40°N
30°N
20°N
10°N
135°W
120°W
105°W
90°W
75°W
20
30
40
50
60
Integrated water vapor (IWV, kg m-2)

A4: October 5, 2005

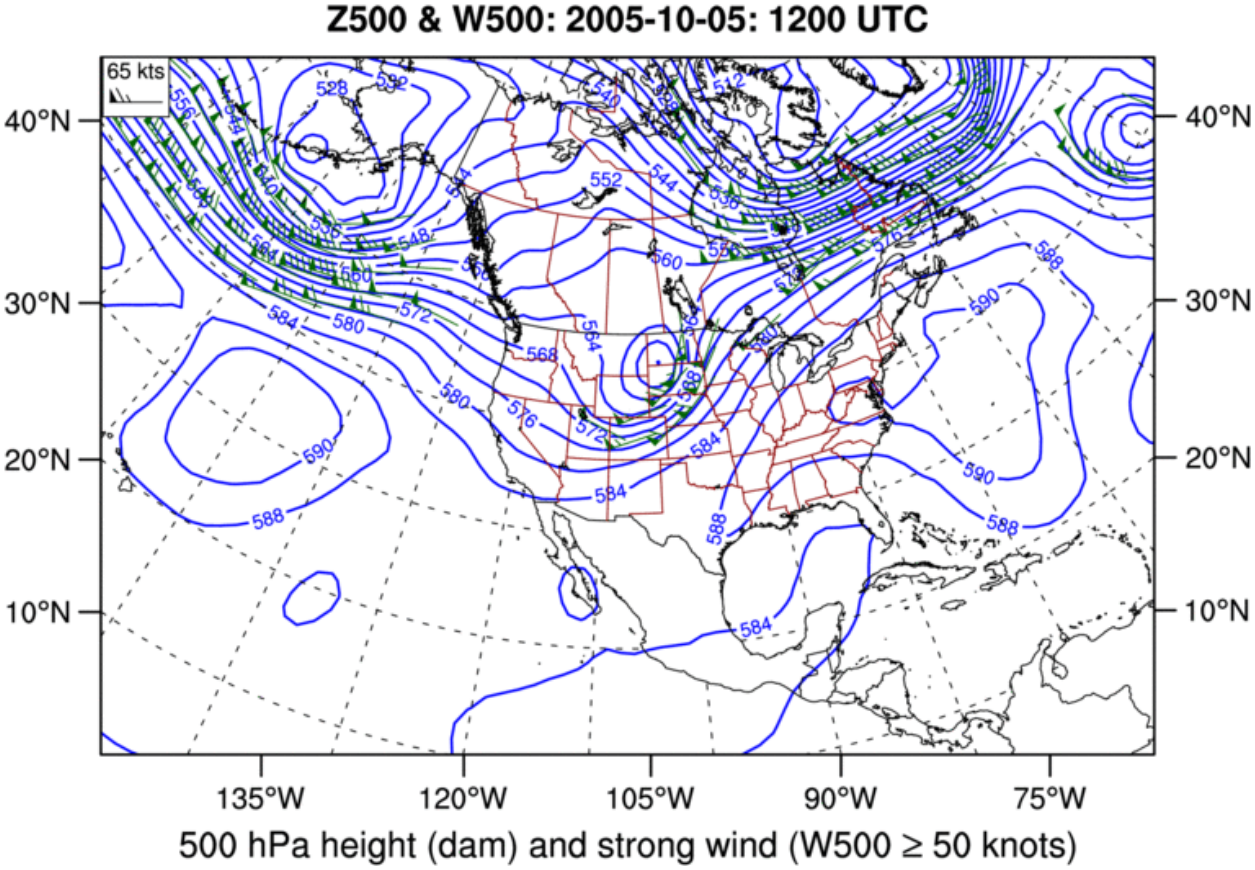

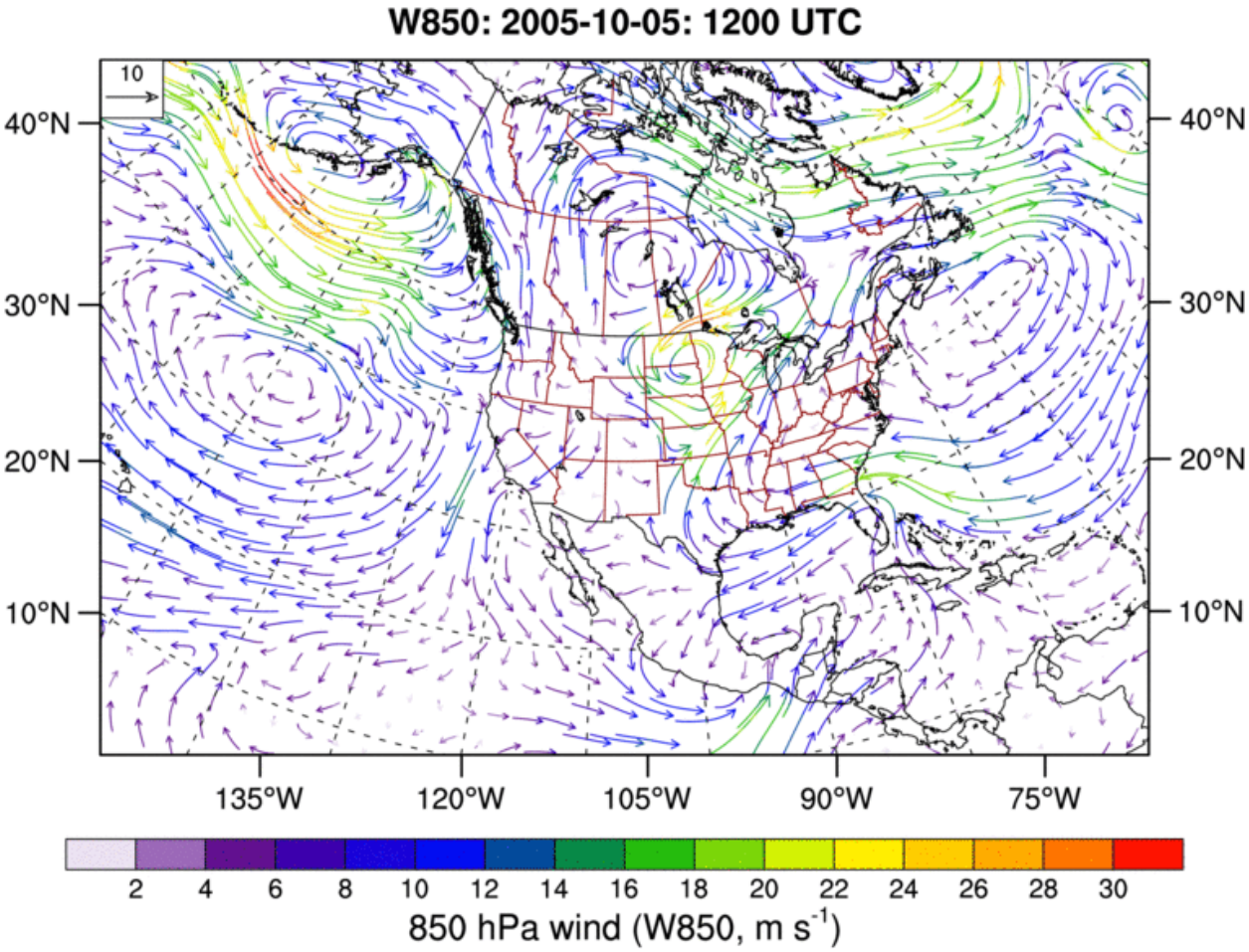
W850: 2005-10-05: 1200 UTC
10
40°N
30°N
20°N
10°N
135°W
120°W
105°W
90°W
75°W
2
4
6
8
10
12
14
16
18
20
22
24
26
28
30
850 hPa wind (W850, m s-1)

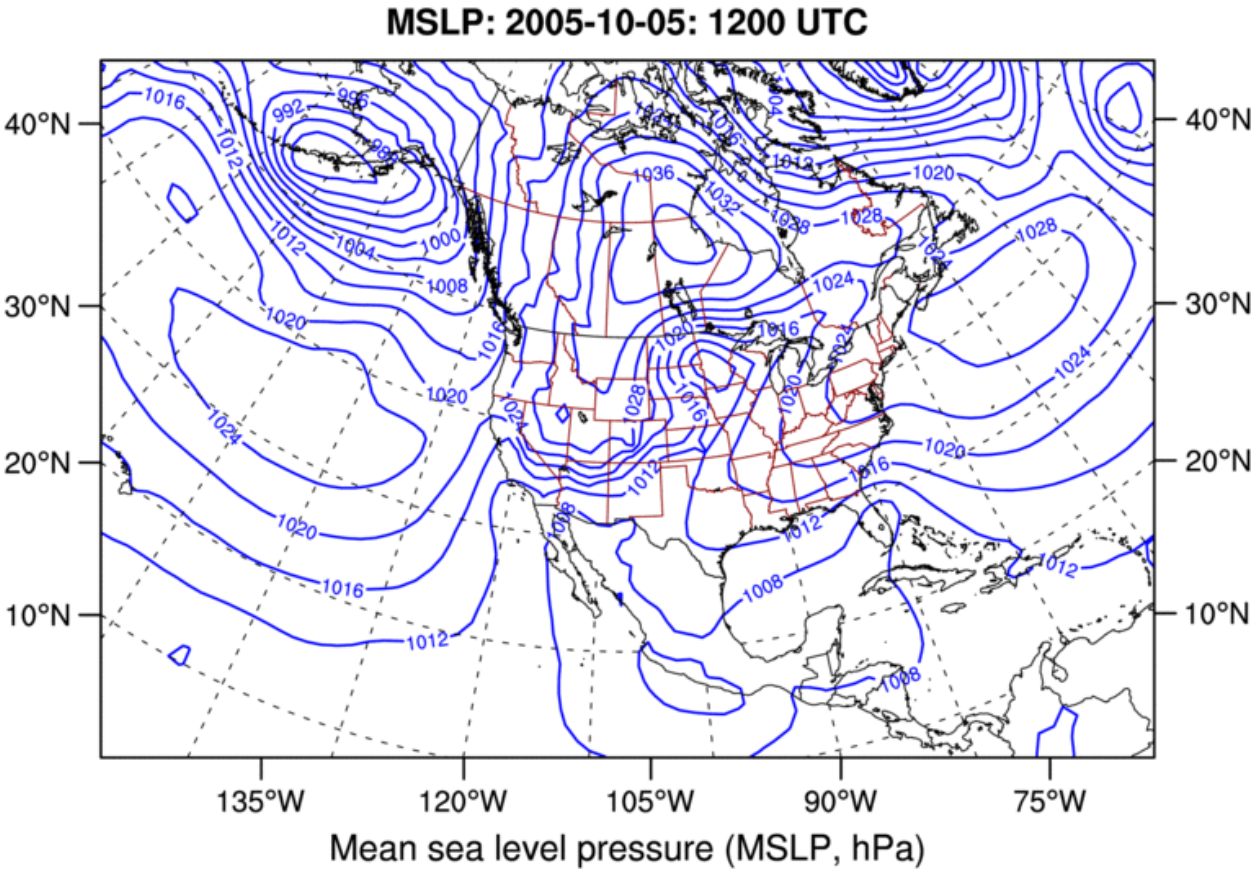
MSLP: 2005-10-05: 1200 UTC
40°N
30°N
20°N
10°N
135°W
120°W
105°W
90°W
75°W
Mean sea level pressure (MSLP, hPa)

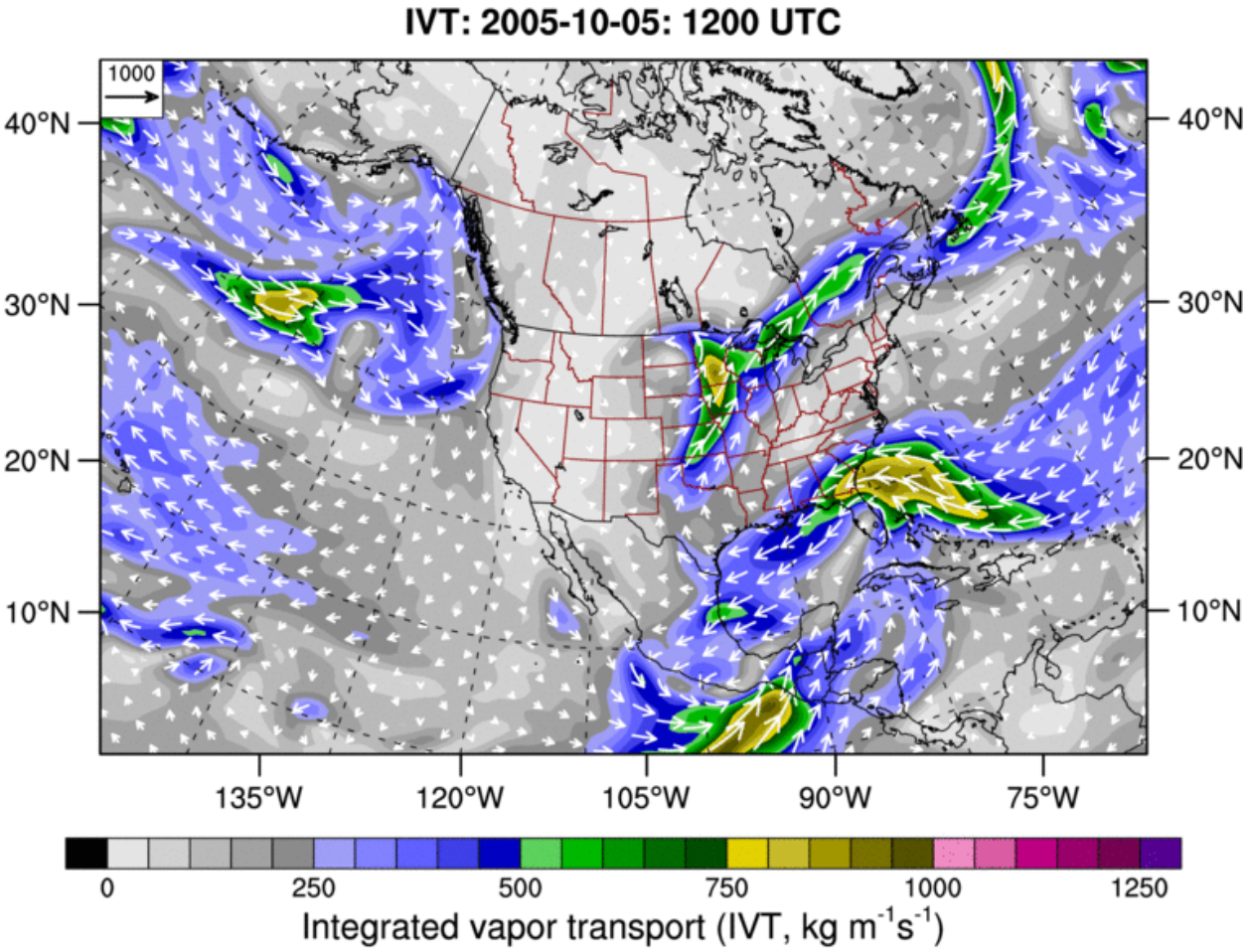
IVT: 2005-10-05: 1200 UTC
1000
40°N
30°N
20°N
10°N
135°W
120°W
105°W
90°W
75°W
0
250
500
750
1000
1250
Integrated vapor transport (IVT, kg m-1s-1)

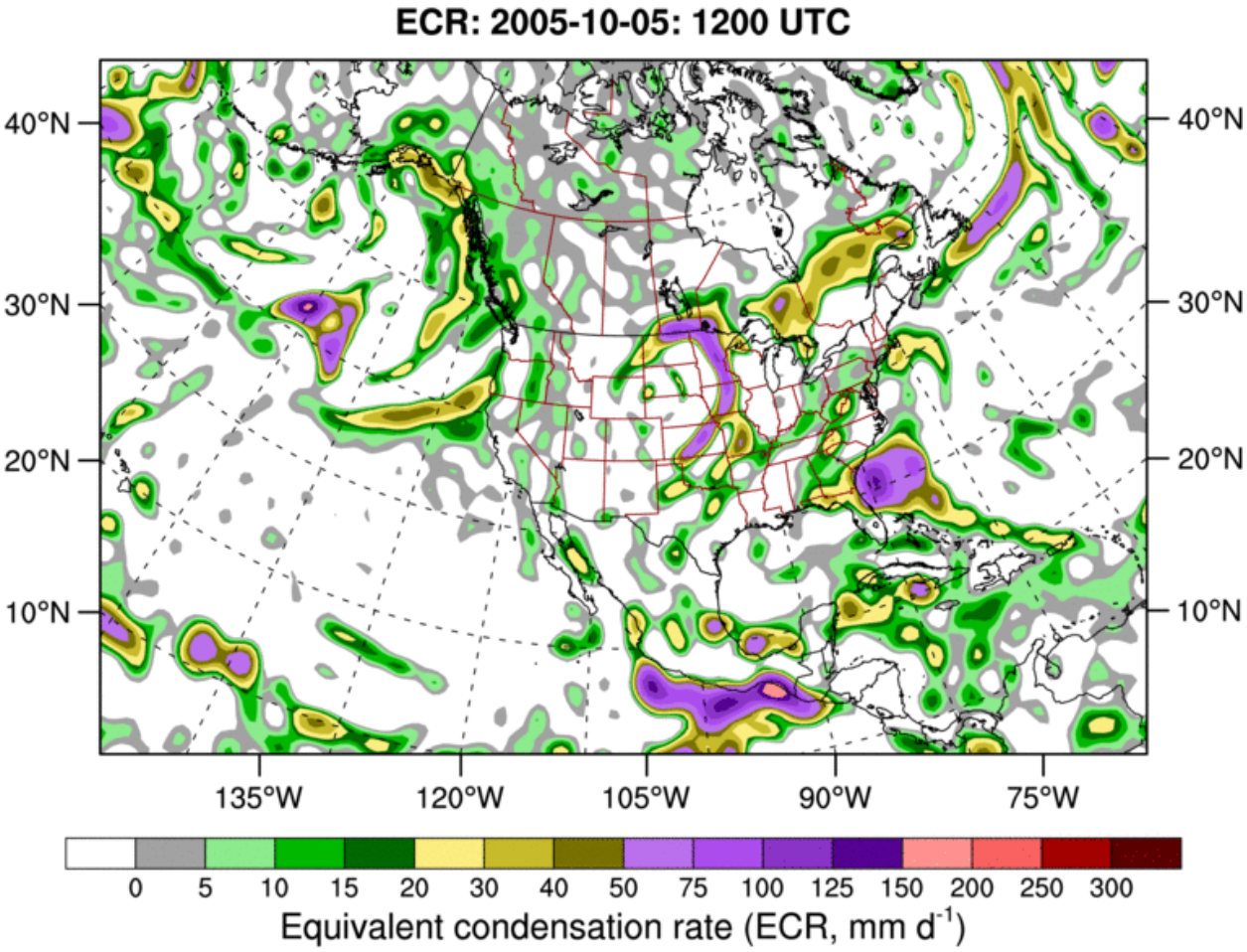
ECR: 2005-10-05: 1200 UTC
40°N
30°N
20°N
10°N
135°W
120°W
105°W
90°W
75°W
0 5 10 15 20 30 40 50 75 100 125 150 200 250 300
Equivalent condensation rate (ECR, mm d-1)

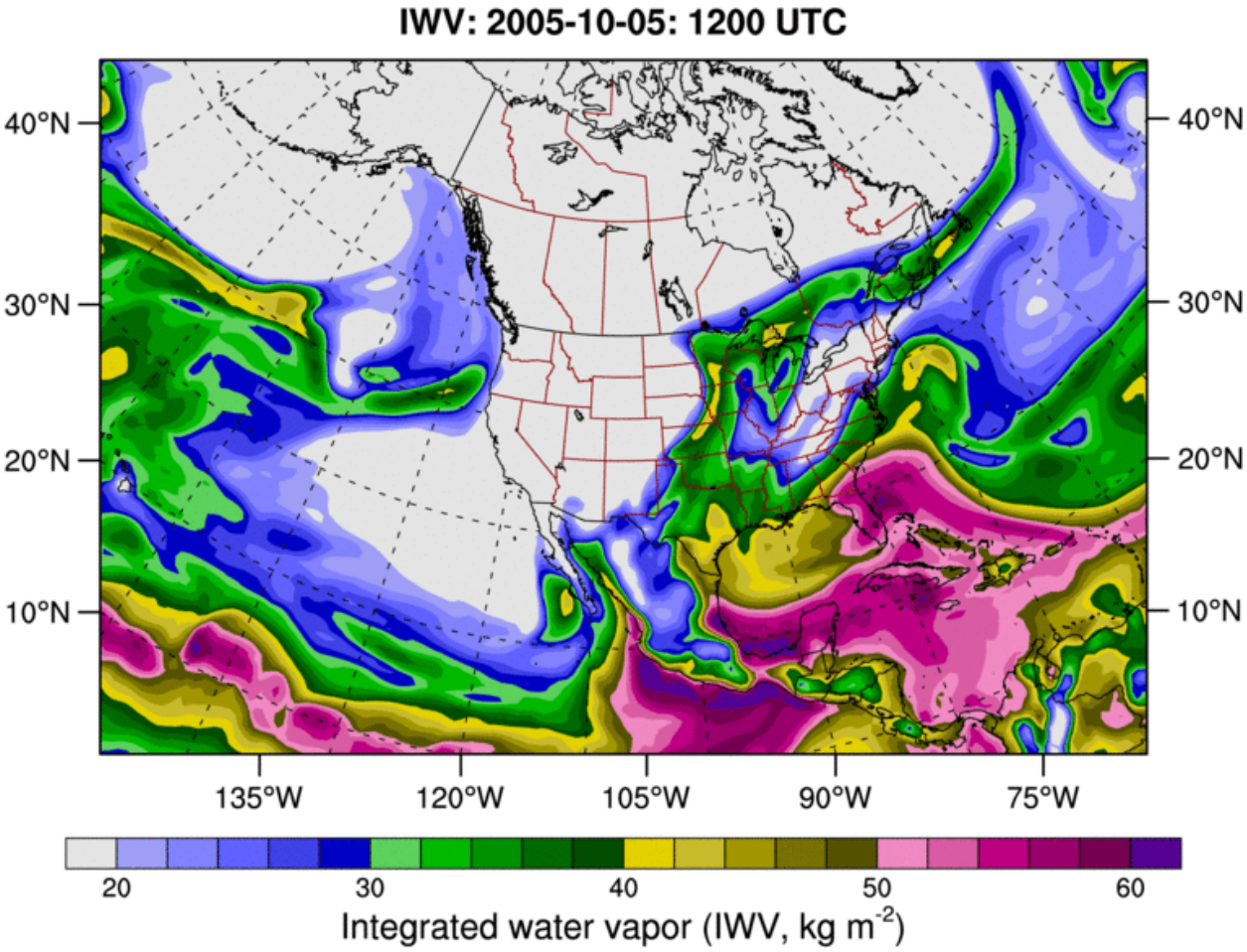
IWV: 2005-10-05: 1200 UTC
40°N
30°N
20°N
10°N
135°W
120°W
105°W
90°W
75°W
20
30
40
50
60
Integrated water vapor (IWV, kg m-2)

A5: December 14-19, 2005

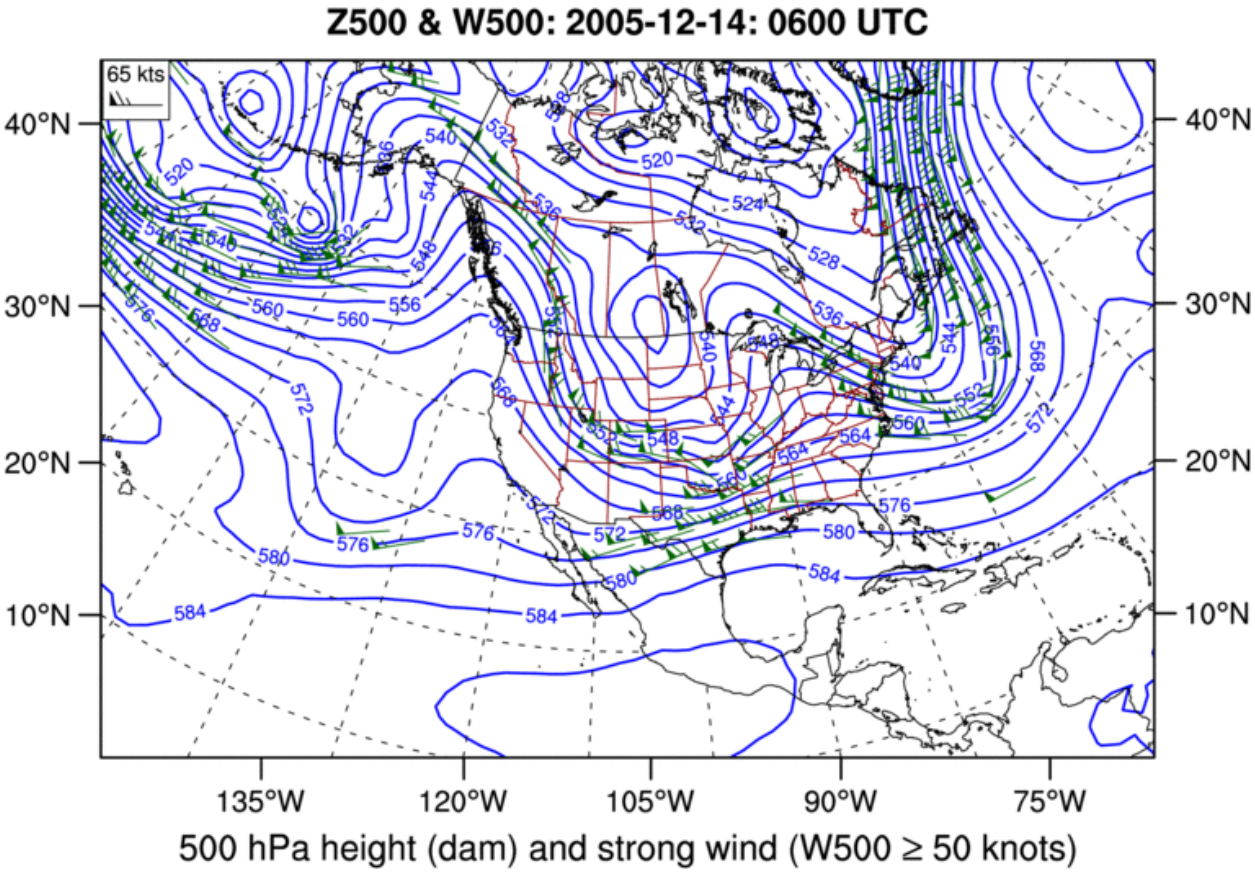

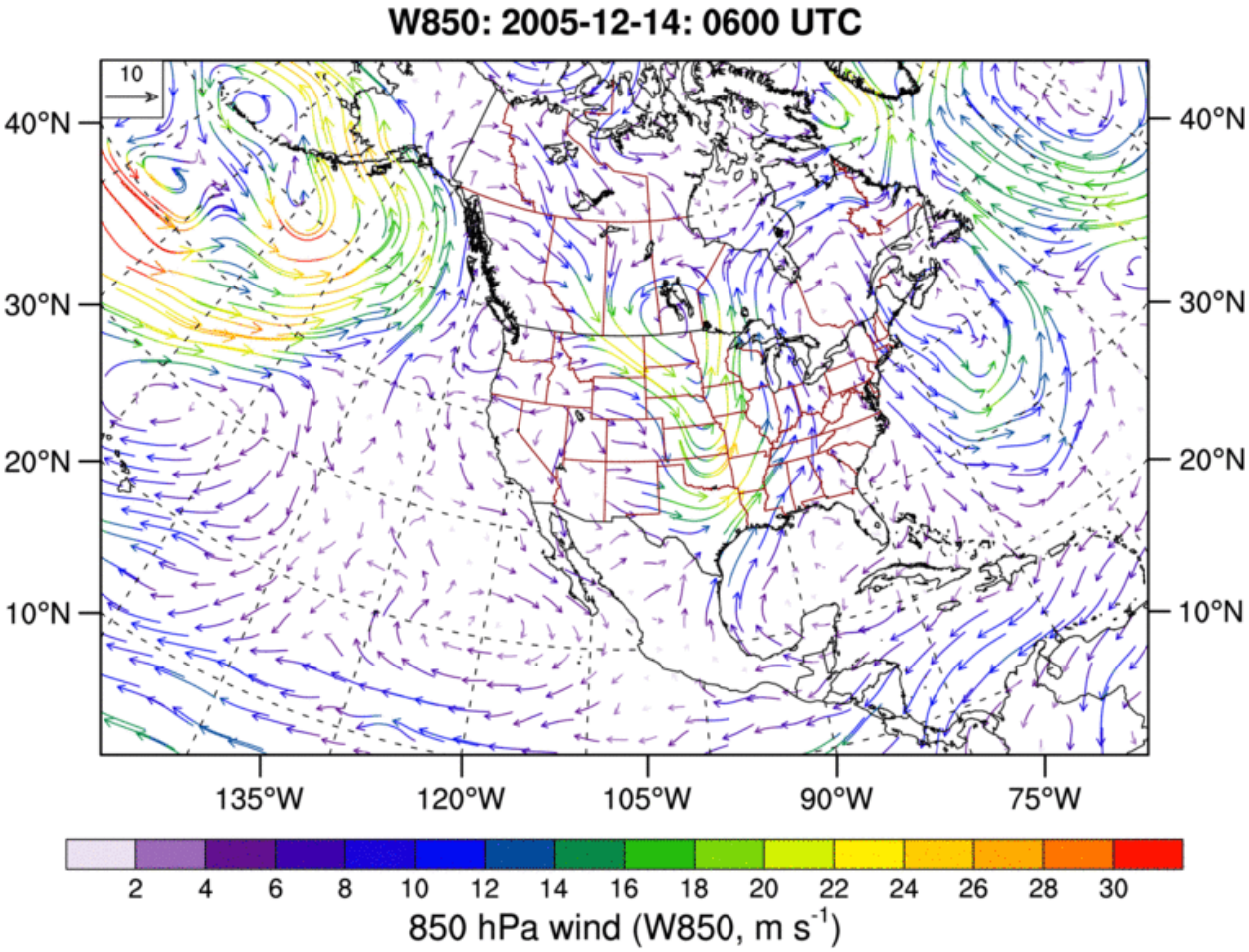
W850: 2005-12-14: 0600 UTC
10
40°N
30°N
20°N
10°N
135°W
120°W
105°W
90°W
75°W
2
4
6
8
10
12
14
16
18
20
22
24
26
28
30
850 hPa wind (W850, m s-1)

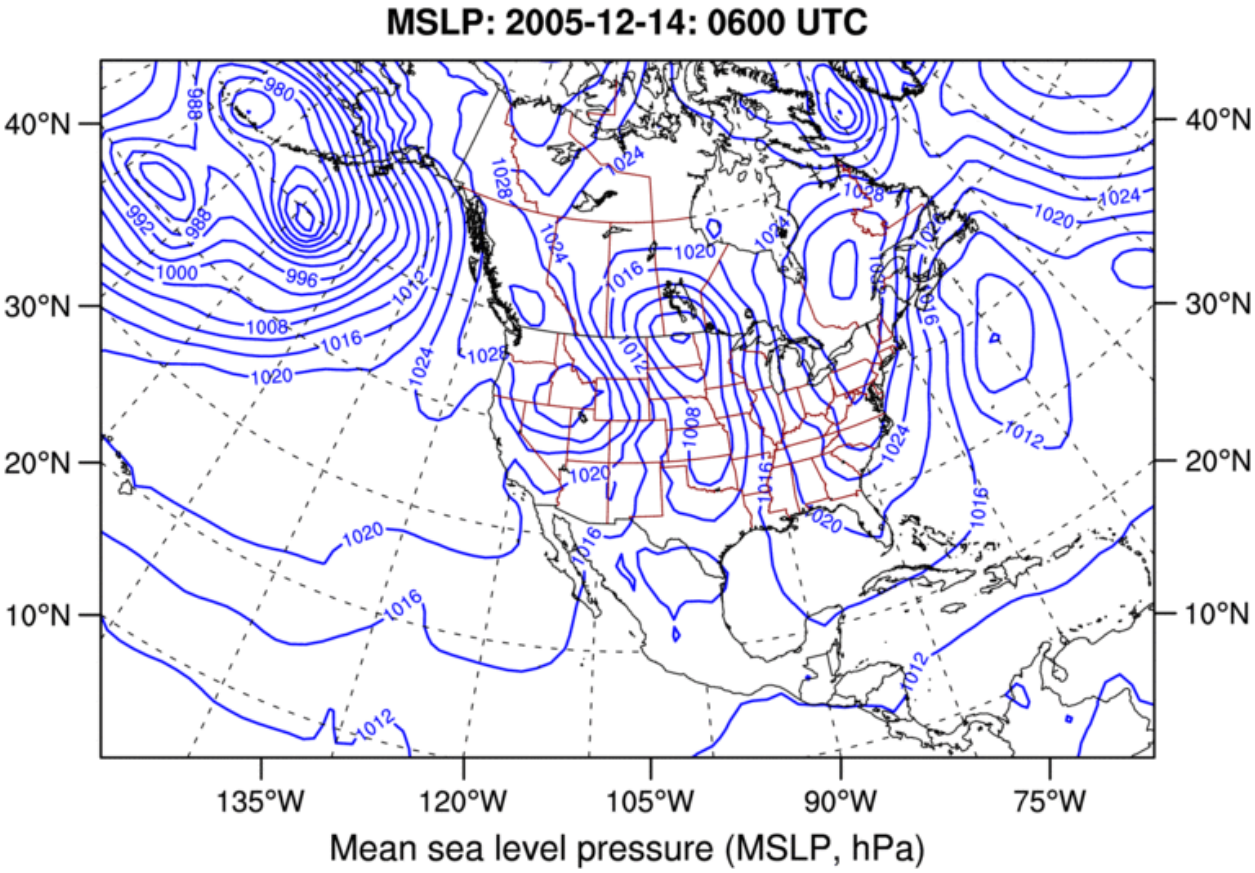
MSLP: 2005-12-14: 0600 UTC
40°N
30°N
20°N
10°N
135°W
120°W
105°W
90°W
75°W
Mean sea level pressure (MSLP, hPa)

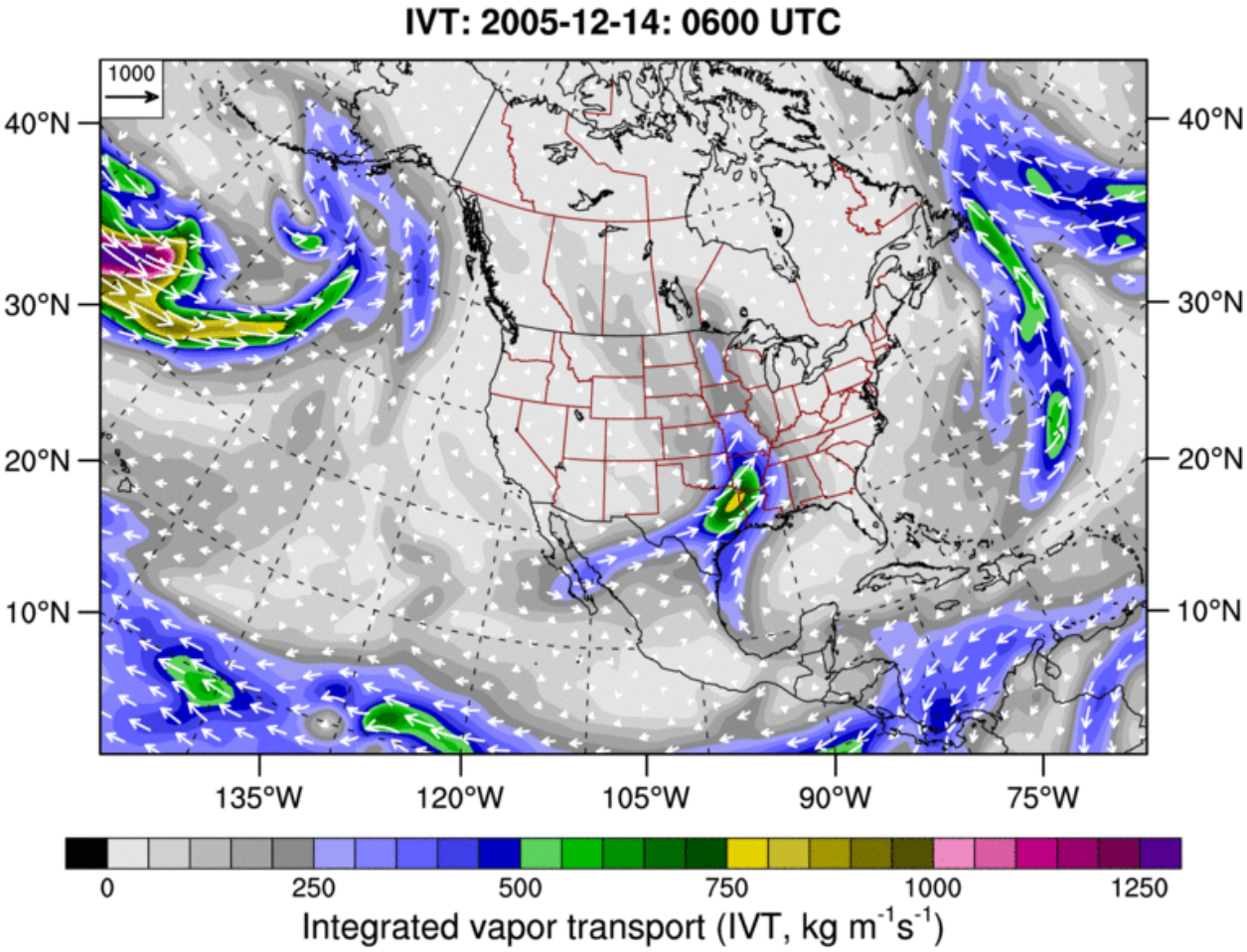
IVT: 2005-12-14: 0600 UTC
1000
40°N
30°N
20°N
10°N
135°W
120°W
105°W
90°W
75°W
0
250
500
750
1000
1250
Integrated vapor transport (IVT, kg m-1s-1)

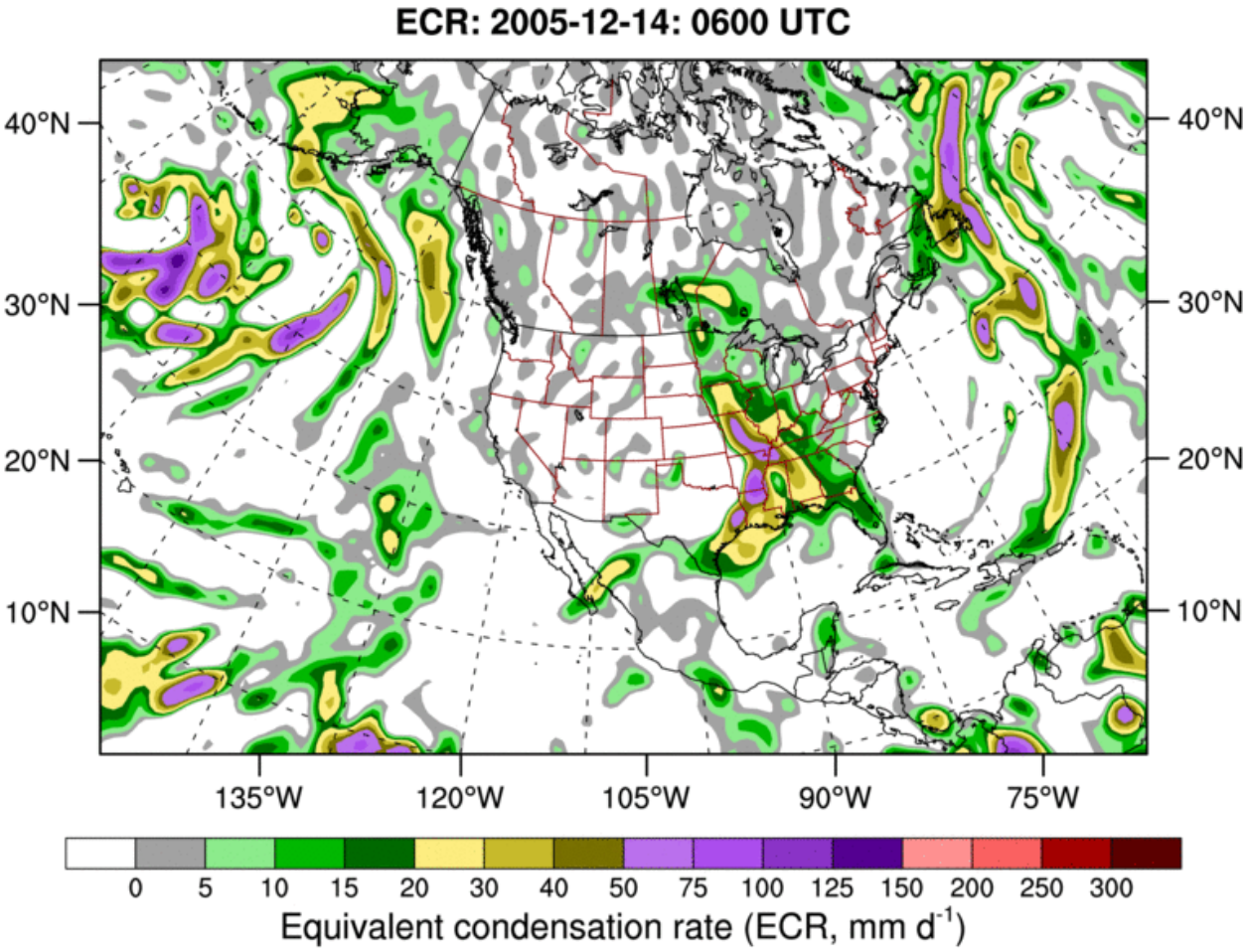
ECR: 2005-12-14: 0600 UTC
40°N
30°N
20°N
10°N
135°W
120°W
105°W
90°W
75°W
0
5
10
15
20
30
40
50
75
100
125
150
200
250
300
Equivalent condensation rate (ECR, mm d-1)

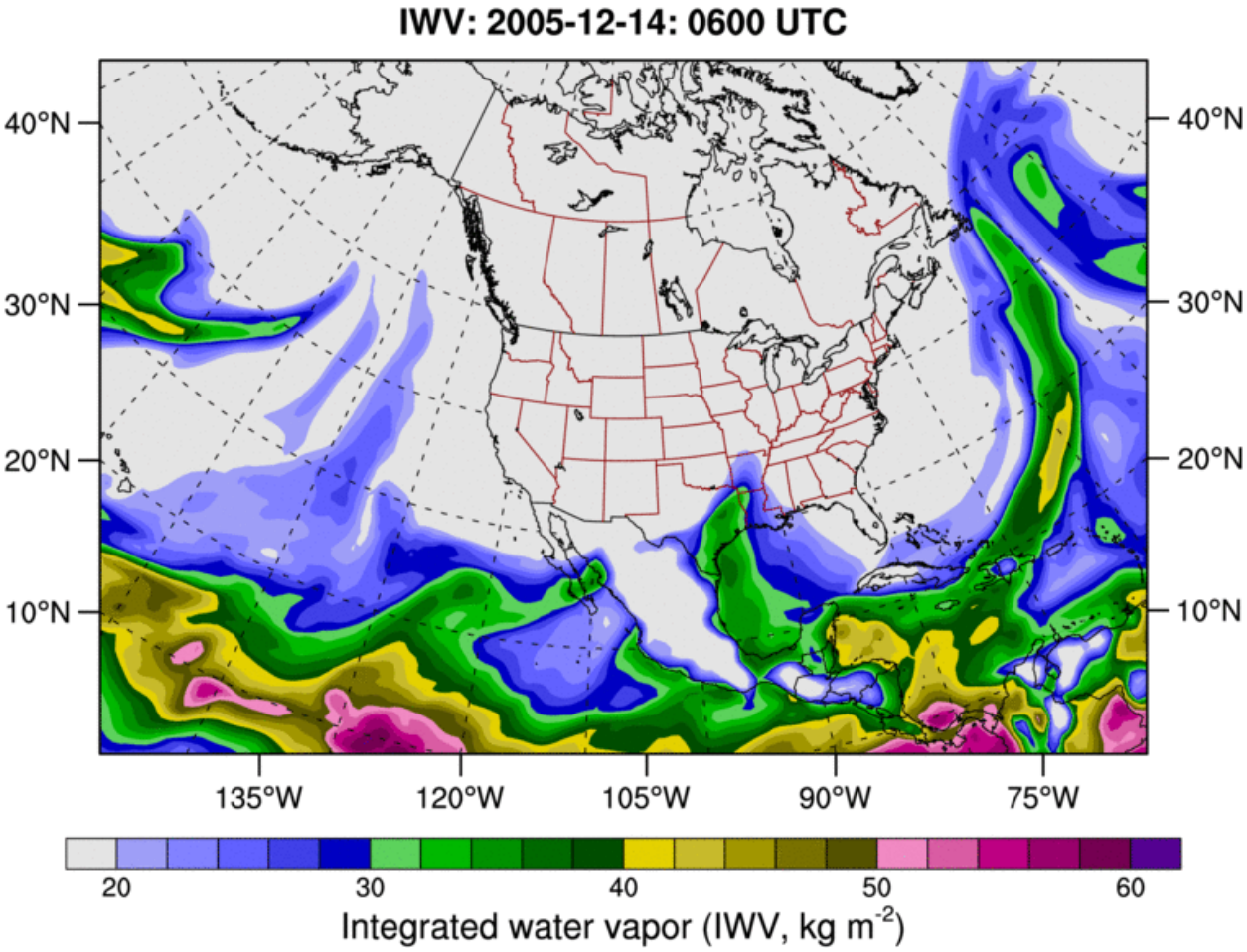
IWV: 2005-12-14: 0600 UTC
40°N
30°N
20°N
10°N
135°W
120°W
105°W
90°W
75°W
20
30
40
50
60
Integrated water vapor (IWV, kg m-2)

A6: December 28, 2005

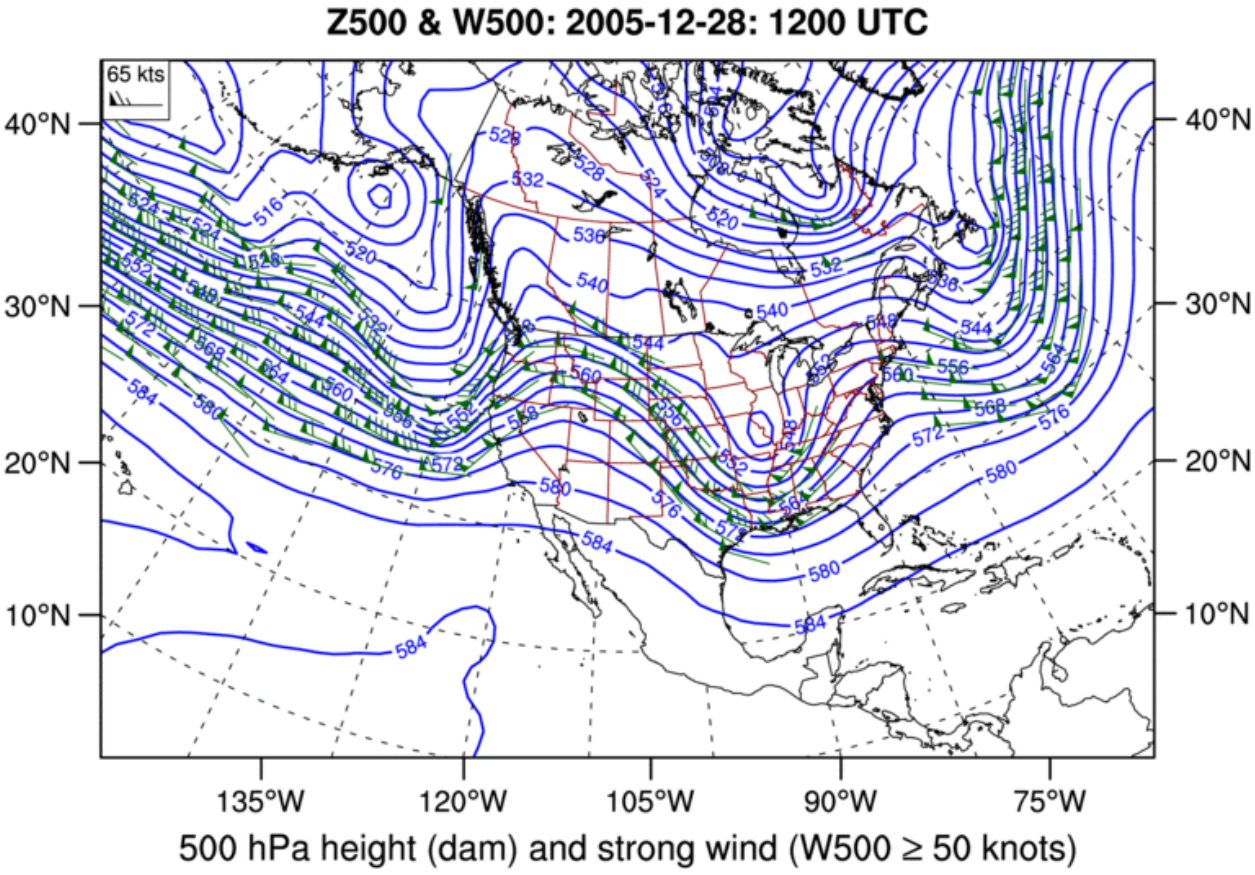

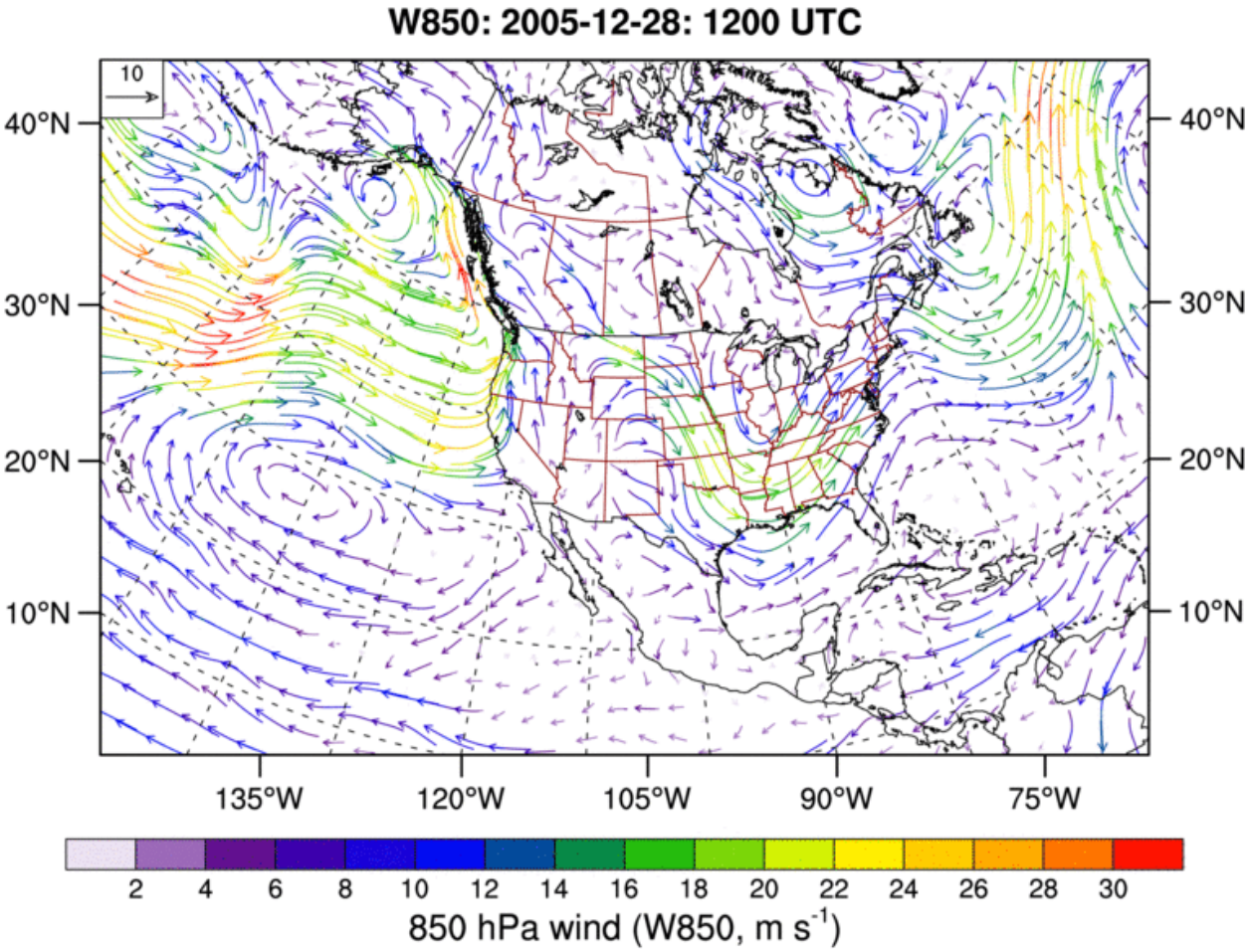
W850: 2005-12-28: 1200 UTC
10
40°N
30°N
20°N
10°N
135°W
120°W
105°W
90°W
75°W
2
4
6
8
10
12
14
16
18
20
22
24
26
28
30
850 hPa wind (W850, m s-1)

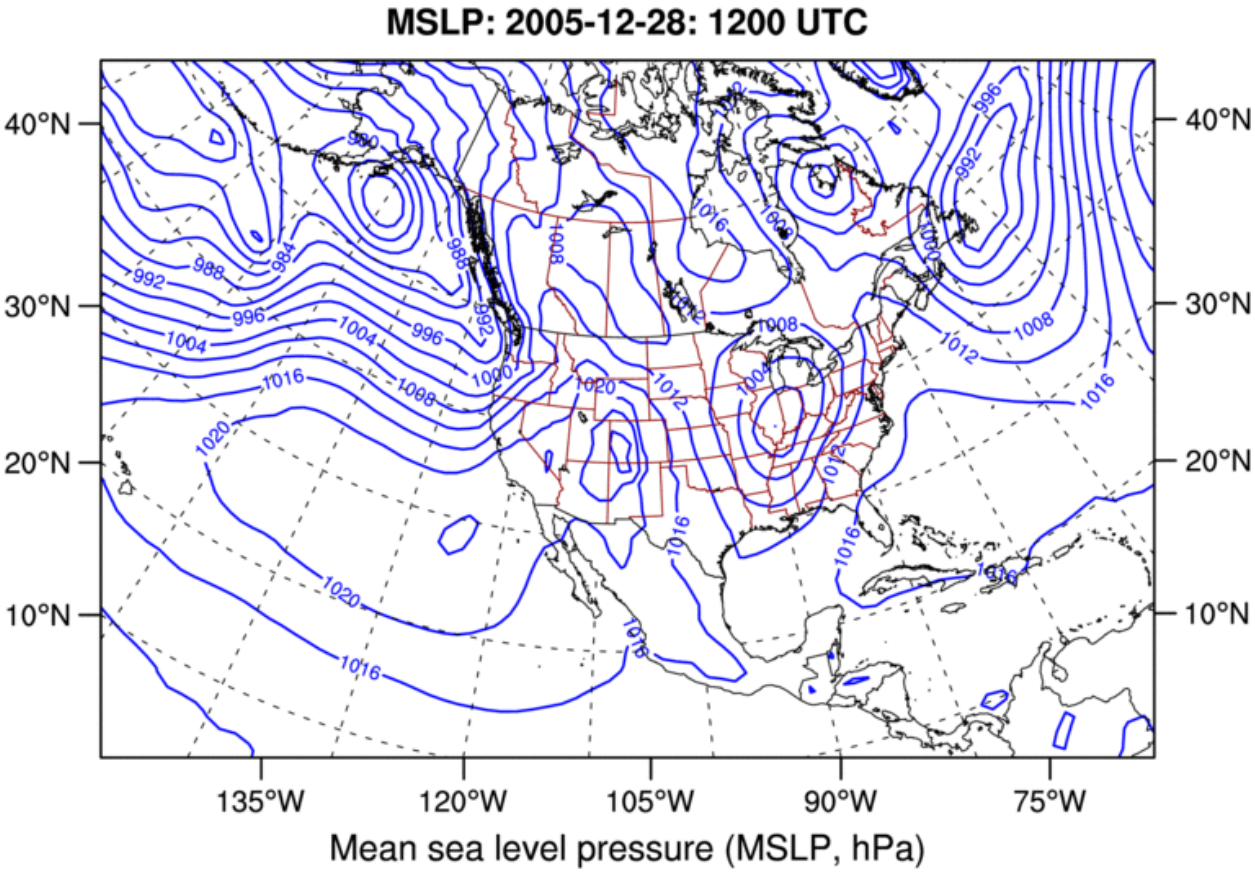
MSLP: 2005-12-28: 1200 UTC
40°N
30°N
20°N
10°N
135°W
120°W
105°W
90°W
75°W
Mean sea level pressure (MSLP, hPa)

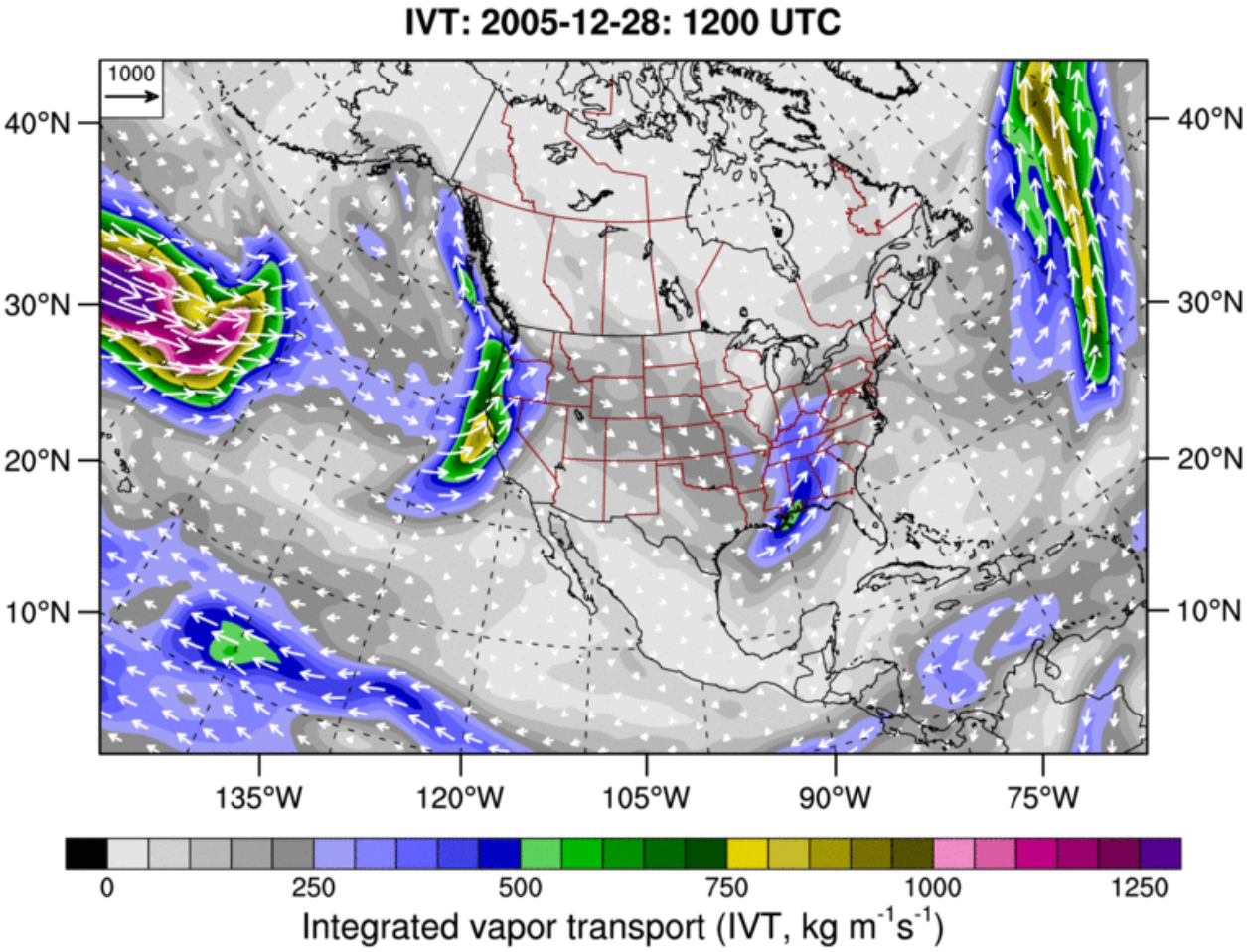
IVT: 2005-12-28: 1200 UTC
1000
40°N
30°N
20°N
10°N
135°W
120°W
105°W
90°W
75°W
0
250
500
750
1000
1250
Integrated vapor transport (IVT, kg m-1s-1)

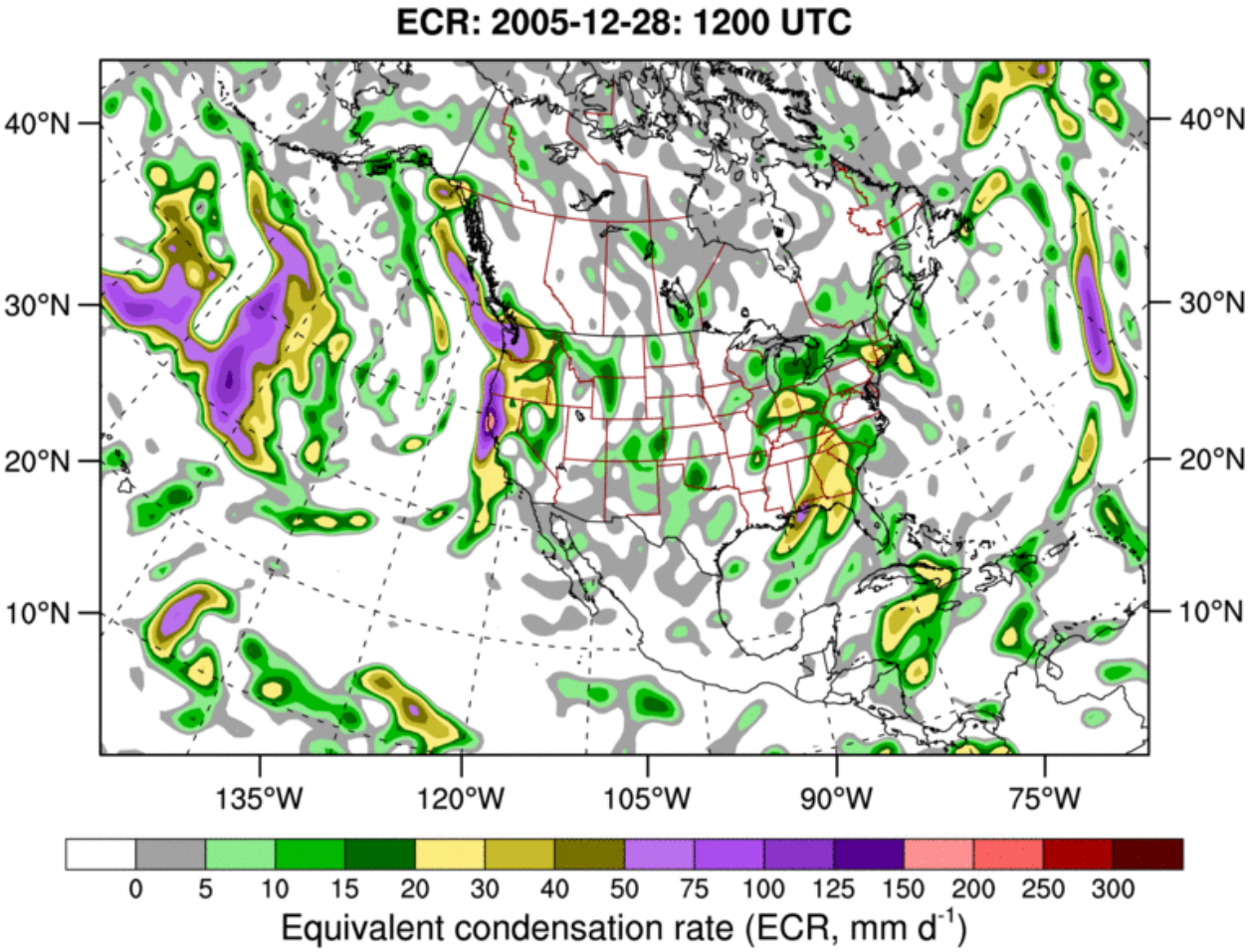
ECR: 2005-12-28: 1200 UTC
40°N
30°N
20°N
10°N
135°W
120°W
105°W
90°W
75°W
0
5
10
15
20
30
40
50
75
100
125
150
200
250
300
Equivalent condensation rate (ECR, mm d-1)

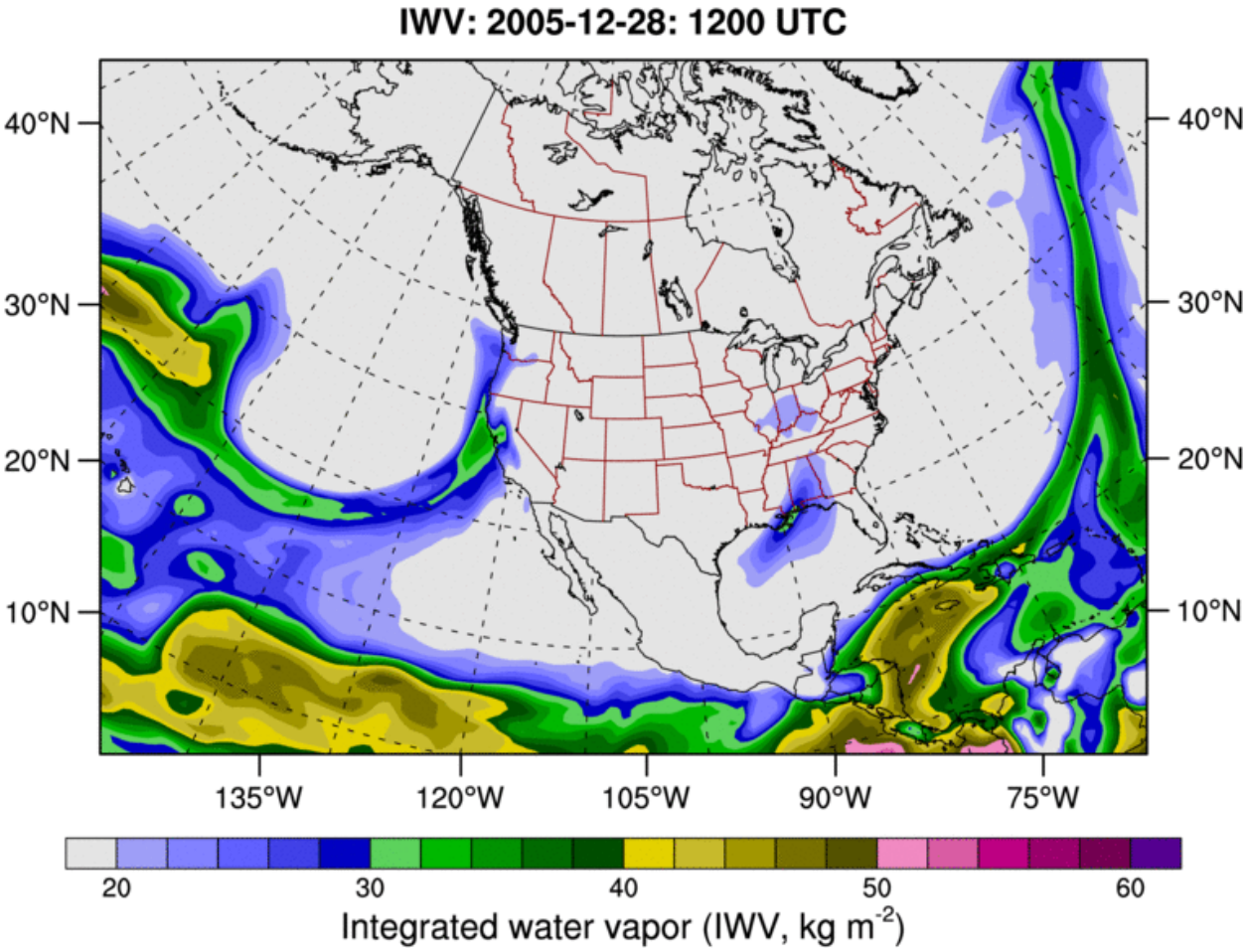
IWV: 2005-12-28: 1200 UTC
40°N
30°N
20°N
10°N
135°W
120°W
105°W
90°W
75°W
20
30
40
50
60
Integrated water vapor (IWV, kg m-2)

A7: January 12-18, 2006

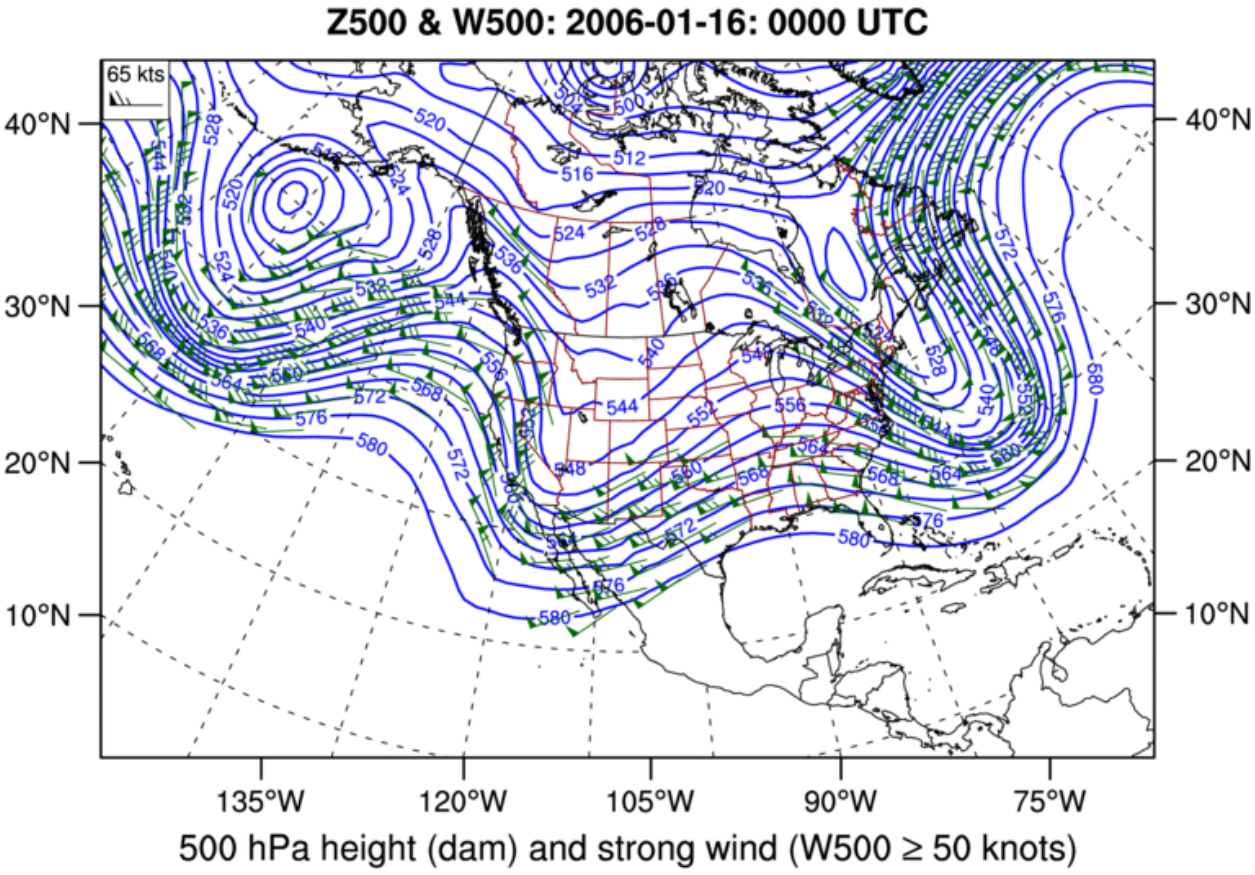

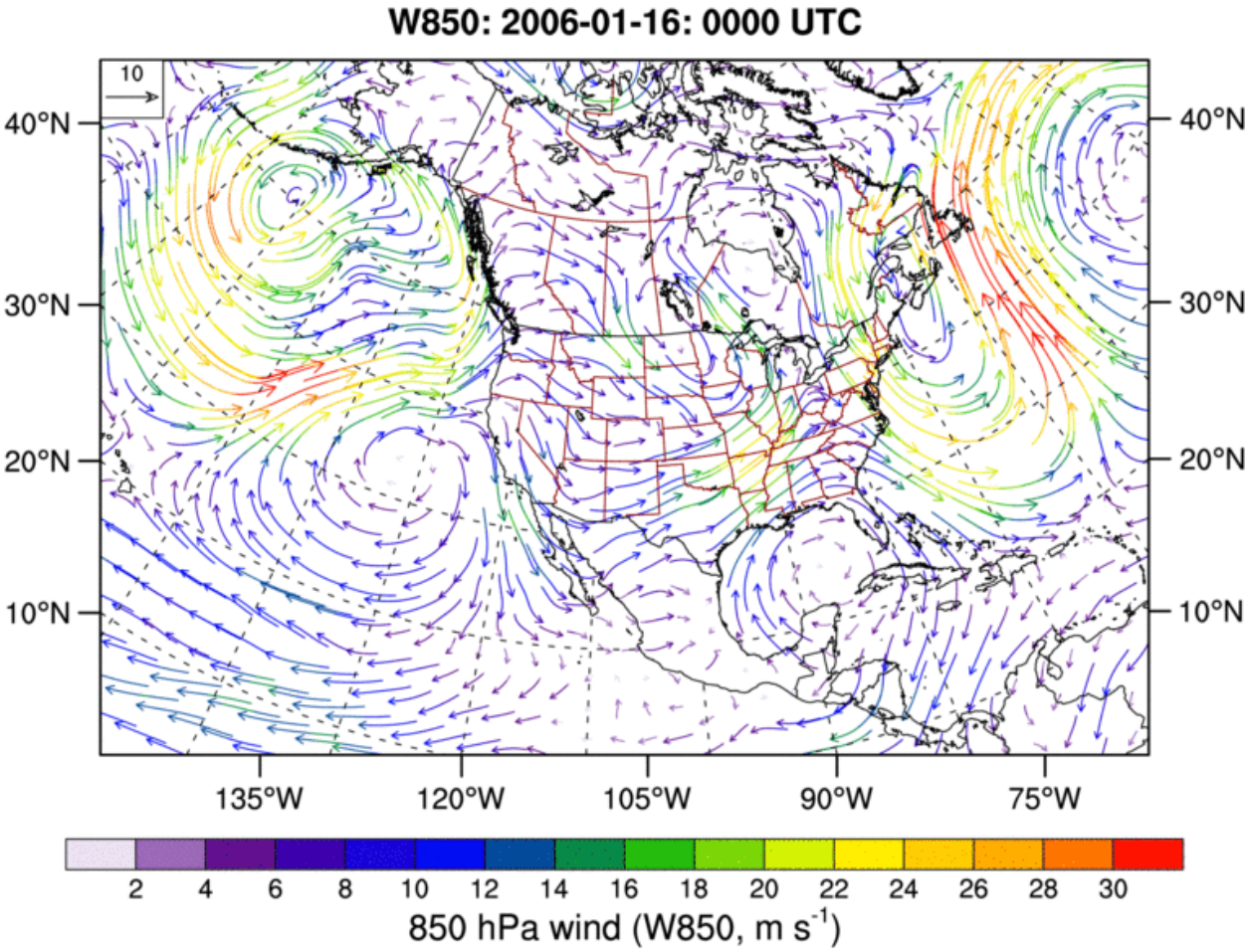
W850: 2006-01-16: 0000 UTC
10
40°N
30°N
20°N
10°N
135°W
120°W
105°W
90°W
75°W
2
4
6
8
10
12
14
16
18
20
22
24
26
28
30
850 hPa wind (W850, m s-1)

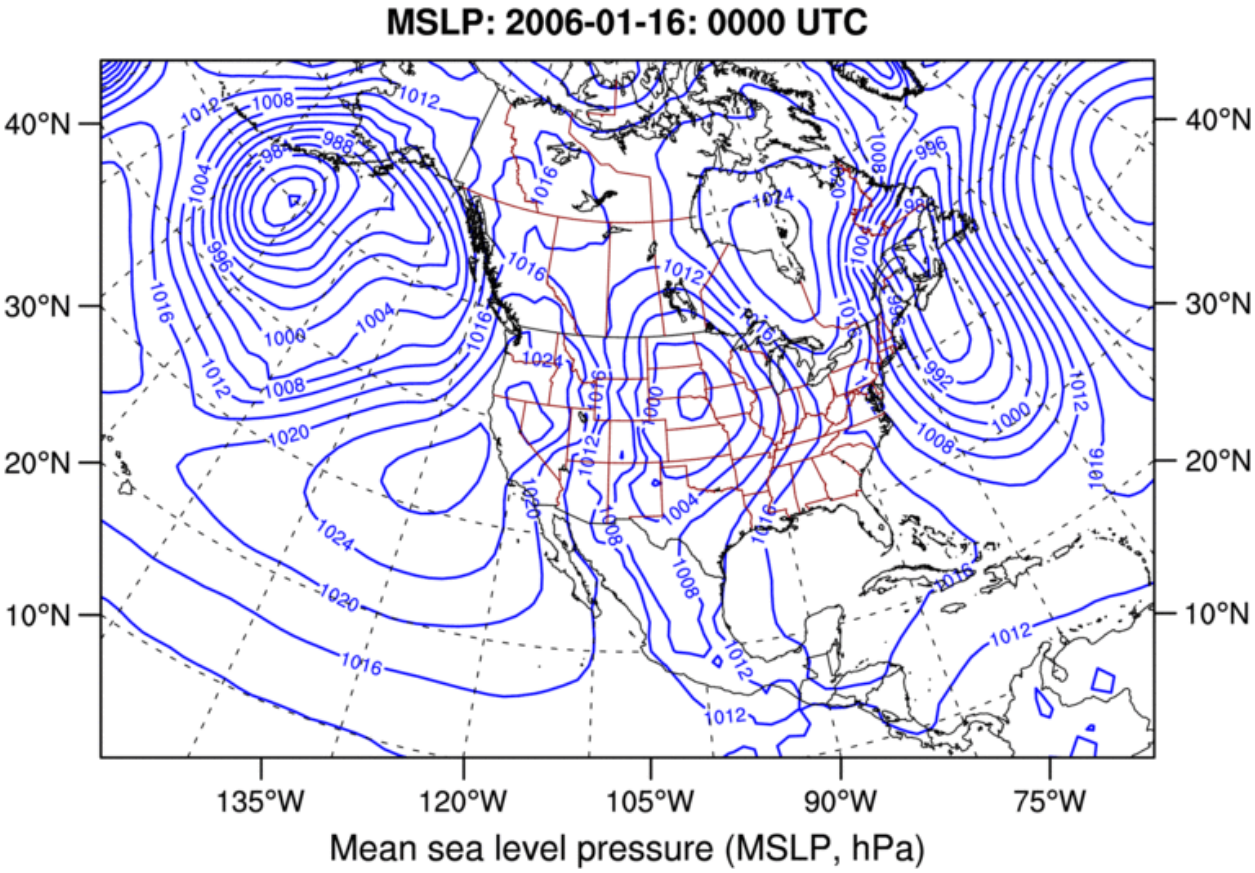
MSLP: 2006-01-16: 0000 UTC
40°N
30°N
20°N
10°N
135°W
120°W
105°W
90°W
75°W
Mean sea level pressure (MSLP, hPa)

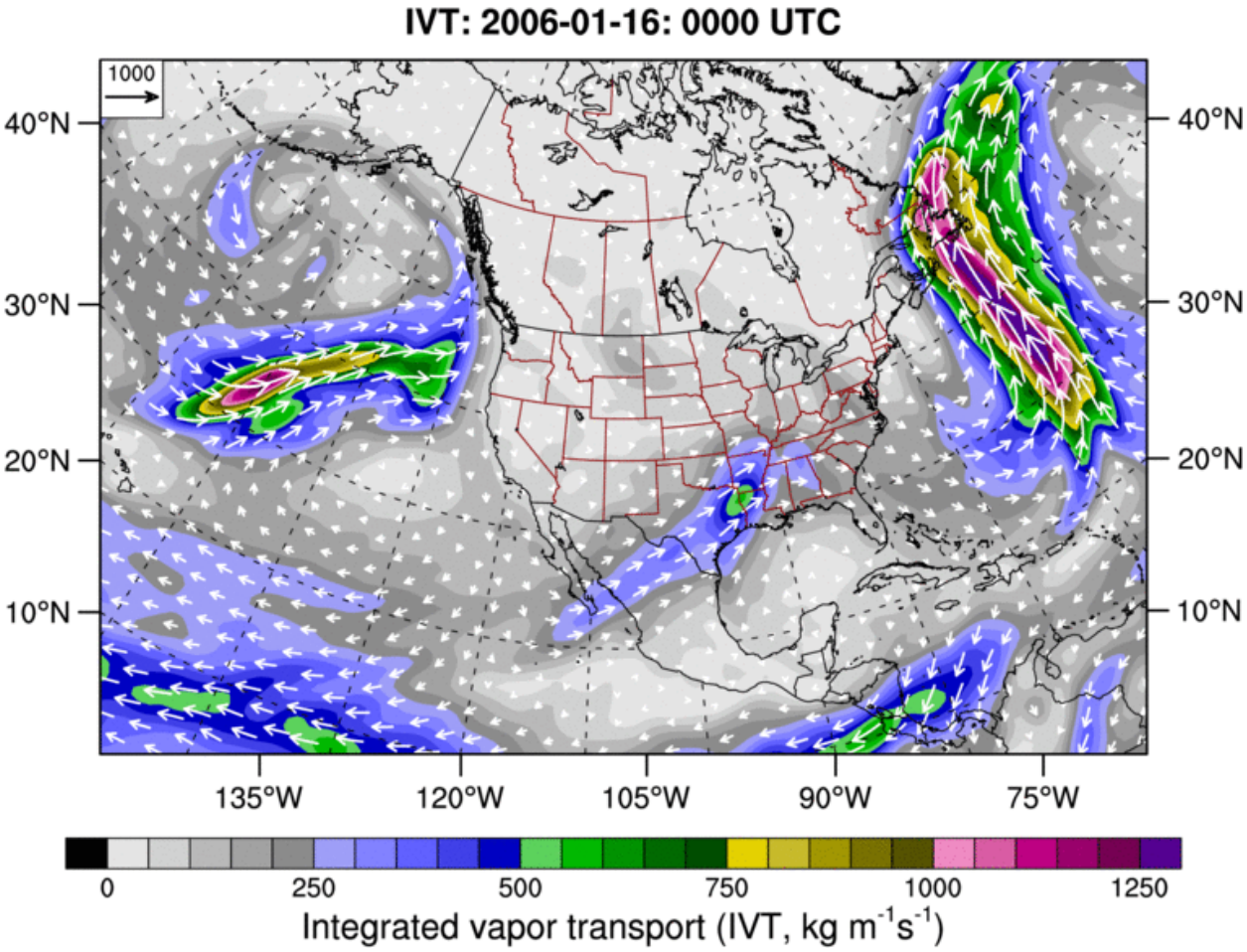
IVT: 2006-01-16: 0000 UTC
1000
40°N
30°N
20°N
10°N
135°W
120°W
105°W
90°W
75°W
0
250
500
750
1000
1250
Integrated vapor transport (IVT, kg m-1s-1)

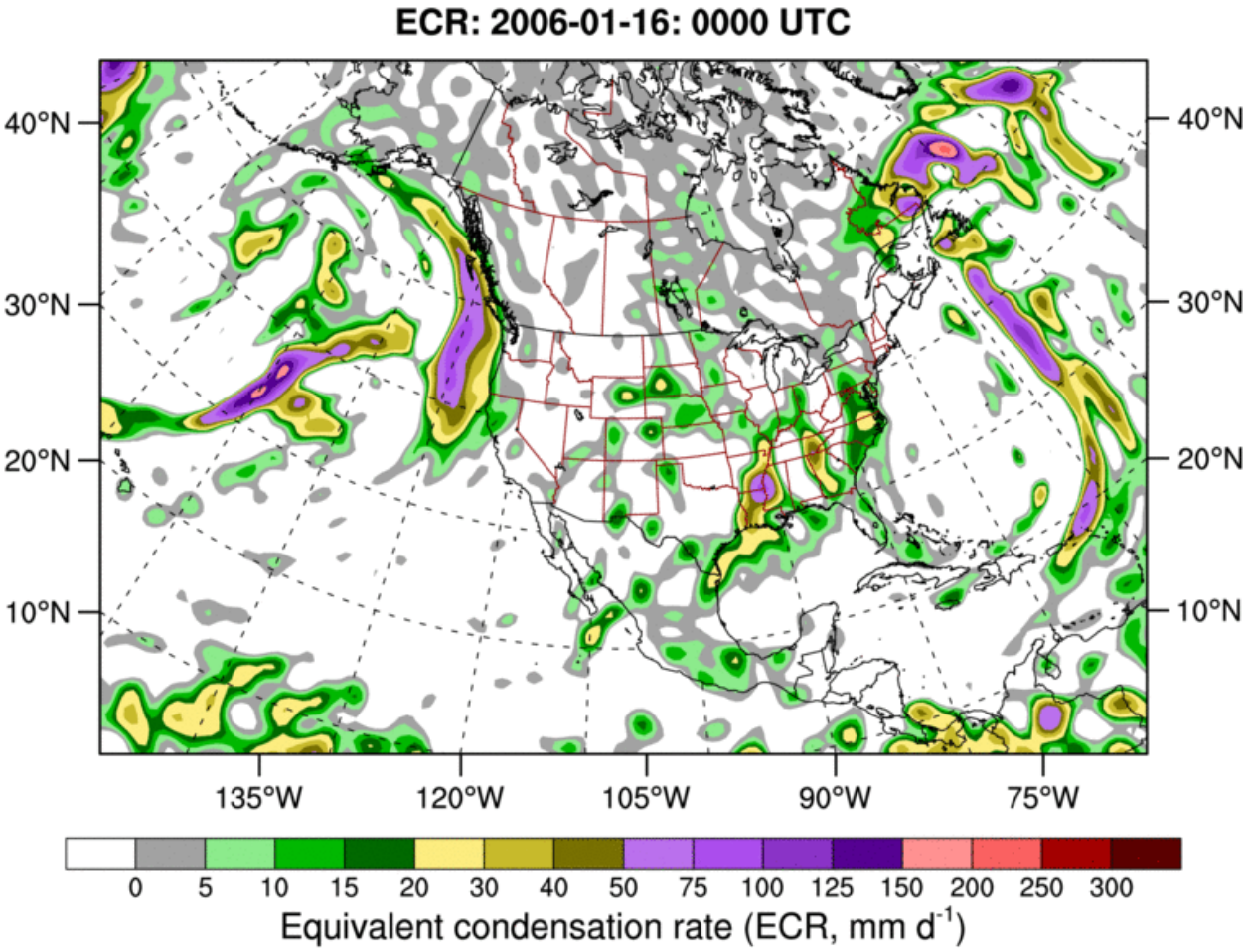
ECR: 2006-01-16: 0000 UTC
40°N
30°N
20°N
10°N
135°W
120°W
105°W
90°W
75°W
0
5
10
15
20
30
40
50
75
100
125
150
200
250
300
Equivalent condensation rate (ECR, mm d-1)

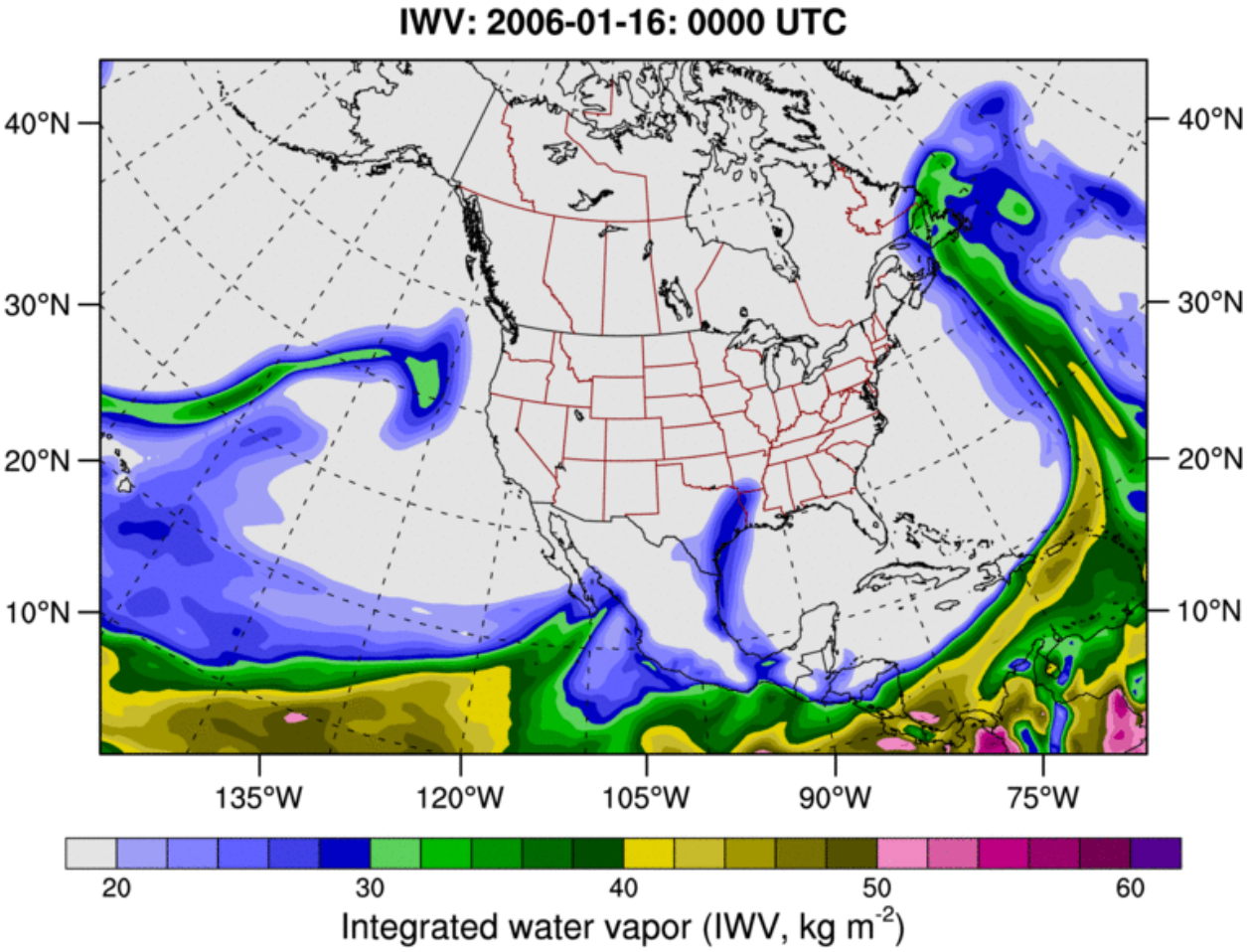
IWV: 2006-01-16: 0000 UTC
40°N
30°N
20°N
10°N
135°W
120°W
105°W
90°W
75°W
20
30
40
50
60
Integrated water vapor (IWV, kg m-2)

A8: October 13, 2006

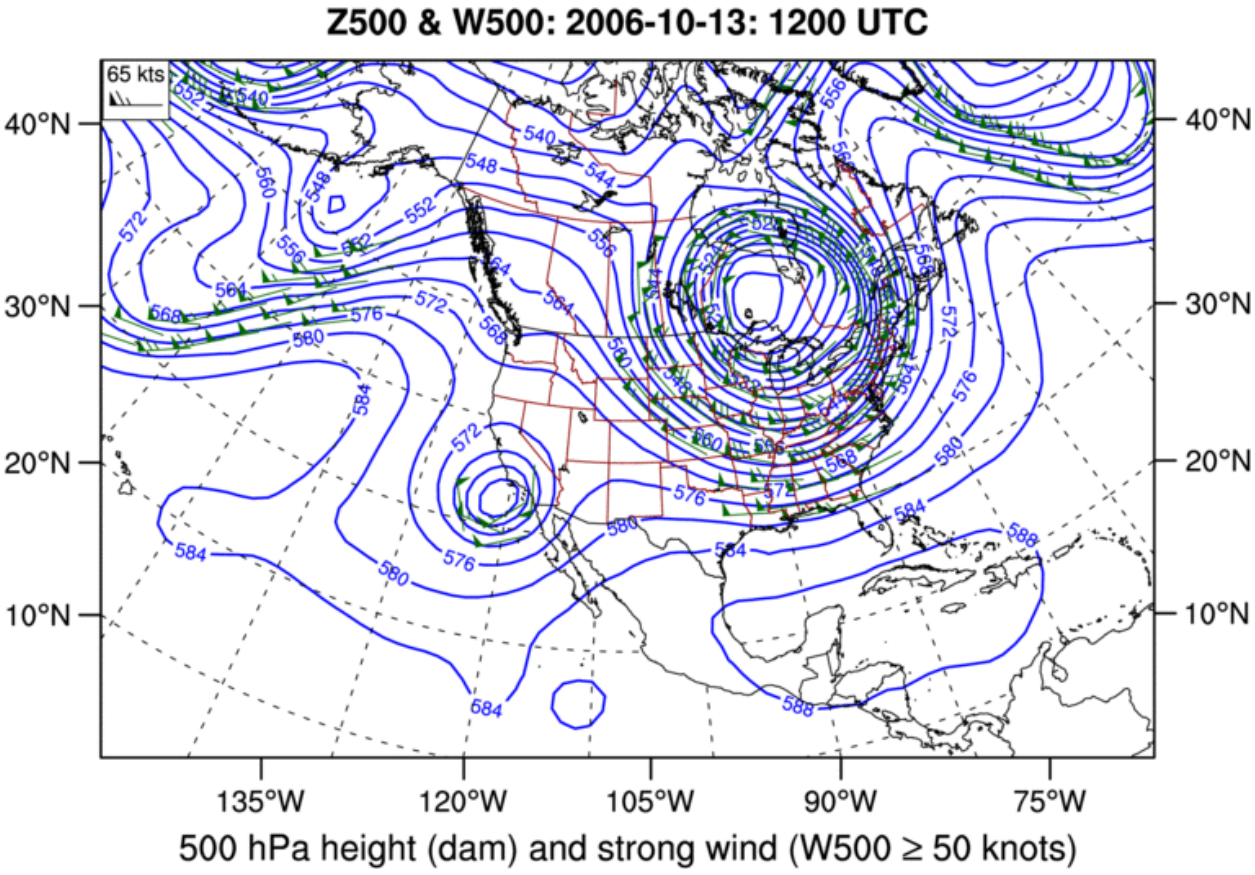

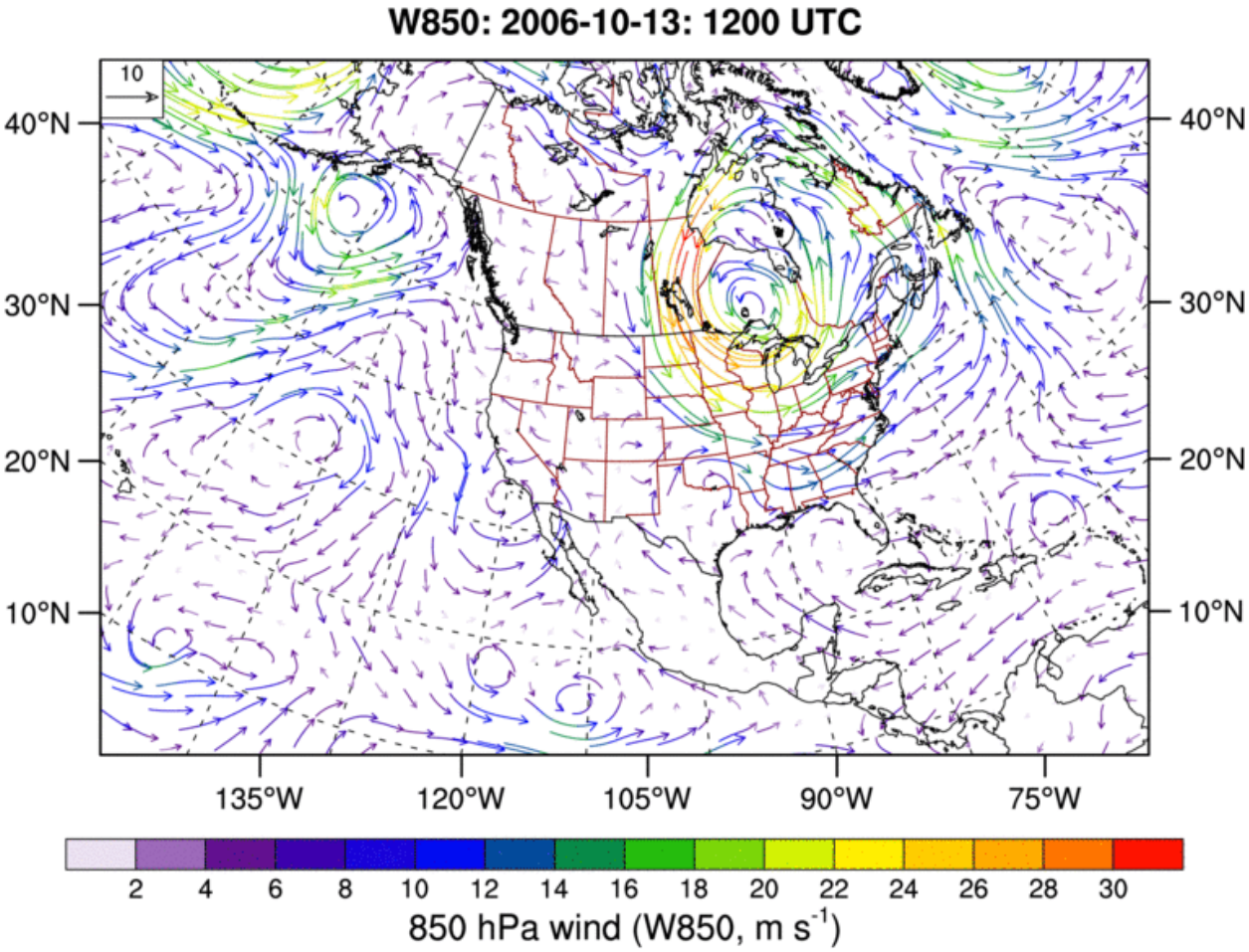
W850: 2006-10-13: 1200 UTC
10
40°N
30°N
20°N
10°N
135°W
120°W
105°W
90°W
75°W
2 4 6 8 10 12 14 16 18 20 22 24 26 28 30
850 hPa wind (W850, m s-1)

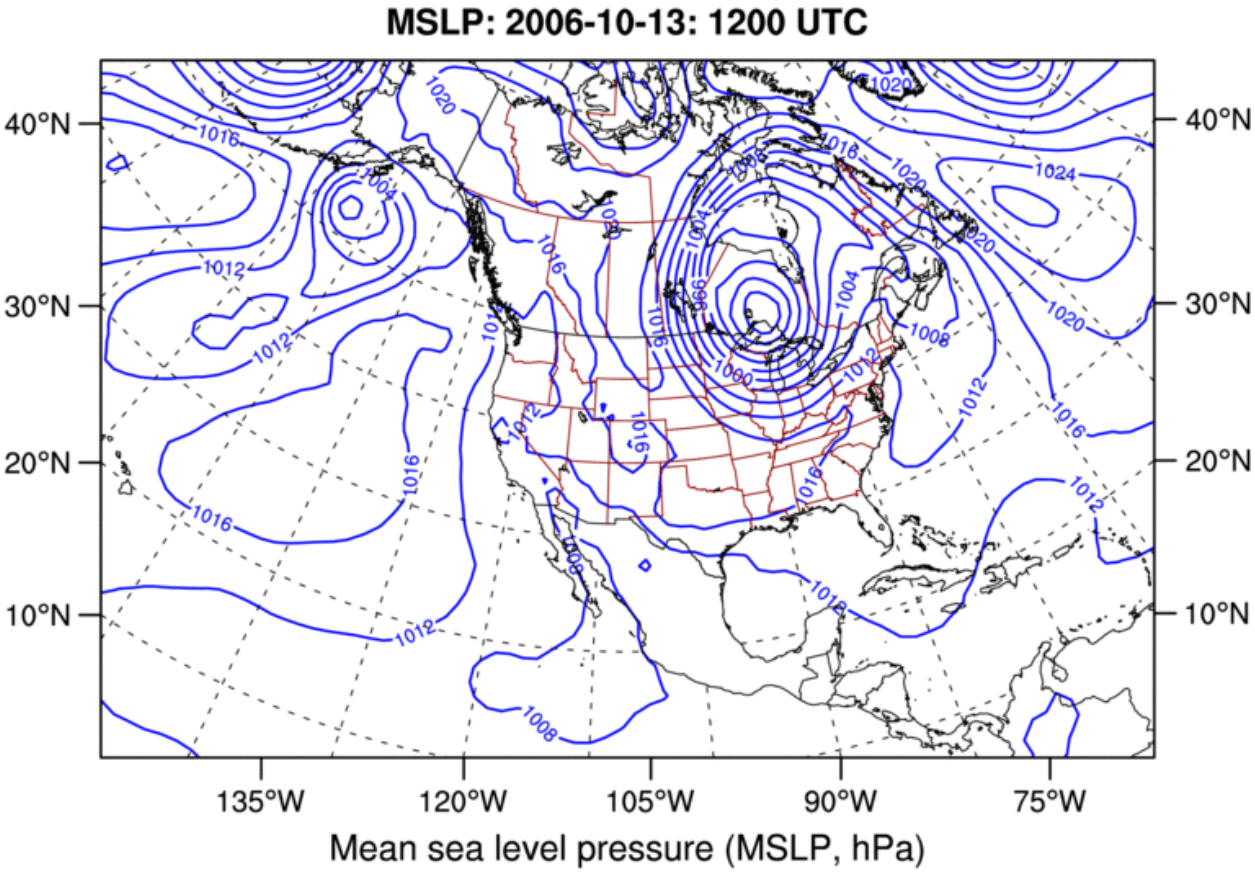
MSLP: 2006-10-13: 1200 UTC
40°N
30°N
20°N
10°N
135°W
120°W
105°W
90°W
75°W
Mean sea level pressure (MSLP, hPa)

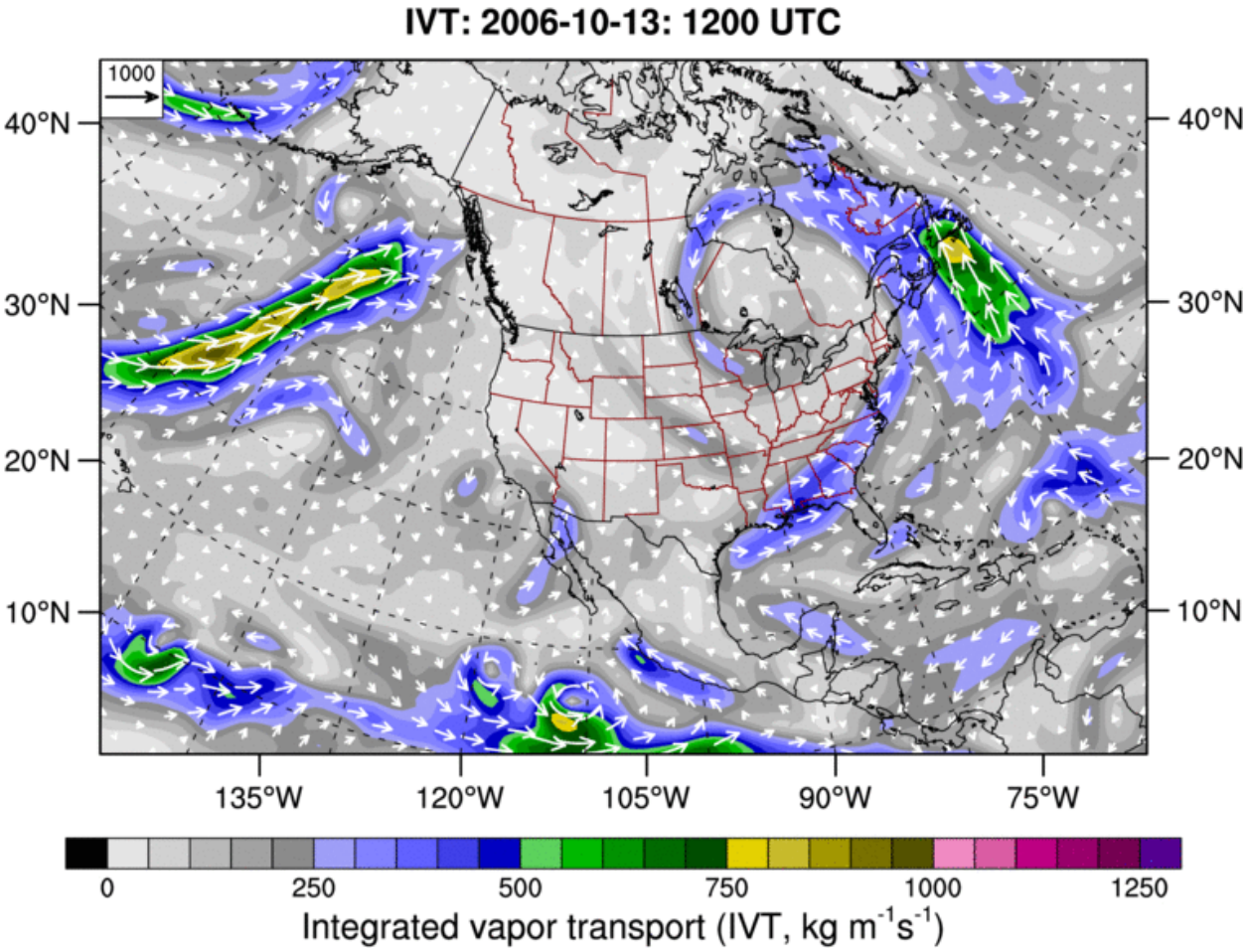
IVT: 2006-10-13: 1200 UTC
1000
40°N
30°N
20°N
10°N
135°W
120°W
105°W
90°W
75°W
0
250
500
750
1000
1250
Integrated vapor transport (IVT, kg m-1s-1)

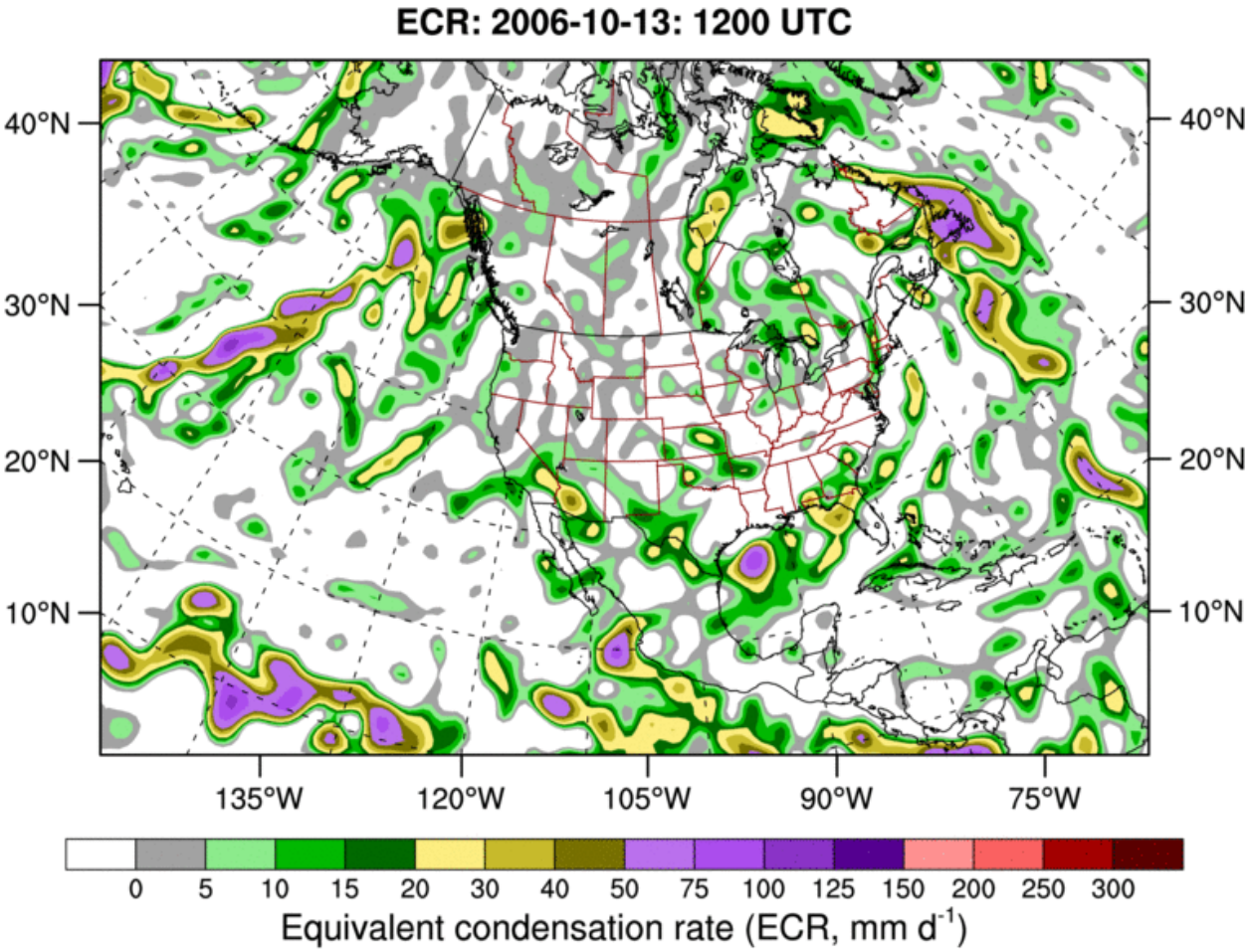
ECR: 2006-10-13: 1200 UTC
40°N
30°N
20°N
10°N
135°W
120°W
105°W
90°W
75°W
0
5
10
15
20
30
40
50
75
100
125
150
200
250
300
Equivalent condensation rate (ECR, mm d-1)

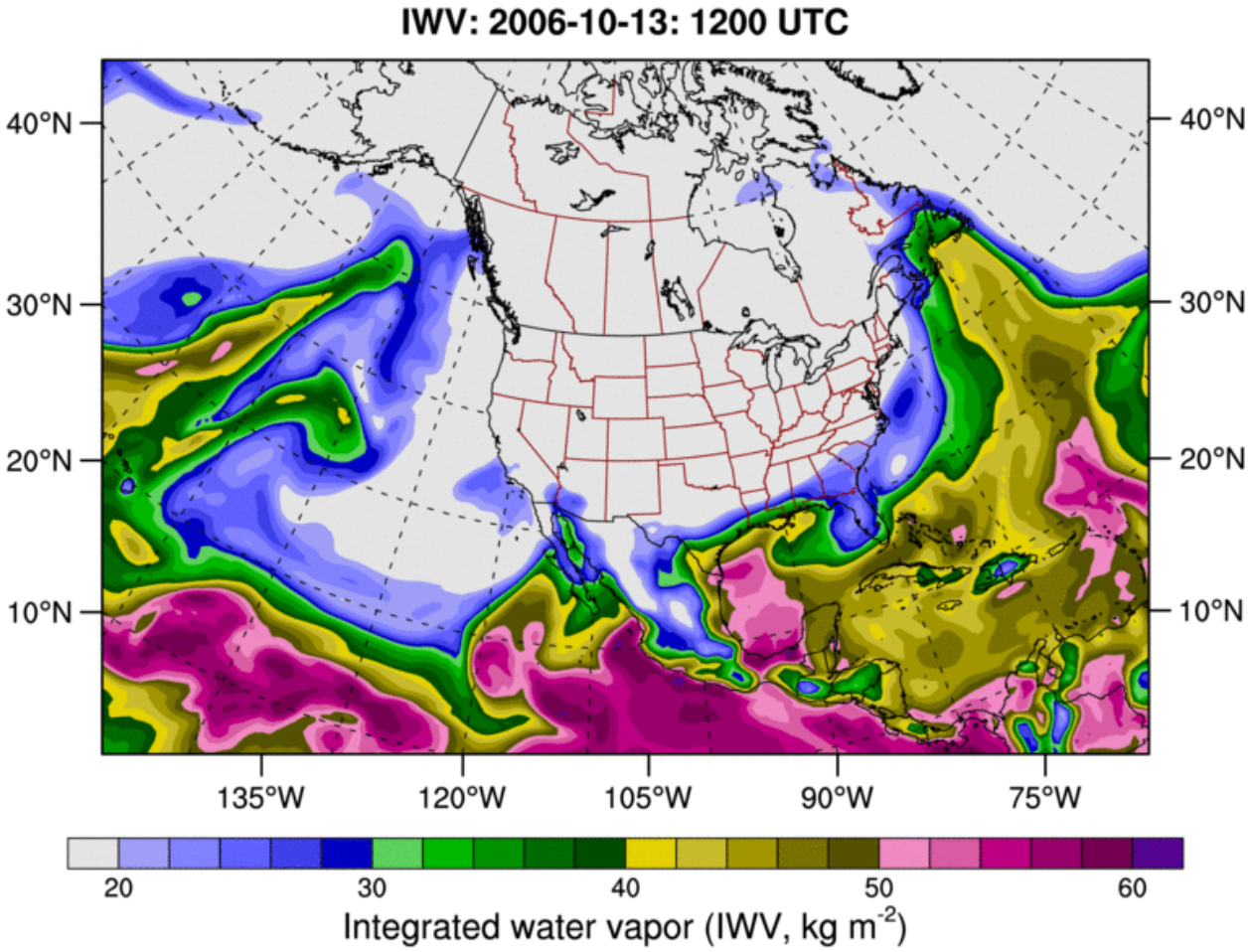
IWV: 2006-10-13: 1200 UTC
40°N
30°N
20°N
10°N
135°W
120°W
105°W
90°W
75°W
20
30
40
50
60
Integrated water vapor (IWV, kg m-2)

A9: October 4-5, 2012

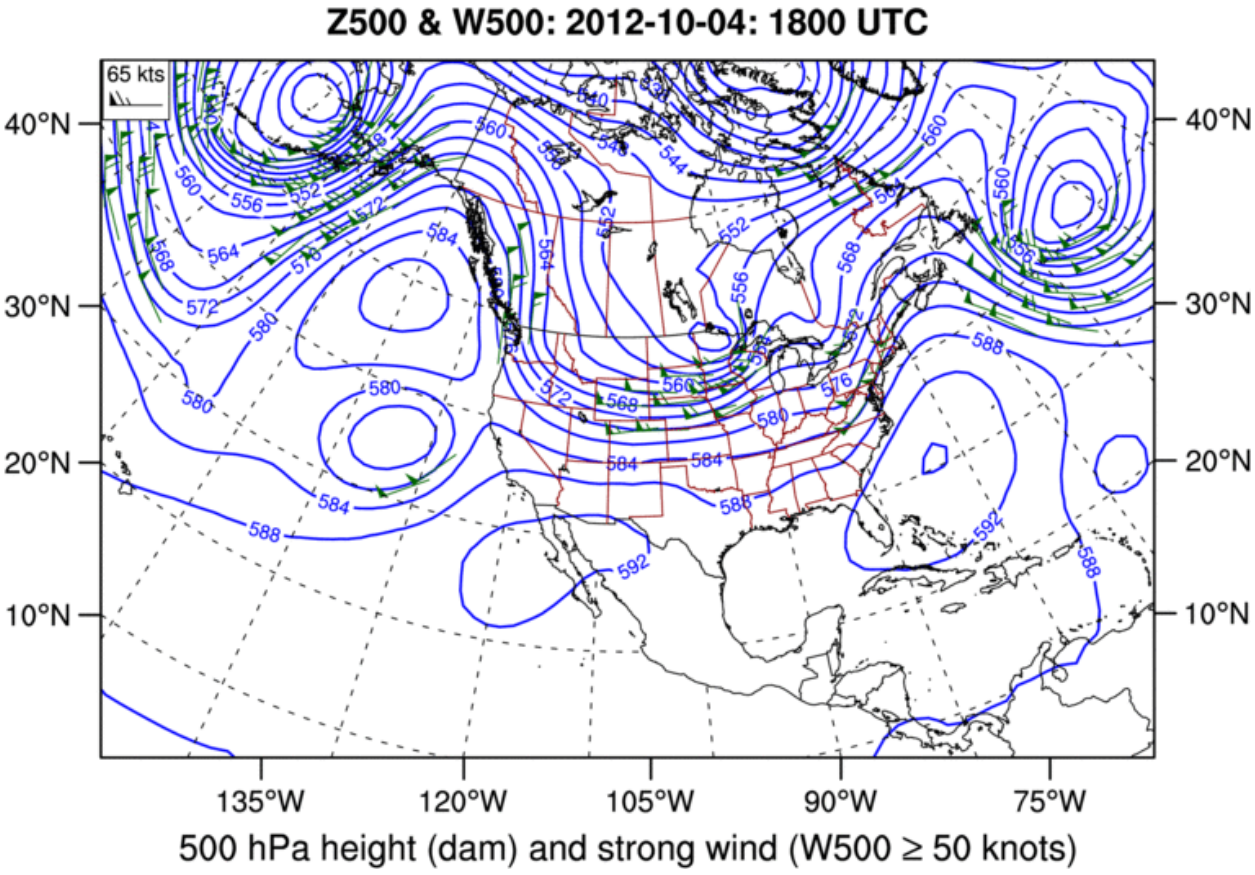

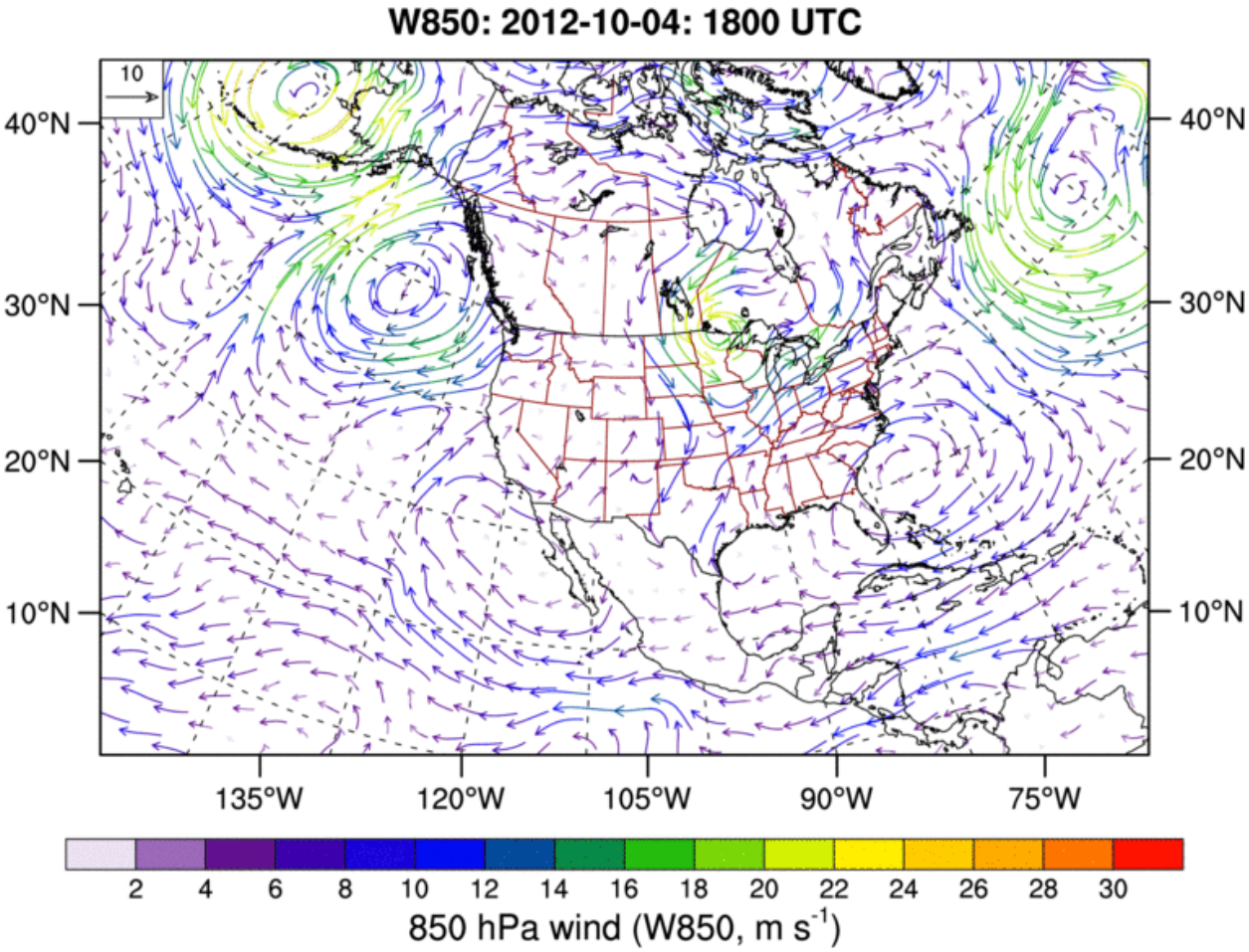
W850: 2012-10-04: 1800 UTC
10
40°N
30°N
20°N
10°N
135°W
120°W
105°W
90°W
75°W
2 4 6 8 10 12 14 16 18 20 22 24 26 28 30
850 hPa wind (W850, m s-1)

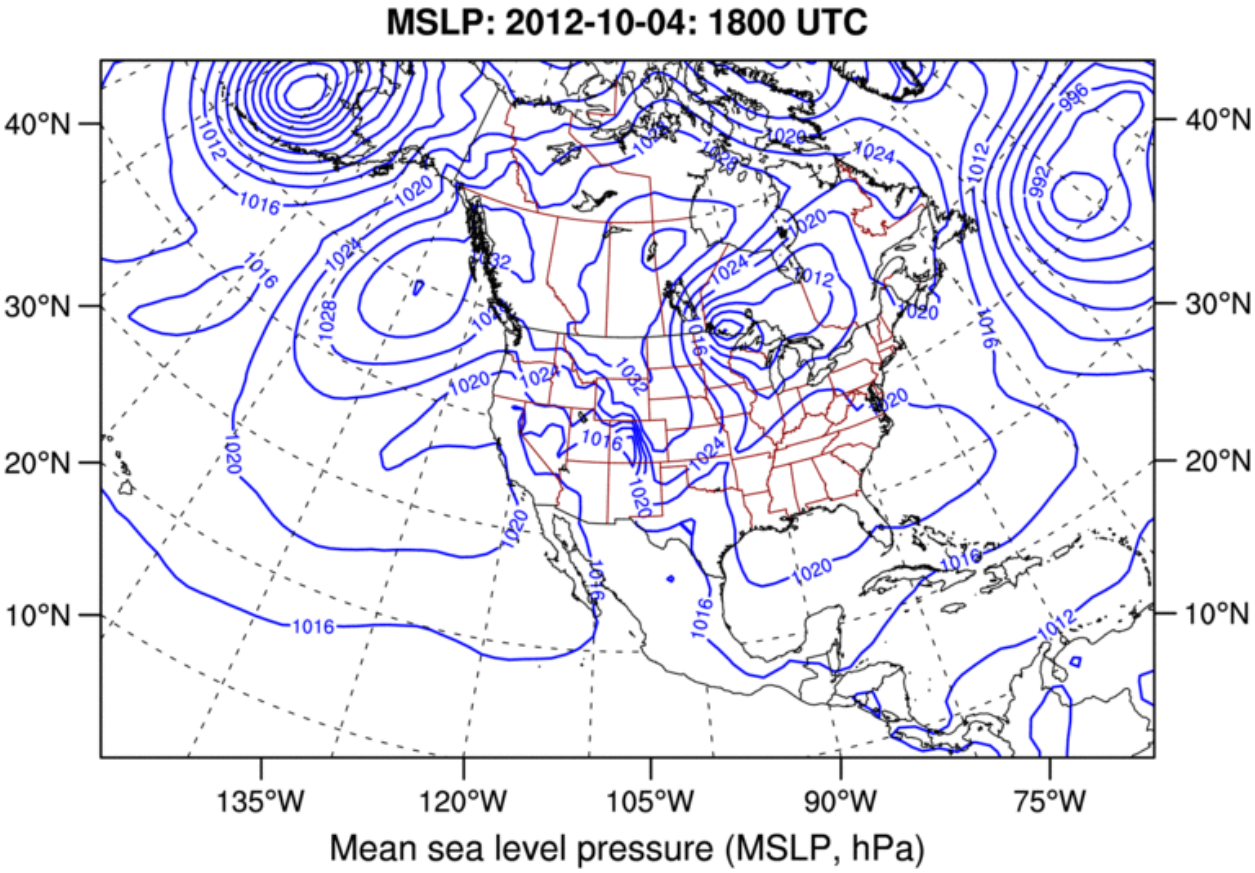
MSLP: 2012-10-04: 1800 UTC
40°N
30°N
20°N
10°N
135°W
120°W
105°W
90°W
75°W
Mean sea level pressure (MSLP, hPa)

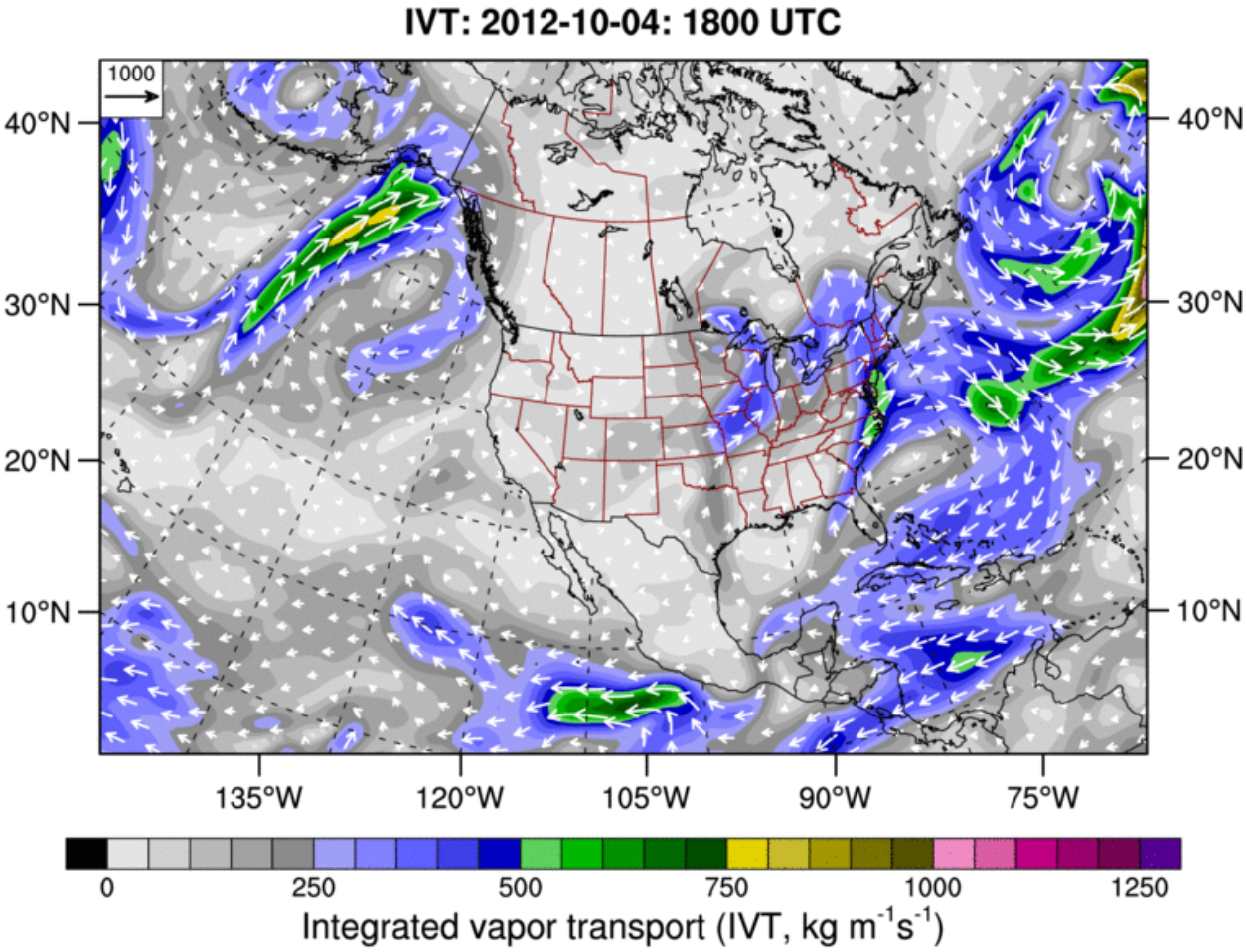
IVT: 2012-10-04: 1800 UTC
1000
40°N
30°N
20°N
10°N
135°W
120°W
105°W
90°W
75°W
0
250
500
750
1000
1250
Integrated vapor transport (IVT, kg m-1s-1)

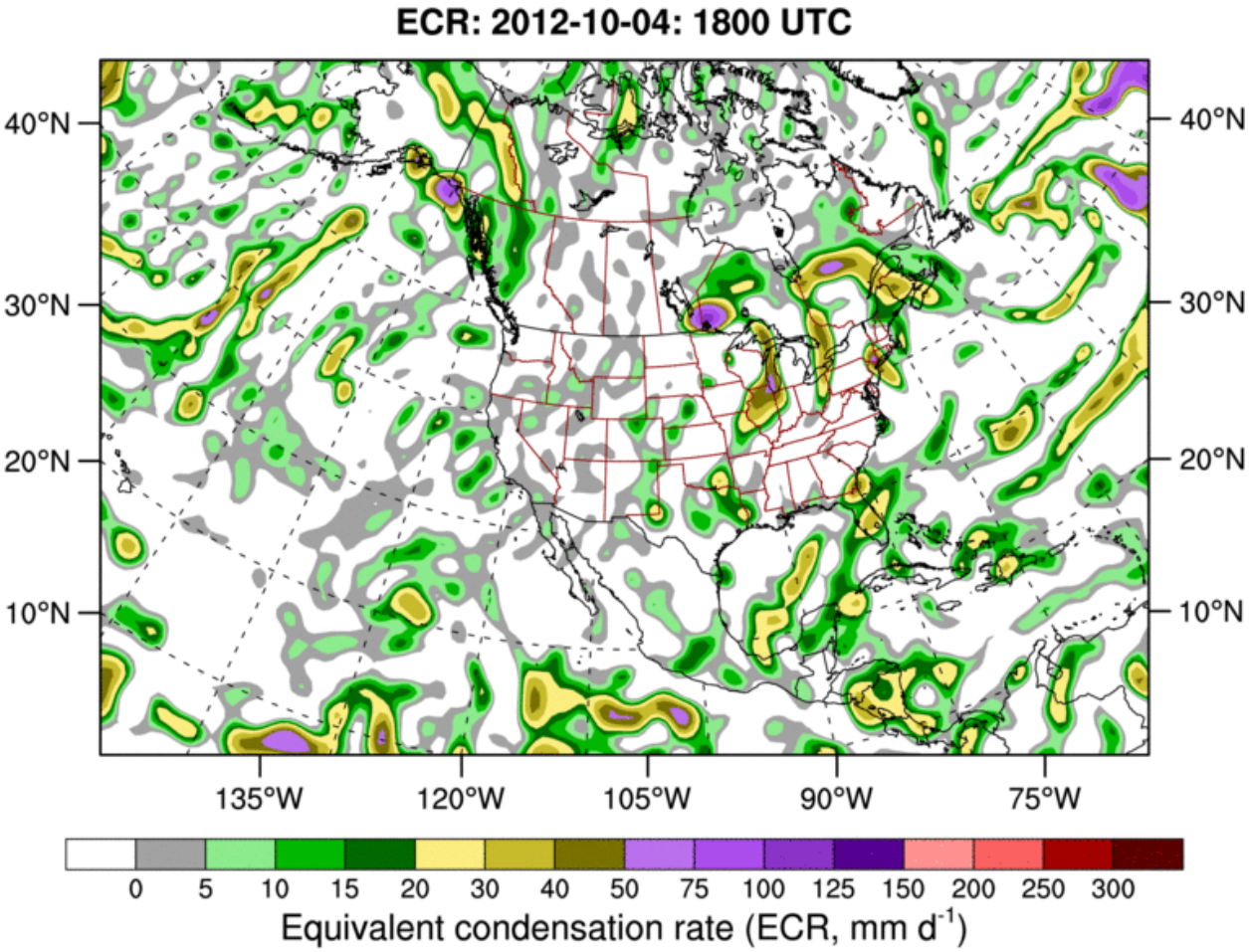
ECR: 2012-10-04: 1800 UTC
40°N
30°N
20°N
10°N
135°W
120°W
105°W
90°W
75°W
0
5
10
15
20
30
40
50
75
100
125
150
200
250
300
Equivalent condensation rate (ECR, mm d-1)

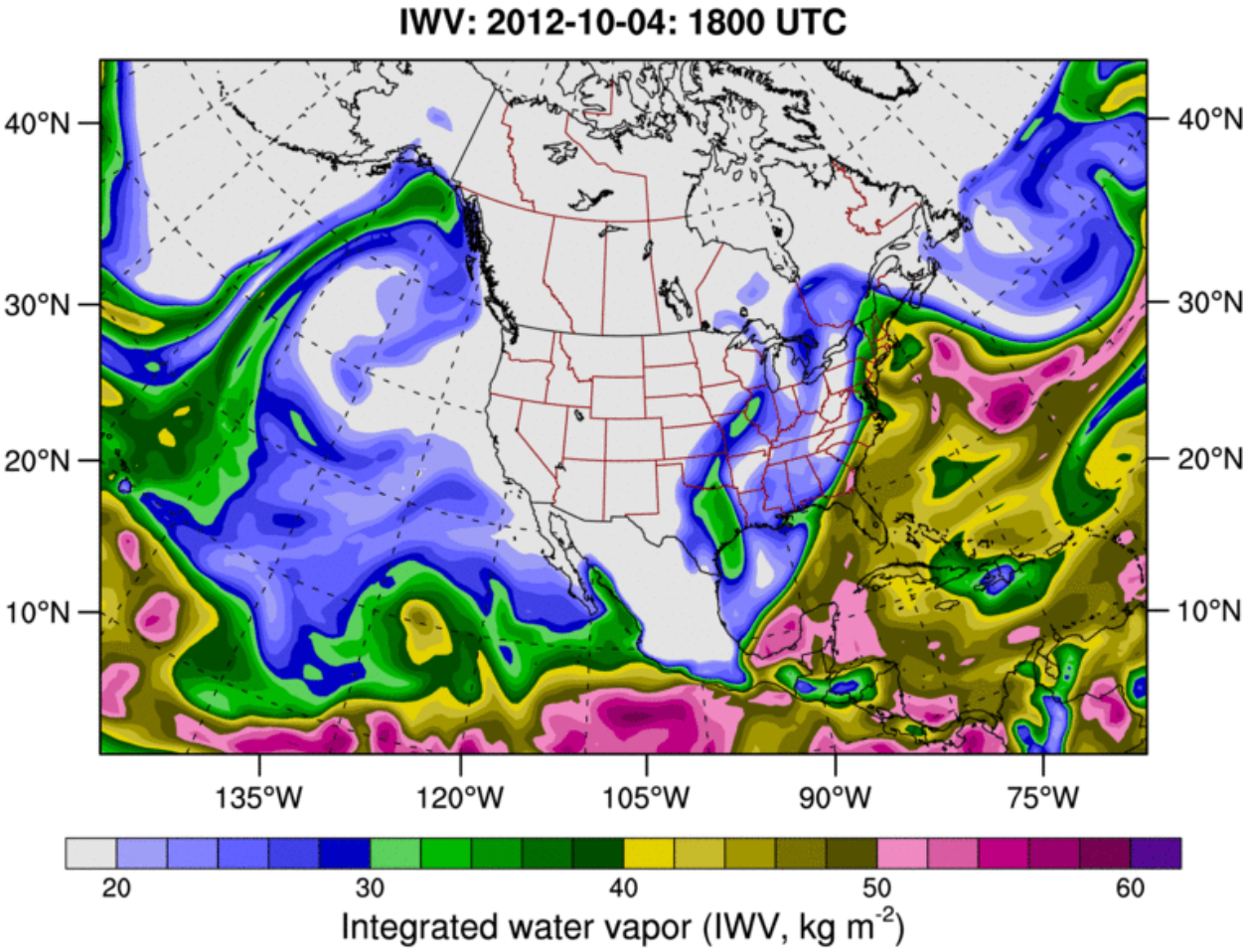
IWV: 2012-10-04: 1800 UTC
40°N
30°N
20°N
10°N
135°W
120°W
105°W
90°W
75°W
20
30
40
50
60
Integrated water vapor (IWV, kg m-2)

A10: March 8, 2017

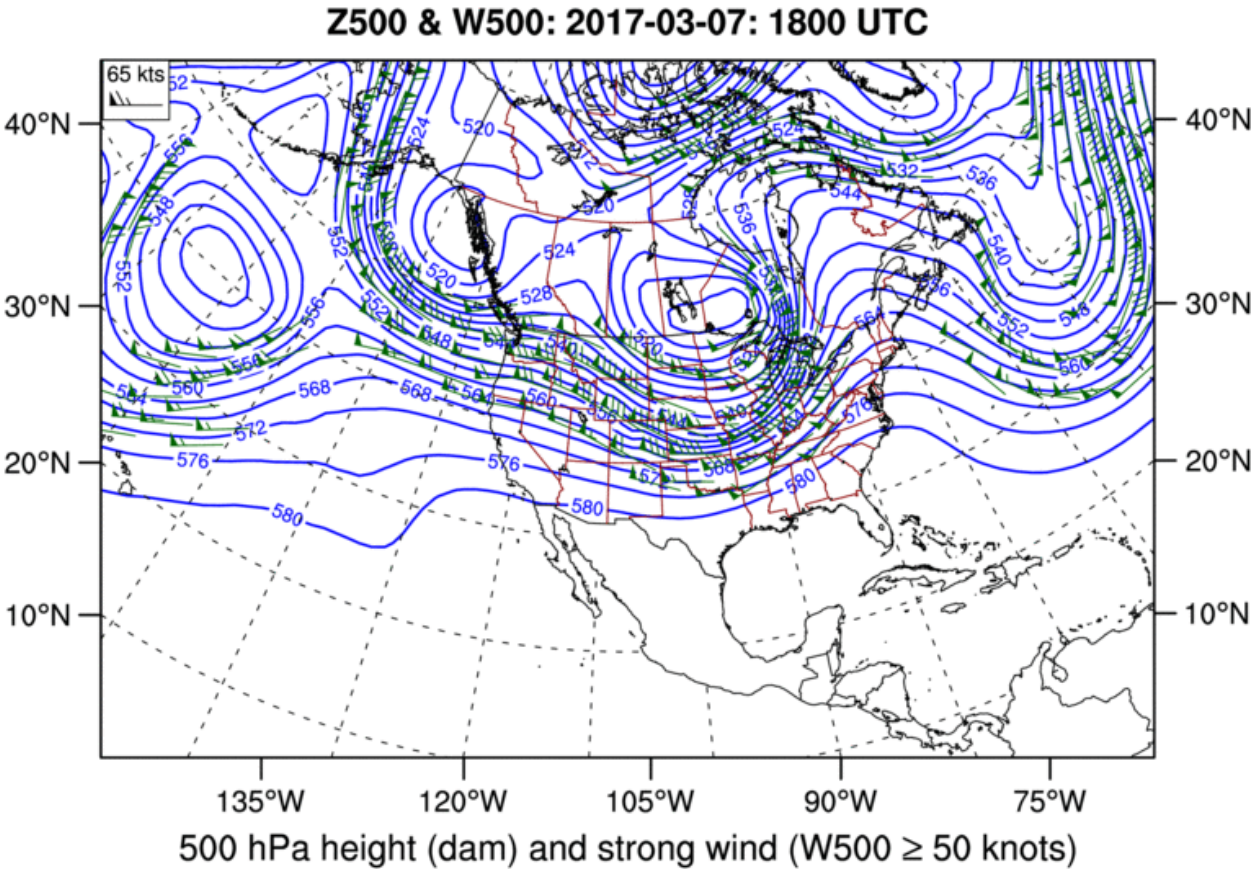

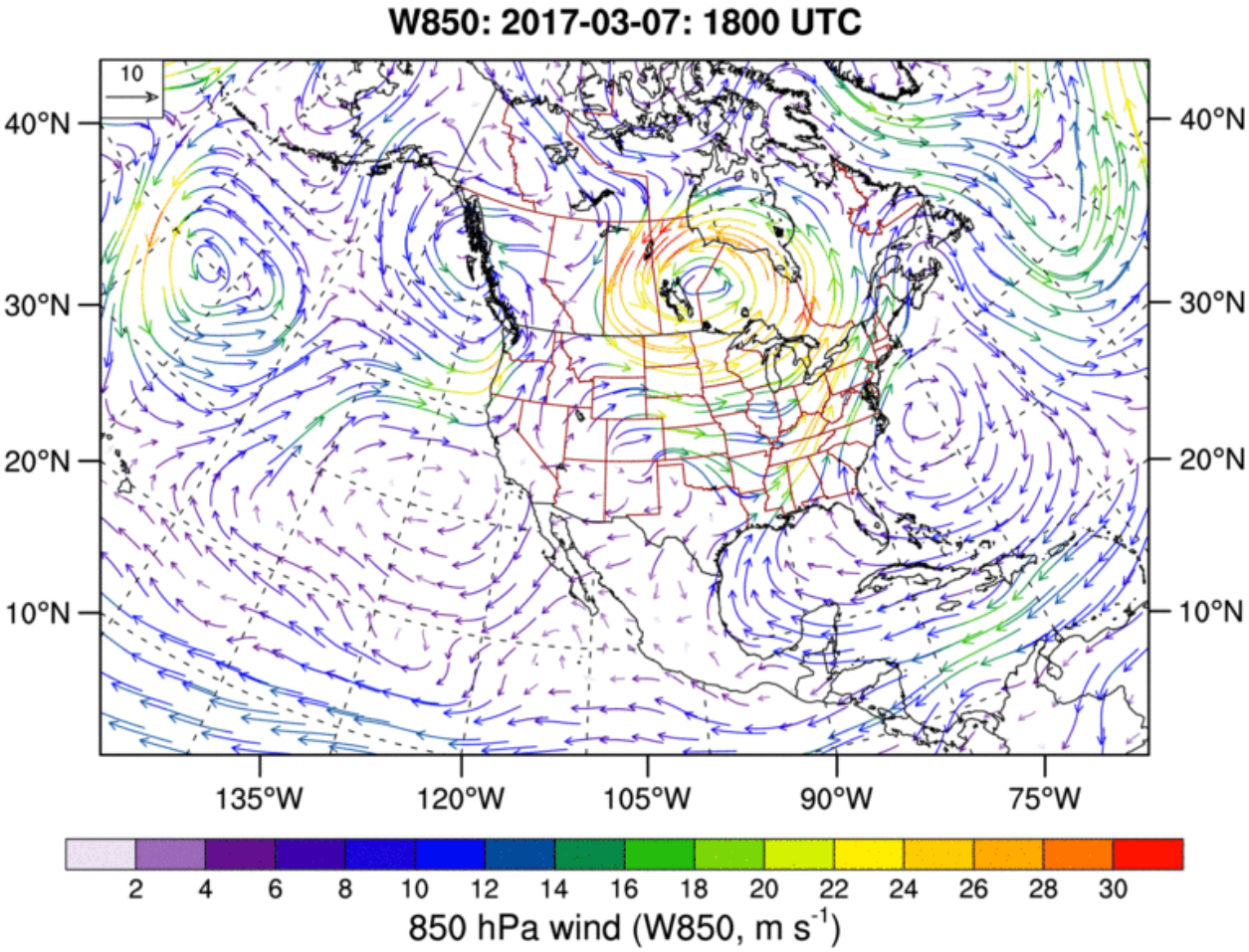
W850: 2017-03-07: 1800 UTC
10
40°N
30°N
20°N
10°N
135°W
120°W
105°W
90°W
75°W
2 4 6 8 10 12 14 16 18 20 22 24 26 28 30
850 hPa wind (W850, m s-1)

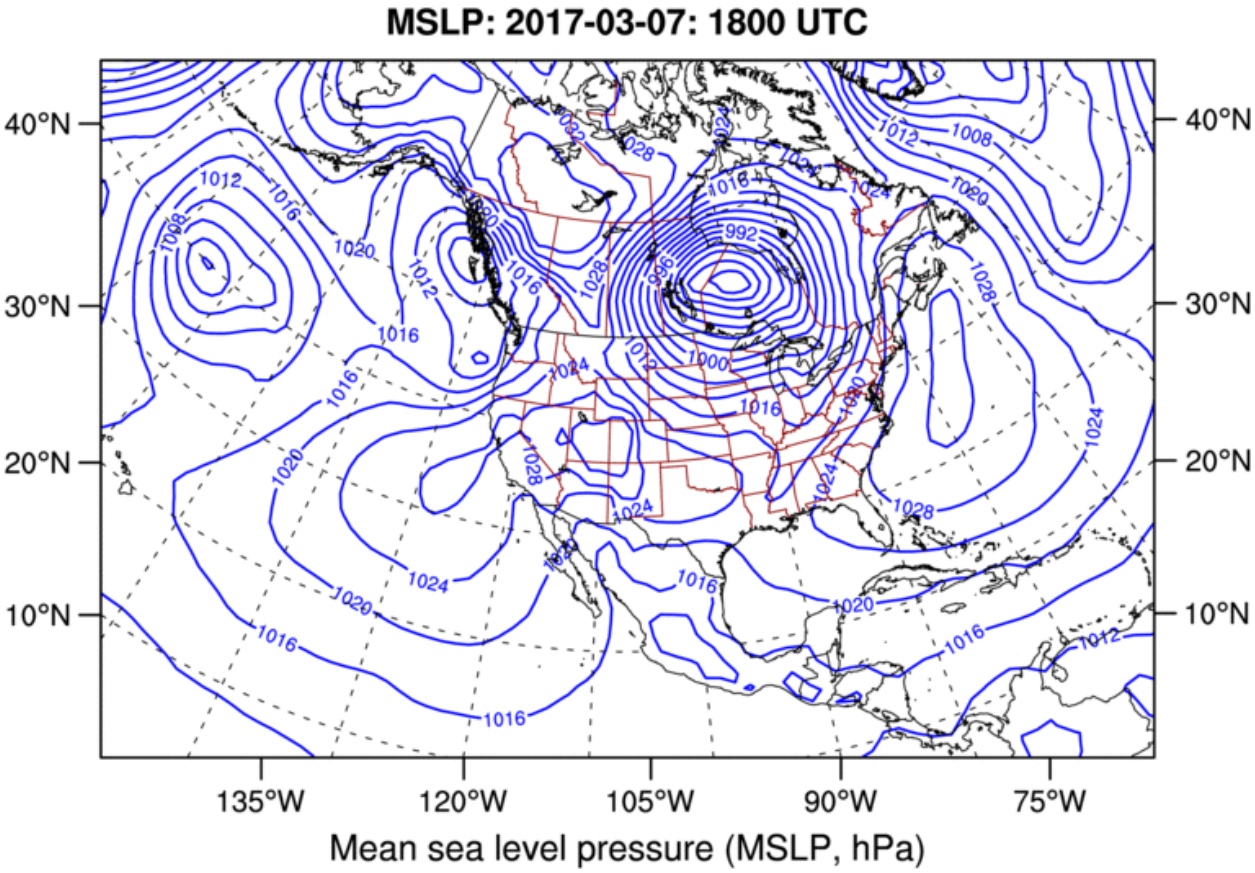
MSLP: 2017-03-07: 1800 UTC
40°N
30°N
20°N
10°N
135°W
120°W
105°W
90°W
75°W
Mean sea level pressure (MSLP, hPa)

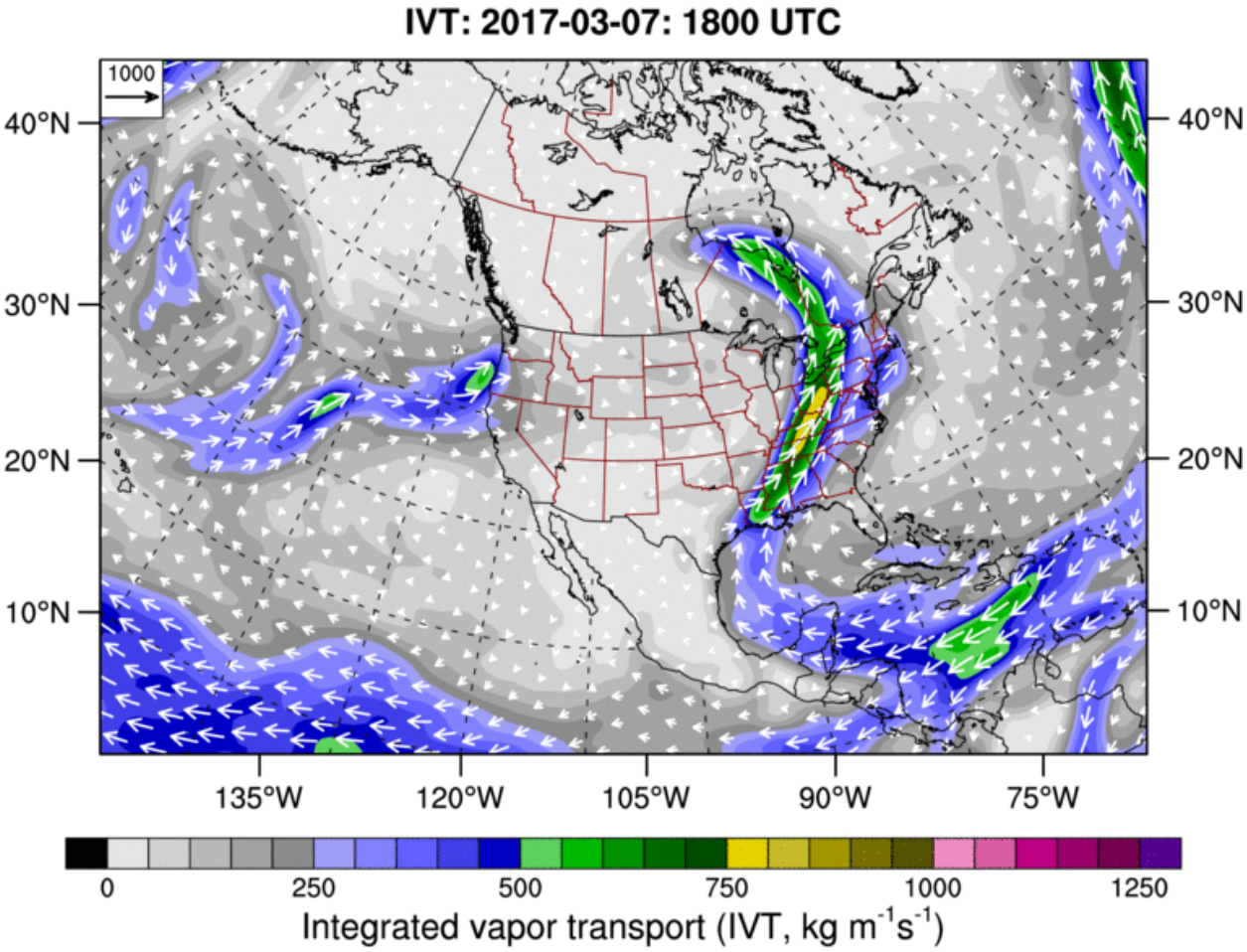
IVT: 2017-03-07: 1800 UTC
1000
40°N
30°N
20°N
10°N
135°W
120°W
105°W
90°W
75°W
0
250
500
750
1000
1250
Integrated vapor transport (IVT, kg m-1s-1)

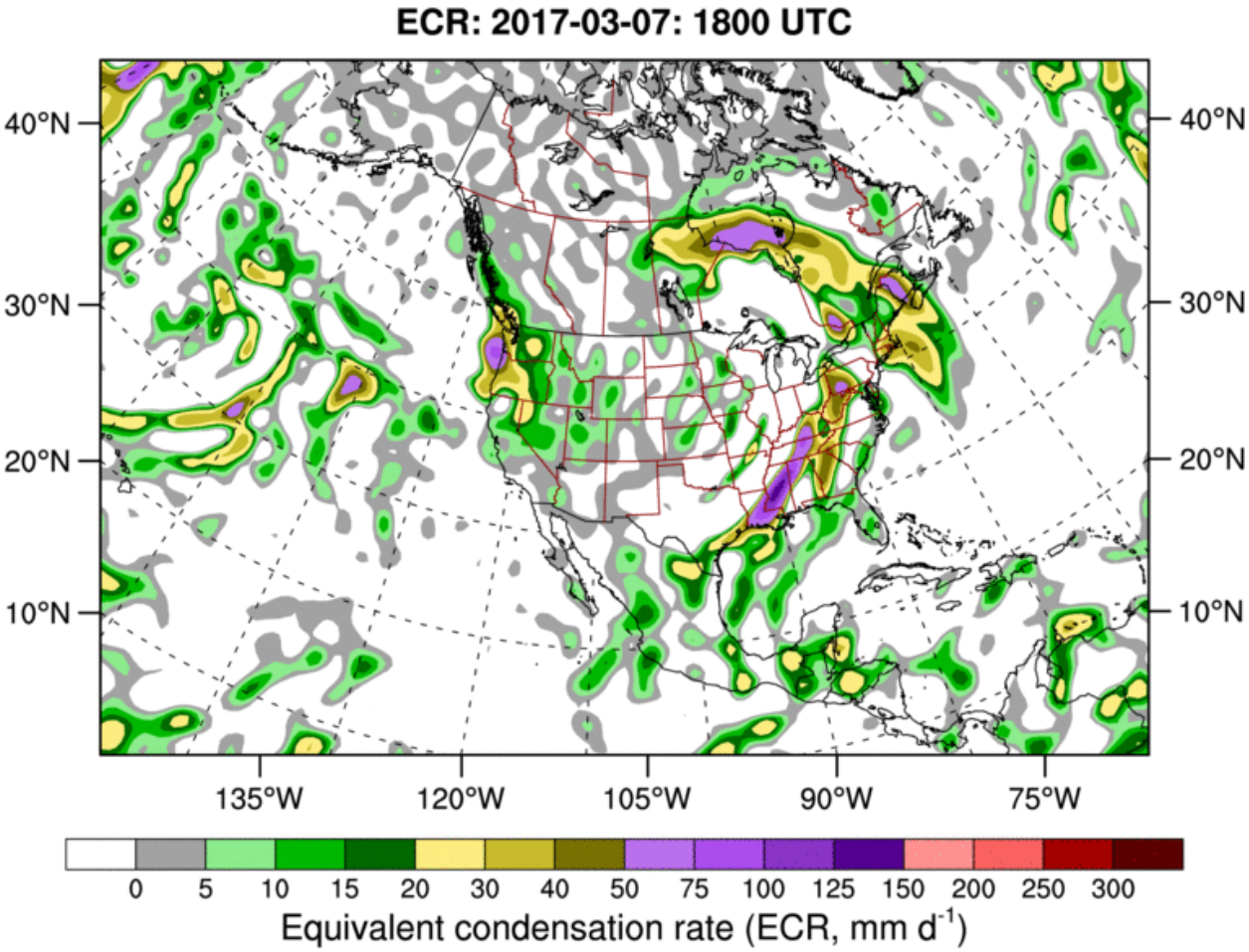
ECR: 2017-03-07: 1800 UTC
40°N
30°N
20°N
10°N
135°W
120°W
105°W
90°W
75°W
0
5
10
15
20
30
40
50
75
100
125
150
200
250
300
Equivalent condensation rate (ECR, mm d-1)

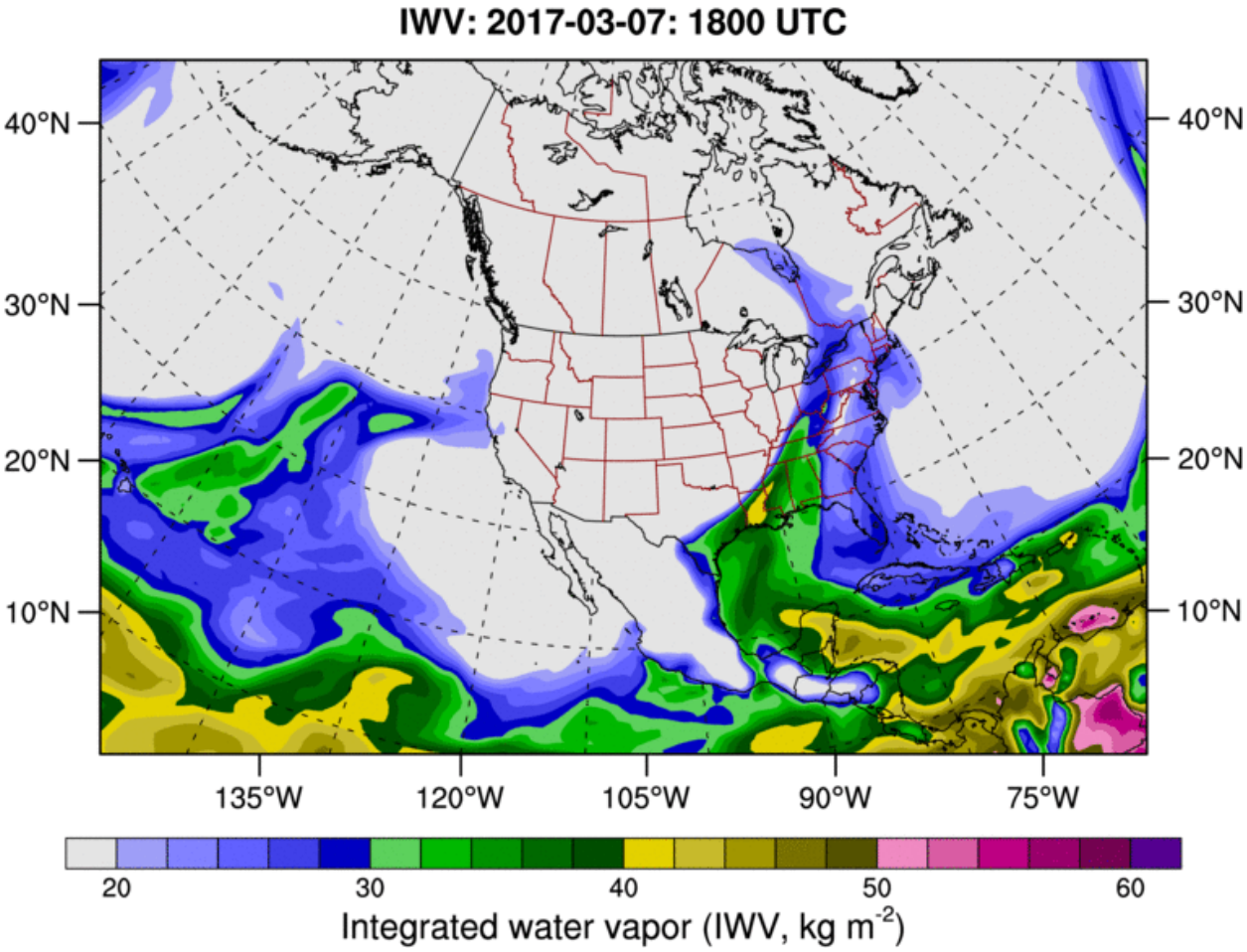
IWV: 2017-03-07: 1800 UTC
40°N
30°N
20°N
10°N
135°W
120°W
105°W
90°W
75°W
20
30
40
50
60
Integrated water vapor (IWV, kg m-2)

Appendix B: GEM Surface/Upper Air Maps

This section contains upper air, surface, and precipitation analyses from ECCC's GEM model. Data are available at 00 UTC, and the second image for each event is a 24 hour forecast for each event. Whenever possible, a date was chosen for these images/events that is similar to the date in Appendix A. The panels in the first images (in order: top left, right, bottom left, right) are:

- 500 hPa height and Vorticity ((1.E-5) s^{-1}
- Mean sea level pressure (hPa) and 1000-500 hPa thickness (dam)
- 700 hPa height analysis and humidity (relative, %)
- 850 hPa height analysis and temperature (°C)

The panels in the second images (in order: top left, right, bottom left, right) are:

- 1000-850 hPa thickness (dam) and 850-700 hPa thickness (dam)
- Mean sea level pressure (hPa) and pressure tendency (hPa 3h $^{-1}$)
- 1000-700 hPa thickness (dam) and vertical motion (0.1 Pa s^{-1})
- Precipitation type (Rain, rain/snow, freezing rain, ice pellets, and snow)

B1: November 6-12, 2000

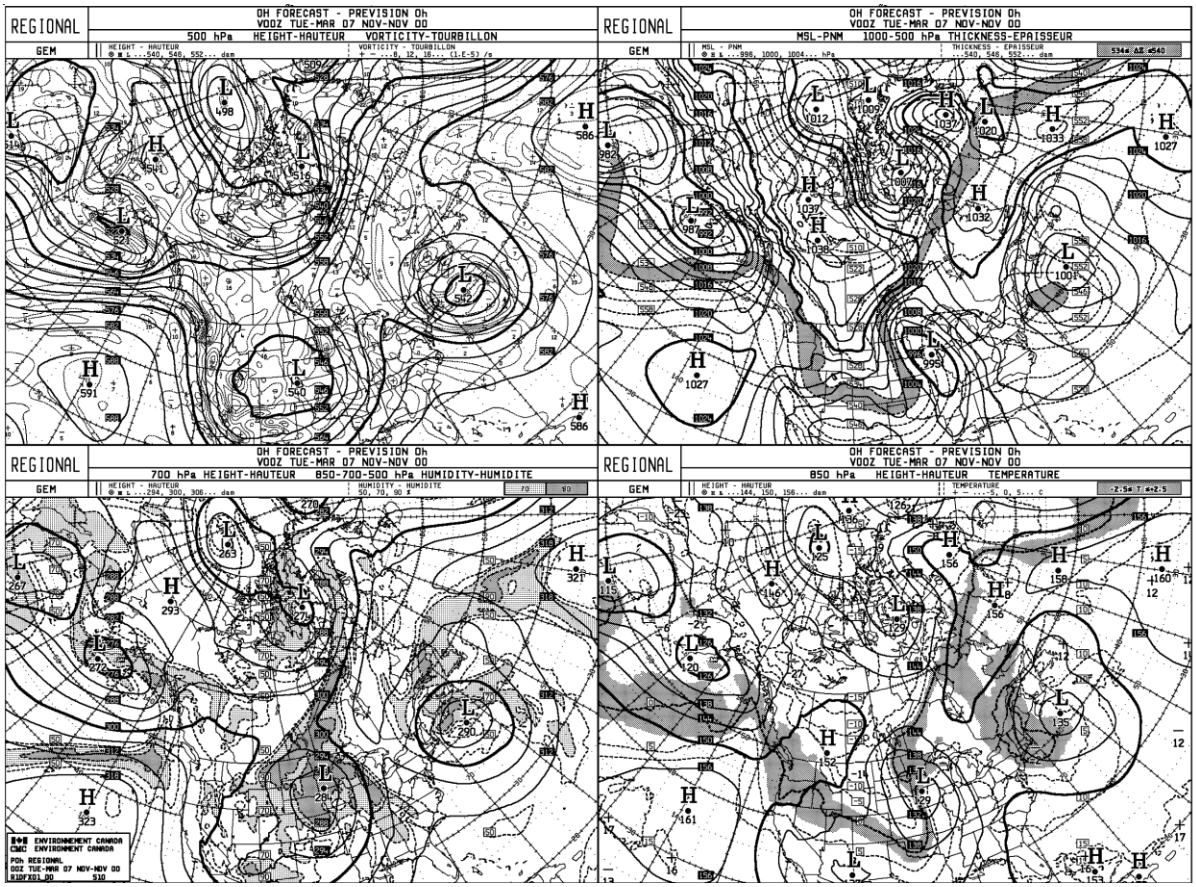

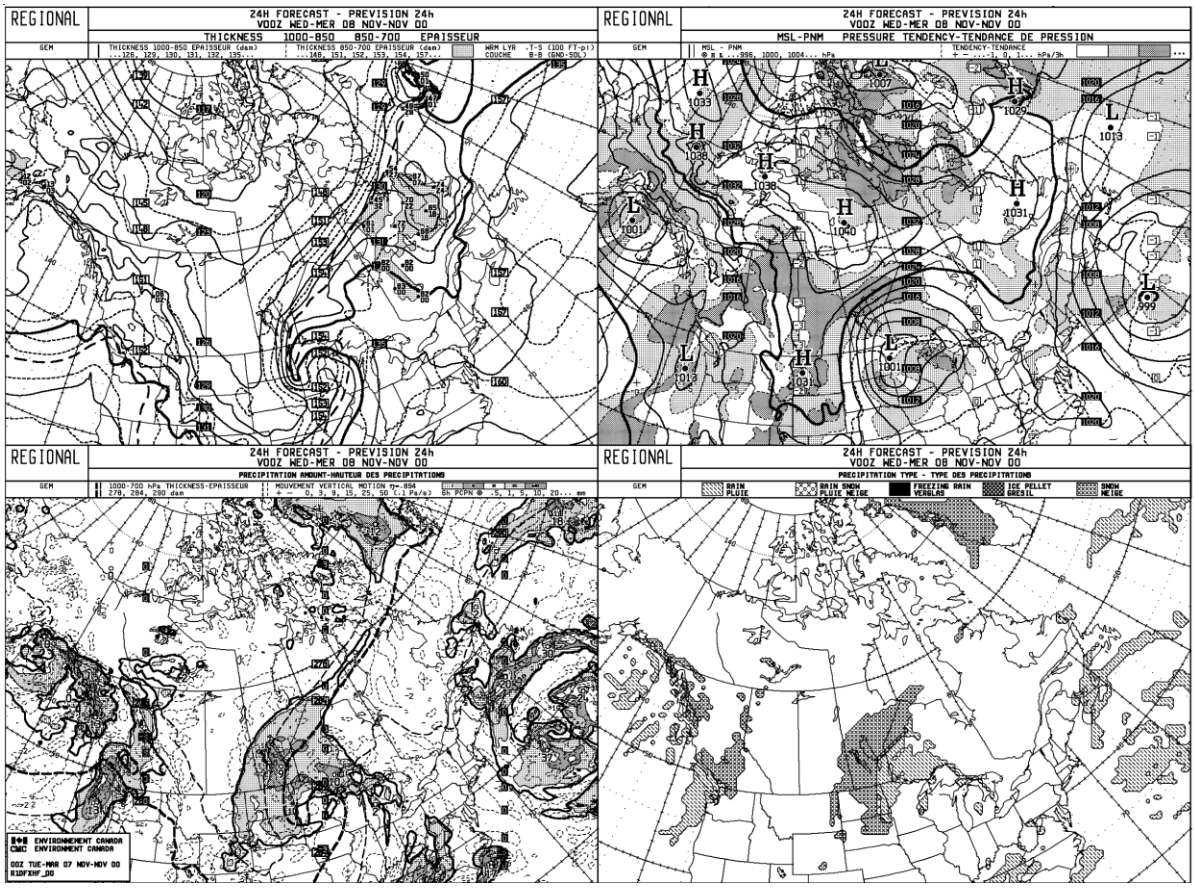
REGIONAL
24H FORECAST - PREVISION 24h
VOOZ WED-MER 08 NOV-NOV 00
THICKNESS 1000-850 850-700 EPAISSEUR
REGIONAL
24H FORECAST - PREVISION 24h
VOOZ WED-MER 08 NOV-NOV 00
MSL-PNM PRESSURE TENDENCY-TENDANCE DE PRESSION
REGIONAL
24H FORECAST - PREVISION 24h
VOOZ WED-MER 08 NOV-NOV 00
PRECIPITATION AMOUNT-HAUTEUR DES PRECIPITATIONS
ENVIRONMENT CANADA
ENVIRONMENT CANADA
REGIONAL
24H FORECAST - PREVISION 24h
VOOZ WED-MER 08 NOV-NOV 00
PRECIPITATION TYPE - TYPE DES PRECIPITATIONS
RAIN
PLUIE
RAIN SNOW
PLUIE MEIGE
FREEZING RAIN
VERGLAS
ICE PELLET
GRESIL
SNOW
NEIGE

B2: May 11, 2004

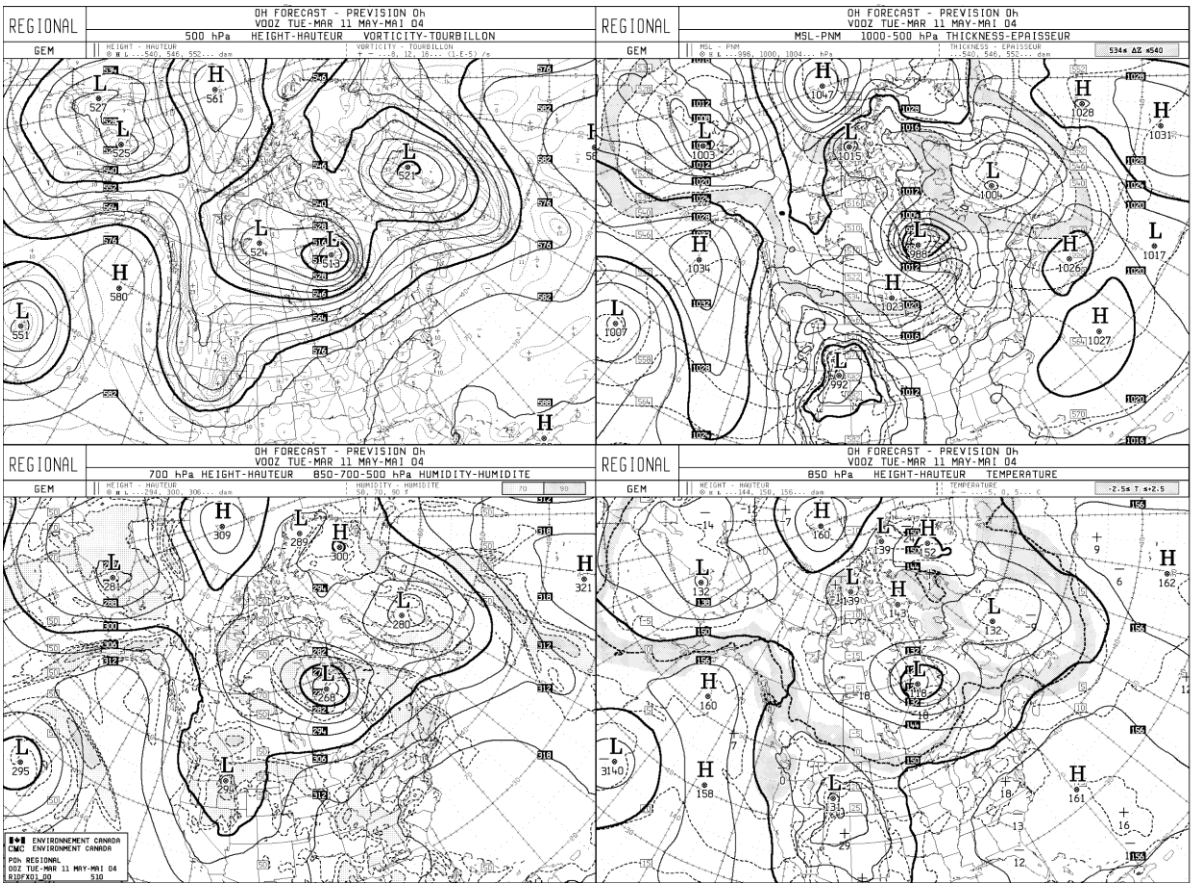

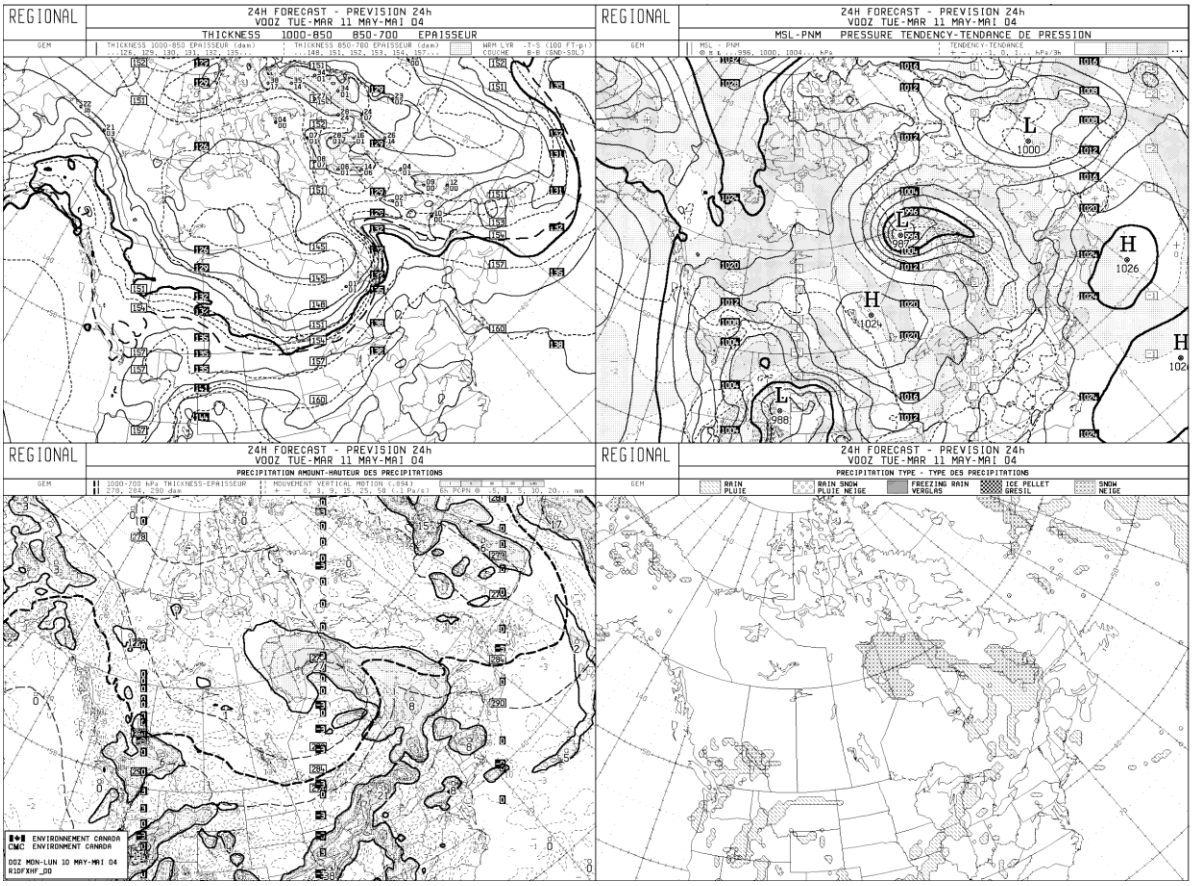
REGIONAL
24H FORECAST - PREVISION 24h
VOOZ TUE-MAR 11 MAY-MAI 04
THICKNESS 1000-850 850-700 EPAISSEUR
REGIONAL
24H FORECAST - PREVISION 24h
VOOZ TUE-MAR 11 MAY-MAI 04
MSL-PNM PRESSURE TENDENCY-TENDANCE DE PRESSION
L
1000
H
1026
H
1024
L
988
REGIONAL
24H FORECAST - PREVISION 24h
VOOZ TUE-MAR 11 MAY-MAI 04
PRECIPITATION AMOUNT-HAUTEUR DES PRECIPITATIONS
ENVIRONNEMENT CANADA
ENVIRONMENT CANADA
00Z MON-LUN 10 MAY-MAI 04
REGIONAL
24H FORECAST - PREVISION 24h
VOOZ TUE-MAR 11 MAY-MAI 04
PRECIPITATION TYPE - TYPE DES PRECIPITATIONS
RAIN
PLUIE
RAIN SNOW
PLUIE NEIGE
FREEZING RAIN
VERGLAS
ICE PELLET
GRESIL
SNOW
NEIGE

B3: October 5, 2005

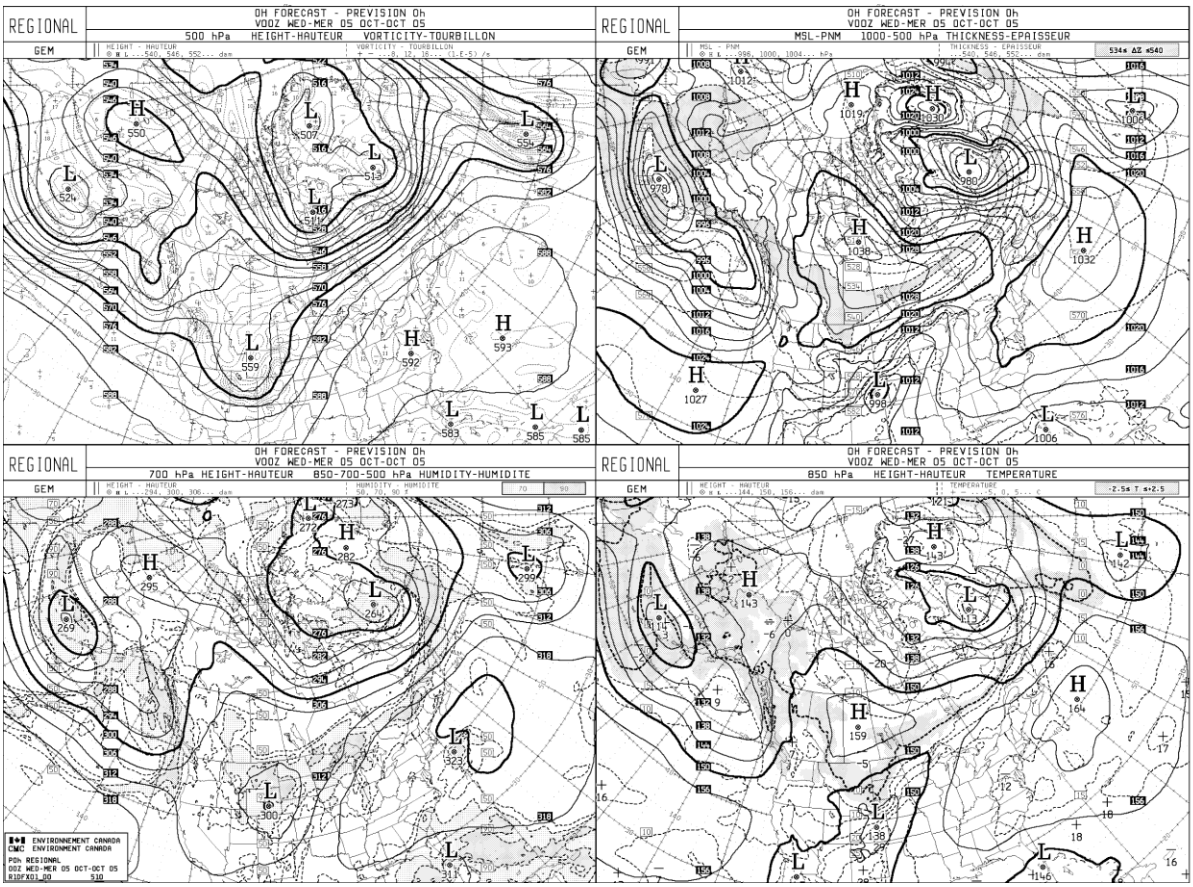

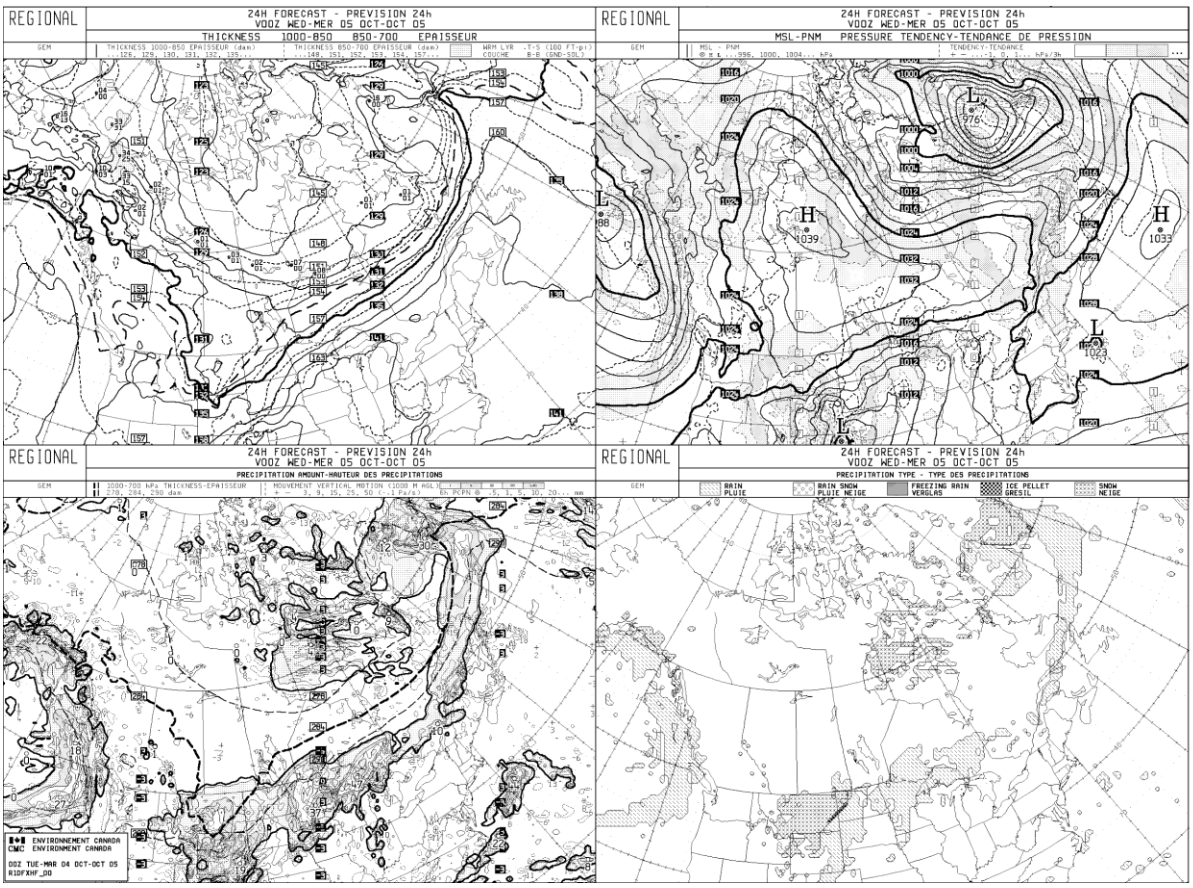
REGIONAL
24H FORECAST - PREVISION 24h
VOOZ WED-MER 05 OCT-OCT 05
THICKNESS 1000-850 850-700 EPAISSEUR
REGIONAL
24H FORECAST - PREVISION 24h
VOOZ WED-MER 05 OCT-OCT 05
MSL-PNM PRESSURE TENDENCY-TENDANCE DE PRESSION
REGIONAL
24H FORECAST - PREVISION 24h
VOOZ WED-MER 05 OCT-OCT 05
PRECIPITATION AMOUNT-HAUTEUR DES PRECIPITATIONS
REGIONAL
24H FORECAST - PREVISION 24h
VOOZ WED-MER 05 OCT-OCT 05
PRECIPITATION TYPE - TYPE DES PRECIPITATIONS
RAIN PLUIE
RAIN SNOW PLUIE NEIGE
FREEZING RAIN VERGLAS
ICE PELLET GRESIL
SNOW NEIGE
ENVIRONNEMENT CANADA
ENVIRONMENT CANADA
00Z TUE-MAR 04 OCT-OCT 05
R1DFXHF_DD

B4: December 14-19, 2005

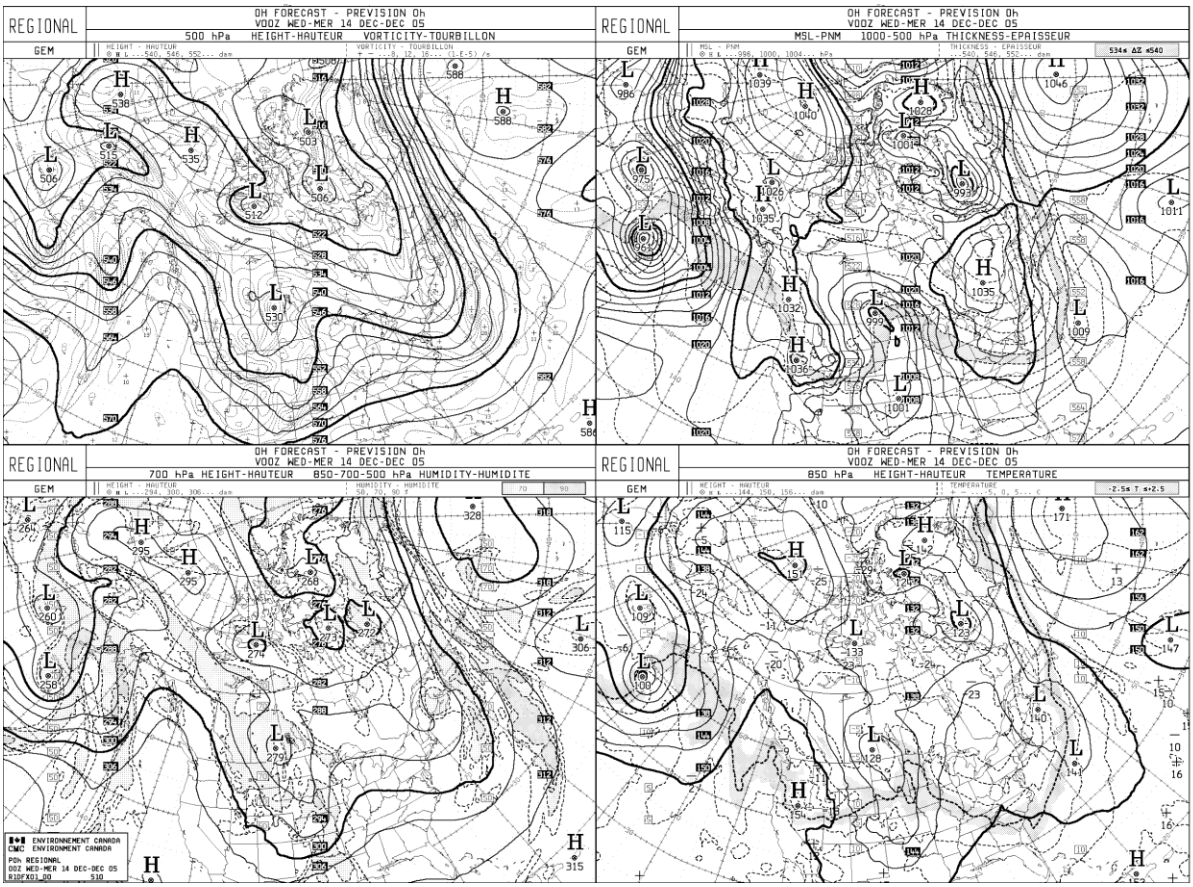

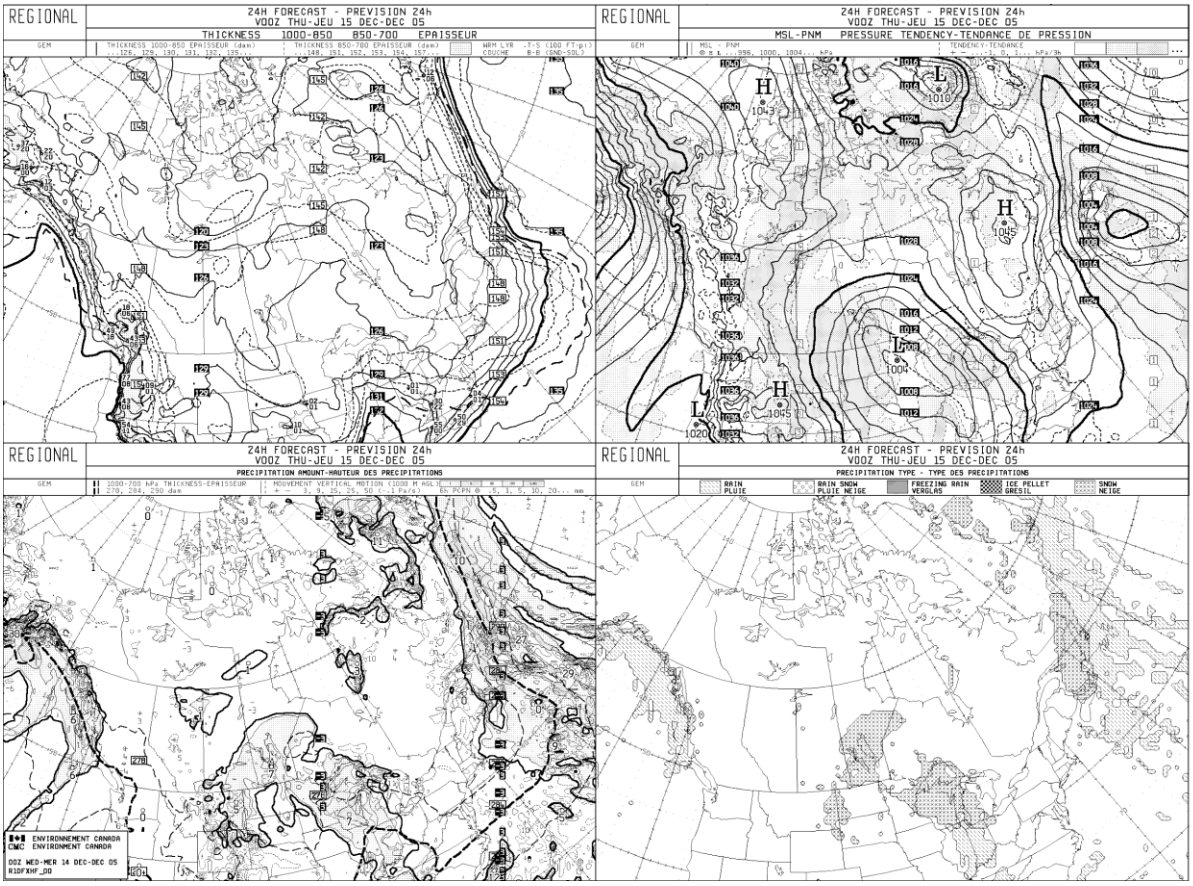
REGIONAL
24H FORECAST - PREVISION 24h
VOOZ THU-JEU 15 DEC-DEC 05
THICKNESS 1000-850 850-700 EPAISSEUR
REGIONAL
24H FORECAST - PREVISION 24h
VOOZ THU-JEU 15 DEC-DEC 05
MSL-PNM PRESSURE TENDENCY-TENDANCE DE PRESSION
REGIONAL
24H FORECAST - PREVISION 24h
VOOZ THU-JEU 15 DEC-DEC 05
PRECIPITATION AMOUNT-HAUTEUR DES PRECIPITATIONS
REGIONAL
24H FORECAST - PREVISION 24h
VOOZ THU-JEU 15 DEC-DEC 05
PRECIPITATION TYPE - TYPE DES PRECIPITATIONS
RAIN
PLUIE
FREEZING RAIN
VERGLAS
ICE PELLET
GRESIL
SNOW
NEIGE
ENVIRONNEMENT CANADA
ENVIRONMENT CANADA
00Z WED-MER 14 DEC-DEC 05

B5: December 28, 2005

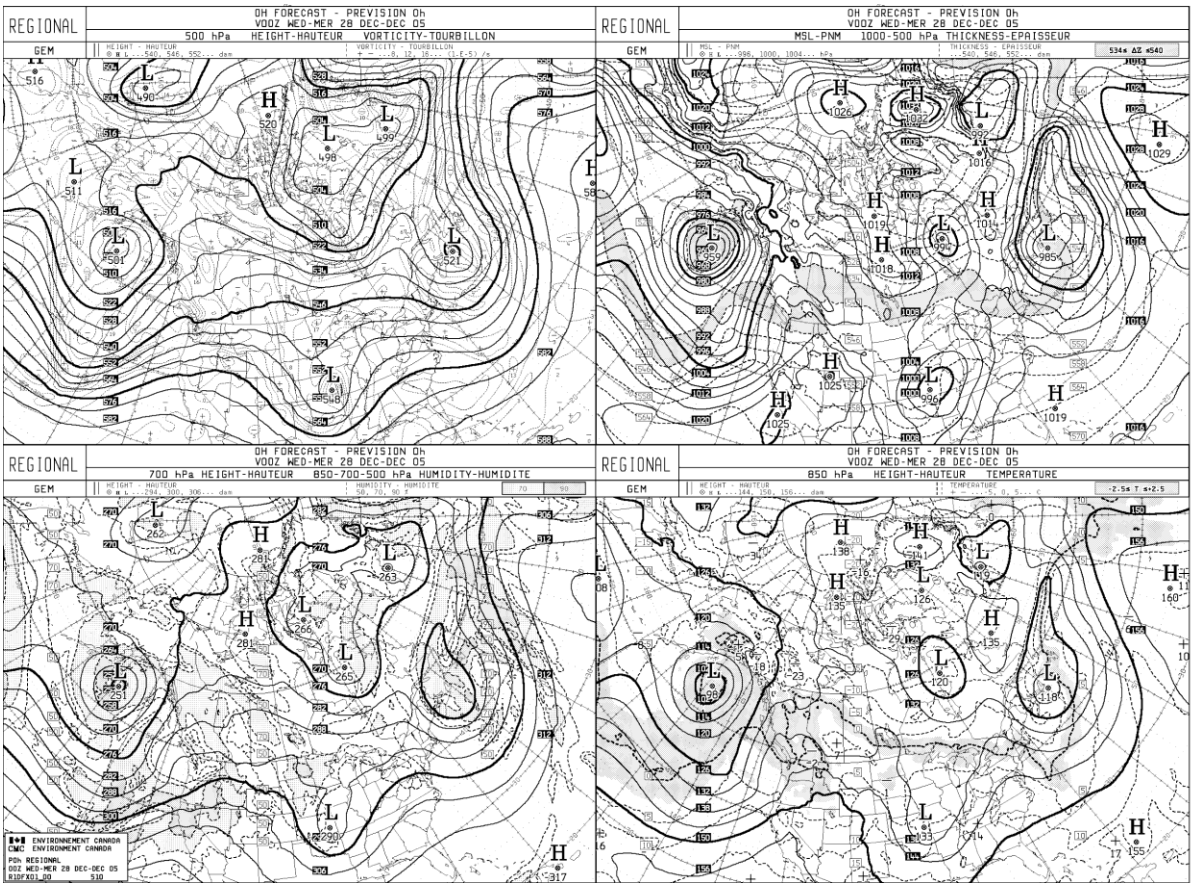

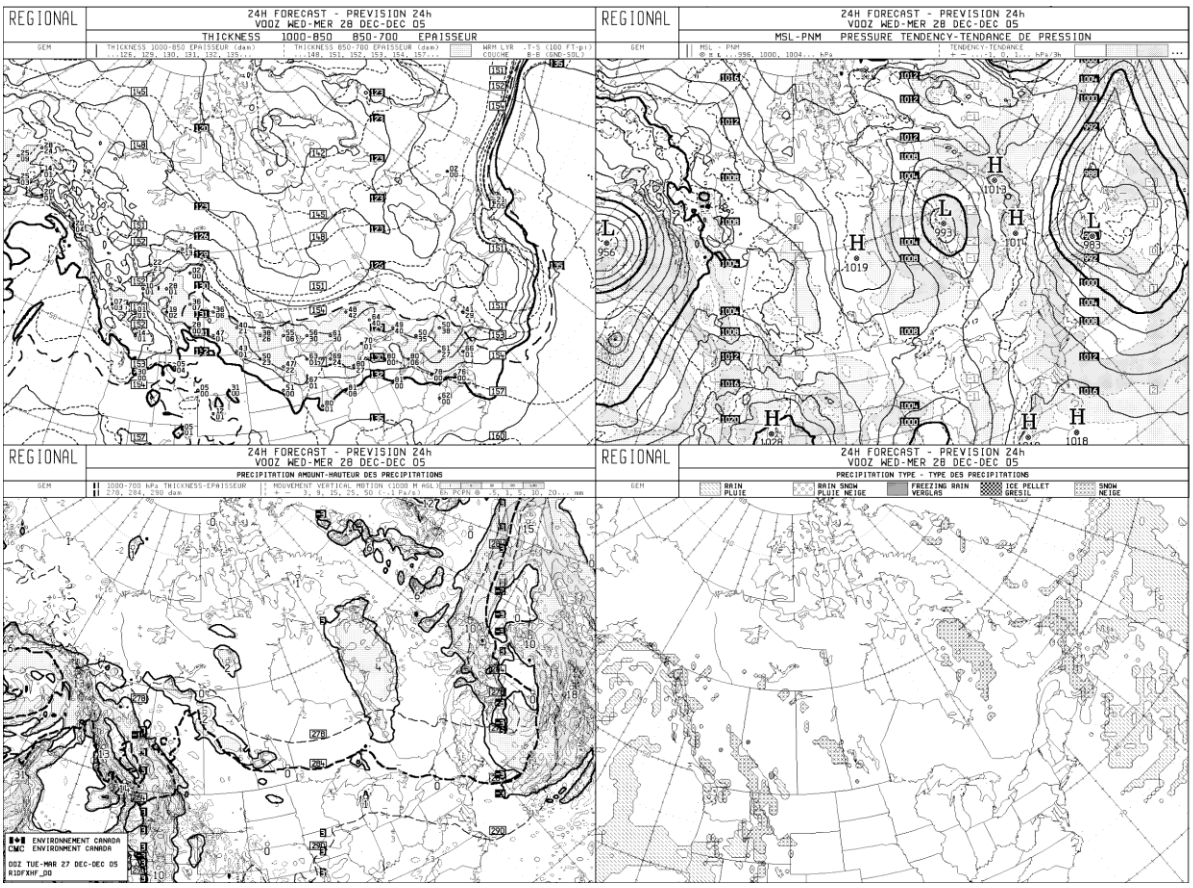
REGIONAL
24H FORECAST - PREVISION 24h
VOOZ WED-MER 28 DEC-DEC 05
THICKNESS 1000-850 850-700 EPAISSEUR
REGIONAL
24H FORECAST - PREVISION 24h
VOOZ WED-MER 28 DEC-DEC 05
MSL-PNM PRESSURE TENDENCY-TENDANCE DE PRESSION
REGIONAL
24H FORECAST - PREVISION 24h
VOOZ WED-MER 28 DEC-DEC 05
PRECIPITATION AMOUNT-HAUTEUR DES PRECIPITATIONS
REGIONAL
24H FORECAST - PREVISION 24h
VOOZ WED-MER 28 DEC-DEC 05
PRECIPITATION TYPE - TYPE DES PRECIPITATIONS
RAIN PLUIE
RAIN SNOW PLUIE NEIGE
FREEZING RAIN VERGLAS
ICE PELLET GRESIL
SNOW NEIGE
ENVIRONNEMENT CANADA
ENVIRONMENT CANADA
00Z TUE-MAR 27 DEC-DEC 05

B6: January 12-18, 2006

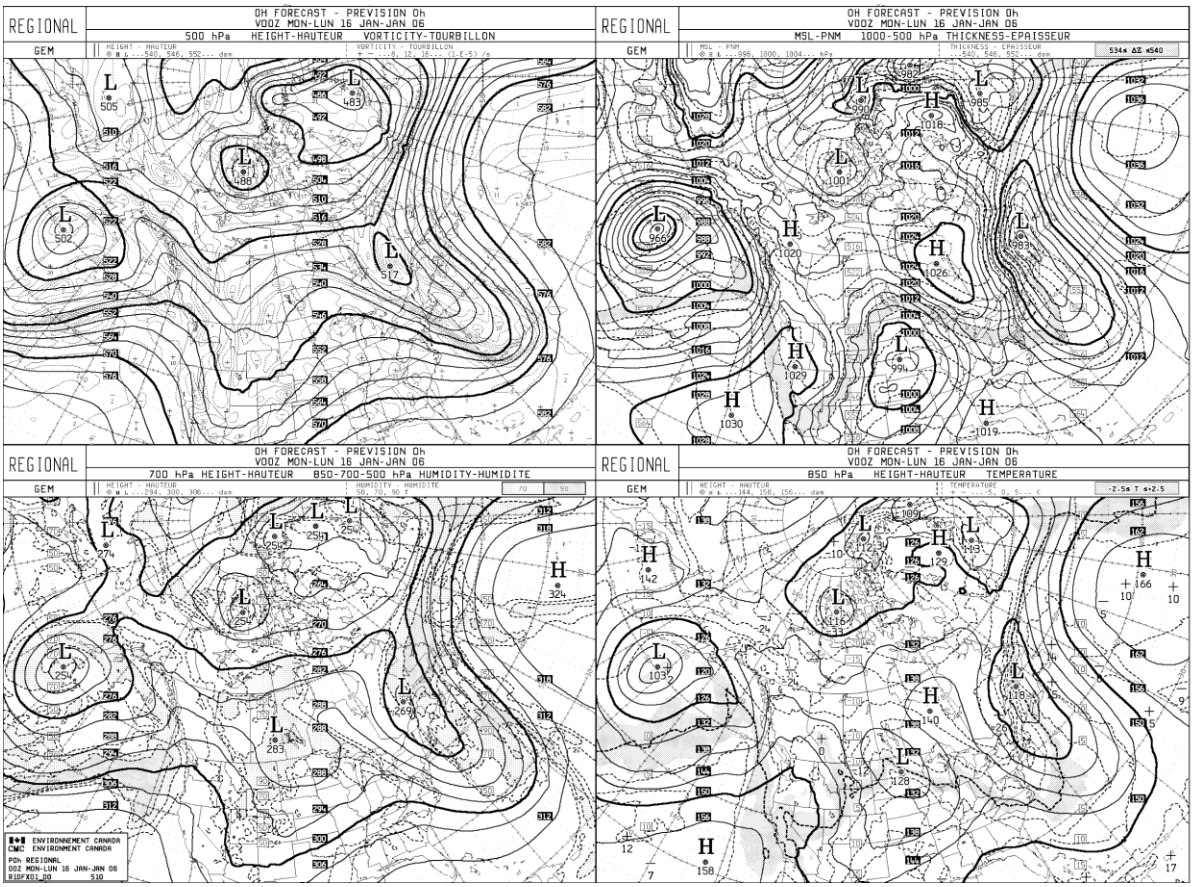

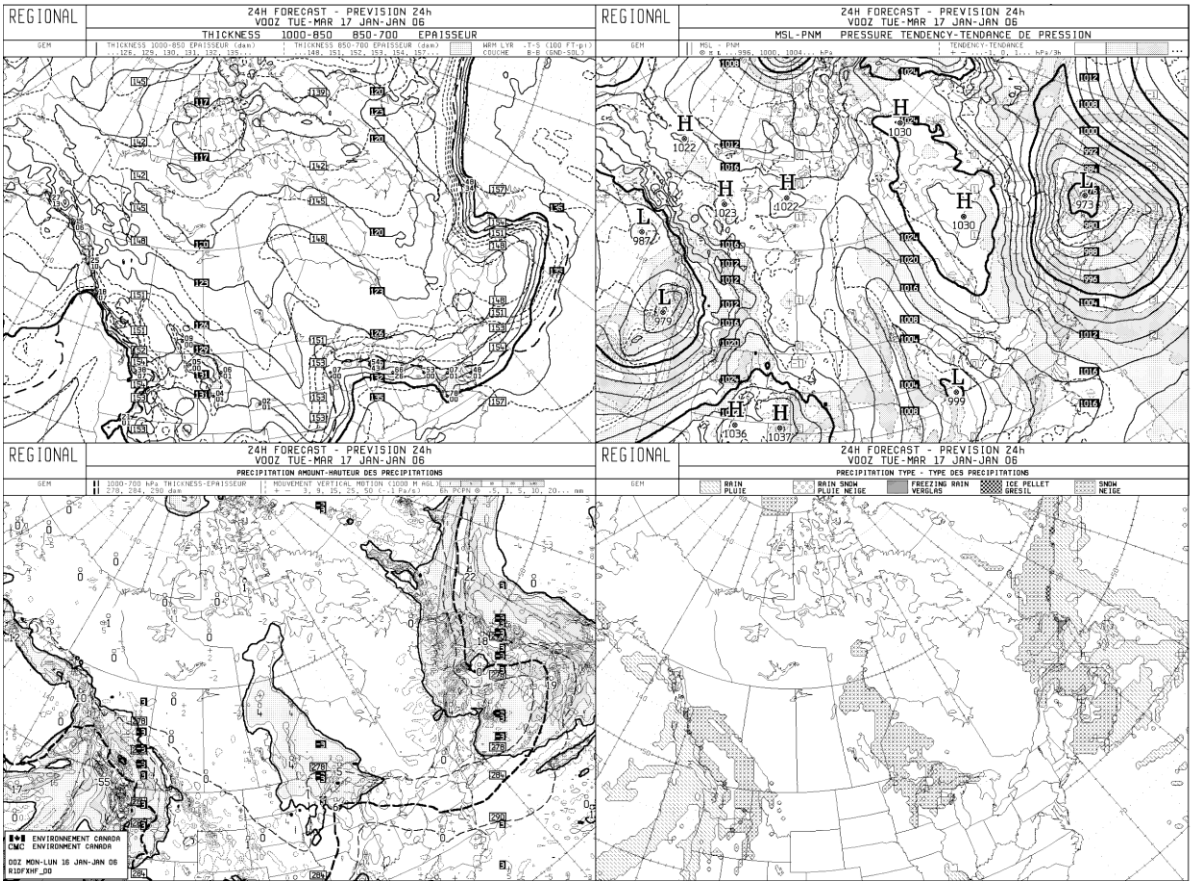
REGIONAL
24H FORECAST - PREVISION 24h
VOOZ TUE-MAR 17 JAN-JAN 06
THICKNESS 1000-850 850-700 EPAISSEUR
REGIONAL
24H FORECAST - PREVISION 24h
VOOZ TUE-MAR 17 JAN-JAN 06
MSL-PNM PRESSURE TENDENCY-TENDANCE DE PRESSION
REGIONAL
24H FORECAST - PREVISION 24h
VOOZ TUE-MAR 17 JAN-JAN 06
PRECIPITATION AMOUNT-HAUTEUR DES PRECIPITATIONS
REGIONAL
24H FORECAST - PREVISION 24h
VOOZ TUE-MAR 17 JAN-JAN 06
PRECIPITATION TYPE - TYPE DES PRECIPITATIONS
RAIN PLUIE
RAIN SNOW PLUIE NEIGE
FREEZING RAIN VERGLAS
ICE PELLET GRESIL
SNOW NEIGE
ENVIRONNEMENT CANADA
ENVIRONMENT CANADA
00Z MON-LUN 16 JAN-JAN 06
R1DFXHF_00

B7: October 13, 2006

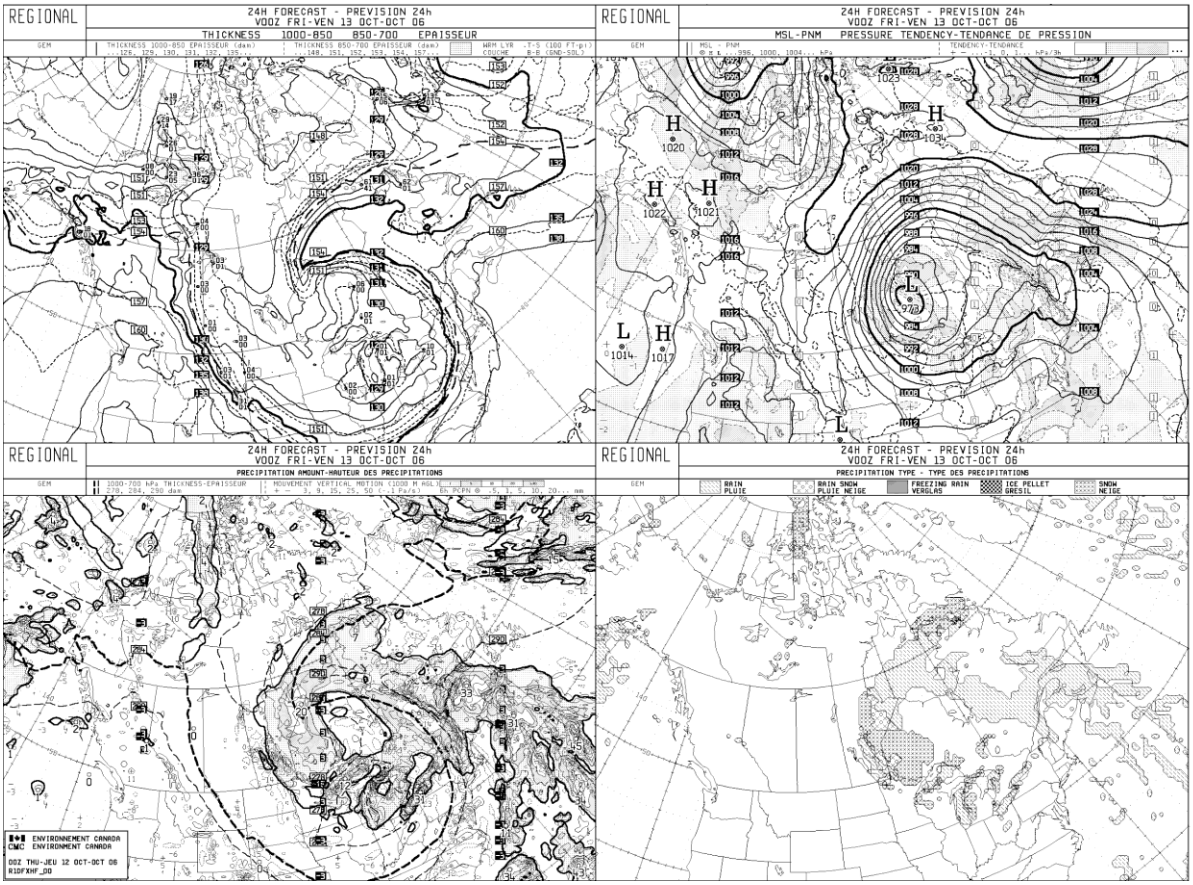

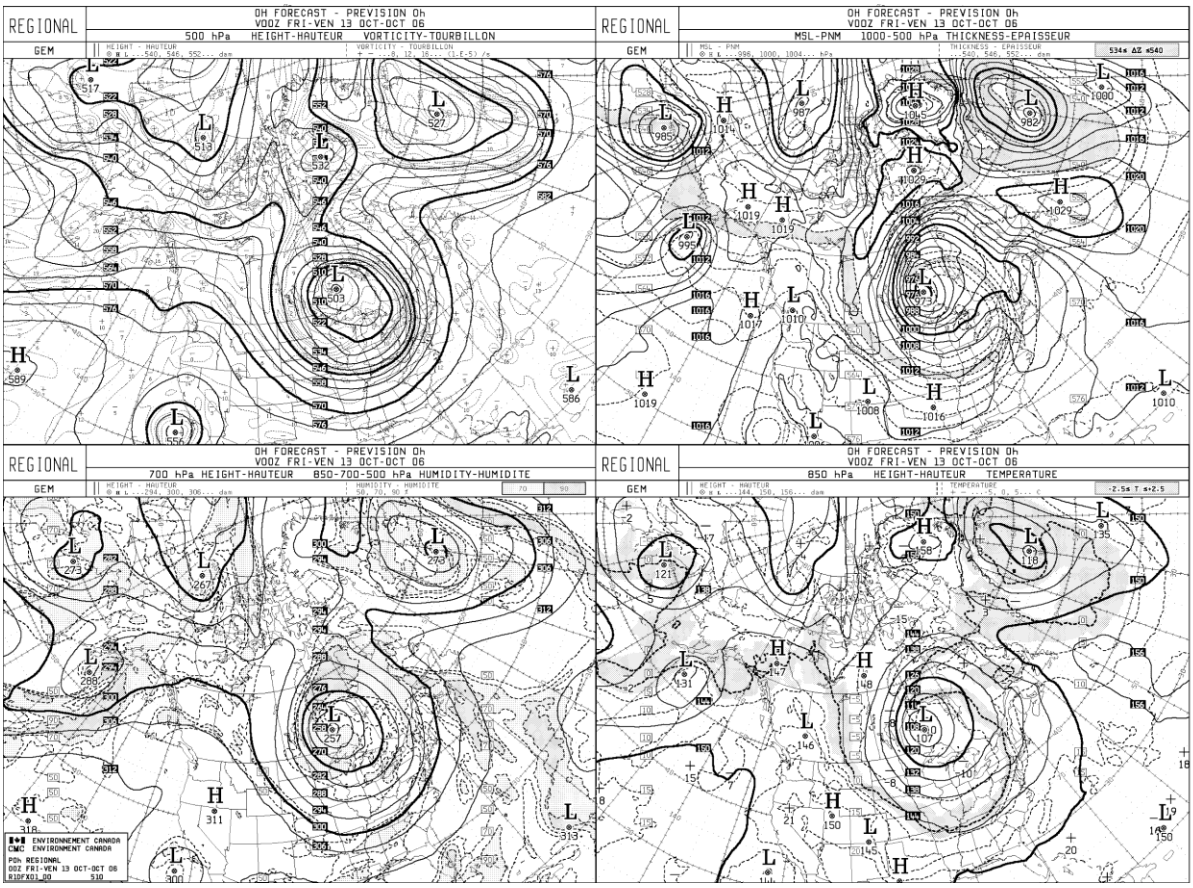
REGIONAL
GEM
0H FORECAST - PREVISION 0h
VOOZ FRI-VEN 13 OCT-OCT 06
500 hPa HEIGHT-HAUTEUR VORTICITY-TOURBILLON
REGIONAL
GEM
0H FORECAST - PREVISION 0h
VOOZ FRI-VEN 13 OCT-OCT 06
MSL-PNM 1000-500 hPa THICKNESS-EPAISSEUR
REGIONAL
GEM
0H FORECAST - PREVISION 0h
VOOZ FRI-VEN 13 OCT-OCT 06
700 hPa HEIGHT-HAUTEUR 850-700-500 hPa HUMIDITY-HUMIDITE
ENVIRONNEMENT CANADA
CMC ENVIRONNEMENT CANADA
PDS REGIONAL
OOZ FRI-VEN 13 OCT-OCT 06
REGIONAL
GEM
0H FORECAST - PREVISION 0h
VOOZ FRI-VEN 13 OCT-OCT 06
850 hPa HEIGHT-HAUTEUR TEMPERATURE

B8: October 4-5, 2012

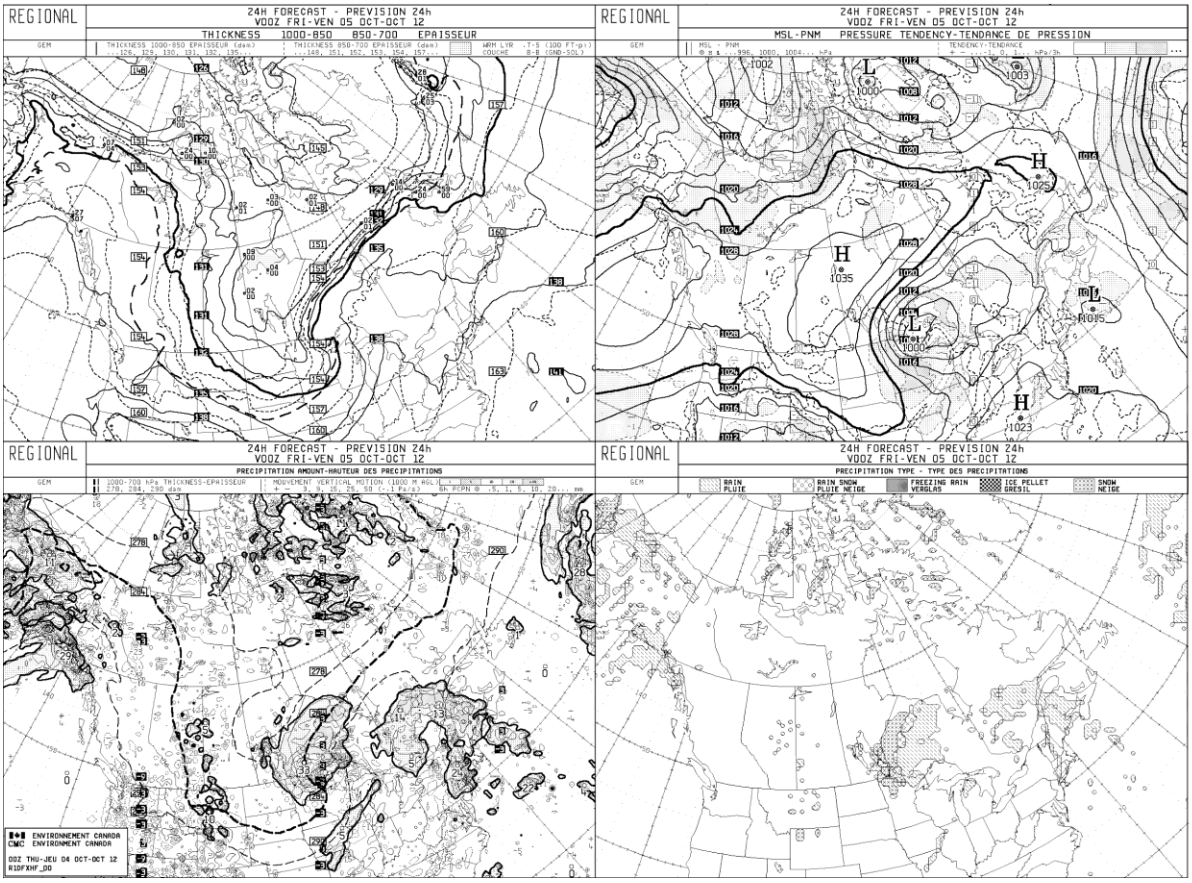

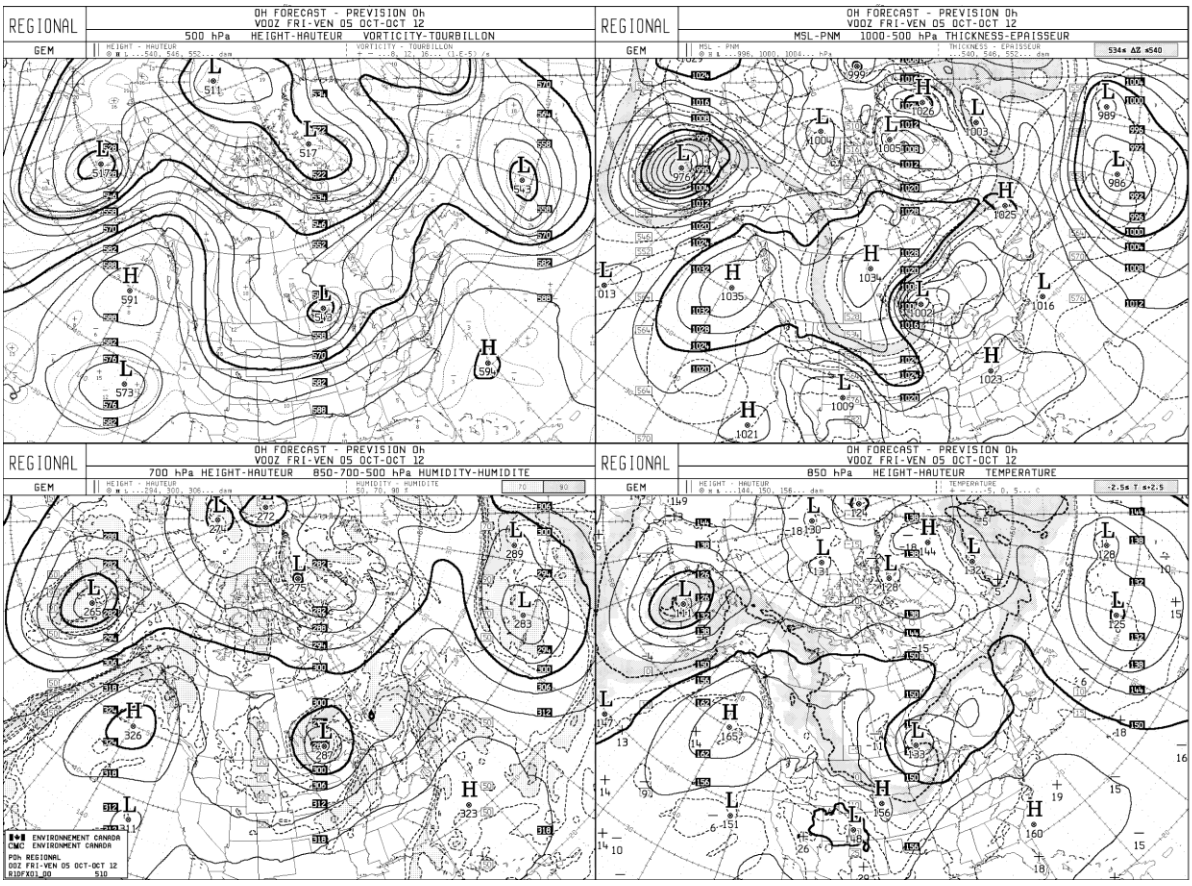
REGIONAL
GEM
00 HR FORECAST - PREVISION 00
VOOZ FRI-VEN 05 OCT-OCT 12
500 hPa HEIGHT-HAUTEUR VORTICITY-TOURBILLON
REGIONAL
GEM
00 HR FORECAST - PREVISION 00
VOOZ FRI-VEN 05 OCT-OCT 12
MSL-PNM 1000-500 hPa THICKNESS-EPAISSEUR
REGIONAL
GEM
00 HR FORECAST - PREVISION 00
VOOZ FRI-VEN 05 OCT-OCT 12
700 hPa HEIGHT-HAUTEUR 850-700-500 hPa HUMIDITY-HUMIDITE
REGIONAL
GEM
00 HR FORECAST - PREVISION 00
VOOZ FRI-VEN 05 OCT-OCT 12
850 hPa HEIGHT-HAUTEUR TEMPERATURE
ENVIRONNEMENT CANADA
ENVIRONMENT CANADA
PDN REGIONAL
OOZ FRI-VEN 05 OCT-OCT 12

Appendix C: January 12-18, 2006 PGW Freezing Rain Cross-Section Time Series

This section contains a time series of cross-sections from the PGW simulation of the January 12-18 freezing rain event. The images are every 3 hours, starting on January 14, 2006 00 UTC to January 16, 2006 21 UTC. Coloured contours indicate the rain mixing ratio in g kg^{-1}. Solid red, thick solid red, and dashed blue contours indicate wet-bulb temperatures above, at, and below 0°C, respectively. Arrows indicate the wind speed and direction. The black area is the terrain. These images show an inversion aloft entering the province from the west, generating freezing rain. It also shows a complex thermal structure, with the release of latent heat as the raindrops freeze along the top and slope of Riding Mountain, as well as upslope flow and cooling. It shows that a combination of mechanisms can be responsible for the spatial patterns seen near elevated terrain. The existence of freezing drizzle is also common throughout, seen as relatively shallow clouds with low rain mixing ratios in cold air.

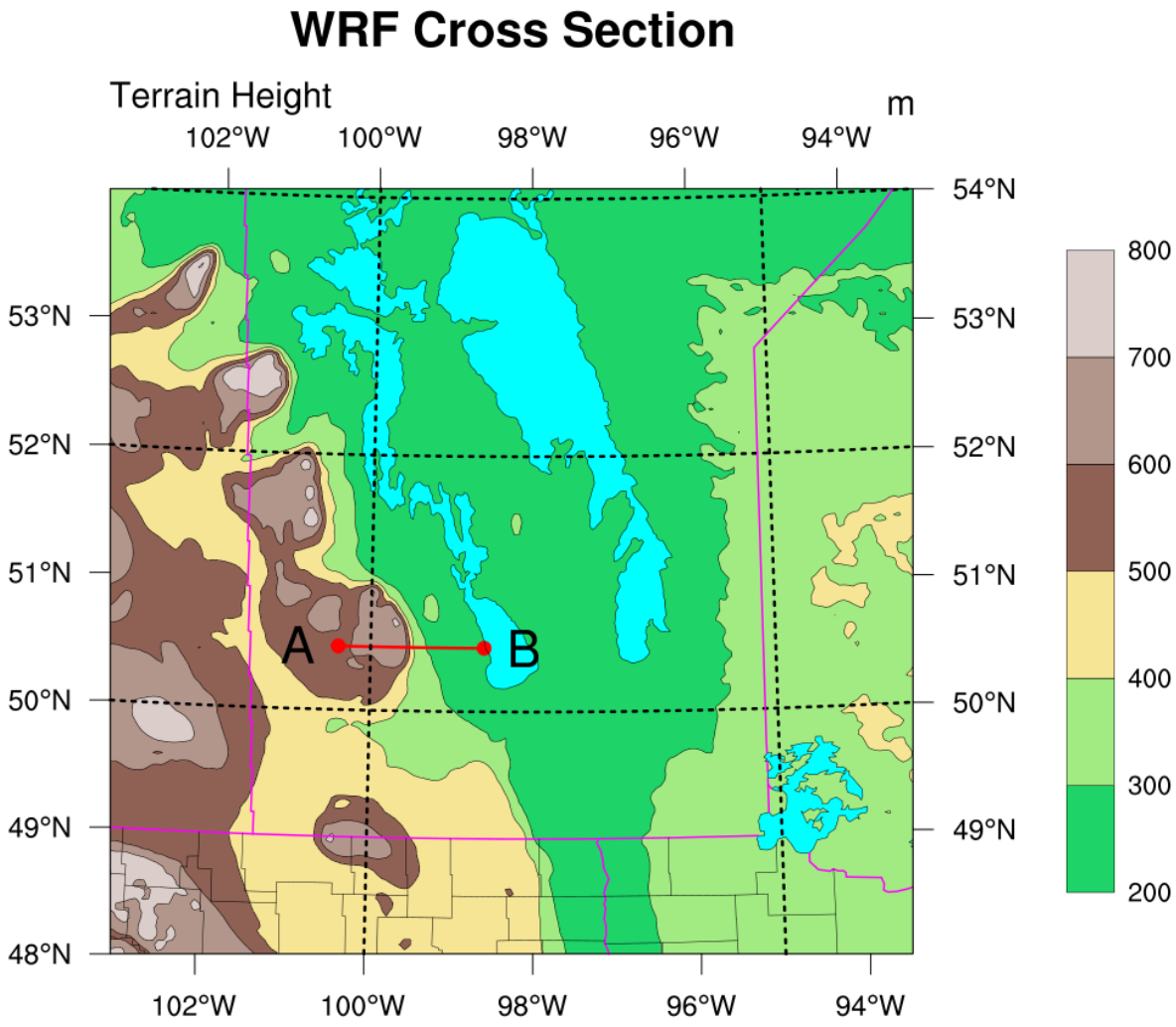
WRF Cross Section
Terrain Height
m
102°W
100°W
98°W
96°W
94°W
54°N
53°N
52°N
51°N
50°N
49°N
48°N
A
B
800
700
600
500
400
300
200

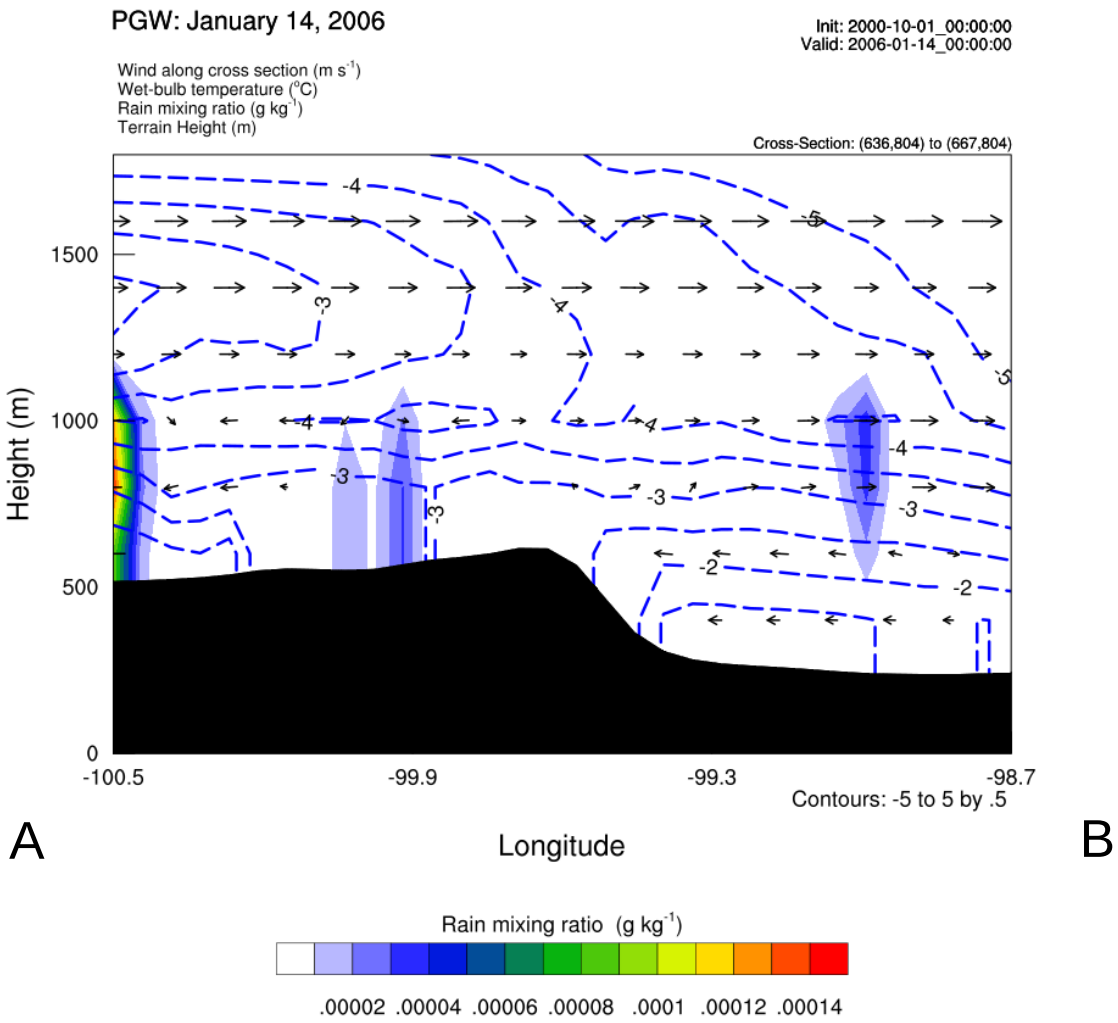
PGW: January 14, 2006
Init: 2000-10-01_00:00:00
Valid: 2006-01-14_00:00:00
Wind along cross section (m s-1)
Wet-bulb temperature (°C)
Rain mixing ratio (g kg-1)
Terrain Height (m)
Cross-Section: (636,804) to (667,804)
Height (m)
1500
1000
500
0
-100.5
-99.9
-99.3
-98.7
Contours: -5 to 5 by .5
A
Longitude
B
Rain mixing ratio (g kg-1)
.00002 .00004 .00006 .00008 .0001 .00012 .00014

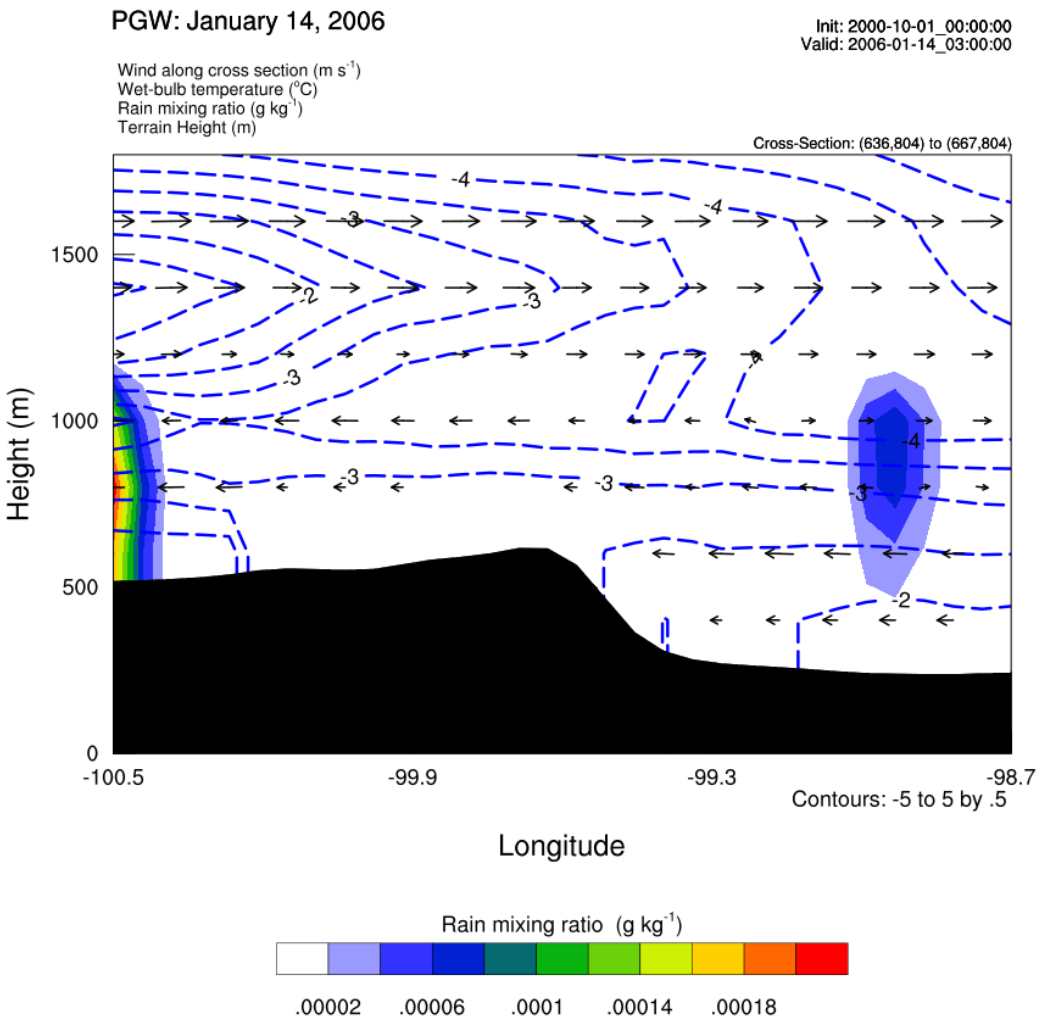
PGW: January 14, 2006
Init: 2000-10-01_00:00:00
Valid: 2006-01-14_03:00:00
Wind along cross section (m s-1)
Wet-bulb temperature (°C)
Rain mixing ratio (g kg-1)
Terrain Height (m)
Cross-Section: (636,804) to (667,804)
Height (m)
1500
1000
500
0
-100.5
-99.9
-99.3
-98.7
Contours: -5 to 5 by .5
Longitude
Rain mixing ratio (g kg-1)
.00002
.00006
.0001
.00014
.00018

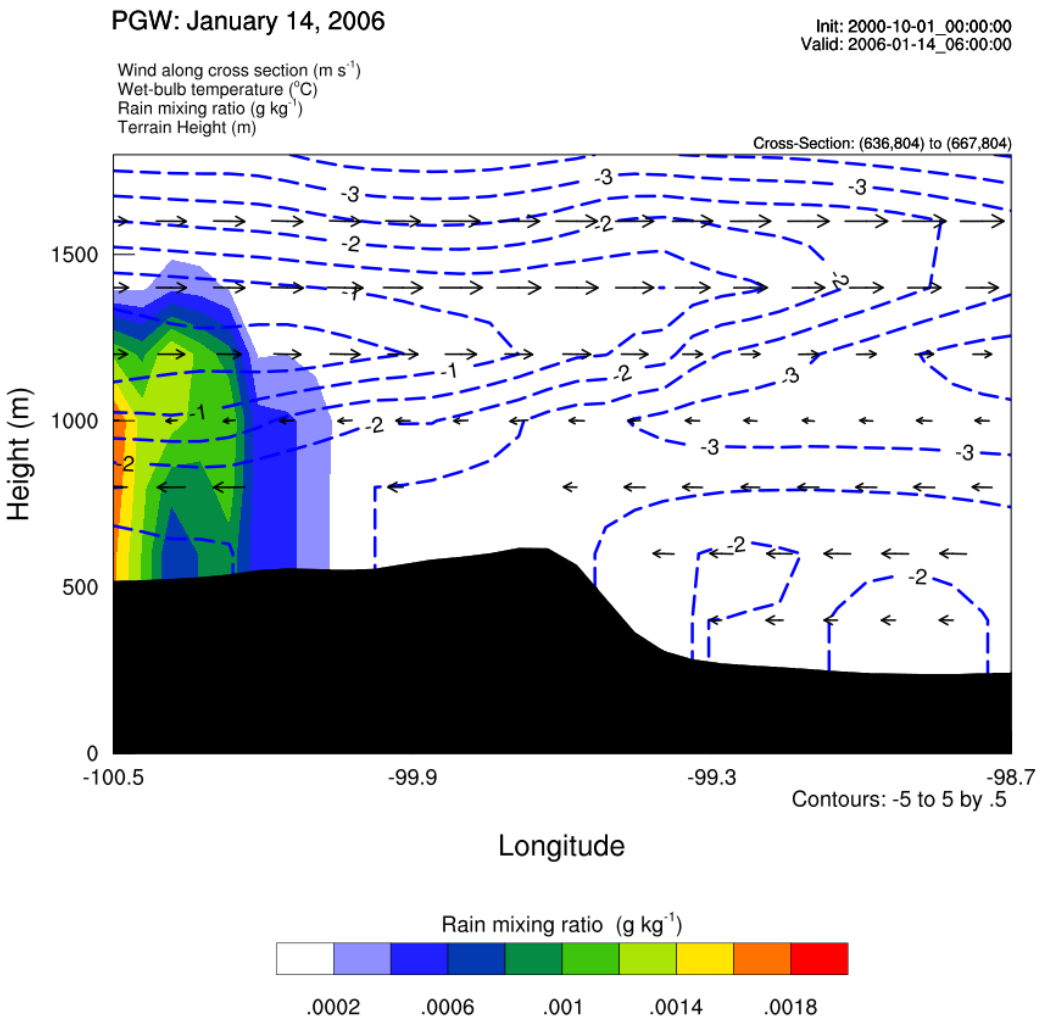
PGW: January 14, 2006
Init: 2000-10-01_00:00:00
Valid: 2006-01-14_06:00:00
Wind along cross section (m s-1)
Wet-bulb temperature (°C)
Rain mixing ratio (g kg-1)
Terrain Height (m)
Cross-Section: (636,804) to (667,804)
Height (m)
0
500
1000
1500
-100.5
-99.9
-99.3
-98.7
Contours: -5 to 5 by .5
Longitude
Rain mixing ratio (g kg-1)
.0002
.0006
.001
.0014
.0018

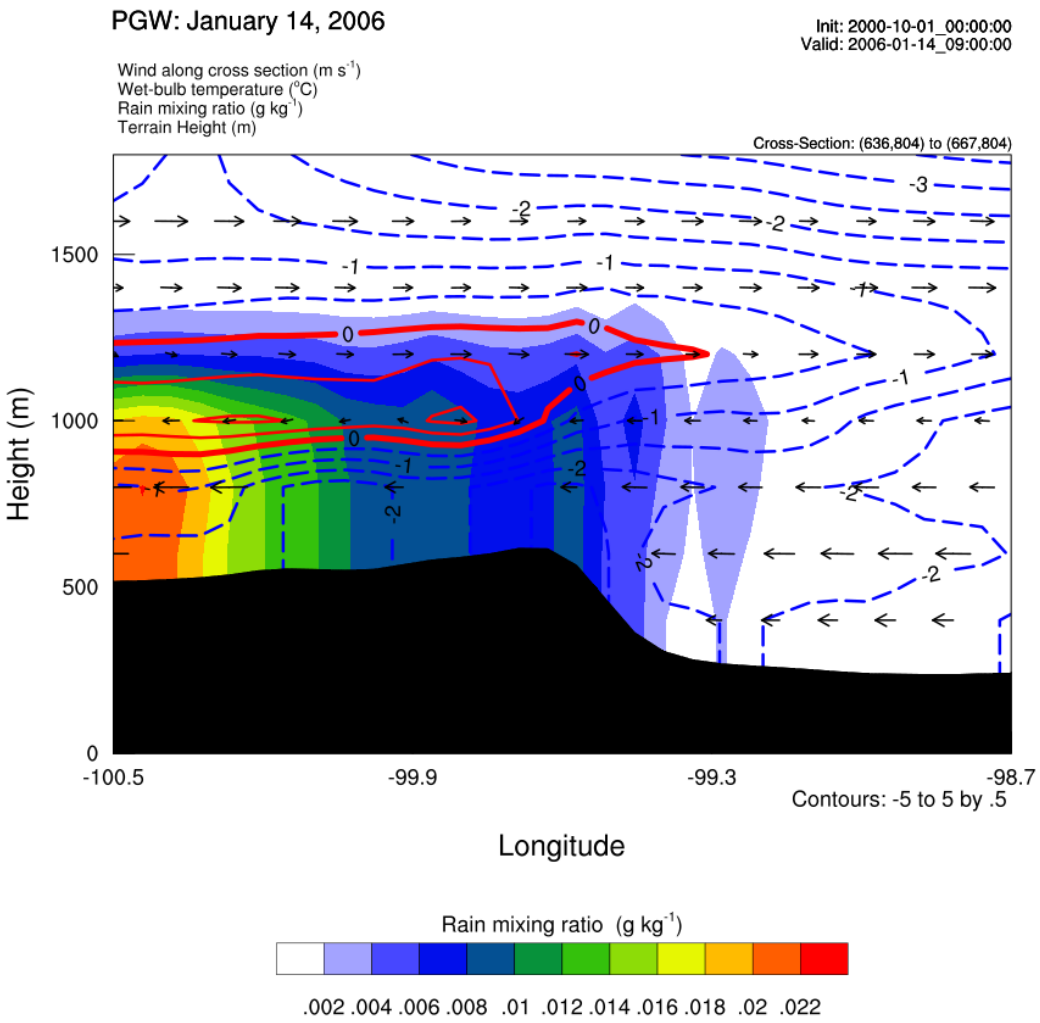
PGW: January 14, 2006
Init: 2000-10-01_00:00:00
Valid: 2006-01-14_09:00:00
Wind along cross section (m s-1)
Wet-bulb temperature (°C)
Rain mixing ratio (g kg-1)
Terrain Height (m)
Cross-Section: (636,804) to (667,804)
Height (m)
1500
1000
500
0
-100.5
-99.9
-99.3
-98.7
Contours: -5 to 5 by .5
Longitude
Rain mixing ratio (g kg-1)
.002 .004 .006 .008 .01 .012 .014 .016 .018 .02 .022

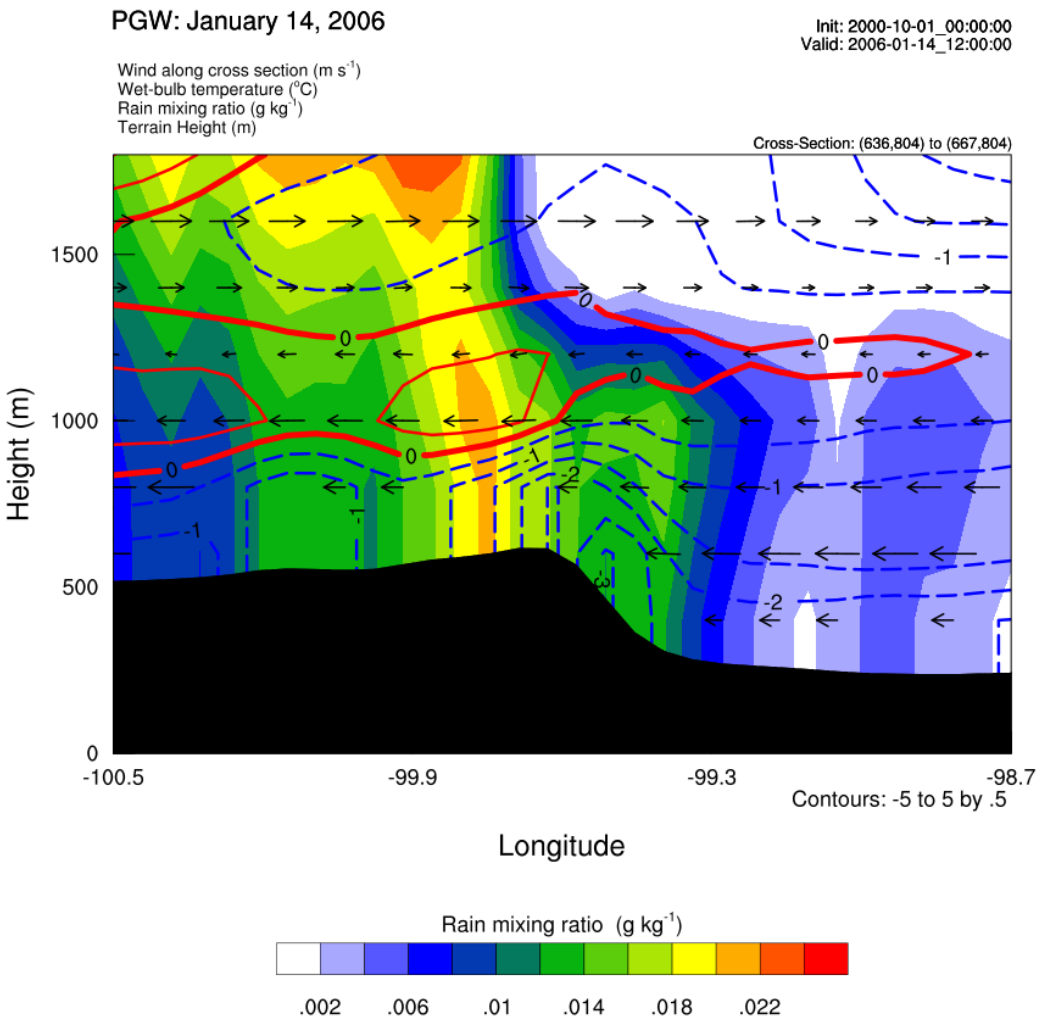
PGW: January 14, 2006
Init: 2000-10-01_00:00:00
Valid: 2006-01-14_12:00:00
Wind along cross section (m s-1)
Wet-bulb temperature (°C)
Rain mixing ratio (g kg-1)
Terrain Height (m)
Cross-Section: (636,804) to (667,804)
Height (m)
1500
1000
500
0
-100.5
-99.9
-99.3
-98.7
Contours: -5 to 5 by .5
Longitude
Rain mixing ratio (g kg-1)
.002
.006
.01
.014
.018
.022

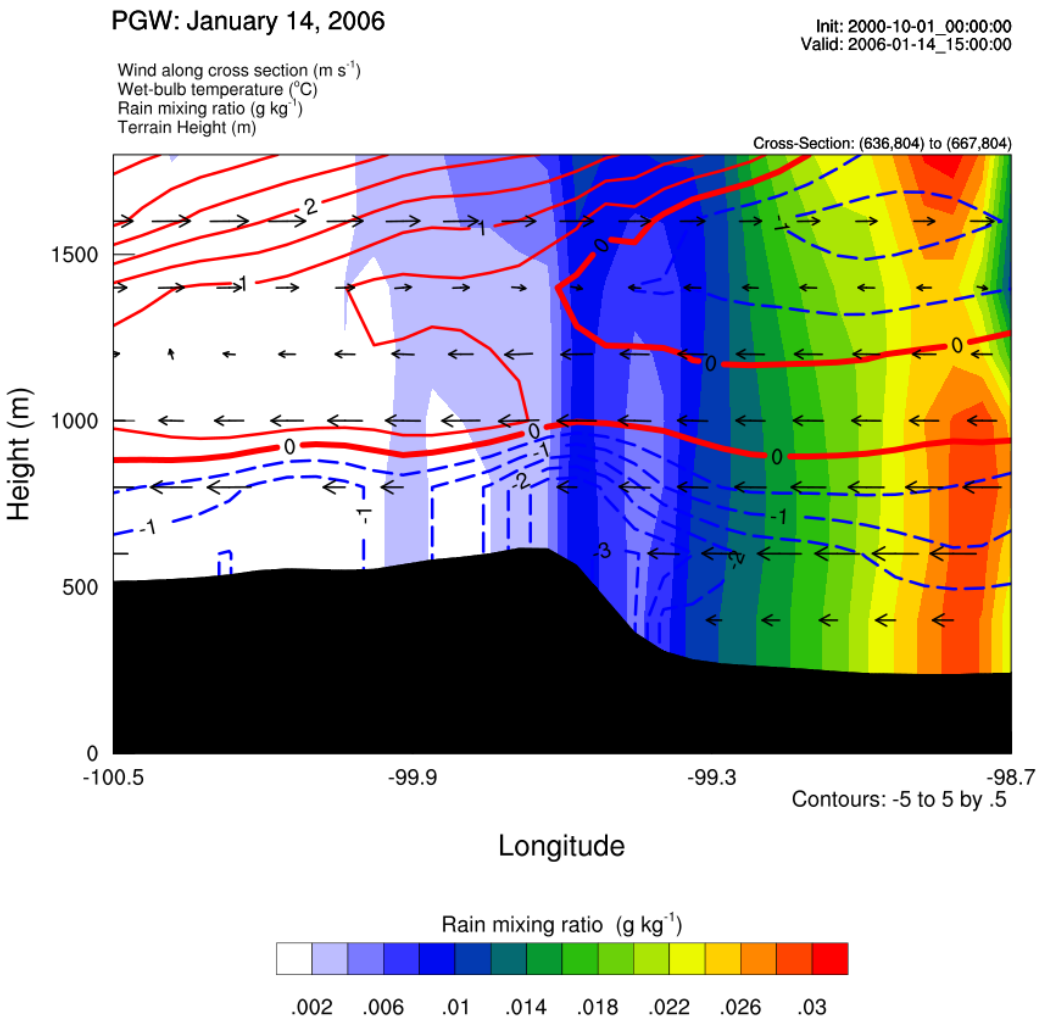
PGW: January 14, 2006
Init: 2000-10-01_00:00:00
Valid: 2006-01-14_15:00:00
Wind along cross section (m s-1)
Wet-bulb temperature (°C)
Rain mixing ratio (g kg-1)
Terrain Height (m)
Cross-Section: (636,804) to (667,804)
Height (m)
1500
1000
500
0
-100.5
-99.9
-99.3
-98.7
Contours: -5 to 5 by .5
Longitude
Rain mixing ratio (g kg-1)
.002
.006
.01
.014
.018
.022
.026
.03

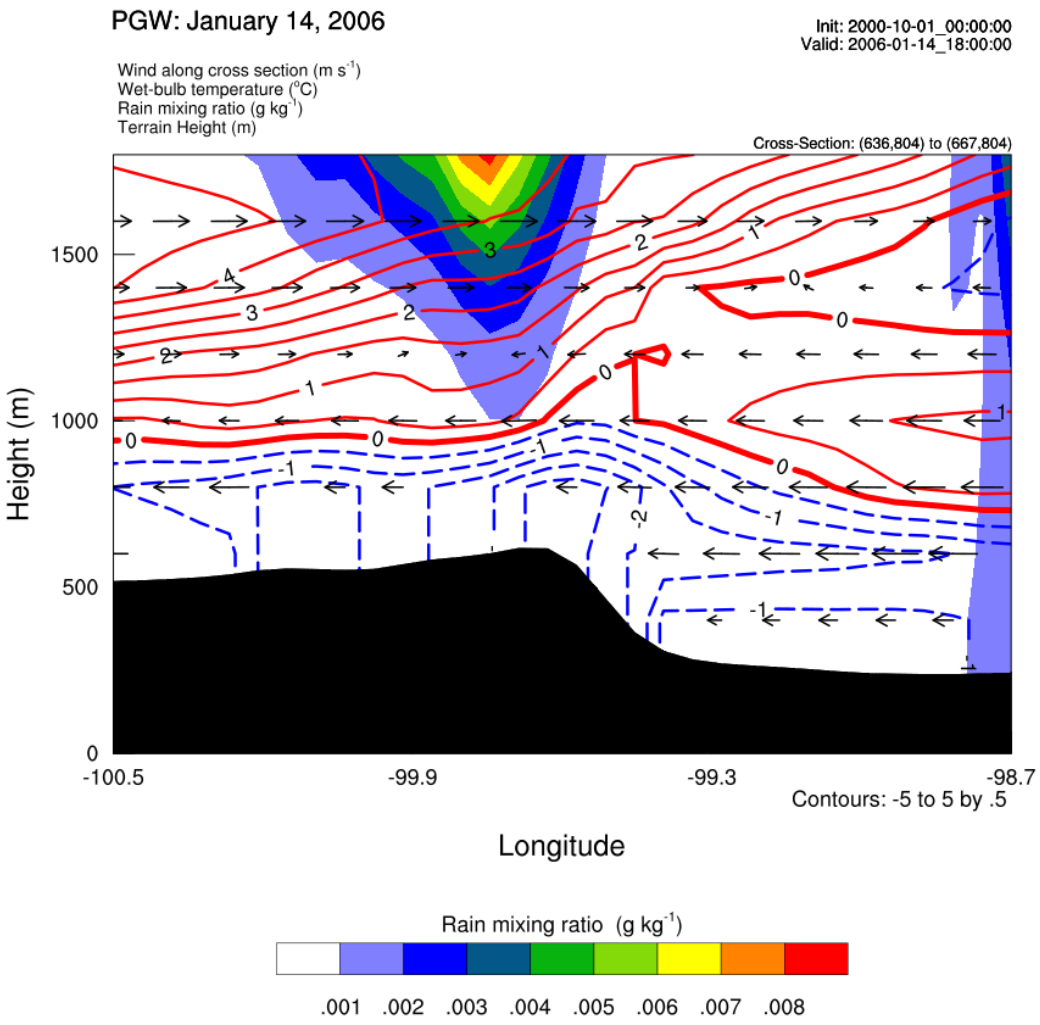
PGW: January 14, 2006
Init: 2000-10-01_00:00:00
Valid: 2006-01-14_18:00:00
Wind along cross section (m s-1)
Wet-bulb temperature (°C)
Rain mixing ratio (g kg-1)
Terrain Height (m)
Cross-Section: (636,804) to (667,804)
Height (m)
1500
1000
500
0
-100.5
-99.9
-99.3
-98.7
Contours: -5 to 5 by .5
Longitude
Rain mixing ratio (g kg-1)
.001 .002 .003 .004 .005 .006 .007 .008

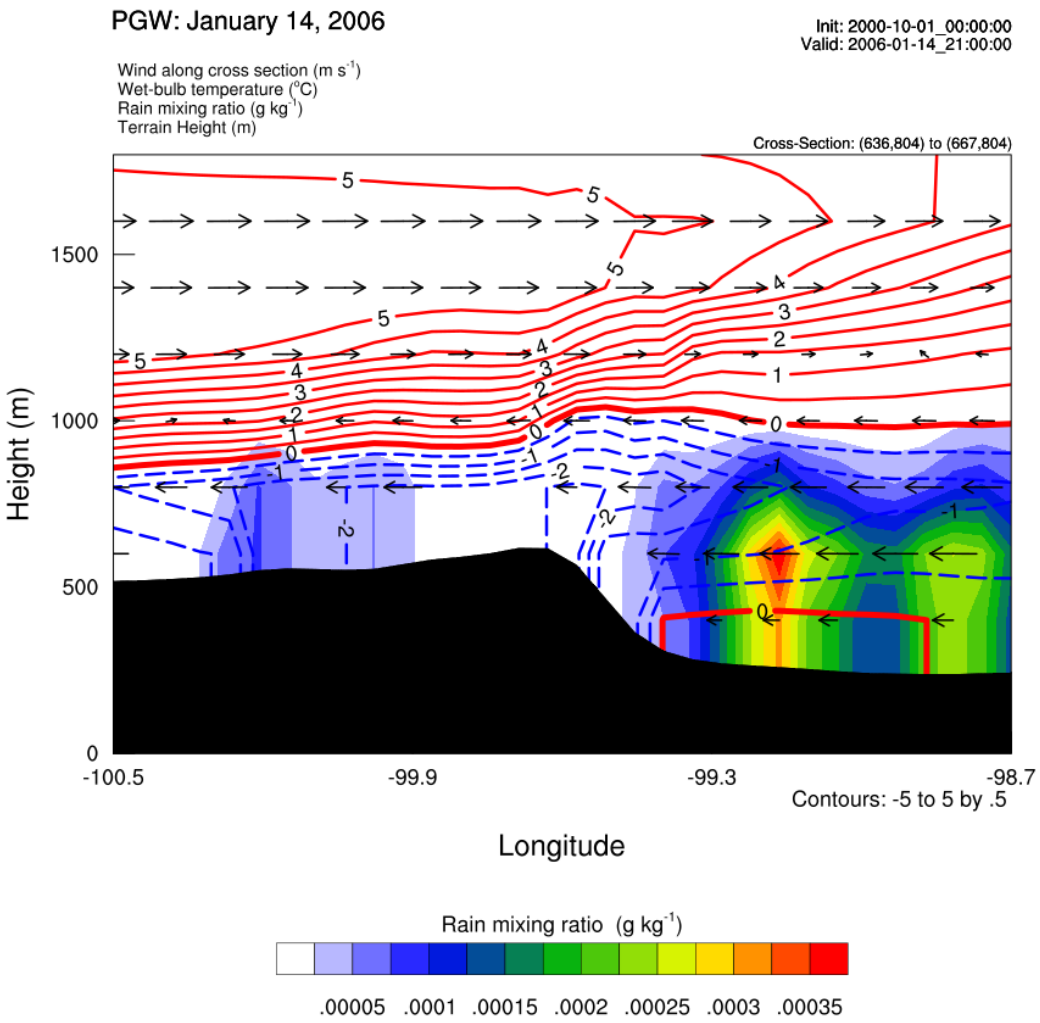
PGW: January 14, 2006
Init: 2000-10-01_00:00:00
Valid: 2006-01-14_21:00:00
Wind along cross section (m s-1)
Wet-bulb temperature (°C)
Rain mixing ratio (g kg-1)
Terrain Height (m)
Cross-Section: (636,804) to (667,804)
Height (m)
1500
1000
500
0
-100.5
-99.9
-99.3
-98.7
Contours: -5 to 5 by .5
Longitude
Rain mixing ratio (g kg-1)
.00005 .0001 .00015 .0002 .00025 .0003 .00035

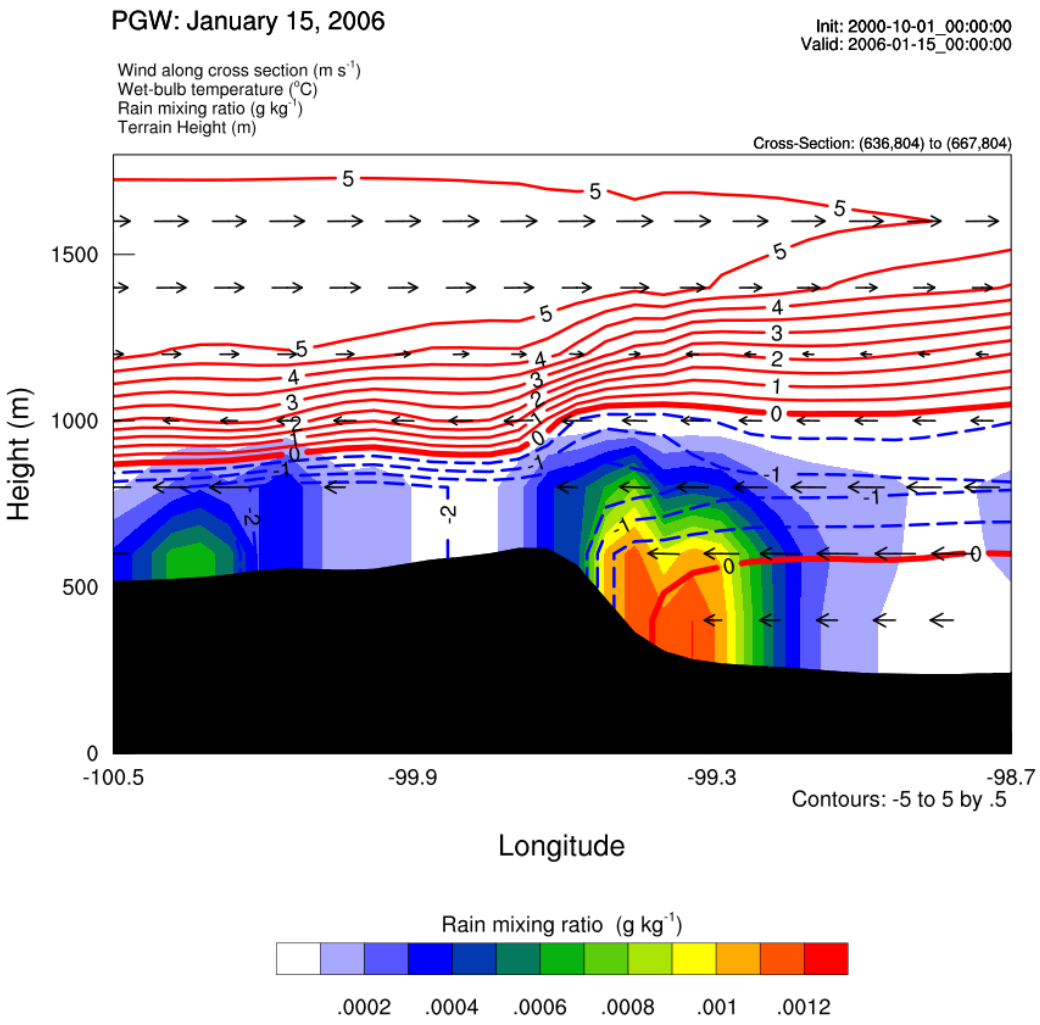
PGW: January 15, 2006
Init: 2000-10-01_00:00:00
Valid: 2006-01-15_00:00:00
Wind along cross section (m s-1)
Wet-bulb temperature (°C)
Rain mixing ratio (g kg-1)
Terrain Height (m)
Cross-Section: (636,804) to (667,804)
Height (m)
1500
1000
500
0
-100.5
-99.9
-99.3
-98.7
Contours: -5 to 5 by .5
Longitude
Rain mixing ratio (g kg-1)
.0002
.0004
.0006
.0008
.001
.0012

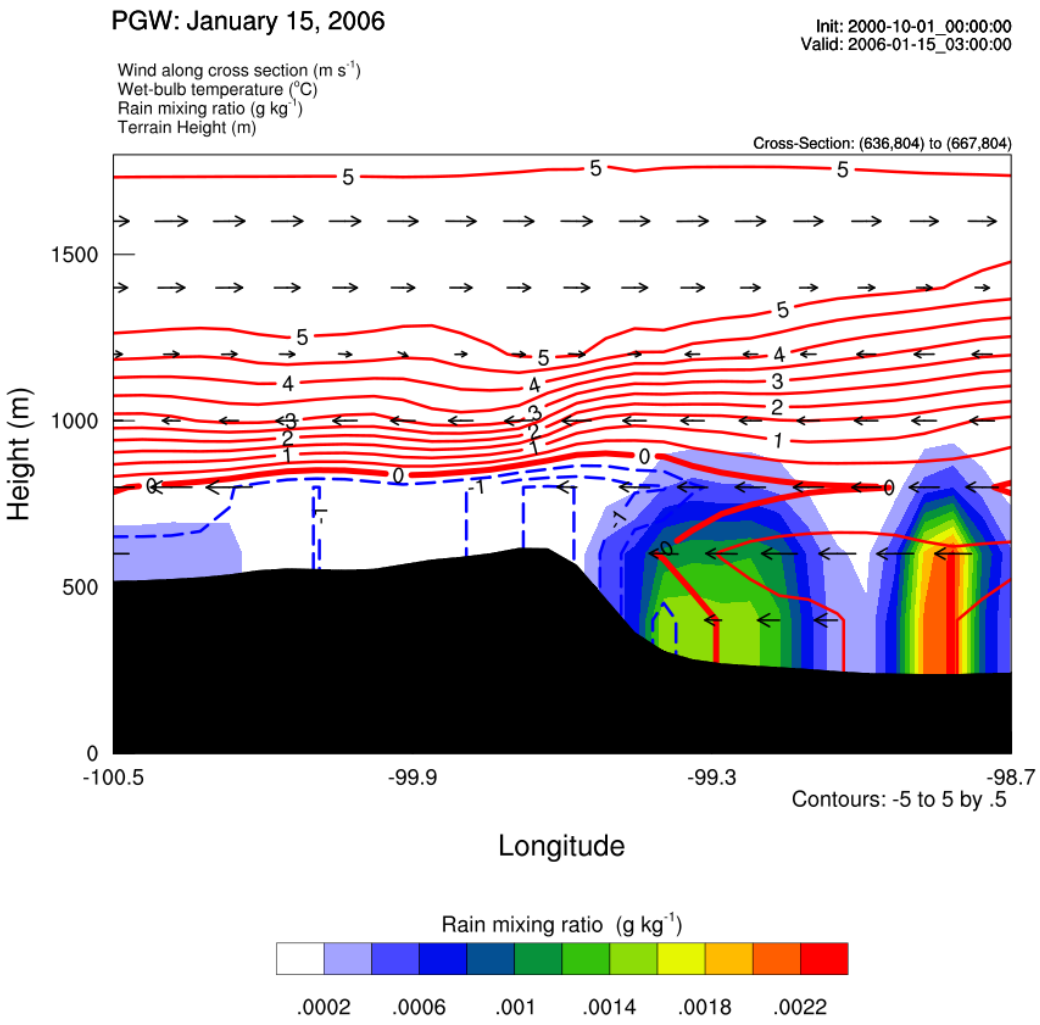
PGW: January 15, 2006
Init: 2000-10-01_00:00:00
Valid: 2006-01-15_03:00:00
Wind along cross section (m s-1)
Wet-bulb temperature (°C)
Rain mixing ratio (g kg-1)
Terrain Height (m)
Cross-Section: (636,804) to (667,804)
Height (m)
1500
1000
500
0
-100.5
-99.9
-99.3
-98.7
Contours: -5 to 5 by .5
Longitude
Rain mixing ratio (g kg-1)
.0002
.0006
.001
.0014
.0018
.0022

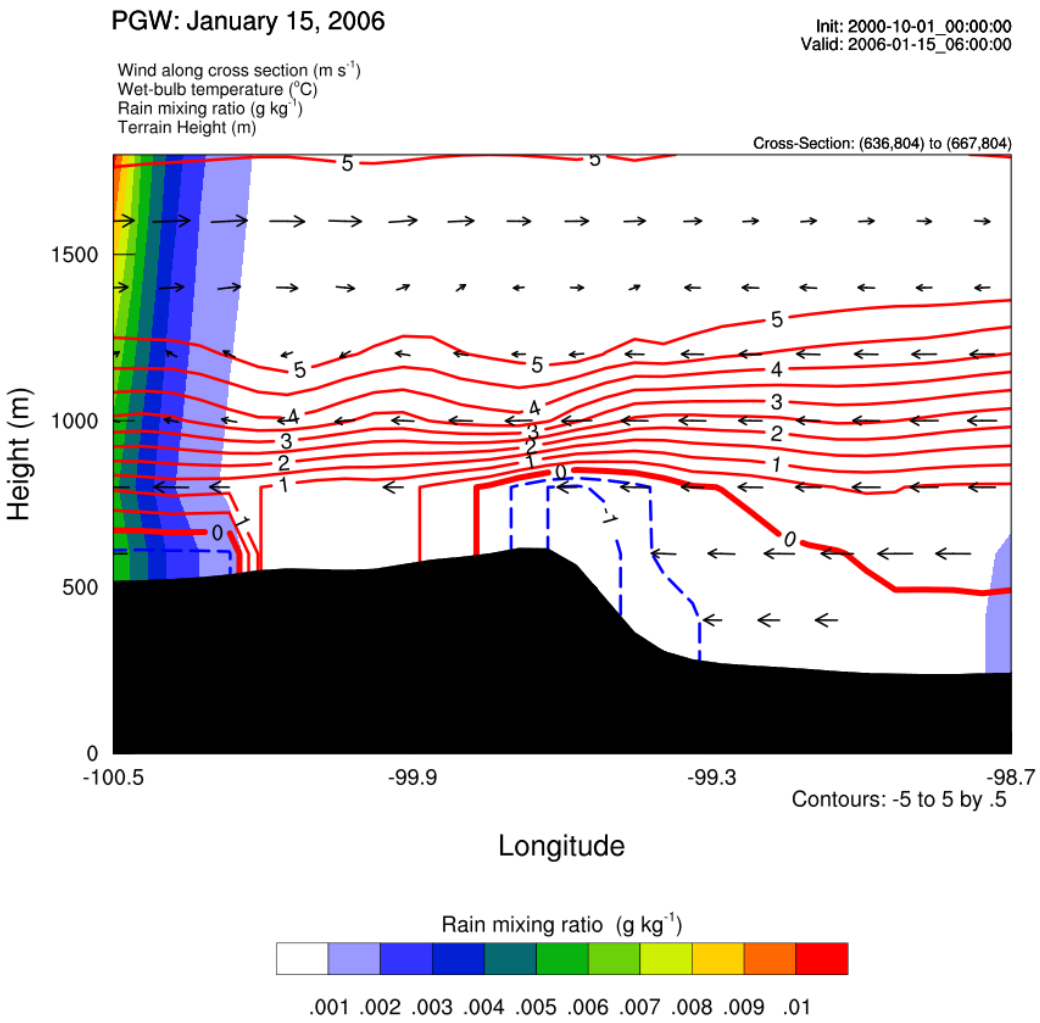
PGW: January 15, 2006
Init: 2000-10-01_00:00:00
Valid: 2006-01-15_06:00:00
Wind along cross section (m s-1)
Wet-bulb temperature (°C)
Rain mixing ratio (g kg-1)
Terrain Height (m)
Cross-Section: (636,804) to (667,804)
Height (m)
1500
1000
500
0
-100.5
-99.9
-99.3
-98.7
Contours: -5 to 5 by .5
Longitude
Rain mixing ratio (g kg-1)
.001 .002 .003 .004 .005 .006 .007 .008 .009 .01

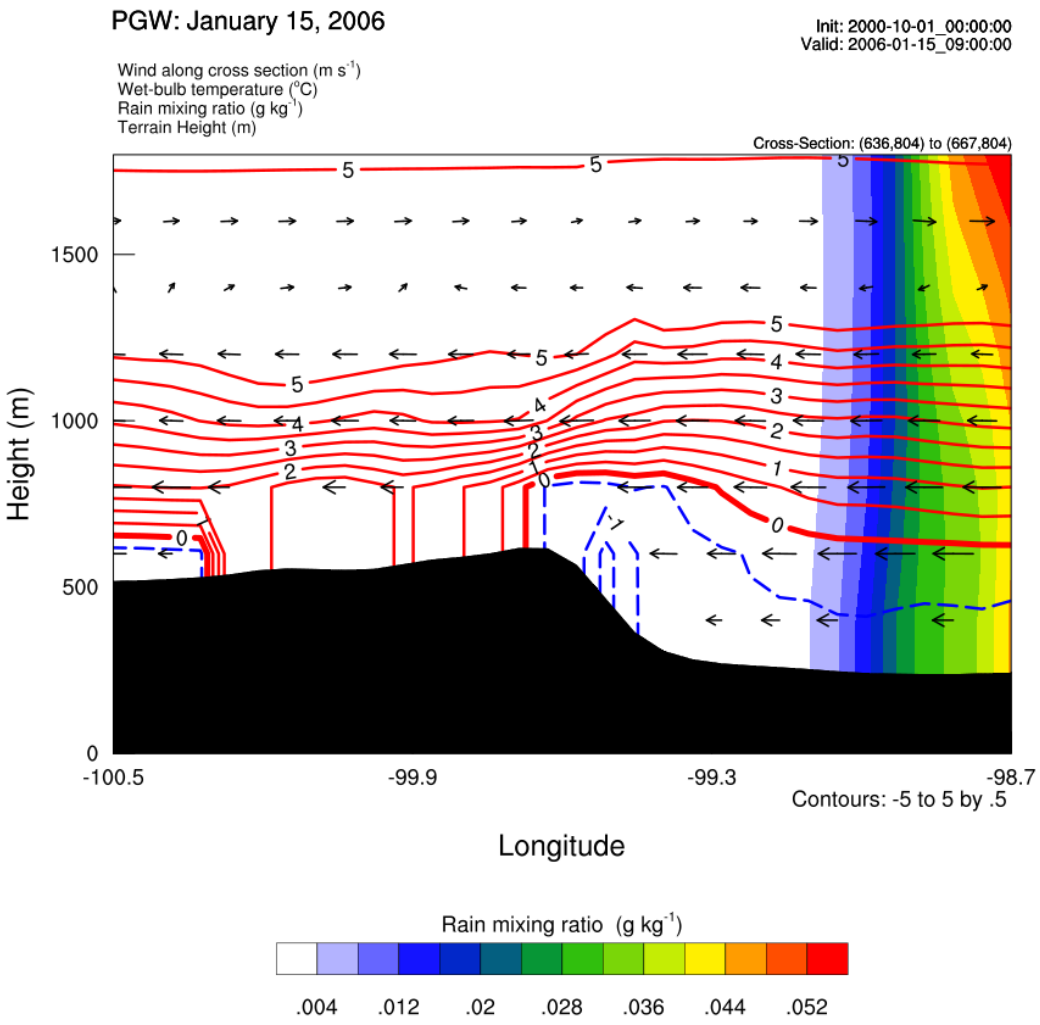
PGW: January 15, 2006
Init: 2000-10-01_00:00:00
Valid: 2006-01-15_09:00:00
Wind along cross section (m s-1)
Wet-bulb temperature (°C)
Rain mixing ratio (g kg-1)
Terrain Height (m)
Cross-Section: (636,804) to (667,804)
Height (m)
1500
1000
500
0
-100.5
-99.9
-99.3
-98.7
Contours: -5 to 5 by .5
Longitude
Rain mixing ratio (g kg-1)
.004
.012
.02
.028
.036
.044
.052

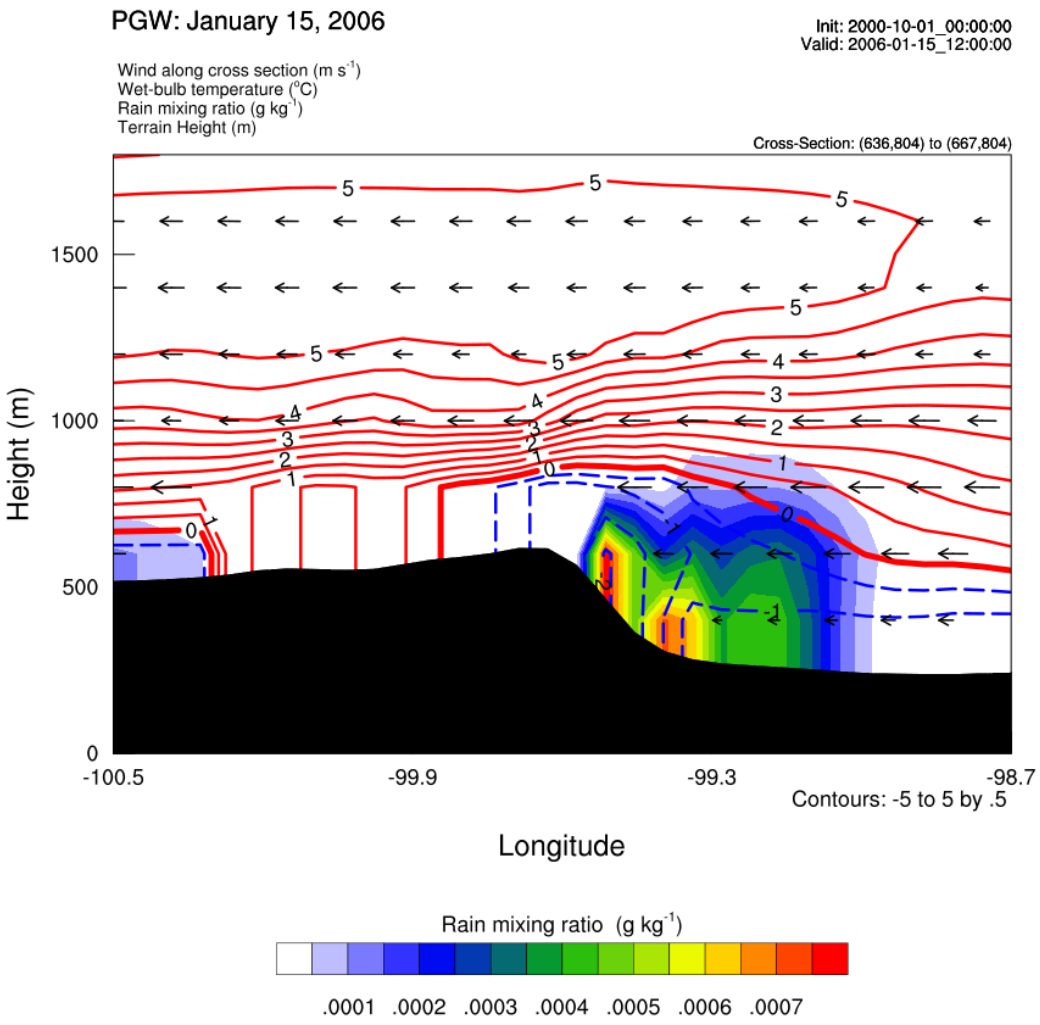
PGW: January 15, 2006
Init: 2000-10-01_00:00:00
Valid: 2006-01-15_12:00:00
Wind along cross section (m s-1)
Wet-bulb temperature (°C)
Rain mixing ratio (g kg-1)
Terrain Height (m)
Cross-Section: (636,804) to (667,804)
Height (m)
1500
1000
500
0
-100.5
-99.9
-99.3
-98.7
Contours: -5 to 5 by .5
Longitude
Rain mixing ratio (g kg-1)
.0001 .0002 .0003 .0004 .0005 .0006 .0007

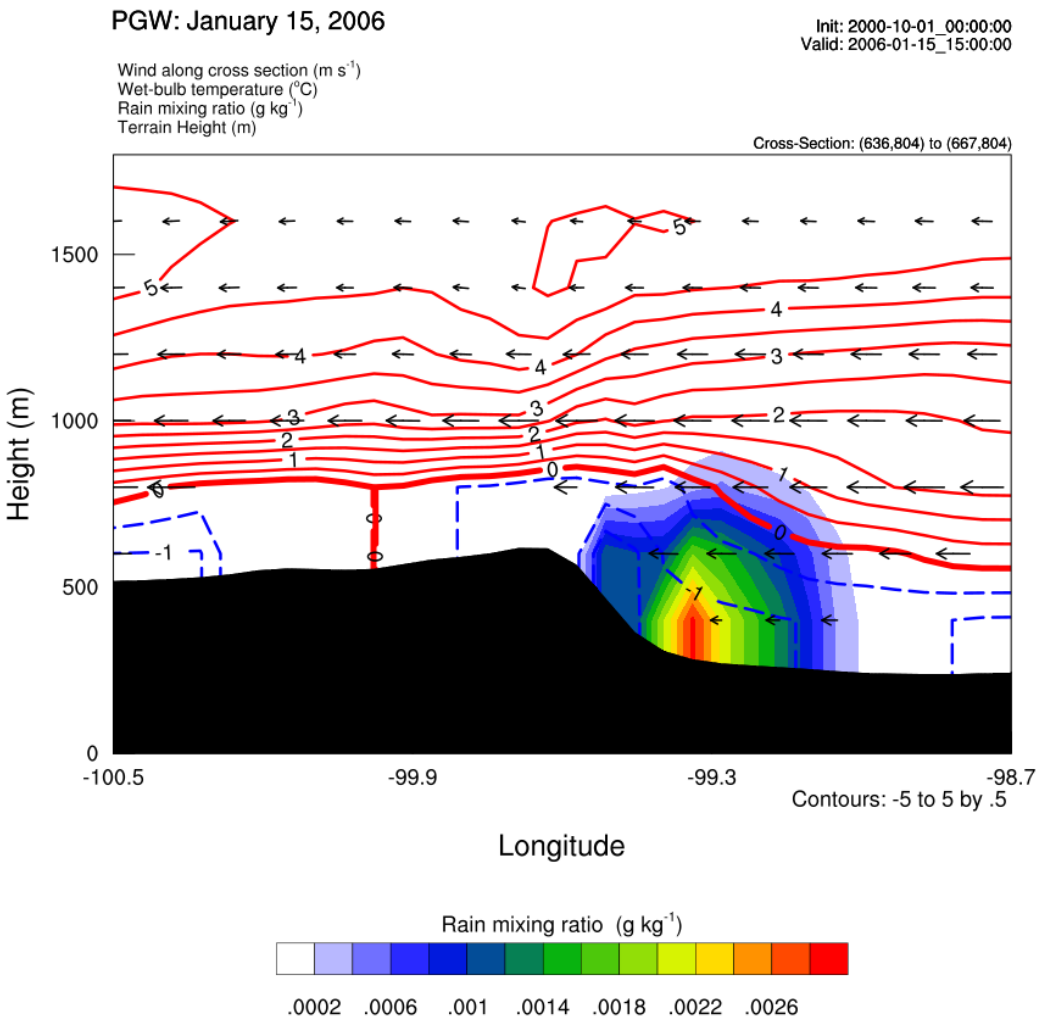
PGW: January 15, 2006
Init: 2000-10-01_00:00:00
Valid: 2006-01-15_15:00:00
Wind along cross section (m s-1)
Wet-bulb temperature (°C)
Rain mixing ratio (g kg-1)
Terrain Height (m)
Cross-Section: (636,804) to (667,804)
Height (m)
1500
1000
500
0
-100.5
-99.9
-99.3
-98.7
Contours: -5 to 5 by .5
Longitude
Rain mixing ratio (g kg-1)
.0002
.0006
.001
.0014
.0018
.0022
.0026

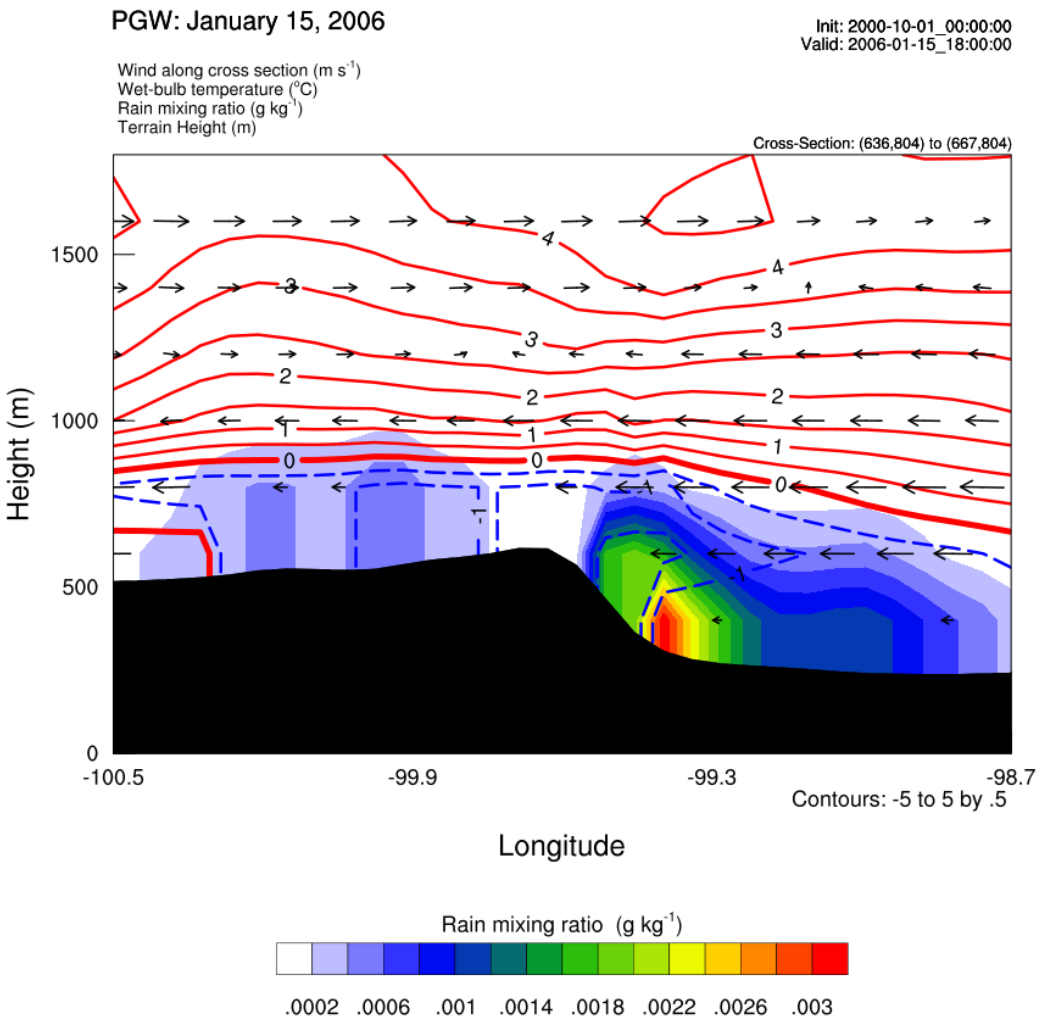
PGW: January 15, 2006
Init: 2000-10-01_00:00:00
Valid: 2006-01-15_18:00:00
Wind along cross section (m s-1)
Wet-bulb temperature (°C)
Rain mixing ratio (g kg-1)
Terrain Height (m)
Cross-Section: (636,804) to (667,804)
Height (m)
1500
1000
500
0
-100.5
-99.9
-99.3
-98.7
Contours: -5 to 5 by .5
Longitude
Rain mixing ratio (g kg-1)
.0002 .0006 .001 .0014 .0018 .0022 .0026 .003

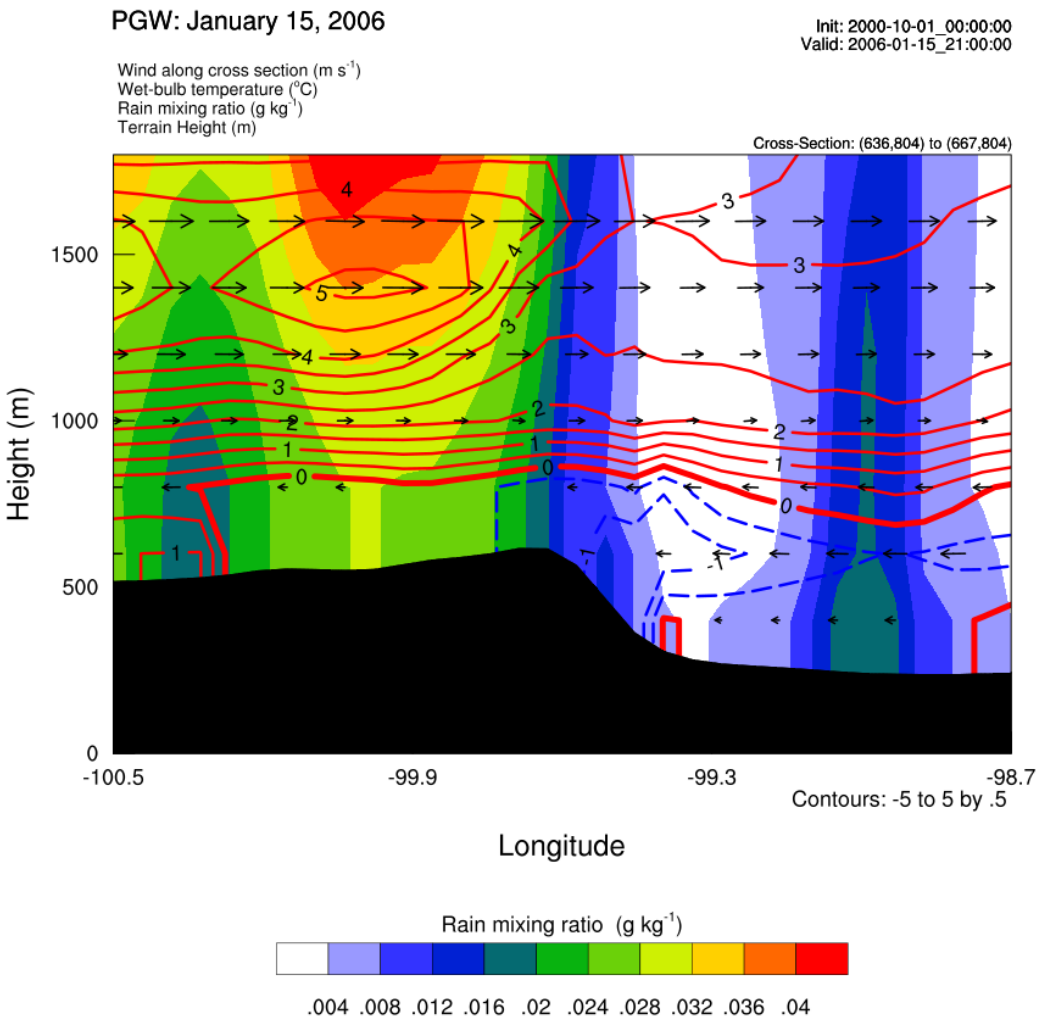
PGW: January 15, 2006
Init: 2000-10-01_00:00:00
Valid: 2006-01-15_21:00:00
Wind along cross section (m s-1)
Wet-bulb temperature (°C)
Rain mixing ratio (g kg-1)
Terrain Height (m)
Cross-Section: (636,804) to (667,804)
Height (m)
1500
1000
500
0
-100.5
-99.9
-99.3
-98.7
Contours: -5 to 5 by .5
Longitude
Rain mixing ratio (g kg-1)
.004 .008 .012 .016 .02 .024 .028 .032 .036 .04

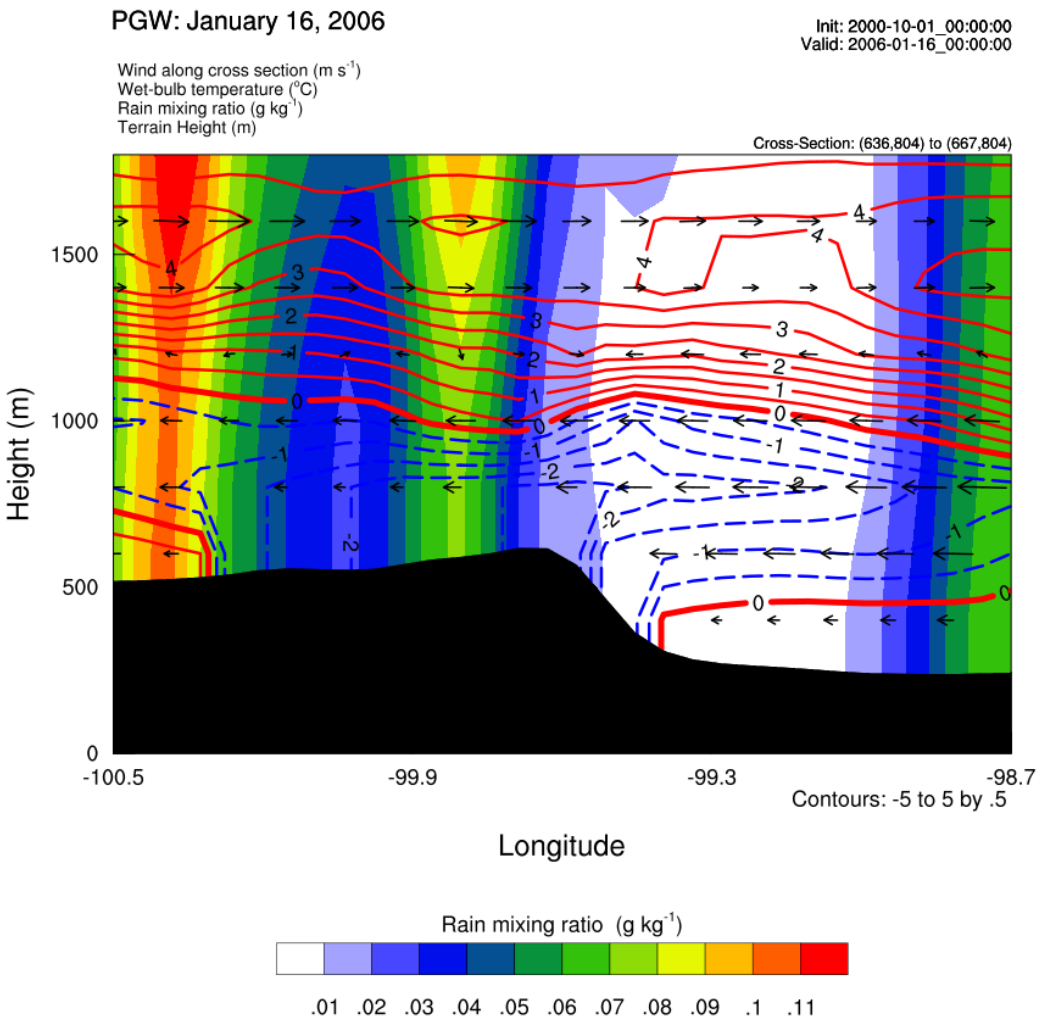
PGW: January 16, 2006
Init: 2000-10-01_00:00:00
Valid: 2006-01-16_00:00:00
Wind along cross section (m s-1)
Wet-bulb temperature (°C)
Rain mixing ratio (g kg-1)
Terrain Height (m)
Cross-Section: (636,804) to (667,804)
Height (m)
1500
1000
500
0
-100.5
-99.9
-99.3
-98.7
Contours: -5 to 5 by .5
Longitude
Rain mixing ratio (g kg-1)
.01 .02 .03 .04 .05 .06 .07 .08 .09 .1 .11

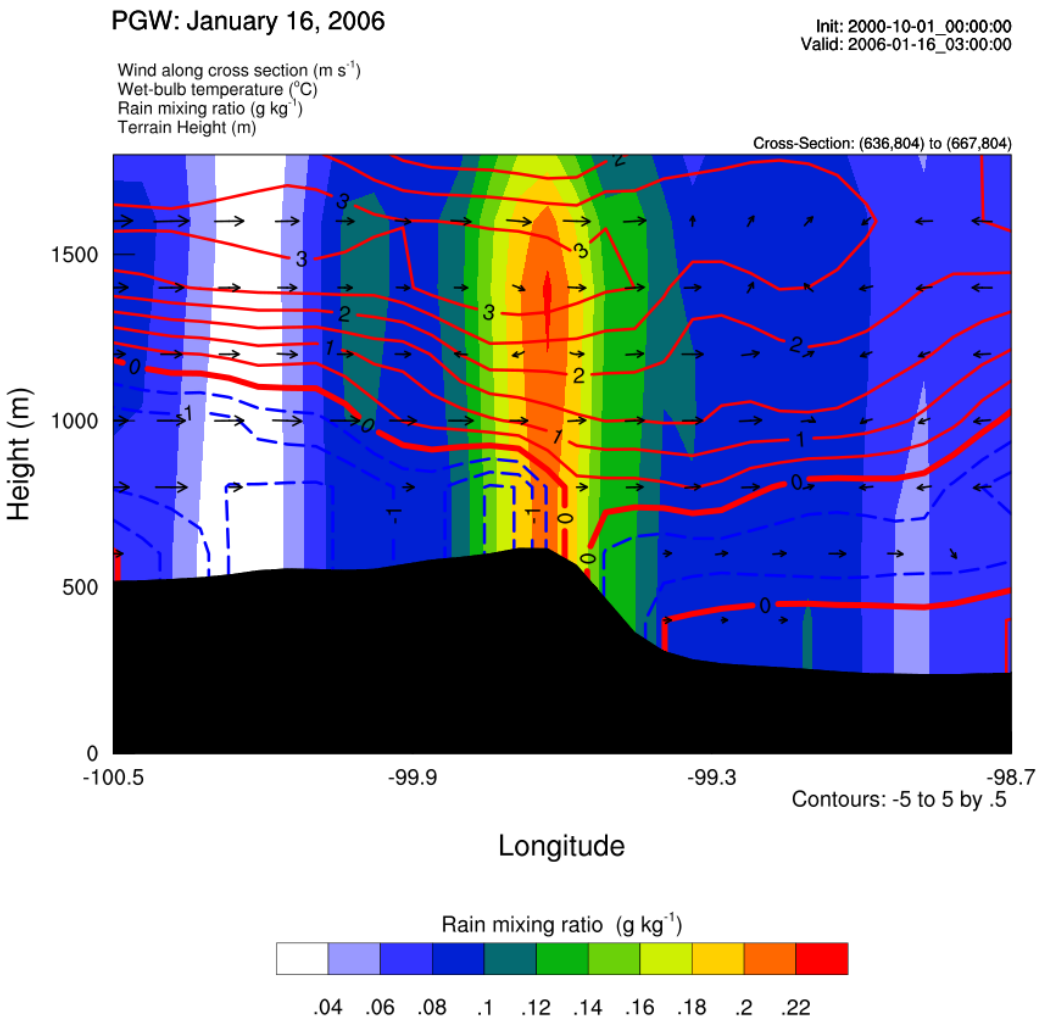
PGW: January 16, 2006
Init: 2000-10-01_00:00:00
Valid: 2006-01-16_03:00:00
Wind along cross section (m s-1)
Wet-bulb temperature (°C)
Rain mixing ratio (g kg-1)
Terrain Height (m)
Cross-Section: (636,804) to (667,804)
Height (m)
1500
1000
500
0
-100.5
-99.9
-99.3
-98.7
Contours: -5 to 5 by .5
Longitude
Rain mixing ratio (g kg-1)
.04 .06 .08 .1 .12 .14 .16 .18 .2 .22

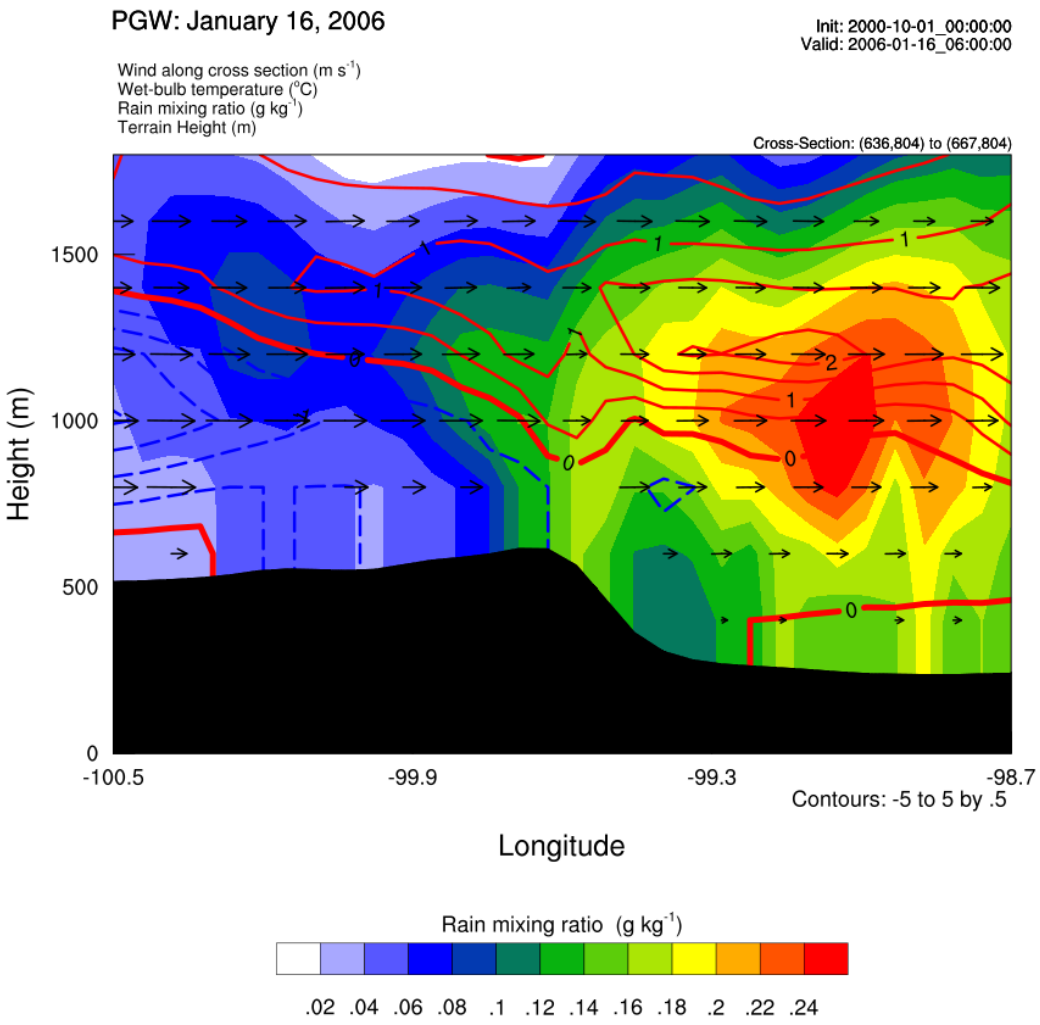
PGW: January 16, 2006
Init: 2000-10-01_00:00:00
Valid: 2006-01-16_06:00:00
Wind along cross section (m s-1)
Wet-bulb temperature (°C)
Rain mixing ratio (g kg-1)
Terrain Height (m)
Cross-Section: (636,804) to (667,804)
Height (m)
1500
1000
500
0
-100.5
-99.9
-99.3
-98.7
Contours: -5 to 5 by .5
Longitude
Rain mixing ratio (g kg-1)
.02 .04 .06 .08 .1 .12 .14 .16 .18 .2 .22 .24

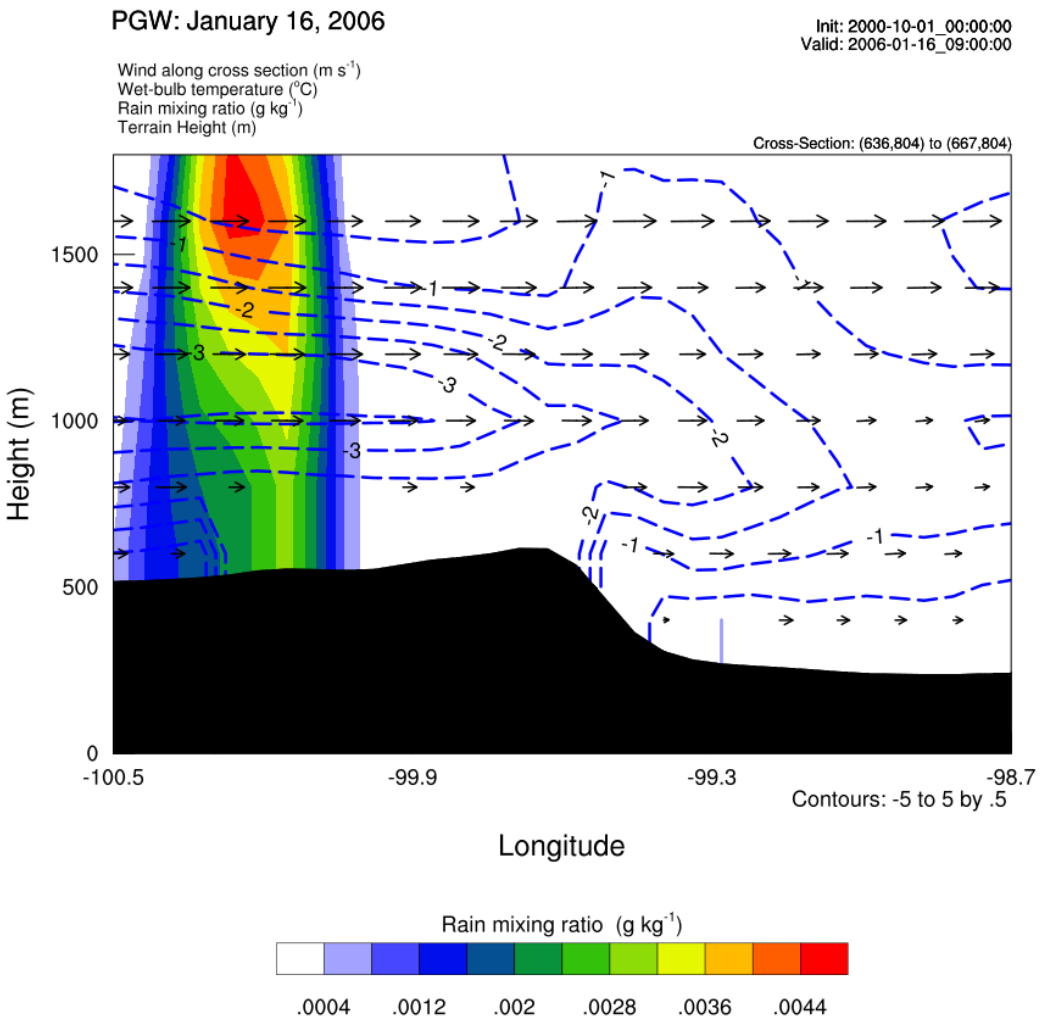
PGW: January 16, 2006
Init: 2000-10-01_00:00:00
Valid: 2006-01-16_09:00:00
Wind along cross section (m s-1)
Wet-bulb temperature (°C)
Rain mixing ratio (g kg-1)
Terrain Height (m)
Cross-Section: (636,804) to (667,804)
Height (m)
1500
1000
500
0
-100.5
-99.9
-99.3
-98.7
Contours: -5 to 5 by .5
Longitude
Rain mixing ratio (g kg-1)
.0004
.0012
.002
.0028
.0036
.0044

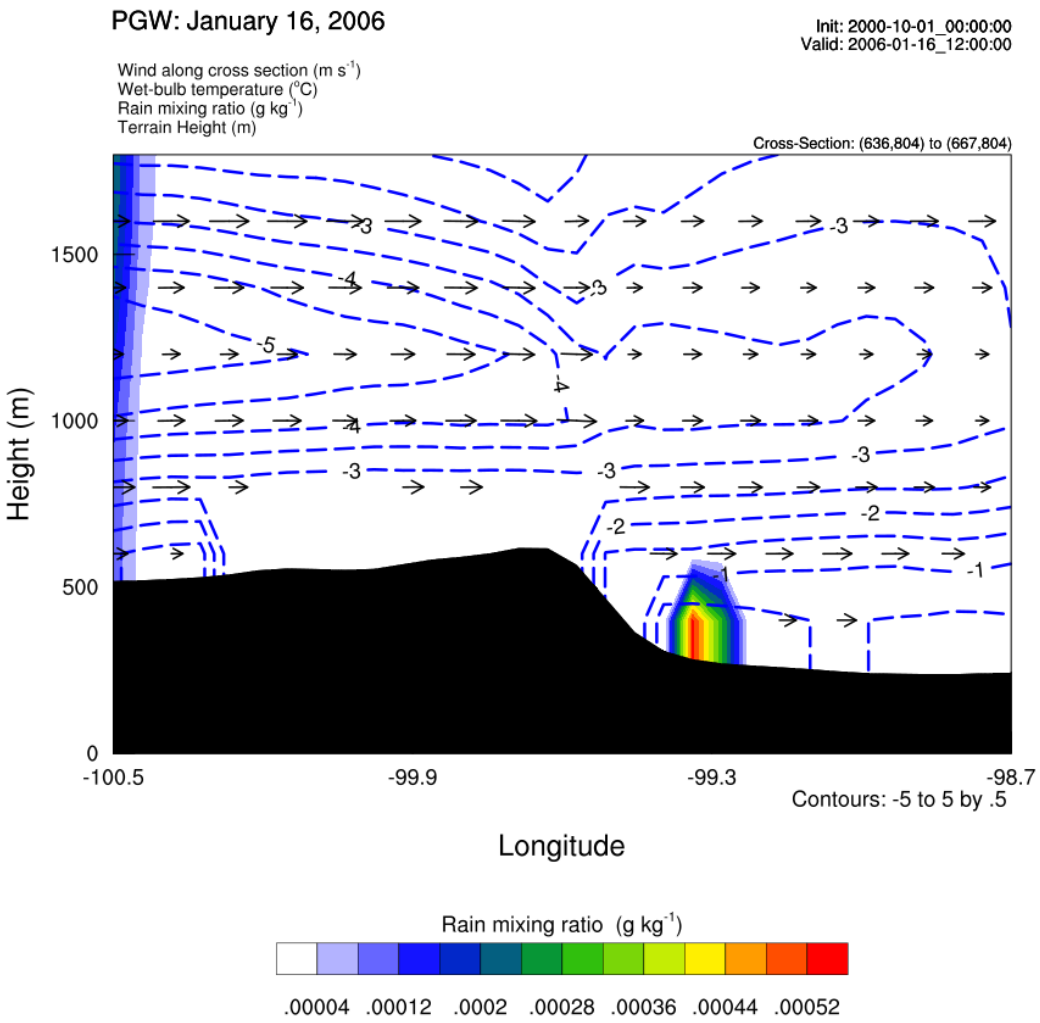
PGW: January 16, 2006
Init: 2000-10-01_00:00:00
Valid: 2006-01-16_12:00:00
Wind along cross section (m s-1)
Wet-bulb temperature (°C)
Rain mixing ratio (g kg-1)
Terrain Height (m)
Cross-Section: (636,804) to (667,804)
Height (m)
1500
1000
500
0
-100.5
-99.9
-99.3
-98.7
Contours: -5 to 5 by .5
Longitude
Rain mixing ratio (g kg-1)
.00004 .00012 .0002 .00028 .00036 .00044 .00052

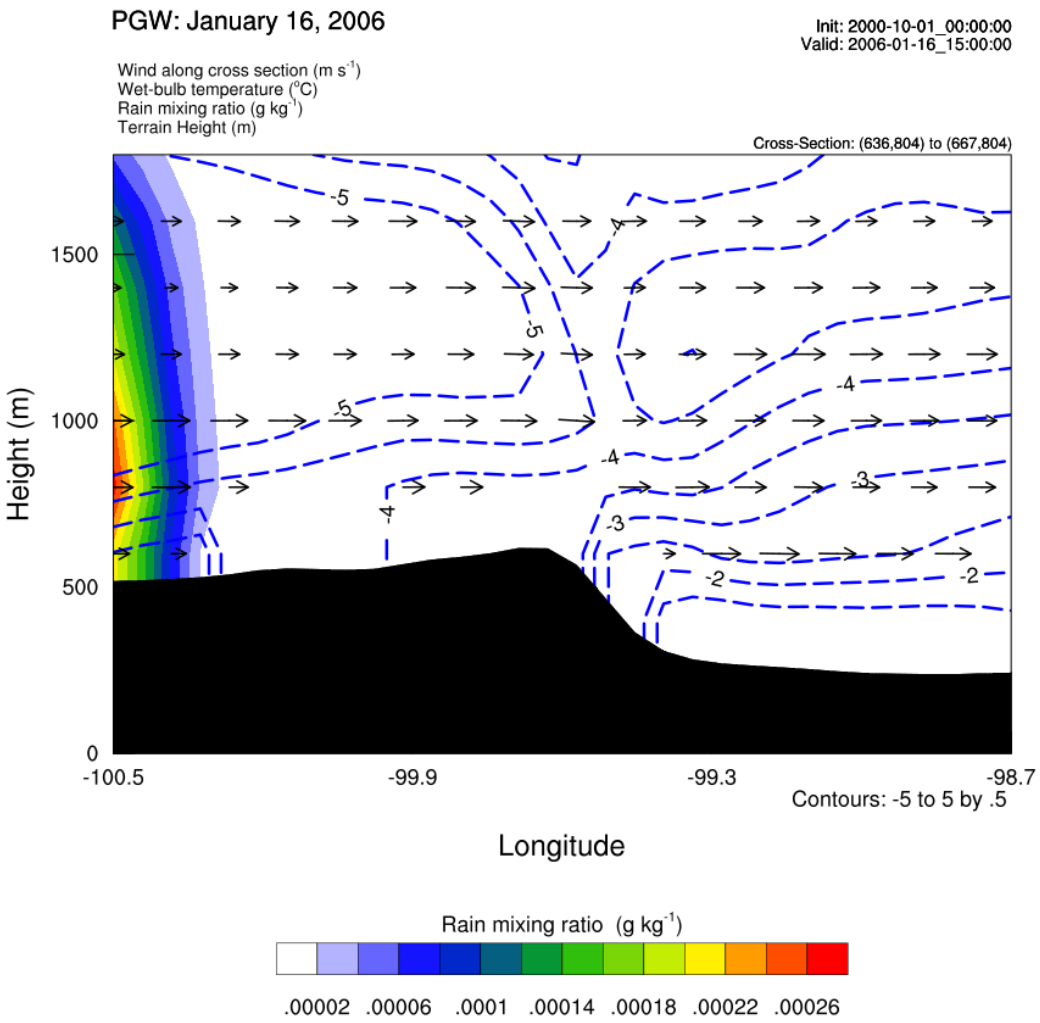
PGW: January 16, 2006
Init: 2000-10-01_00:00:00
Valid: 2006-01-16_15:00:00
Wind along cross section (m s-1)
Wet-bulb temperature (°C)
Rain mixing ratio (g kg-1)
Terrain Height (m)
Cross-Section: (636,804) to (667,804)
Height (m)
1500
1000
500
0
-100.5
-99.9
-99.3
-98.7
Contours: -5 to 5 by .5
Longitude
Rain mixing ratio (g kg-1)
.00002 .00006 .0001 .00014 .00018 .00022 .00026

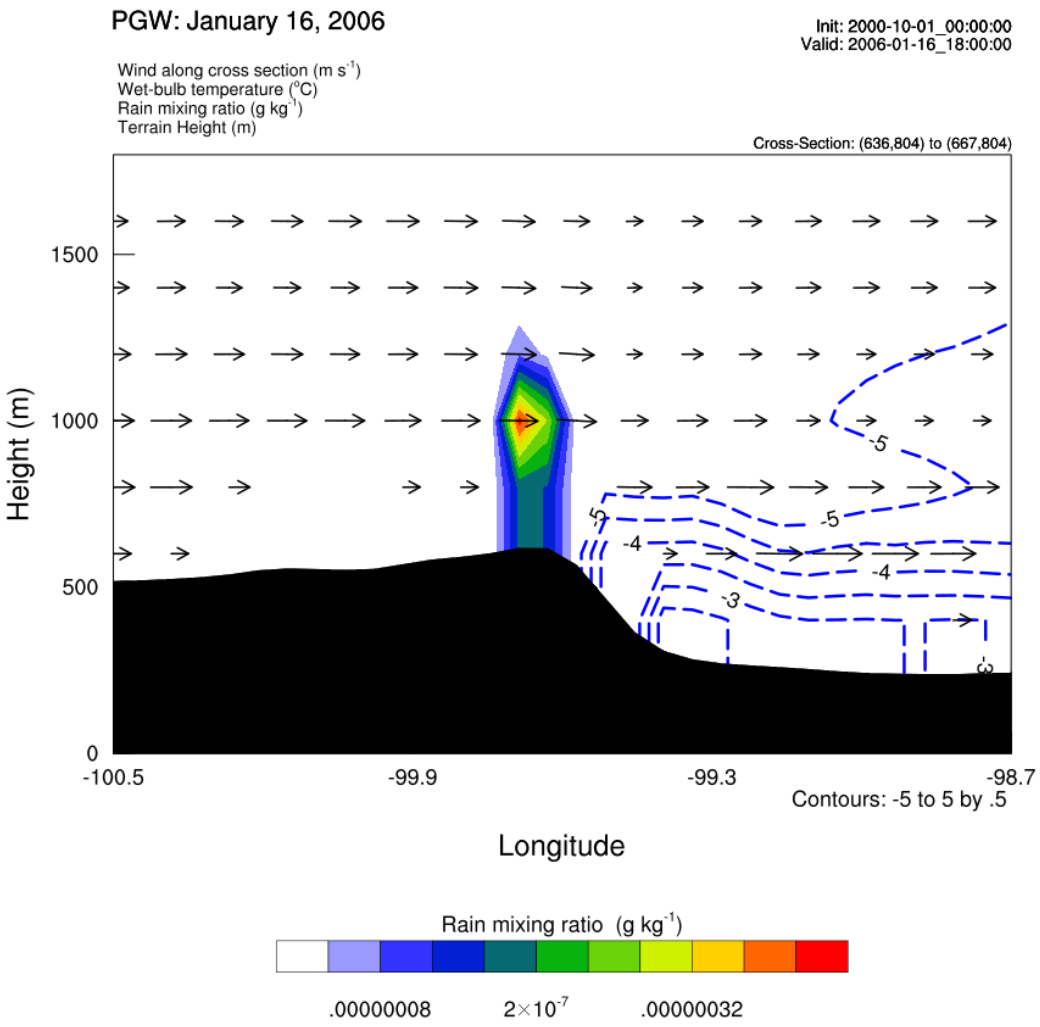
PGW: January 16, 2006
Init: 2000-10-01_00:00:00
Valid: 2006-01-16_18:00:00
Wind along cross section (m s-1)
Wet-bulb temperature (°C)
Rain mixing ratio (g kg-1)
Terrain Height (m)
Cross-Section: (636,804) to (667,804)
Height (m)
1500
1000
500
0
-5
-4
-3
-100.5
-99.9
-99.3
-98.7
Contours: -5 to 5 by .5
Longitude
Rain mixing ratio (g kg-1)
.00000008
2×10-7
.00000032

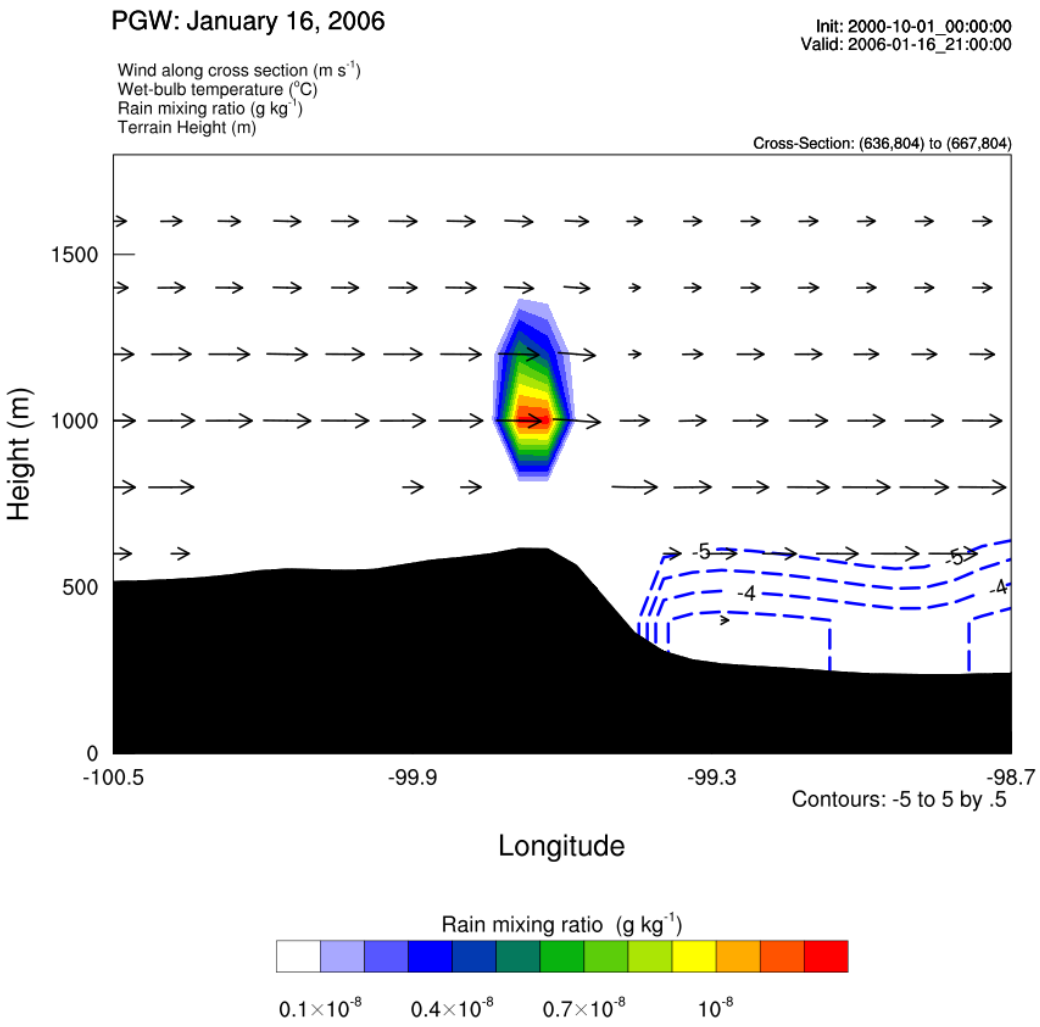
PGW: January 16, 2006
Init: 2000-10-01_00:00:00
Valid: 2006-01-16_21:00:00
Wind along cross section (m s-1)
Wet-bulb temperature (°C)
Rain mixing ratio (g kg-1)
Terrain Height (m)
Cross-Section: (636,804) to (667,804)
Height (m)
1500
1000
500
0
-5
-4
-100.5
-99.9
-99.3
-98.7
Contours: -5 to 5 by .5
Longitude
Rain mixing ratio (g kg-1)
0.1×10-8
0.4×10-8
0.7×10-8
10-8

Appendix D: WRF CTRL vs Surface Observations

Time Series

This section contains time series from 8 different surface weather stations across Manitoba. The first image shows a map of these stations, indicated with a red dot, or a yellow star for the capital city of Winnipeg. The time series show the 2 m temperature, relative humidity, and 10 m winds for both the WRF CTRL simulation and ECCC Observations, as indicated by the legend at the top of the image. The left axis is the temperature and the right is the relative humidity. Winds are shown as wind barbs in m s^{-1}.

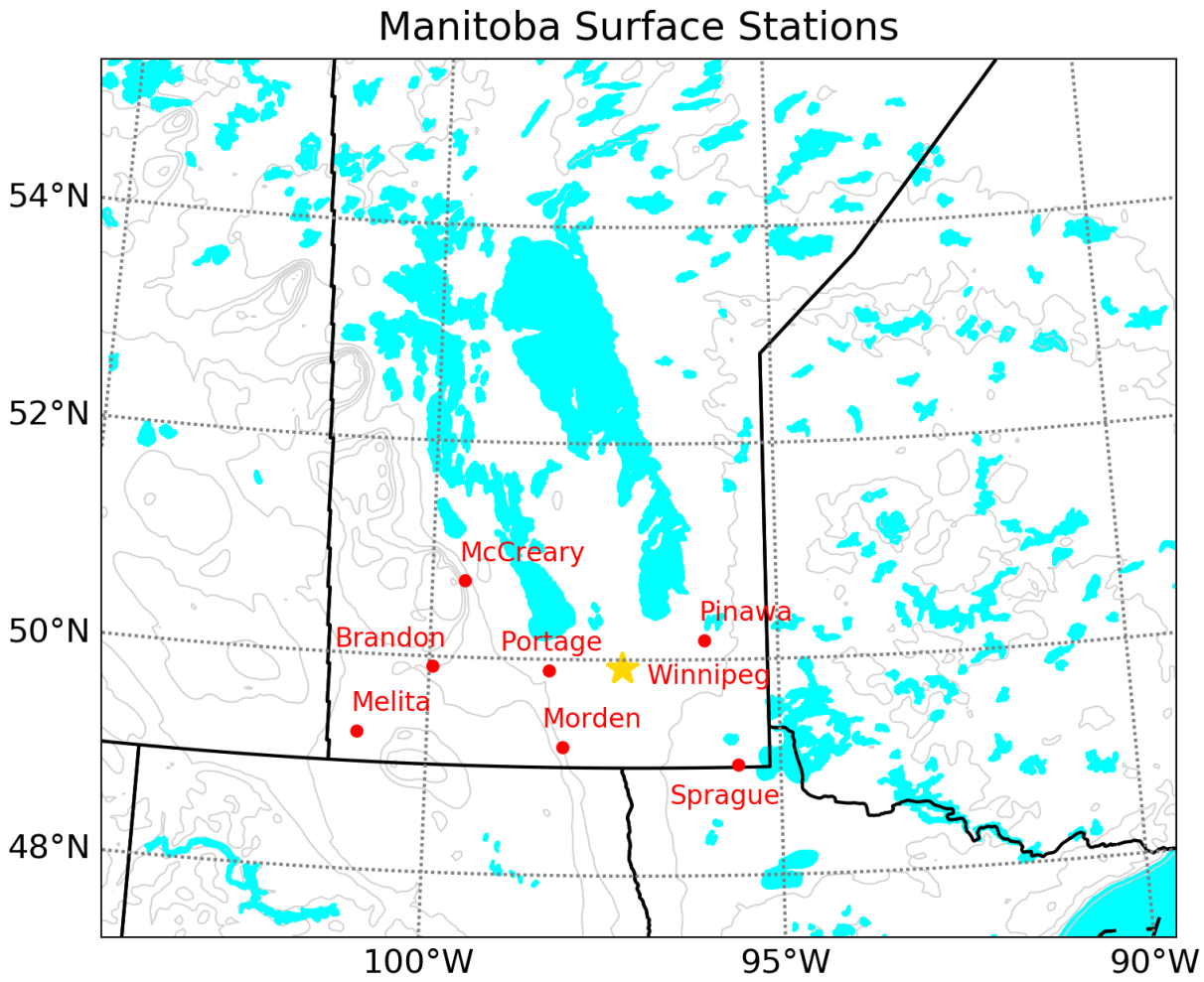
Manitoba Surface Stations
54°N
52°N
50°N
48°N
100°W
95°W
90°W
McCreary
Brandon
Portage
Pinawa
Winnipeg
Melita
Morden
Sprague

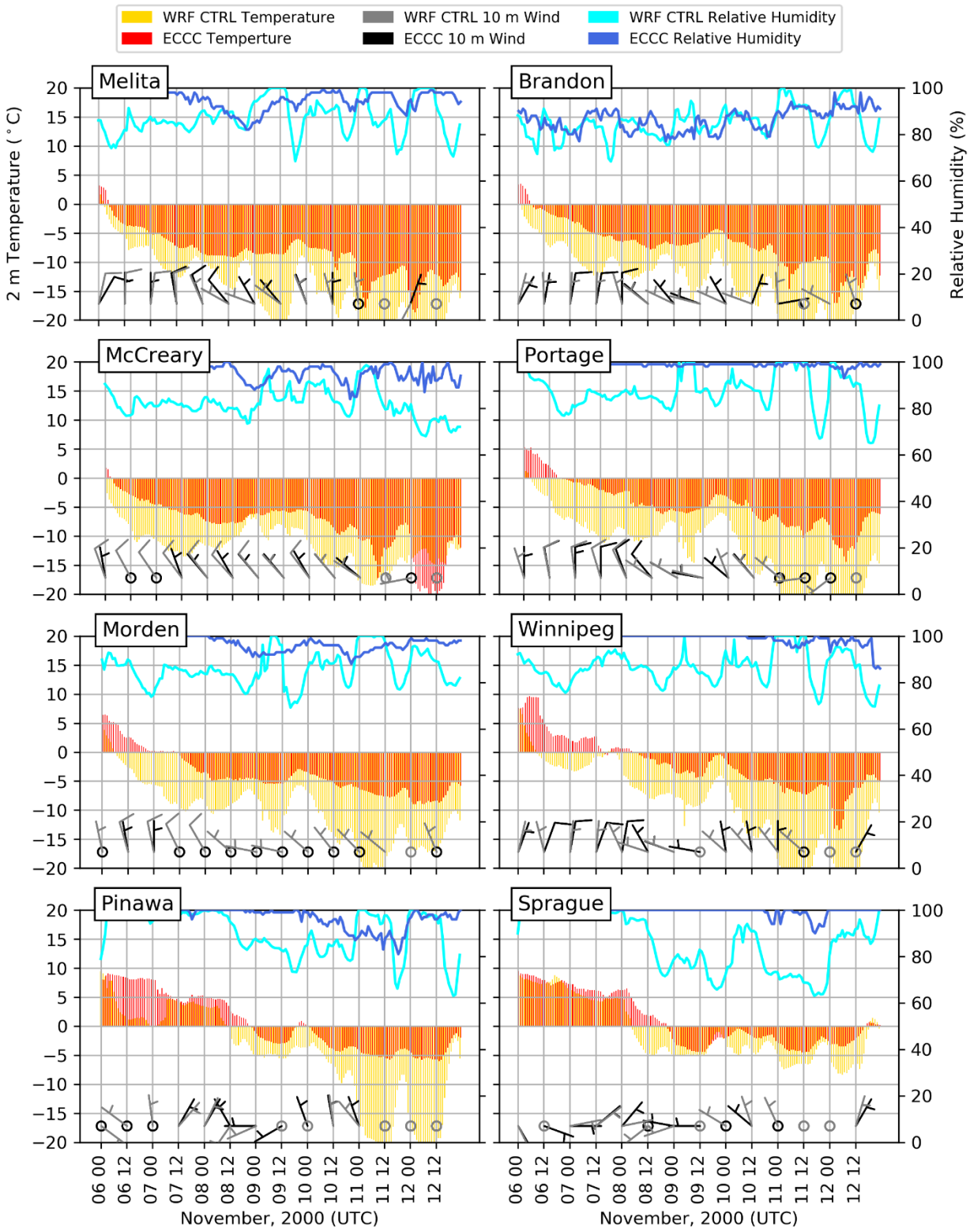
WRF CTRL Temperature
ECCC Temperture
WRF CTRL 10 m Wind
ECCC 10 m Wind
WRF CTRL Relative Humidity
ECCC Relative Humidity
Melita
Brandon
McCreary
Portage
Morden
Winnipeg
Pinawa
Sprague
2 m Temperature (° C)
Relative Humidity (%)
06 00
06 12
07 00
07 12
08 00
08 12
09 00
09 12
10 00
10 12
11 00
11 12
12 00
12 12
November, 2000 (UTC)

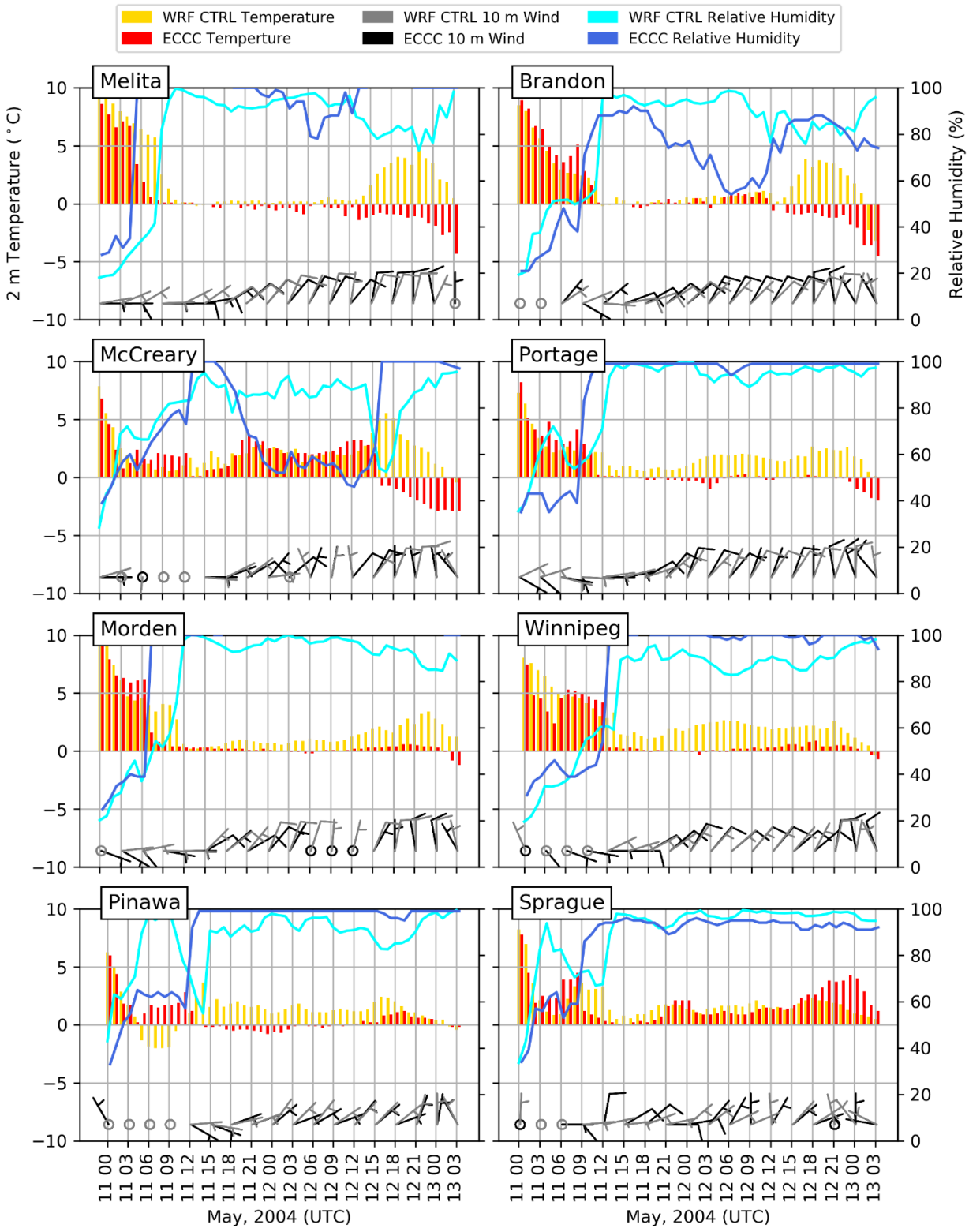
WRF CTRL Temperature
ECCC Temperture
WRF CTRL 10 m Wind
ECCC 10 m Wind
WRF CTRL Relative Humidity
ECCC Relative Humidity
Melita
Brandon
McCreary
Portage
Morden
Winnipeg
Pinawa
Sprague
2 m Temperature (° C)
Relative Humidity (%)
May, 2004 (UTC)
May, 2004 (UTC)

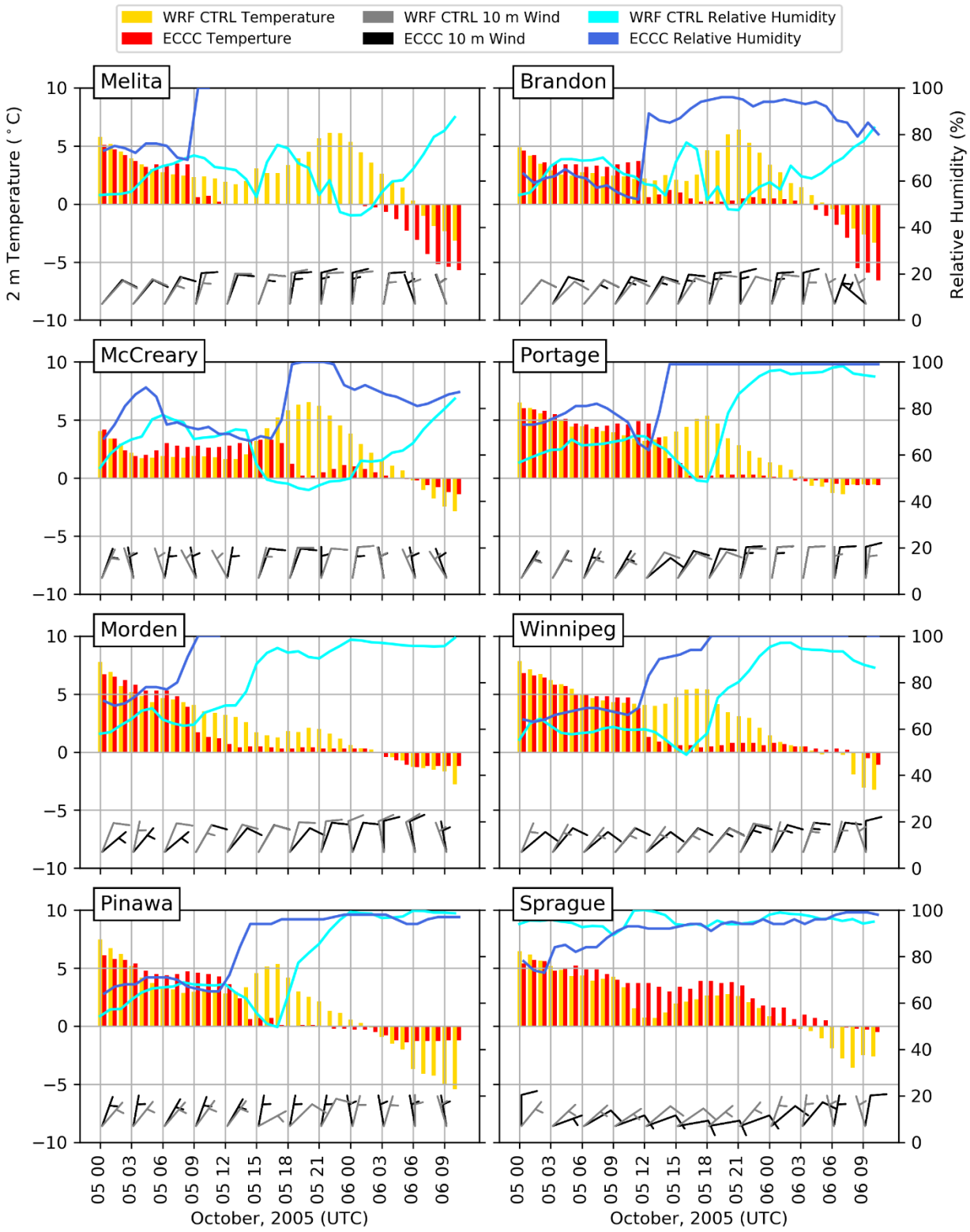
WRF CTRL Temperature
ECCC Temperture
WRF CTRL 10 m Wind
ECCC 10 m Wind
WRF CTRL Relative Humidity
ECCC Relative Humidity
Melita
Brandon
McCreary
Portage
Morden
Winnipeg
Pinawa
Sprague
2 m Temperature (°C)
Relative Humidity (%)
October, 2005 (UTC)
October, 2005 (UTC)

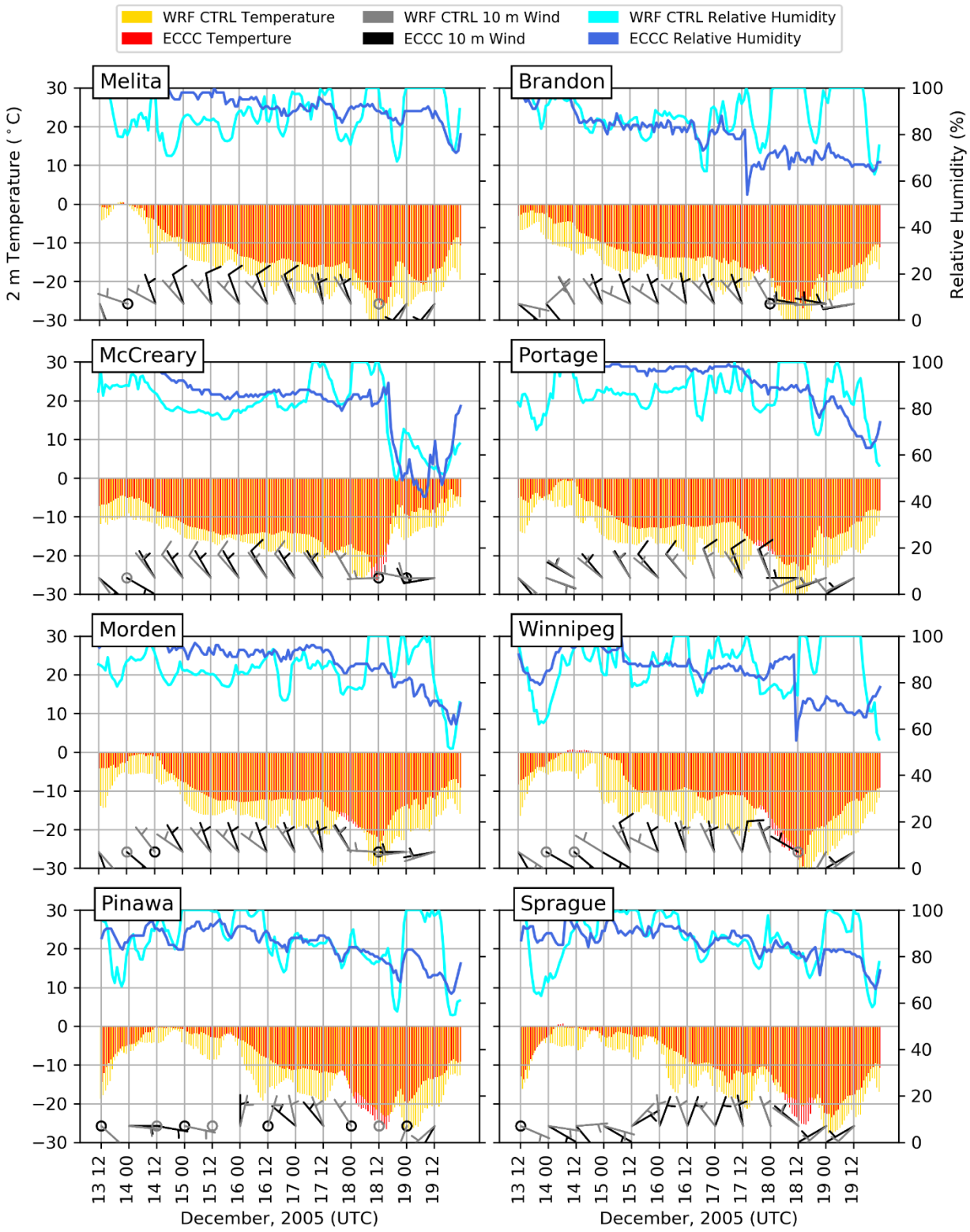
WRF CTRL Temperature
ECCC Temperture
WRF CTRL 10 m Wind
ECCC 10 m Wind
WRF CTRL Relative Humidity
ECCC Relative Humidity
Melita
Brandon
McCreary
Portage
Morden
Winnipeg
Pinawa
Sprague
2 m Temperature (° C)
Relative Humidity (%)
13 12
14 00
14 12
15 00
15 12
16 00
16 12
17 00
17 12
18 00
18 12
19 00
19 12
December, 2005 (UTC)

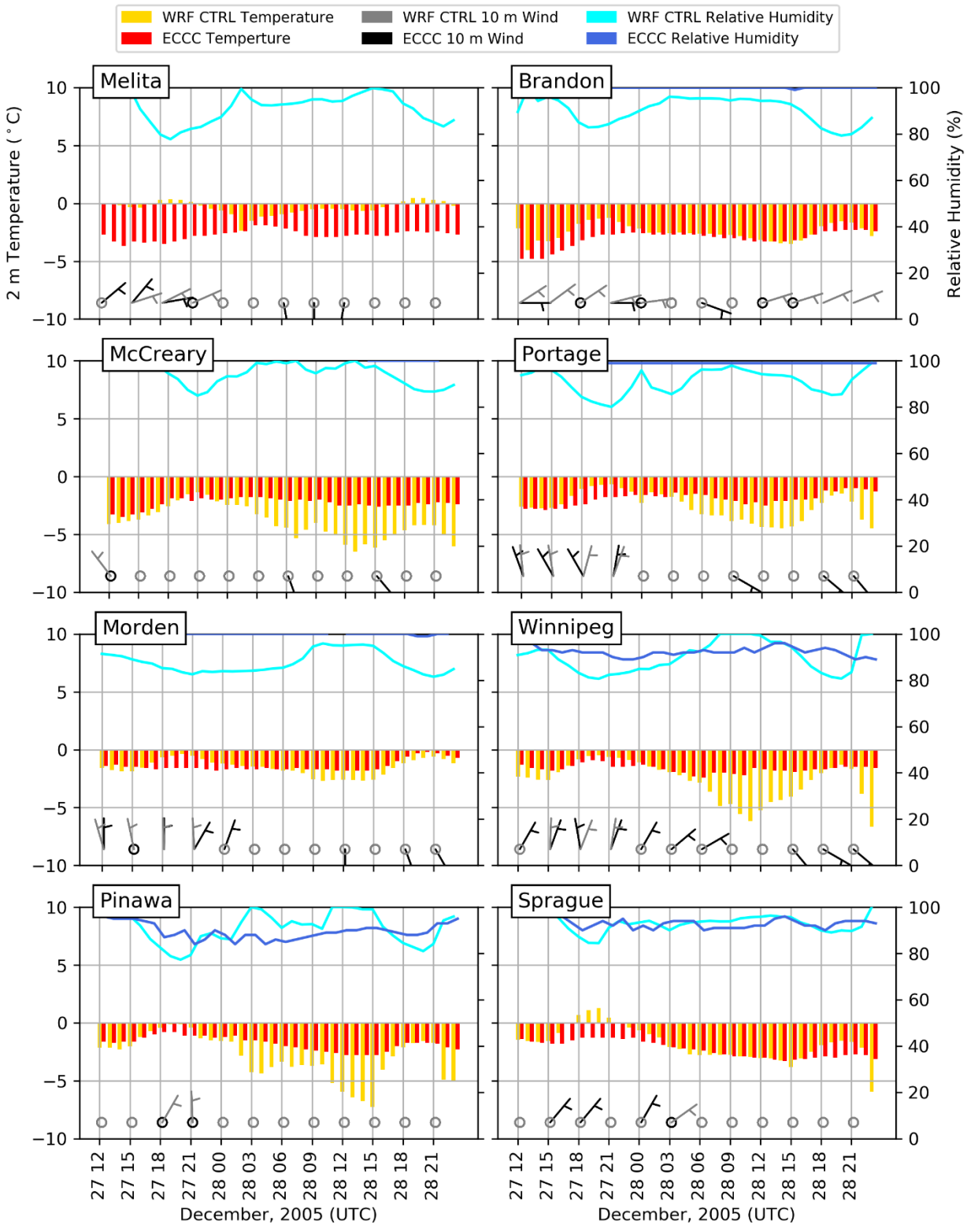
WRF CTRL Temperature
ECCC Temperture
WRF CTRL 10 m Wind
ECCC 10 m Wind
WRF CTRL Relative Humidity
ECCC Relative Humidity
Melita
Brandon
McCreary
Portage
Morden
Winnipeg
Pinawa
Sprague
2 m Temperature (° C)
Relative Humidity (%)
27 12
27 15
27 18
27 21
28 00
28 03
28 06
28 09
28 12
28 15
28 18
28 21
December, 2005 (UTC)

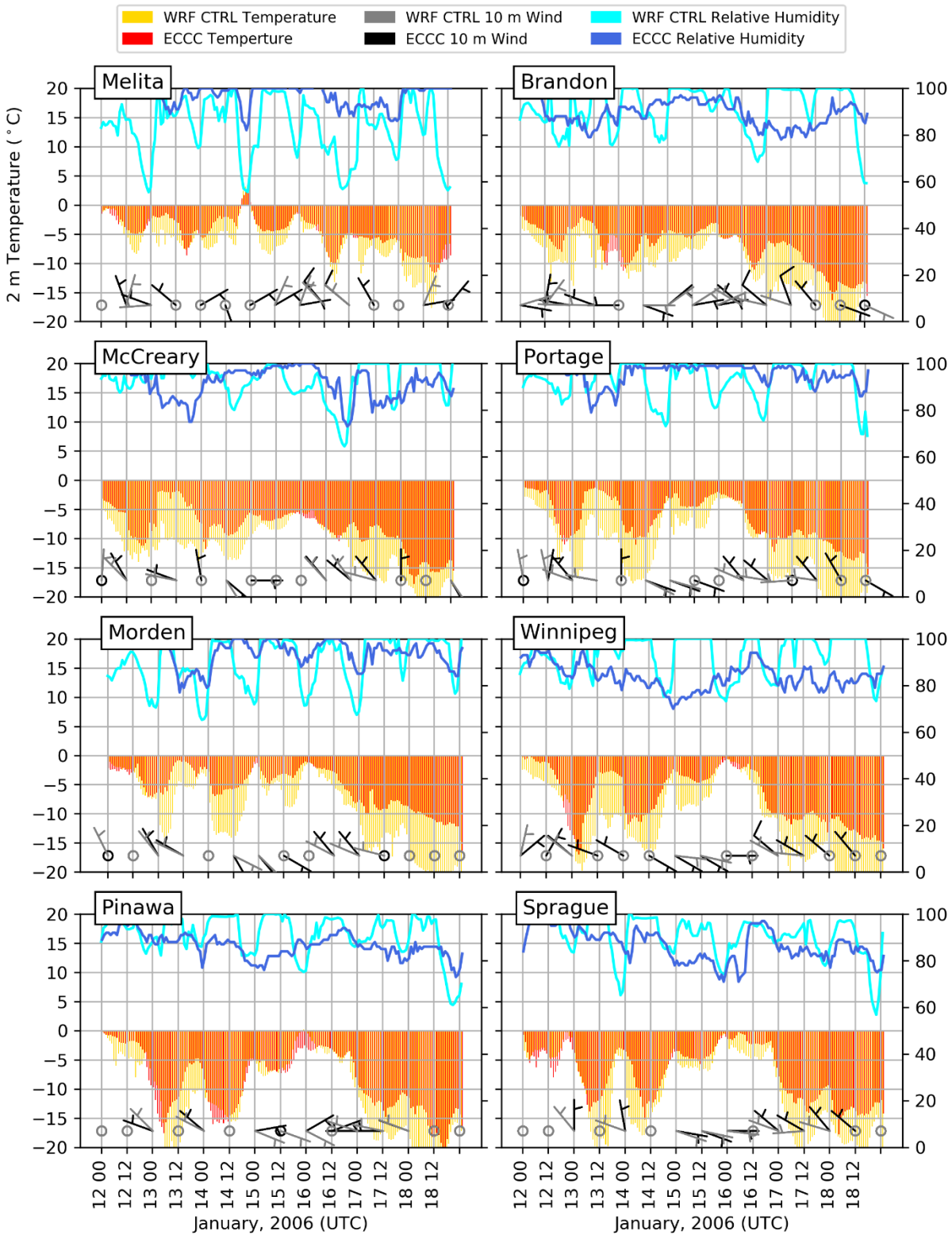
WRF CTRL Temperature
ECCC Temperture
WRF CTRL 10 m Wind
ECCC 10 m Wind
WRF CTRL Relative Humidity
ECCC Relative Humidity
Melita
Brandon
McCreary
Portage
Morden
Winnipeg
Pinawa
Sprague
2 m Temperature (°C)
Relative Humidity (%)
January, 2006 (UTC)

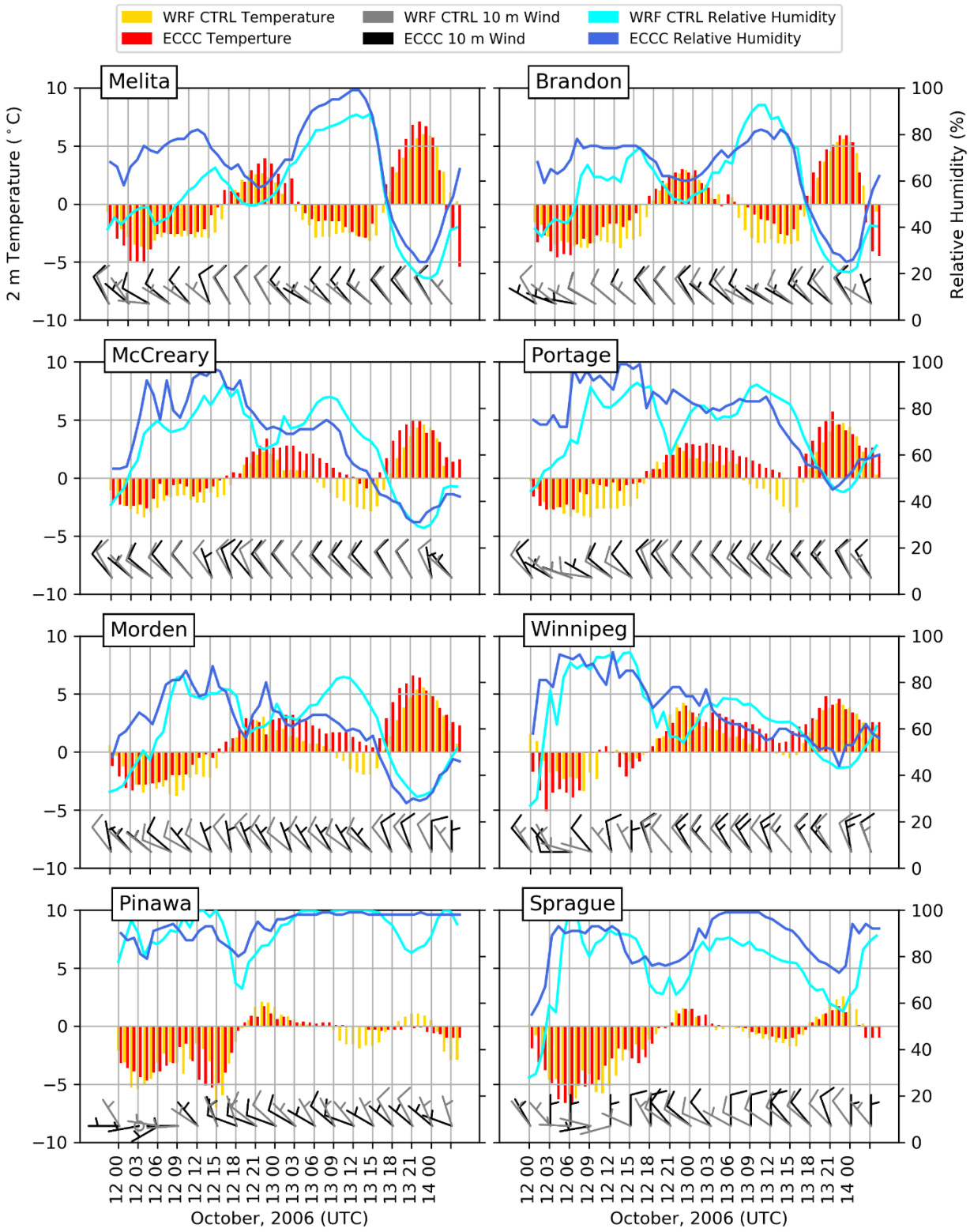
WRF CTRL Temperature
ECCC Temperture
WRF CTRL 10 m Wind
ECCC 10 m Wind
WRF CTRL Relative Humidity
ECCC Relative Humidity
Melita
Brandon
McCreary
Portage
Morden
Winnipeg
Pinawa
Sprague
2 m Temperature (° C)
Relative Humidity (%)
October, 2006 (UTC)
October, 2006 (UTC)

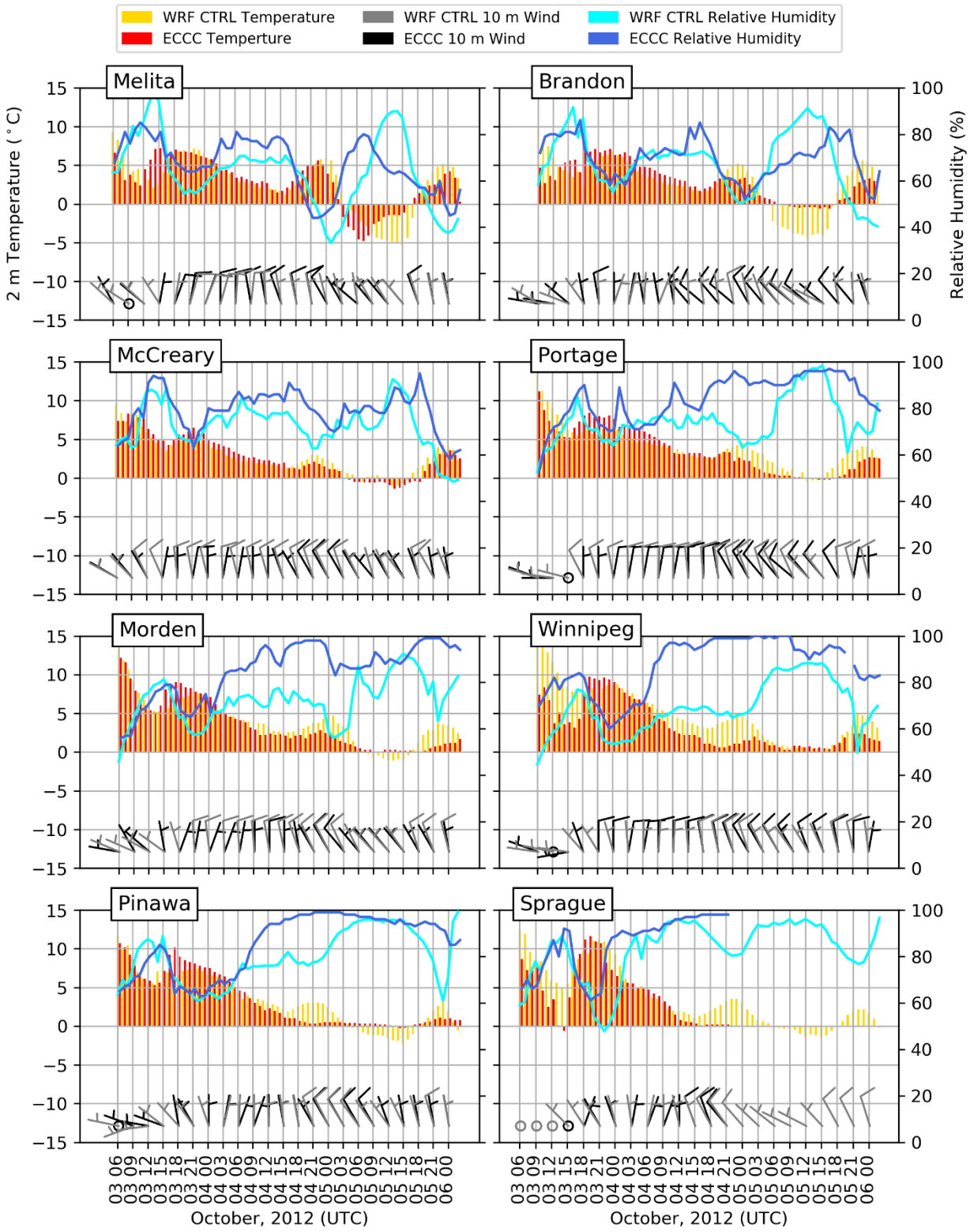
WRF CTRL Temperature
ECCC Temperture
WRF CTRL 10 m Wind
ECCC 10 m Wind
WRF CTRL Relative Humidity
ECCC Relative Humidity
Melita
Brandon
McCreary
Portage
Morden
Winnipeg
Pinawa
Sprague
2 m Temperature (° C)
Relative Humidity (%)
October, 2012 (UTC)
October, 2012 (UTC)